Drivers of Southern Ocean food web structure and impacts of environmental change

Patrick Eskuche-Keith

Thesis submitted in fulfilment of the requirements of the University of Essex for the degree of Doctor of Philosophy

School of Life Sciences

University of Essex

July 2024

"It seems to me that the natural world is the greatest source of excitement; the greatest source of visual beauty; the greatest source of intellectual interest. It is the greatest source of so much in life that makes life worth living".

Sir David Attenborough

Abstract

The Southern Ocean is experiencing major environmental and ecological changes which could drastically alter communities and impact ecosystem functioning. We still have a poor understanding of the structure of Southern Ocean food webs and their likely responses to ongoing and future changes, which limits our ability to develop and implement effective management and conservation strategies. This thesis employs multiple approaches to investigate several aspects relating to the structure and dynamics of Southern Ocean food webs. First, the links between morphological traits and trophic niches are explored within the demersal fish community of the subantarctic island of South Georgia, highlighting the role of functional traits in driving community structure. Second, functional traits including body size, mobility, foraging habitat and feeding mode are used to identify the drivers of stabilising sub-structures (modularity) across regional food webs. This leads to the hypothesis that habitat heterogeneity is a major determinant of the distribution of modules within networks. Third, an extensive dataset of mesopelagic fish and zooplankton samples from across a latitudinal temperature gradient is used to determine the impact of warming on predator-prey body mass ratios (PPMR). This reveals that ongoing environmental change may reorganise the size-structure of Southern Ocean ecosystems, with implications for their stability. Fourth, the possible consequences of ongoing baleen whale population recovery for competitor biomasses are explored using the Ecopath framework, with the conclusion that strong trade-offs between conservation objectives are likely unless substantial increases in suitable primary production occur. This thesis finishes with a synthesis of these new insights into the structure and dynamics of Southern Ocean food webs and discusses the major future directions for food web research more generally.

Contributions statement

I hereby declare that the chapters and associated papers that make up this thesis are the result of my own work. My supervisory team (Drs Eoin O'Gorman, Simeon Hill, Michelle Taylor and Phil Hollyman) provided conceptual guidance and editorial feedback on drafts. Various external collaborators (Drs Lucía López-López, Ryan Saunders, Geraint Tarling, Benjamin Rosenbaum and Martin Collins) also provided invaluable help with various aspects of this thesis, including contributing data, aiding in fieldwork and providing feedback on manuscript drafts.

Acknowledgements

Writing this thesis broadened my appreciation for the interconnectedness of the natural world and has strengthened my passion for understanding how the interactions between organisms mediate the patterning of biodiversity and maintenance of ecosystem processes. Pursuing this PhD has brought me into contact with amazing people and allowed me to experience mind-blowing places, and for that I will be ever grateful.

This thesis has been a long journey and I've only made it through thanks to the support and encouragement of my supervisors, friends and family. First and foremost, thank you to my supervisory team, Dr Eoin O'Gorman, Dr Simeon Hill, Dr Michelle Taylor and Dr Phil Hollyman. Your feedback and guidance helped me develop my skills and independence as a researcher, and I am hugely grateful for your encouragement throughout this project. Thank you for all of the opportunities you created, from conducting fieldwork to collaborations with other researchers and publishing articles – it's been a blast!

Much of this thesis came about through collaborations with incredible researchers at various institutes. In no particular order, thanks to Dr Ryan Saunders, Prof. Geraint Tarling and Dr Martin Collins (British Antarctic Survey), Dr Benjamin Rosenbaum (iDiv), and Dr Lucía López-López (IEO). Thanks also to the UK NERC and ARIES DTP for funding my project. The British Antarctic Survey also provided logistical support to facilitate the fieldwork underlying my first chapter, and the EU COST Action Sea-Unicorn funded the research stay in Santander which ultimately led to the development of my third chapter.

Having a strong support network is key to success and I was lucky enough to have an excellent group of friends to see me through. You are too many to thank individually so here it goes in no particular order: Amy, Howard, Alex (thanks for all the shenanigans and for introducing me to the bliss that is freediving), Zelin, Mike, Alice (I hope you cure your plant obsession soon, for all our sakes), Peter, Lucy, Haleigh, Nonny, Jake, Hugo and Joe. Thanks also to the various friends I made at BAS (Paul, maybe one day you'll have a functional air mattress for me) and at KEP. In the words of a wise man, keep crushing it! Turns out that light in the tunnel isn't a train after all.

To my parents Hugh and Lisa, you got me to this point through thick and thin and I hope I've made you proud. Maybe now I'll finally get a real job. And to my wonderful partner Melissa, thanks for sticking it out with me, I'm so proud of what you have achieved in the meantime. Here's to the future!

Contents

1 General Introduction

Our oceans are experiencing unprecedented environmental and ecological changes. These include climate-driven warming of waters (including more frequent, stronger marine heatwaves), melting of sea ice, and changes in primary productivity (Cooley et al. 2022). Additionally, the growing human population is resulting in ever-increasing demand for food, driving the over-exploitation of marine resources (Costello et al. 2020). These stressors often do not act in isolation, but instead interact additively and synergistically to increase the vulnerability of species and communities (Gissi et al. 2021). It is predicted that climate change will soon become the single greatest driver of global biodiversity loss (Newbold 2018; He et al. 2019). A primary response of marine ectotherms to changing conditions (particularly temperature rises) is to shift their distribution to track favourable conditions, and regional species turnover rates are far greater within the marine environment than on land (Blowes et al. 2019). Species that are unable to track favourable conditions may experience physiological impacts resulting in fundamental changes such as decreases in size-at-age, changes to fecundity, or even local extinctions (Nikolaou and Katsanevakis 2023; Niu et al. 2023). Such shifts in the distribution and local abundance of marine species will alter regional community composition, with impacts on ecosystem structure.

Polar regions are particularly under threat, as many endemic species have limited capacity to undergo compensatory distribution shifts due to the shrinking of suitable habitat (such as sea ice or waters within their thermal tolerance range) or the presence of physical barriers (e.g. the Antarctic continental shelf). Polar ecosystems will thus be increasingly impacted both by abiotic and biotic factors, as environmental changes drive the decline of native species and influxes of sub-polar species alter the composition of regional species assemblages. Such biodiversity changes and homogenisation are of great concern from both conservation and management perspectives, as they may increase the vulnerability of ecosystems to further changes and could disrupt ecosystem functioning and the maintenance of ecosystem services (Olden et al. 2004).

1.1 Biodiversity and ecosystem stability

Recognition of ongoing biodiversity change has led to a focus on the links between diversity and the dynamics and stability of communities and maintenance of ecosystem processes. Ecological stability has numerous definitions (as reviewed by Ives and Carpenter 2007), the most common being the overall temporal variability or amplitude of fluctuations in the focal

community properties (dynamic stability), the extent to which discrete perturbations alter these properties (resistance), and the ability or rate at which the properties return to equilibrium (recovery) (McCann 2000; Ives and Carpenter 2007) (Figure 1.1). Species diversity may enhance community stability through mechanisms such as the 'portfolio effect' (statistical averaging) and the 'covariance effect' (whereby negative covariance in abundance of competing species increases with higher diversity) (Tilman and Downing 1994; Tilman et al. 2006). Ecosystem resilience (the combination of resistance and recovery) often increases with diversity. This is due to the greater variety of ecological roles present within the community and the number of species able to perform the same roles (functional redundancy), which increases the overall capacity to tolerate perturbations (Biggs et al. 2020; Yachi and Loreau 1999).

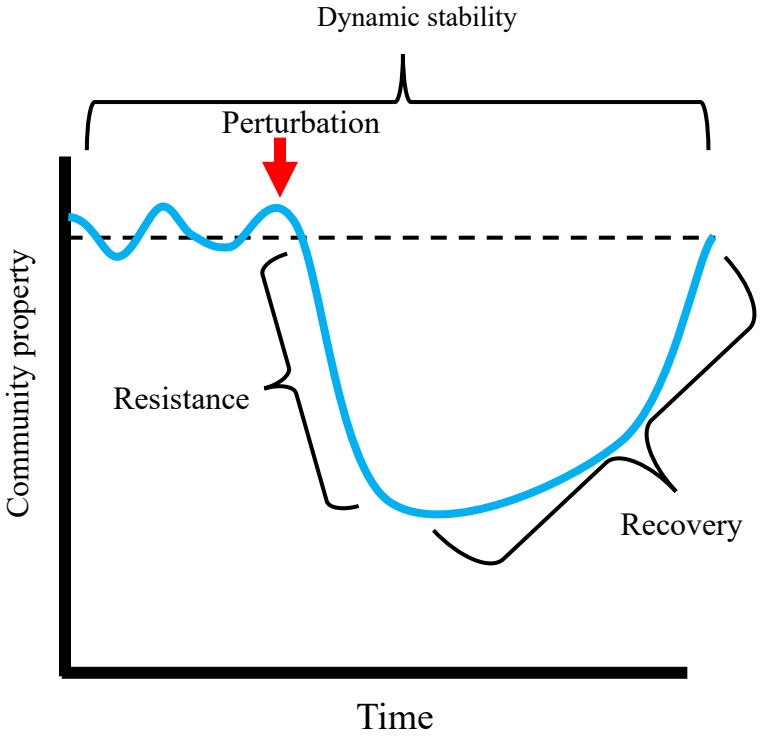

Figure 1.1: Conceptual visualisation of three common stability measures. The blue line represents a community property (e.g. biomass). Dynamic stability generally describes the temporal variability or amplitude of fluctuations in the property, resistance measures the degree of change in the property after perturbation, and recovery represents the rate at which of the property returns to baseline (dashed line) after perturbation, or the relative quantity of the community property that is recovered post-disturbance.

Much diversity-stability research has focussed on simple communities spanning single or few trophic levels and may therefore fail to consider important ways in which species diversity in larger, more complex ecological networks can modify ecosystem properties. As discussed by Stachowicz et al. (2007), changes to predator and prey diversity in multi-trophic marine communities can modify diversity-stability relationships through mechanisms such as altered strength of top-down and bottom-up control, and trophic cascades. In the context of climate change, there is evidence that fluctuations in species populations and overall diversity are driven as much by changes in the interactions between species as by direct environmental effects on organisms themselves (Ockendon et al. 2014). If we are to disentangle and predict the likely ecosystem-level responses to changes in species distributions, then it is important that we gain an understanding of how ecological communities are structured and what implication this structure has for ecosystem stability. This approach requires the explicit consideration of species interactions, which can be achieved using food web models.

1.2 Food web models

Food web models depict the feeding relationships between species and provide a useful framework for relating the structure of multitrophic communities to ecosystem functioning, given that they incorporate not only their constituent species but also the relevant patterning of interactions (i.e. energy flow) within the system (Thompson et al. 2012; Hines et al. 2019). Models are generally constructed using information on the diet of each species within the focal ecosystem. This data may come from a range of sources including direct observation of feeding interactions, morphological analysis of stomach or scat samples, and methods such as stable isotope analysis or the DNA sequencing of tissue samples (Horswill et al. 2018). The limitations to these different methods are well described. Morphological methods are biased towards identifying prey species with hard structures and the resulting information only represents recent dietary composition, while isotope analysis can identify more long-term diet in addition to providing quantitative estimates of diet reliance but cannot resolve prey taxonomy to the species-level (Nielsen et al. 2017; Horswill et al. 2018). DNA sequencing sits somewhere in-between, as it can resolve recent prey taxonomy without requiring intact prey specimens to be present but fails to provide information on the relative proportions of species in the diet (Nielsen et al. 2017; Horswill et al. 2018). Despite their individual limitations, these methods can provide invaluable contributions to the creation of comprehensive food web models for a wide range of ecosystems, and recent research has begun combining some of these techniques to maximise the reliability of inferred diets (e.g.

Horswill et al. 2018; Bonin et al. 2020). Data on feeding relationships are often also supplemented with information from the primary literature to infer interactions for species that are known to occur in the system concerned.

There are various approaches to modelling food webs, which exist along a spectrum of capabilities and data requirements (Figure 1.2). At their most basic, food webs can be described using simple unweighted binary network models, whereby species (or groups of taxonomically or functionally similar organisms) are represented by nodes and their interactions are described by the links between them. Such models are relatively easy to construct, as they only require knowledge of which groups consume each other. Despite their simplicity, these models can provide useful insights, with a variety of metrics that can be calculated to describe the position and role of individual nodes within the wider ecosystem or provide an understanding of the overall structure of the food web, both of which are relevant to determining the implications of perturbations for ecosystem functioning (Table 1.1). Qualitative network models can be particularly useful in data-poor systems, as they require only a general understanding of the interactions between ecosystem components, and have been used to explore possible ecological consequences of climate change or management activities (Melbourne-Thomas et al. 2013; Forget et al. 2020).

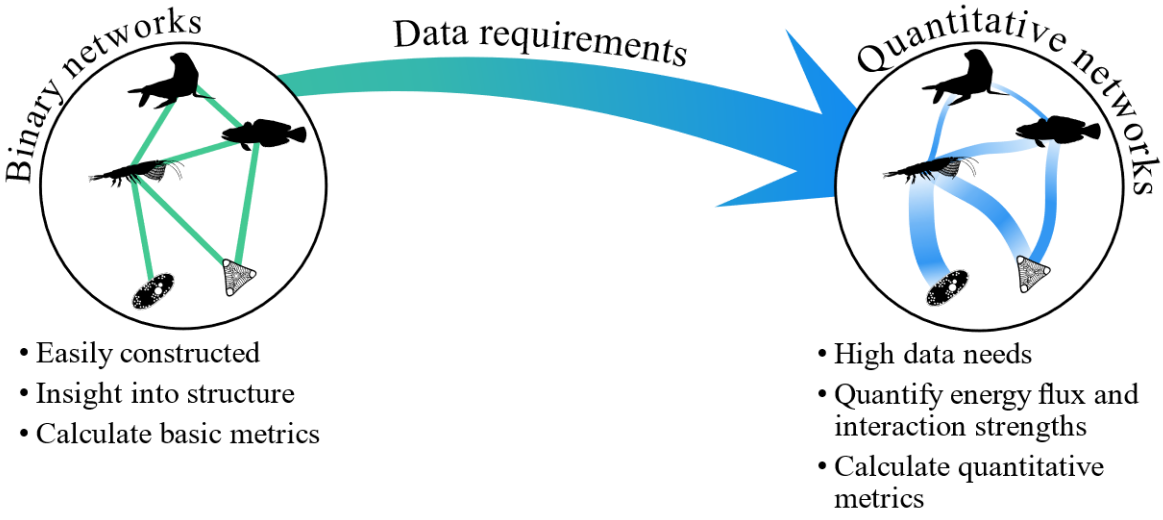

Figure 1.2: Conceptual diagram highlighting the requirements and capabilities of binary and quantitative food web models.

278 Table 1.1: List of common node-level and network-level food web metrics, their descriptions,
279 and implications for our understanding of food web structure.

Metric	Description	Implication	References
Species richness (S)	Number of nodes within the food web.	Provides information on food web size.	Thompson et al. 2012; Kortsch et al. 2019
Link richness (L)	Number of feeding links between nodes.	Provides information on food web size.	Thompson et al. 2012; Kortsch et al. 2019
Average food chain length	The number of nodes that energy passes through from the base to the top predator in the food chain.	Provides information about network structure and organisation of interactions.	Post 2002; Thompson et al. 2012
Linkage density (L/S)	Average number of links per node (unweighted).	Indicates food web complexity.	Kortsch et al. 2019
Connectance (L/S^2)	Proportion of total possible trophic links that actually occur in a network (unweighted).	Indicates food web complexity.	Thompson et al. 2012
Clustering coefficient	For a given node, indicates the degree to which connected nodes are also linked to each other. At the network level, indicates the average level of clustering.	Indicates food web complexity and structure.	Kortsch et al. 2019; Marina et al. 2018
Degree	Number of incoming and outgoing links to a specific node.	Indicates how connected the node is. Used to estimate generality and vulnerability.	Thompson et al. 2012; Kortsch et al. 2019; Marina et al. 2018
Degree distribution	Overall frequency distribution of the number of interactions for each node in the network	Can help identify species/groups with important roles in connecting the community.	Thompson et al. 2012; Kortsch et al. 2019; Marina et al. 2018
Generality	Number of prey consumed by a node. At network scale, estimated as the mean number of prey per consumer.	Indicates node/network sensitivity to bottom-up processes influencing prey dynamics.	Thompson et al. 2012
Vulnerability	Number of predators of a given node. At network scale, estimated as the mean number of consumers per prey.	Indicates node/network sensitivity to top-down processes influencing predator dynamics.	Thompson et al. 2012
Modularity	How densely nodes within subgroups interact with each other compared to with nodes from other subgroups.	Provides an indication of the structure and organization of links within the food web.	Grilli et al. 2016; Kortsch et al. 2019
Proportion of basal, intermediate, and top species	Fraction of species with no resources, with both consumers and resources, and with no consumers, respectively.	Provides an indication of food web structure and possible top-down or bottom-up control.	Kortsch et al. 2019; Gibert 2019
Omnivory	Variety in prey trophic level for a given consumer node.	Proportion of omnivory has implications for network stability and energy flow.	McCann and Hastings 1997; Kratina et al. 2012; Heymans et al. 2014

280

281

More complex models can provide additional knowledge about structure and patterns of energy transfer that is not available in unweighted models. For example, these weighted networks can reveal the energy flux between groups and capture the strengths of interactions (Marina et al. 2024; Gauzens et al. 2019). The development of such quantitative models comes with greater data requirements, such as abundances, body masses, metabolic rates and relative dietary contributions, limiting their application to regions where such information is available. Modelling frameworks such as Ecopath with Ecosim are used to construct models of energetic fluxes that meet the assumption of mass-balance over a specific time period (often a single year) (Christensen and Walters 2004). Ecopath models lie at the far end of the complexity and data needs scale, with key parameters including the biomass, diet composition by weight, production per unit biomass, consumption per unit biomass and assimilation efficiency of each group, while additional parameters representing biomass accumulation rates, fishery catches and discards, and migration rates can also be supplied (Christensen and Walters 2004). Parameters are ideally location- and group-specific but can also be taken from other models or literature where necessary. These form the basis of linear equations underlying the production of each group, as determined both by their parameters and those of their consumers. A key parameter which is often an output of Ecopath models is the ecotrophic efficiency (*EE*), representing the proportion of the production or mortality of each group that is explained in the model. Values range from zero (limited to top predators that are not fished) to one (100% of production is consumed by other groups in the model). As such, the *EE* is a key parameter representing whether or not the model is in balance, with values above one indicating groups with mortality rates that cannot be sustained by production rates. Extensive adjustments to group parameters must often be made before the assumption of mass balance ($EE \leq 1$) is met for all groups. Balanced Ecopath models represent a powerful tool for exploring topics including the direct and indirect impacts of fisheries on trophic interactions (Coll et al. 2006; Subramaniam et al. 2020), the consequences of climate change for aquaculture (Chapman et al. 2020), and the effect of multiple climate and anthropogenic stressors on trophic dynamics (Stock et al. 2023). Additionally, the inclusion of temporal population trends for key groups can also facilitate the development of time-dynamic models using the Ecosim plugin, and spatially resolved models can also be constructed (Christensen and Walters 2004).

1.3 The drivers of food web structure

Early research into the relationship between diversity and stability used random matrices to describe the structure of species communities (e.g. May 1973). We now know that complex networks are non-randomly structured, and that their topology may be influenced by a variety of factors.

A major driver of the structure of food webs is the distribution of functional traits across the community (Gravel et al. 2016; Brose et al. 2019). Predator and prey traits influence both the likelihood of co-occurrence of interacting species, and the ability of each species to capture and consume, or escape, the other. Marine food webs are often strongly size-structured, as body size determines gape limitation, prey density, handling time and energy content (Petchey et al. 2008; Rall et al. 2012; Potapov et al. 2019). The relative size of predators to their prey (the predator prey mass ratio, PPMR), can be used to predict food web structure (Petchey et al. 2008; Morales-Castilla et al. 2015; Laigle et al. 2017). PPMR generally decreases with trophic height of the consumer (Jonsson and Ebenman 1998; Tucker and Rogers 2014), and may also predict the strength of trophic interactions, with a positive relationship between PPMR and interaction strength identified for some consumer-resource pairs (Emmerson and Raffaelli 2004; Woodward et al. 2005). Body size is also often related to important life-history traits such as generation time and reproductive rate (Stearns 1983; Janis and Carrano 1991; Gillooly 2000) and is therefore also strongly linked to abundance, which typically declines as size increases (White et al. 2007). This relationship, in combination with the fact that predator body masses are generally one to three orders of magnitude greater than those of their prey (Woodward et al. 2005), often results in a pyramidal structure of declining abundance with increasing trophic level (Cohen et al. 2003; Jacquet et al. 2020). Further traits such as taxonomy, prey type, habitat type, and motility can also be used to infer interactions (Morales-Castilla et al. 2015; Laigle et al. 2017; Brose et al. 2019), and phylogeny, feeding habitat and feeding method have been found to explain food web structure in various marine communities (Rezende et al. 2009; Jacob et al. 2011; Cirtwill and Eklöf 2018).

As previously discussed, environmental changes are driving extensive reorganisation of marine communities, so abiotic factors can clearly also have a major influence on food web structure. Gradients of seawater temperature, depth, and days of ice cover are associated with significant variation in local food web metrics, and food web complexity (i.e. the number of species and interactions) increases with local habitat heterogeneity (Kortsch et al. 2019).

Similarly, warming may drive declines in the proportion of basal species, and changes in metrics such as connectance and omnivory level (Gibert 2019). Within both terrestrial and aquatic food webs, warming and nutrient enrichment are expected to drive significant changes in producer and consumer activity and biomass, altering the patterns of energy flow within the communities (O'Connor et al. 2009; Sentis et al. 2017; O'Gorman et al. 2017; 2019). The greater metabolic demands associated with warming may drive declines in the body size distribution of many marine communities, through changes in species composition and size at age (Coghlan et al. 2024; Saunders and Tarling 2018). Larger organisms may decline in size more rapidly than smaller organisms, due to reduced surface area to body mass ratios and the associated challenge of maintaining a higher metabolic rate (Forster et al. 2012; Petrik et al. 2020). As a result, warming may drive substantial changes to PPMR and the size structure of communities, with implications for the patterning of interaction strengths and energy flow. Ultimately, changes to the distribution of many marine organisms may result in the gain or loss of species with key traits and disproportionately large influence on food web structure and ecosystem functioning. These changes could disrupt key structural features and might reduce the stability of food webs.

1.4 Food web stability

Several different mechanisms have been found to influence the stability of food webs. One such driver is the pattern and coupling of weak and strong interactions. Interaction strength quantifies the magnitude of the effect that individual species have on one another (Berlow et al. 1999). Food webs are dominated by weak interactions, which provide stability by dampening population oscillations between consumers and their resources (Paine 1992; McCann et al. 1998). As a result, removal of either strong or weak interactors can reduce the temporal stability of ecosystem processes and resistance to changes in community composition (O'Gorman and Emmerson 2009; 2010). In general, highly connected generalist species display weaker net effects than specialist predators, which rely heavily on a small number of food sources (Montoya et al. 2009; O'Gorman and Emmerson 2010; Wootton and Stouffer 2016). Larger body size ratios often lead to greater interaction strengths, therefore the size distribution of the different components of the food web may be an important determinant of system stability (Woodward et al. 2005). The coupling of different energy channels (e.g. from primary production versus detritus) can also enhance the dynamic stability of higher consumers, by generating asynchrony in energy flux (Blanchard et al. 2011). Similarly, larger mobile consumers may also drive food web flexibility and stability

when basal resource availability fluctuates asymmetrically, either spatially or temporally, by coupling multiple distinct sub-food webs (McCann et al. 2005; McCann and Rooney 2009; Mougi 2018).

There has been much focus on the organisation of nodes into 'modules': subgroups of species that interact often with one-another but have few connections to species outside their subgroup. This structuring has been identified in a variety of social and biological networks including food webs (Newman and Girvan 2004; Krause et al. 2003; Rezende et al. 2009; Pérez-Matus et al. 2017; Zhao et al. 2017), although the prevalence of modules in marine food webs has recently been disputed (Marina et al. 2018). Modularity has been found to increase stability in both theoretical and modelled empirical food webs by restricting the propagation of secondary extinctions to the subgroups in which the initial species loss occurs (Teng and McCann 2004; Thébault and Fontaine 2010; Stouffer and Bascompte 2011; Zhao et al. 2017) (Figure 1.3). Stability in this context is generally estimated as robustness using the R50 value, the proportion of species that need to be primarily removed to cause 50% of the food web to become extinct (Jonsson et al. 2015). A value of 0.5 indicates a robust food web, as no secondary extinctions occur (Figure 1.3). The relationship between modularity and robustness to species extinctions is not necessarily clear-cut, however, as the degree to which it promotes network stability may depend on spatial scale, with smaller systems benefiting the most from this structure (Mougi 2018). Few papers have explicitly investigated the mechanisms driving modular structure, but species' traits appear to play an important role. Modules have been characterised using species' niche organisation and diets (Guimera et al. 2010), and may contain separate trophic groups (clusters of species with common prey and predators) (Gauzens et al. 2015). Furthermore, modularity has previously been linked with body size distributions and phylogeny, and further traits such as foraging mode and habitat are also suggested to contribute to this structure (Rezende et al. 2009; Kortsch et al. 2015).

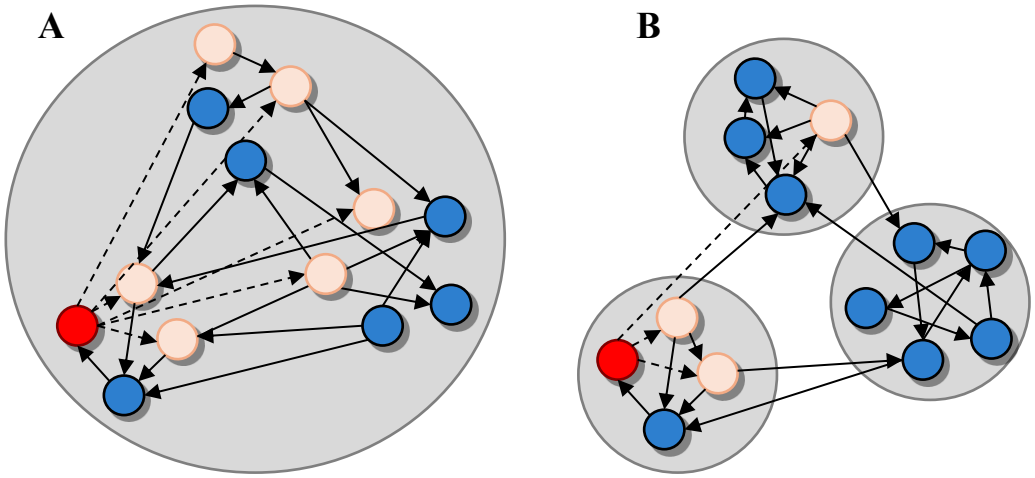

Figure 1.3: The theoretical stabilising effects of modularity. A species extinction (red node) could potentially drive secondary extinctions in species that prey on it directly (pale orange nodes connected by dashed line). **A)** In a non-modular food web, the high inter-connectedness of species means that secondary extinctions are likely to propagate widely throughout the network. **B)** In a modular food web, the low number of links between modules means that secondary extinctions are primarily restricted to the same module as the initial extinction. Results of random extinction analysis confirm that the more modular network, with an R_{50} value of 0.46, exhibits greater robustness than the non-modular food web, which has an R_{50} of 0.31.

1.5 The Southern Ocean

Given the mounting pressures of climate change and human activities, it is imperative that we establish which biotic and abiotic factors drive the structure of different marine food webs, and how this structure relates to their stability. This is particularly true in polar regions, where our understanding of the ecology of many species and the structuring of different food webs is still limited.

The Southern Ocean plays a key role in global oceanic circulation and nutrient distribution, linking the world's major ocean basins (Carter et al. 2008). A major feature is the Antarctic Circumpolar Current (ACC), a wind-driven, eastward-flowing current that surrounds the continent (Carter et al. 2008) (Figure 1.4). The ACC acts as a thermal barrier, maintaining stable low water temperatures in the Southern Ocean, particularly in high-latitude shelf regions where temperatures range from around +2 °C down to -1.9 °C (Weiss et al. 2012; Mintenbeck 2017). As a result, many Antarctic organisms are highly stenothermal (Peck et al. 2014). A further major physical feature of the Southern Ocean is sea ice. The Southern Ocean

can be split into broad zones based on their differing sea ice dynamics and coverage (Deppeler and Davidson 2017). At high latitudes, sea ice coverage is nearly complete and persists throughout the year, while areas further north experience seasonal fluctuations between winter maxima and summer minima (Convey et al. 2009; Deppeler and Davidson 2017) (Figure 1.4). Further north still, the open ocean zone remains almost completely ice-free throughout the year (Deppeler and Davidson 2017). Sea ice plays an important role in structuring the water column and driving the formation of water masses (Cherkasheva et al. 2014). It also acts to limit the penetration of light into surface waters, which, in conjunction with the strong seasonal variation in light conditions, means that light availability is a major factor affecting Southern Ocean ecosystems (Park et al. 2017).

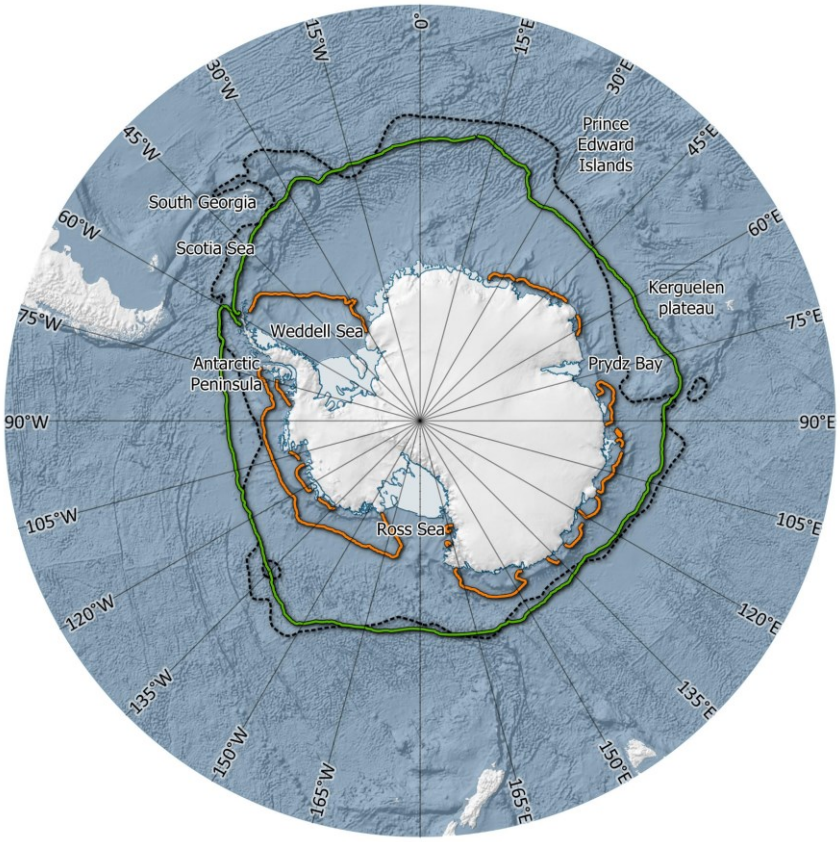

Figure 1.4: The Southern Ocean and Antarctic continent. Solid orange and green lines indicate the median February minimum and September maximum sea ice extent 1981-2010, respectively. Dashed black line represents the general position of the Southern Antarctic Circumpolar Current front. All map layers obtained from Quantarctica 3.0 (Matsuoka et al. 2021) and displayed in Antarctic Stereographic projection. Text labels identify locations of particular relevance to this thesis.

Southern Ocean food webs have traditionally been viewed as relatively simple and centered primarily around the Antarctic krill (*Euphausiia superba*). This species is highly abundant in regions such as the south-west Atlantic Ocean, and acts as prey for many species including baleen whales, penguins, seals, squid and fish (Trathan and Hill 2016). Other zooplankton are also important components of regional Southern Ocean ecosystems, such as the smaller ice krill (*Euphausia crystallorophias*) which is abundant in the permanent ice zone (Thomas and Green 1988), hyperiid amphipods such as *Themisto gaudichaudii,* and the many copepod species which can represent over 45% of pelagic filter-feeder biomass in some areas (Voronina 1998; Kouwenberg et al. 2014). While some top predators may feed directly on the zooplankton component, squid and fishes make up another major link in energy flow within the Southern Ocean ecosystem. The Southern Ocean fish community has relatively low diversity, with only 322 recognised species relative to the ~28,000 fish species known globally, but their contribution to the Antarctic marine ecosystem is substantial (Eastman 2004). Most species are demersal, found on and around the continental shelves, and display a variety of different feeding strategies and diets ranging from purely planktivorous to omnivorous and in some cases primarily piscivorous (Casaux and Barrera-Oro 2013; Bansode et al. 2014). Mesopelagic lanternfish (family Myctophidae) are also a key component of Southern Ocean food webs, with a biomass of potentially over 200 million tonnes, and may represent a key krill-independent pathway of energy flow to higher trophic levels (Saunders et al. 2018; 2019; McCormack et al. 2020). Clearly, while it is true that Antarctic krill are a central component of many ecosystems, the complexity of Southern Ocean food webs has been underestimated. If we wish to assess the impacts of environmental and anthropogenic change on these ecosystems, it is important that we gain a better understanding of their structure and dynamics.

The popular view of Antarctica and its surrounding waters is often that of a pristine, undisturbed landscape. In fact, the Southern Ocean has been subject to significant human activities. Exploitation of Antarctic fur seals and Southern elephant seals during the early 19th century resulted in the near extinction of their populations on sub-Antarctic islands like South Georgia, although their populations have subsequently grown rapidly (Miller 1991; Hucke-Gaete et al. 2004). The early 20th century then marked the beginning of the commercial exploitation of whales within the Southern Ocean, which drove severe declines in their abundance (Miller 1991). Some whale species have recently shown evidence of recovery (Zerbini et al. 2019; Calderan et al. 2020), but populations of others have displayed

much slower recovery rates and are still at only a fraction of their pre-exploitation numbers (Crespo et al. 2019; Tulloch et al. 2019). The major declines in the abundance of these top predator species are likely to have had significant effects on the wider regional food webs by altering levels of top-down regulation and potentially reducing the competitive pressure on other predator species. The ongoing recovery of many whale species may therefore represent further changes in energy flow within Southern Ocean ecosystems, as their predatory and competitive influence is restored. Exploitation in the Southern Ocean has since shifted to focus on finfish such as toothfish (*Dissostichus mawsoni* and *D. eleginoides*) and mackerel icefish (*Champsocephalus gunnari*), in addition to a large krill fishery which operates primarily in the South Atlantic (Kock et al. 2007). These fisheries are managed by the Commission for the Conservation of Antarctic Marine Living Resources (CCAMLR), which practices an ecosystem approach to management involving regular monitoring of target and non-target species and abiotic conditions to minimise human impacts on ecological relationships and conserve Antarctic species and ecosystem functioning (Kock et al. 2007). Despite this careful approach, these fisheries still represent an important additional pressure on Antarctic marine ecosystems, and their potential future expansion may have significant implications for the functioning of Southern Ocean food webs, particularly when viewed in combination with the effects of climate change.

It is becoming increasingly clear that the Antarctic is vulnerable to the effects of climate change. The Southern Ocean has displayed regional variation in temperature trends, with some areas remaining stable or cooling while others, such as the western Antarctic Peninsula and Scotia Sea, have warmed significantly (Meredith and King 2005; Whitehouse et al. 2008). Similarly, there has been regional variation in sea ice trends, with rapid declines in sea ice extent and concentration in some areas and increases in others (Parkinson 2019). These changes have serious implications for regional ecosystems. Changes to the timing and extent of seasonal sea ice expansion and contraction, and strengthened water column stratification following ice melt, could alter the timing and magnitude of primary production, potentially reducing the amount of food available for consumers (Quetin et al. 2007). Reductions in the availability of sea ice could also directly impact the populations of key mid-trophic species such as Antarctic krill and the Antarctic silverfish, *Pleuragramma antarcticum*, as they use this substrate for refuge and spawning (Massom and Stammerjohn 2010; La Mesa and Eastman 2011). Temperature rises and sea ice declines have already driven a southward contraction in the distribution of Antarctic krill, while fish species such as the Antarctic

toothfish are also expected to exhibit range shifts in the future (Cheung et al. 2008; Kawaguchi et al. 2024). Ocean warming is also expected to drive range shifts in the benthos due to the thermal sensitivity of many benthic species (Barnes et al. 2009). Temperature-driven shifts in body size could alter the structure of communities, while changes in the dominance of certain mid-trophic species (e.g. krill versus the tunicate *Salpa thompsoni*) might reduce the efficiency of energy flow to higher trophic levels (Pauli et al. 2021; Pietzsch et al. 2023). Warming and reductions in sea ice cover could also facilitate the influx and successful establishment of invasive species, which will lead to changes in community composition and novel interactions (Morley et al. 2020; Queirós et al. 2024).

If we are to manage Southern Ocean ecosystems effectively in the face of the varied anthropogenic and environmental threats discussed above, then we must improve our understanding of the drivers of food web structure and their likely responses to change. Much previous research on Southern Ocean ecosystems has involved species-specific models of habitat-use or population dynamics, and simple trophic models (see McCormack et al. 2021a, and references therein). Various ecological network modelling studies have also been conducted to investigate the structure and dynamics of regional food webs. To date, food web models have been developed for various Southern Ocean regions (e.g. Ballerini et al. 2014; Hill et al. 2012; López-López et al. 2021; Jacob et al. 2011; Pinkerton and Bradford-Grieve 2014; McCormack et al. 2020, amongst others). Such models have provided insights into regional food webs, including the major energy pathways (McCormack et al. 2020; McCormack et al. 2021b), the importance of environmental variables for structuring networks (López-López et al. 2021; Rossi et al. 2019), and the association between species' functional traits and network structure (Jacob et al. 2011). Researchers have also modelled the possible ecosystem responses to scenarios of climate change and anthropogenic activities including the historic exploitation of baleen whales (Surma et al. 2014) and future changes in primary production (Ballerini et al. 2014), declines in the biomass of Antarctic krill (Hill et al. 2012), and increased exploitation of Antarctic toothfish (Pinkerton and Bradford-Grieve 2014).

There remain a variety of knowledge gaps surrounding the structure of Southern Ocean food webs and their likely responses to future change. In particular, there is still a poor understanding of the role that body size, mobility, feeding-mode and other morphological and behavioural traits play in driving the structure of Southern Ocean food webs. Additionally, identifying the presence and distribution of stabilising features such as modularity, and

546 determining their underlying drivers, will bring our knowledge of Southern Ocean food webs
547 more in line with wider food web theory and improve our understanding of how robust they
548 are to perturbations. There is also a need to investigate what the consequences of changes in
549 environmental and ecological conditions will be for ecosystem structure. Comparisons of
550 regional food webs are still largely lacking and would provide us with a clearer understanding
551 of the resilience of different Southern Ocean ecosystems to the above changes, which would
552 improve our ability to implement suitable management and conservation measures.

553 *1.6 Thesis outline*

554 This thesis combines a number of approaches from theoretical and empirical ecology and
555 ecosystem modelling at a variety of spatial scales to provide insight into the structure of
556 Southern Ocean food webs and their possible responses to environmental and ecological
557 change. The component data chapters can be split into two main themes, encompassing the
558 relationships between functional traits and trophic structure and the impacts of changing
559 ecological and environmental conditions on communities and ecosystems, although these
560 themes overlap for some chapters, as visualised in Figure 1.5.

561 **Chapter 2** focusses on the demersal fish community around South Georgia, using stomach
562 content analysis and morphological measurements to identify how simple morphological
563 traits map onto broad feeding guilds. This is a novel approach within Southern Ocean food
564 webs which provides a baseline understanding of how morphological traits underlie the
565 ecology of demersal fish and highlights the role that krill may play in bridging ecological
566 niches imposed by morphology.

567 **Chapter 3** expands upon the trait-based approach, applying it to a comparison of four highly
568 taxonomically resolved food webs across the Southern Ocean and northern hemisphere to
569 determine how functional traits (both morphological and behavioural) underlie the
570 distribution of modules. Traits such as body size, foraging habitat, feeding mode and mobility
571 are found to be good predictors of module membership. Differences in the relative
572 importance of traits, and in the structuring of modules across trophic levels, are postulated to
573 be tied to the degree of habitat heterogeneity between systems.

574 **Chapter 4** then focuses on how warming alters body size relationships in the myctophid
575 community of the Scotia Sea, using an extensive dataset of myctophid stomach contents and
576 environmental zooplankton samples. A clear decline in predator-prey mass ratio (PPMR) with
577 warming is driven by shifts in the size distribution of both the myctophids and their prey. This

provides insight into the possible implications of environmental change for the size structure and distribution of interaction strengths within Southern Ocean food webs.

Chapter 5 explores the possible ecological consequences of the recovery of Southern Ocean baleen whale populations and implications for management. This makes use of a suite of published regional Ecopath models, which were then standardised and subject to a custom balancing algorithm to generate ensembles of plausible alternative models. Clear trade-offs between whale recovery and the biomass of key competitors are identified, and the potential structural features and environmental factors which could mitigate these are discussed.

Chapter 6 provides a synthesis of the insights gained in the previous chapters and puts them into context of the wider state of knowledge regarding contemporary and future Southern Ocean food webs.

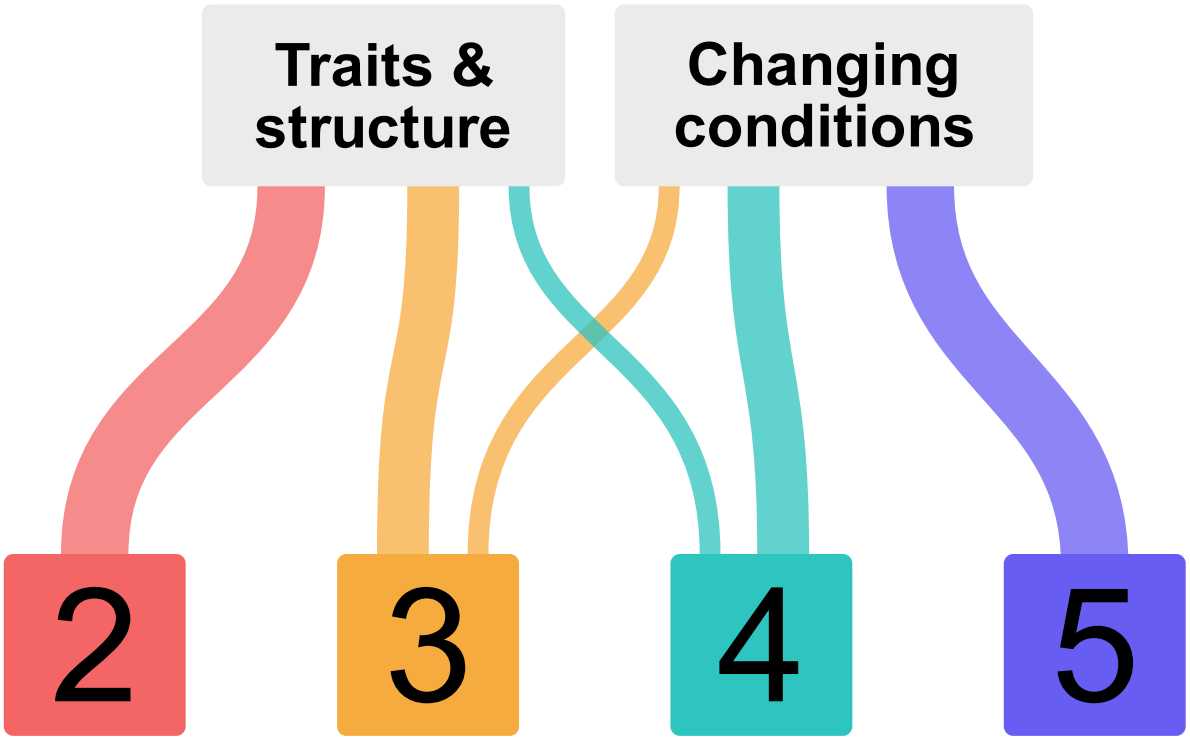

Figure 1.5: Conceptual diagram displaying the main linkages between the primary themes of this thesis and each of the four data chapters. The thickness of the links indicates the extent to which the chapters fall within each theme.

2 Morphological traits distinguish feeding guilds in a Southern Ocean fish community

Submitted to *Functional Ecology*

Abstract

Morphological traits reflect an organism's ecological niche and role within ecosystems, thus improving our understanding of the drivers of community structure. Here, we combined morphological measurements with stomach contents analysis of nine demersal fish species from the subantarctic island of South Georgia, where climate change has already affected the distribution of a key prey species, Antarctic krill. Although most species include krill in their diets, cluster analysis identified five distinct feeding guilds, with traits such as gape size proving especially useful for determining guild membership. Individuals feeding primarily on fish had larger gapes and higher caudal and pectoral fin aspect ratios, enhancing their ability to capture and consume such large, fast prey. In contrast, benthic feeders had smaller gapes and lower fin aspect ratios, reflecting their reliance on suction feeding and higher manoeuvrability. Continued research into the relationship between morphology and diet will improve understanding of the drivers of trophic dynamics in marine ecosystems and aid our ability to predict the effects of environmental change on community composition and structure.

2.1 Introduction

The field of ecology is increasingly focusing on how complex interactions between individuals shape the structure and functioning of ecosystems (Åkesson et al. 2021). A key component of this approach is the consideration of how functional traits including physiological, morphological, behavioural and life history attributes shape how organisms respond to each other and to their environment (Violle et al. 2007). This trait-based approach to ecology seeks to identify how the functional traits of organisms combine to determine their interactions and thus drive the organisation of ecological communities. By describing the distribution of traits within ecosystems, it is possible to generalize the mechanisms underlying complex ecological processes and predict the resilience of key ecosystem functions to perturbations (Kiørboe et al. 2018).

Ecomorphology is a key component of trait-based ecology, whereby an individual's body form is linked to its behaviour and interactions with others (Barr 2018). An organism's

624 physical features represent adaptation to its environment, and therefore the combination of
625 different morphological traits largely underlie its ecological niche. As such, morphological
626 traits may be strongly tied to the distribution and functional role of organisms within
627 ecosystems, e.g. wing shape and beak dimensions strongly predict diet and foraging niche in
628 birds (Pigot et al. 2016); eye size is linked to adult habitat and activity level in amphibians
629 (Thomas et al. 2020); whilst diet and habitat preferences are driven by traits including body
630 size, eye position and head shape in ants (Gibb et al. 2015).

631 Marine ecosystems are often strongly size structured due to gape limitations and the interplay
632 between body size and feeding (Jennings et al. 2001; Potapov et al. 2019). In fish, gape size
633 often reflects feeding mode, with ambush piscivores generally exhibiting large gapes while
634 suction feeding planktivores tend to have small gapes (Luiz et al. 2019). Gape size also often
635 constrains the maximum size of prey that can be consumed, thus determining the structure of
636 feeding relationships (Christensen 1996). Allometric scaling relationships have been
637 identified for tropical and temperate fish species, whereby gape size, and thus also average
638 and maximum prey size, generally increase with predator body size (Bachiller and Irigoien
639 2013; Dunic and Baum 2017). In many species maximum prey size increases more rapidly
640 than minimum prey size as fish become larger, resulting in a widening of their trophic niche
641 (Scharf et al. 2000). Differences in allometric relationships for body size and gape
642 morphology could also influence levels of resource partitioning and competitive interactions
643 within the fish community (Schuckel et al. 2012; Barnes et al. 2021). Other traits may also be
644 important, such as fin morphology which is linked to habitat use and prey acquisition: e.g.
645 high aspect ratios of the caudal and pectoral fins are linked with greater swimming efficiency
646 and maximum speed (Higham 2007; Sambilay 1990) and generally found in more active
647 species that feed on pelagic or mobile prey such as zooplankton and fish (Bridge et al. 2016;
648 Hobson 1979). Lower aspect ratios provide greater manoeuvrability and thrust at low speeds
649 and may therefore be better suited to less active benthic or ambush feeding (Higham 2007;
650 Bridge et al. 2016).

651 While an increasing number of marine studies use trait-based approaches, these often involve
652 competition models focused primarily on basal groups and overlook trophic interactions
653 between predators and their prey (Kiørboe et al. 2018). There is therefore a need to further
654 describe the traits driving trophic relationships, particularly in remote and understudied
655 marine ecosystems. Here we describe the relationships between morphology and diet for nine
656 of the most abundant demersal fish species around the sub-Antarctic island of South Georgia

in the Atlantic sector of the Southern Ocean. Previous research on the diet and biology of these species has revealed a system largely dominated by consumption of Antarctic krill, *Euphausia superba*, in addition to fish and macrozooplankton such as amphipods, particularly in periods of low krill availability (Kock et al. 2012). There is some evidence of interspecies dietary differentiation (McKenna 1991; Targett 1981), but to date there has been no comprehensive investigation of the links between morphological traits and dietary niches across the wider groundfish community. Such information will improve our understanding of the mechanisms underlying community structure and energy flow through this component of demersal food webs. Many marine species at South Georgia are at the northern edge of their distributions and may therefore be vulnerable to ocean warming, which has been particularly rapid in this region (Whitehouse et al. 2008). A southward range contraction by *E. superba* has already been observed (Kawaguchi et al. 2024) and changes in the dynamics and distribution of other zooplankton groups might also be expected (Whitehouse et al. 2008), ultimately driving significant changes in community composition and associated feeding interactions. Identifying how morphological traits influence prey selection will provide insight into the possible consequences of such shifts in prey availability for community structure. The general relationships between feeding ecology and morphology identified here will also be broadly applicable to other regions, furthering our ability to generalize the drivers of marine ecosystem assembly.

We hypothesise that dietary differences between and within species are explained by differences in their functional traits. We expect that predators with larger gape sizes and higher fin aspect ratios primarily consume fish and krill due to their ability to capture and consume such larger, mobile prey, while those feeding on smaller, less mobile prey such as benthic invertebrates or amphipods display smaller gape sizes and lower fin aspect ratios to provide the necessary manoeuvrability for benthic foraging.

2.2 Materials and methods:

2.2.1 Sample collection:

Sampling of the groundfish community was conducted from the FV *Robin M Lee* over the South Georgia and Shag Rocks shelves between the 1st and 10th of February 2023 as part of the biennial groundfish survey conducted by the British Antarctic Survey and the Government of South Georgia and the South Sandwich Islands. The survey utilises a random stratified design across five shelf areas and two depth strata (100-200m and 200-350m). A

total of 47 bottom trawls were completed using an FP-120 net (Caedmon Nets, UK; Figure 2.1). See Hollyman et al. (2023) for further details on sampling methodology. For this study, nine fish species were sampled: icefish (*Champsocephalus gunnari*, *Chaenocephalus aceratus*, and *Pseudochaenichthys georgianus*); rockcods (*Notothenia rossii*, *Trematomus hansoni, Lepidonotothen squamifrons*, *L. larseni*, and *Gobionotothen gibberifrons*); and dragonfish (*Parachaenichthys georgianus)*. Fish were opportunistically sampled from catches, with efforts made to choose specimens representing a range of body lengths for each species. Selected individuals were frozen at -20°C for later analysis at King Edward Point research station, South Georgia.

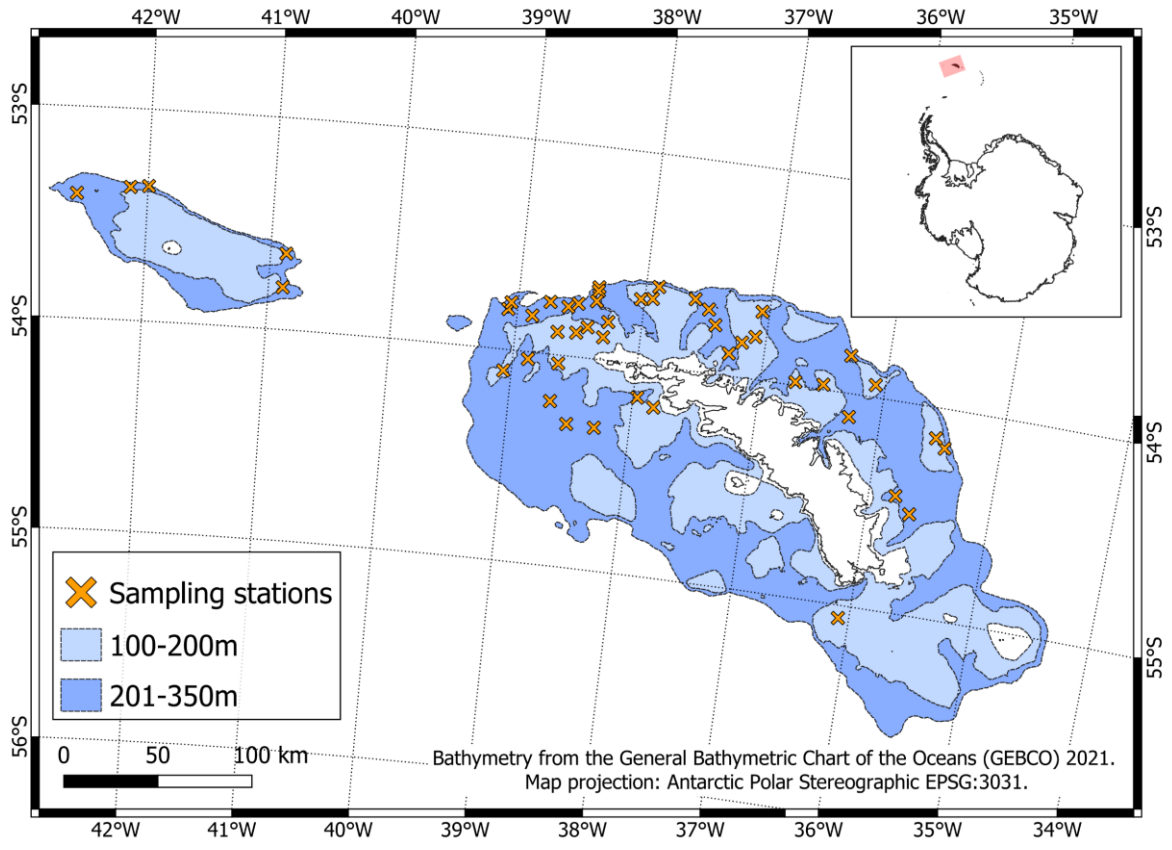

Figure 2.1: Distribution of haul locations, identifying the two depth zones sampled. Inset map displays the sampling region (red rectangle) in the context of the wider Antarctic continent. Map generated in QGIS 3.28.0-Firenze.

2.2.2 Morphological measurements and stomach contents dissection:

In the laboratory, each fish was thawed before being weighed using either a small (Kern, PCB1000-2, +/- 0.01 g) or large (M3, WPL industries, +/- 1 g) top-loading scale depending on the size of the fish. For large fish (>400 mm total length, *TL*), measurements of *TL* were

recorded using a fish board and dissecting ruler. All other specimens were photographed using a Sony RX100i digital camera mounted on a copy stand (Kaiser R2N), with length later measured in ImageJ software (Schneider et al. 2012). Gape measurements to the nearest mm were taken for each specimen using Vernier callipers for maximum vertical gape (G_{height}) and a dissecting ruler for maximum horizontal gape (G_{width}). The gape height and width of each fish were then combined to estimate the maximum oral gape area (G_{area}) using the following equation (Ward-Campbell et al. 2005):

$$G_{area} = \pi(0.5G_{height} * 0.5G_{width})$$

Photographs were also taken of each specimen's caudal and pectoral fins, with the latter excised at the fin base and laid flat. The aspect ratio (*AR*) of each fish's caudal and pectoral fins was estimated using the following equation:

$$AR = \frac{h^2}{a}$$

where *a* is the fin area (in mm) and *h* is either the caudal fin height or length of the leading edge of the pectoral fin, measured in ImageJ (Pauly 1989).

Each fish stomach was dissected, and non-empty stomachs were weighed to the nearest 0.01 g. Stomach contents were grouped according to the lowest identifiable taxonomic level, weighed, and counted, excluding fish prey displaying no evidence of digestion (likely to be the result of net feeding). Where stomachs contained many individuals of a prey group, 30 individuals were subsampled and weighed, and the total number of individuals in the stomach was estimated.

To investigate potential ontogenetic shifts in diet, each individual fish was assigned to a size class, estimated by splitting the range of sampled *TL* across the community into four size bins of 176 mm. These were numbered 1 to 4 in ascending size order. This split, whilst arbitrary, provided the best balance of sample sizes across size classes for most species. We defined size classes at the community level rather than at the species level to ensure that size classes were comparable across species. The relative importance of each prey group in the diet of each species-size class combination was estimated from three separate measures of importance using the % Index of Relative Importance (%IRI), calculated as:

$$\%IRI_i = \frac{(\%N_i + \%W_i) * \%FO_i}{\sum_{i=1}^{n}(\%N_i + \%W_i) * \%FO_i} * 100$$

Where *%FO* is the percentage frequency of occurrence, *%N* is the proportional abundance and *%W* is the proportional weight of each prey group in the diets of each species-size class (Pinkas et al. 1970). We set a minimum sample size of five non-empty stomachs, resulting in the exclusion of the largest and smallest size classes of *Parachaenichthys georgianus* and *Chaenocephalus aceratus*, respectively (n = 2 in both cases).

2.2.3 Identification of feeding guilds

All analyses were conducted using R statistical software version 4.3.0 (R Core Team 2023; see Table A1 for an overview of the various packages used). Species-size classes were grouped into feeding guilds with hierarchical cluster analysis, using Bray-Curtis dissimilarities calculated from the prey %IRI values. Prey were grouped into eight broad taxonomic groups: 1) krill (all members of the Euphausiidae); 2) *Themisto gaudichaudii* (an abundant swarming amphipod); 3) other non-swarming amphipods (primarily *Vibilia sp.*, *Primno macropa*, and individuals of superfamily Lysianassoidea); 4) isopods; 5) fish; 6) mysids; 7) benthic decapods (*Notocrangon sp.* and *Chorismus sp.*); 8) miscellaneous benthos (including polychaetes, annelids, bivalves, gastropods, and echinoderms which were sporadically found in stomachs). Differences between assigned feeding guilds were identified using the similarity percentage routine (SIMPER).

2.2.4 Predator-prey size relationships

We explored the relationship between predator mass and average prey mass using a linear mixed effects model. This model included the count-weighted average prey body mass ($\log_{10}$ g) of each prey type within each stomach as a response, and predator body mass ($\log_{10}$ g) and feeding guild plus their interaction as predictors, to identify predator-prey size relationships specific to different dietary groups. Prey type was included as a random effect to account for potential differences in size relationships across prey taxa, and different covariate weighting structures were investigated to account for any systematic variance in the residuals (e.g. exponential, fixed, constant). Model selection by BIC comparison was used to identify the best random effects, variance weighting, and fixed effects structures (in that order).

2.2.5 Morphological trait distributions

We first explored inter- and intra-specific trait variation, to provide context for later trait analyses. This included nonparametric Kruskal-Wallis analysis of variance (due to non-normality of residuals), and pairwise comparisons of trait distributions from the post-hoc

766 Dunn's test with Bonferroni correction. We also plotted trait-body size relationships to
767 describe ontogenetic trends across species.

768 To identify relationships between morphological traits and feeding guild membership, the
769 distribution of trait values (gape area, caudal fin *AR*, and pectoral fin *AR*) across individuals
770 within each feeding guild were again compared using Kruskal-Wallis analysis of variance and
771 Dunn's test. We also used a principal components analysis (PCA) based on Euclidian
772 distances for gape area and caudal and pectoral fin *AR*, to explore the distribution of feeding
773 guilds in multi-dimensional trait space. To minimise the influence of individual body size on
774 the ordination, we standardised each measurement to the *TL* of the individual using the
775 following equation:

776 $$Y_i^* = Y_i \left| \frac{TL_0}{TL_i} \right|^b$$

777 Where Y_i^* is the standardized predicted value of trait *Y* for individual *i*, Y_i is the measured
778 value of the trait for individual *i*, TL_i is the measured *TL* of individual *i*, TL_0 is the mean *TL*
779 for all individuals and the parameter *b* is the slope from an ordinary least-squares (OLS)
780 regression of log-transformed *Y* and *TL* (Lleonart et al. 2000). This standardization effectively
781 adjusts the trait measurements to values they would have if the individuals were of the
782 average body size for the sampled population (Lleonart et al. 2000). We conducted this
783 standardisation for all individuals of the same species that were assigned to the same feeding
784 guild, to reduce allometric effects while still reflecting situations where different size classes
785 of a given species were assigned to separate guilds.

786 We then implemented a random forest (RF) model to assess whether feeding guild
787 membership could be predicted from the standardised morphological traits. RF modelling is a
788 classification tool that uses bootstraps for the prediction of group membership and provides
789 an indication of the relative importance of predictor variables for partitioning individuals into
790 clusters (Cutler et al. 2007). We implemented a cross-validation approach by randomly sub-
791 sampling 70% of the data to calibrate the model and then using the remaining 30% for
792 prediction. This was repeated 100 times to investigate the variability around classification
793 accuracy and relative importance of each trait. We assessed the predictive ability of the RF
794 model through the True Skill Statistic (TSS), with values of 1 and 0 indicating perfect and
795 completely random predictions, respectively (Allouche et al. 2006).

2.3 Results

A total of 893 individuals were sampled for this study (Table 2.1). In most species, stomach contents were present for the majority of individuals, although for Scotia Sea icefish (*Chaenocephalus aceratus*) only 25% of stomachs were non-empty (Table 2.1).

Table 2.1: Species sampled in this study, including Food and Agriculture Organization 3-alpha taxonomic identification code for each species, number of individuals sampled, range of total lengths (TL mm) of individuals sampled, and the number of non-empty stomachs. The number of stomachs by size group is shown in Figure 2.2.

Species	Common name	Code	*N* fish	*TL* range (mm)	*N* stomachs
Family Channichthyidae (icefish)					
Champsocephalus gunnari	Mackerel icefish	ANI	135	154-573	88
Chaenocephalus aceratus	Scotia Sea icefish	SSI	119	164-622	30
Pseudochaenichthys georgianus	South Georgia icefish	SGI	117	187-523	75
Family Nototheniidae (rockcod)					
Notothenia rossii	Marbled rockcod	NOR	75	336-795	66
Trematomus hansoni	Striped rockcod	TRH	69	169-383	61
Lepidonotothen squamifrons	Grey rockcod	NOS	101	100-462	86
Lepidonotothen larseni	Painted notie	NOL	81	93-216	67
Gobionotothen gibberifrons	Humped rockcod	NOG	104	150-572	95
Family Bathydraconidae (dragonfish)					
Parachaenichthys georgianus	South Georgia dragonfish	PGE	92	123-434	58

2.3.1 Species trait relationships

The sampled fish displayed various interspecific differences in their traits. The icefish *P. georgianus* and *C. aceratus* and rockcod *N. rossii* had the largest gapes, while the remaining rockcods, particularly *L. larseni*, had the smallest gapes (Figure A1a). The intercepts of the species-specific gape-size relationships showed a similar rank order (with the icefish *P. georgianus* highest and *G. gibberifrons* and *L. larseni* lowest) with consistent slopes across species (Figure A1b). *C. gunnari* and *C. aceratus* displayed the highest caudal *AR*s and *N. rossii* and the icefish *P. georgianus* exhibited the highest pectoral *AR*s, while the dragonfish *P. georgianus* had the lowest caudal and pectoral *AR*s (Figure A1c,e). The relationships between fin *AR* and body size varied considerably between species (Figure A1d,f).

2.3.2 Feeding guilds

The cluster analysis identified five feeding guilds at a dissimilarity level of 50% (Figure 2.2; see A2 for pairwise similarities for each guild): (i) 'krill feeders' included all size classes of the icefish *C. gunnari* and *P. georgianus,* and the rockcod *L. larseni* (which was only represented by the smallest size class); (ii) 'benthos feeders' consumed miscellaneous benthos and isopods, and represented all size classes of *G. gibberifrons*; (iii) '*Themisto* and krill feeders' contained all size classes of *T. hansoni,* in addition to the smallest *L. squamifrons* and size class 2 *C. aceratus*, though fish were also important in their diet; (iv) 'fish feeders' contained the larger *C. aceratus* and *L. squamifrons,* and all *N. rossii*; and (v) 'benthic shrimp feeders', represented by the dragonfish *P. georgianus*, which fed primarily on mysids and the decapods *Notocrangon sp.* and *Chorismus sp.*

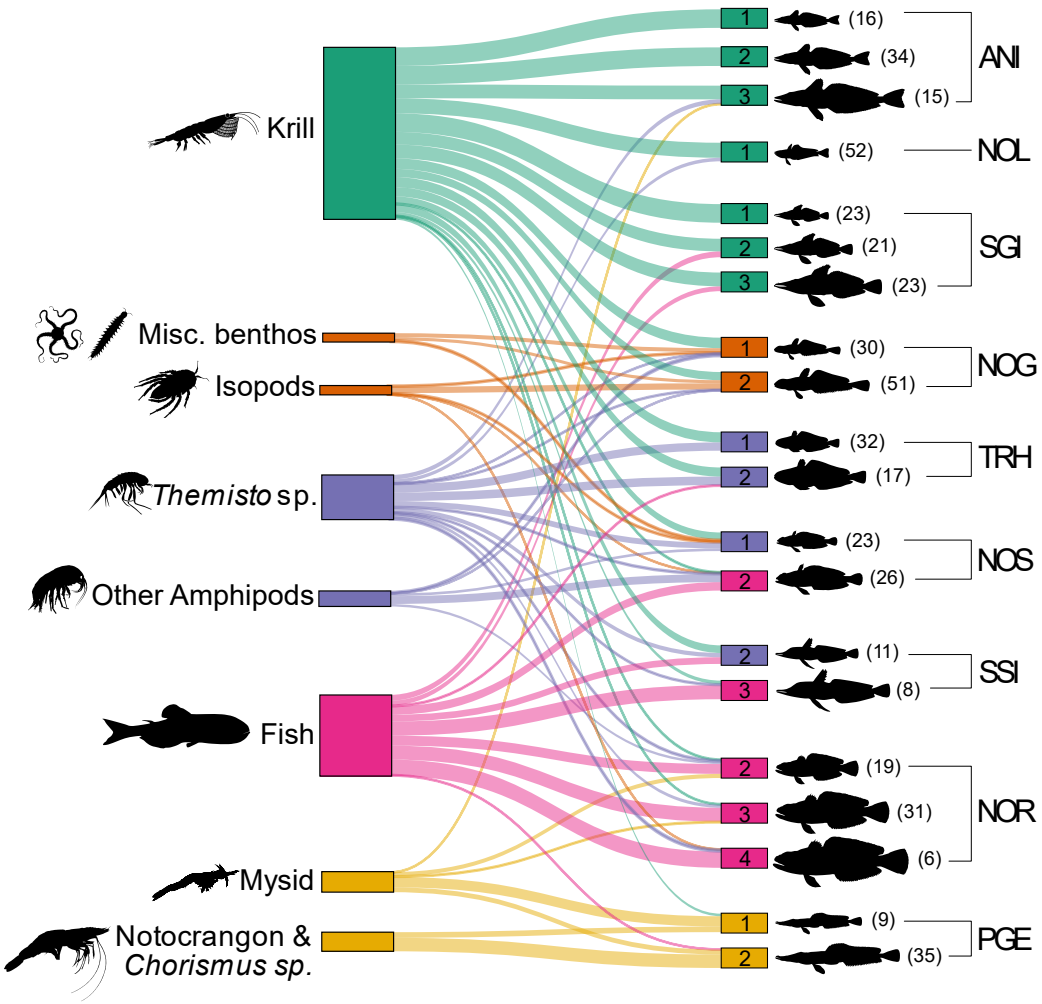

829

830 Figure 2.2: Sankey diagram depicting the trophic interactions between prey groups (left) and
831 predators (right). Link thickness is proportional to the %IRI (links representing <1% are
832 omitted for clarity). Node colours represent the feeding guilds determined by cluster analysis
833 (green = 'krill feeders', orange = 'benthos feeders', purple = '*Themisto* and krill feeders',
834 pink = 'fish feeders', yellow = 'benthic shrimp feeders'). Numbers within predator boxes
835 indicate the size class (also represented by silhouette size), and numbers in brackets indicate
836 sample size (number of non-empty stomachs). See Table 2.1 for a key to species codes.

837 The final selected linear mixed effects model of prey mass as a function of predator mass
838 included a random intercept for prey type (reflecting different average body sizes for prey
839 taxa), and a combination of fixed variance weighting structure for predator body mass and
840 constant variance weighting structure for prey type (Table A3). The fixed effect structure
841 included predator body mass and feeding guild as additive predictors, with no significant
842 interaction identified (Table A4). Overall, the linear mixed effects model identified a
843 significant increase in prey size with predator size, with a consistent slope but different

intercepts of the relationship across feeding guilds ($F_{6,599} = 134.80$, $p < 0.001$; Figure 2.3; Table A5).

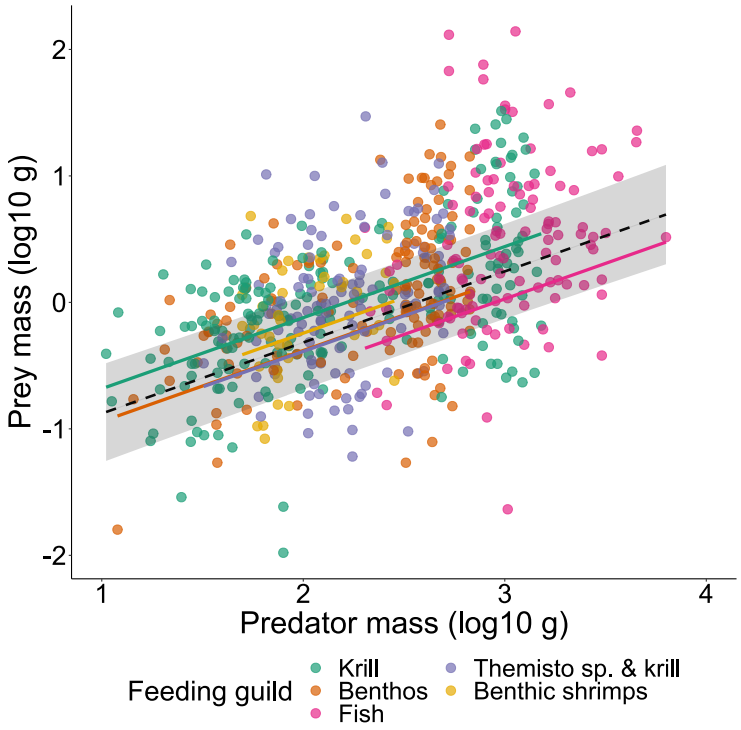

Figure 2.3: Partial residuals plot from a linear mixed effects model of the relationship between predator body mass and count-weighted average prey mass consumed across feeding guilds. Each point represents one predator. Dashed line represents the overall model fit, with shading representing 95% confidence intervals. Solid lines represent fits for each feeding guild. Model coefficients are provided in Table A5.

2.3.3 Distinguishing feeding guilds with functional traits

Significant differences in trait values between feeding guilds were observed for all traits (Figure 2.4; Table A6-A7). 'Fish feeders' had the largest gape areas, while 'krill feeders' and 'benthic shrimp feeders' generally had intermediate gape areas, with 'benthos feeders' and '*Themisto* and krill feeders' having the smallest gape areas (Figure 2.4a). There were only small differences in caudal fin AR across guilds, with the largest values observed in the 'fish feeders' and 'krill feeders' and the smallest observed in the 'benthic shrimp feeders' (Figure 2.4b). Similarly, the 'fish feeders' had the highest pectoral fin ARs while the 'benthic shrimp feeders' had significantly lower values compared to other groups (Figure 2.4c). These differences between feeding guilds were captured in multi-dimensional space by the PCA of length-standardised fish traits, which consisted of three dimensions with Dim1 and Dim2 together explaining 86% of the variance (Table A8). Gape area and pectoral fin *AR* were most

strongly related to Dim1 (r = 0.62 and r = 0.59, respectively), while caudal fin *AR* was strongly correlated with Dim2 (r = 0.84; Figure 2.5a; Table A9). The PCA indicated substantial overlap in the trait space for each feeding guild, with the primary differentiation of the feeding guilds being between the 'fish feeders', which generally had positive Dim1 scores, and the 'benthic shrimp feeders', '*Themisto* and krill feeders', and 'benthos feeders' which generally had negative Dim1 scores and overlapped considerably with one another (Figure 2.5a). Additionally, 'benthic shrimp feeders' were separated from the '*Themisto* and krill feeders' guild along Dim2 (Figure 2.5a). The 'krill feeders' were the least differentiated by the traits, with individuals spread across most of the trait space (Figure 2.5a).

Despite the high levels of overlap in trait space for some feeding guilds, the Random Forest model could predict feeding guild membership from the length-standardised traits relatively well, with an average TSS score of 0.77 ± 0.12 over 100 cross-validation runs. The most important trait for predicting guild membership was gape area (84% relative importance), followed by caudal and pectoral fin *AR* (both 8% relative importance; Figure 2.5b).

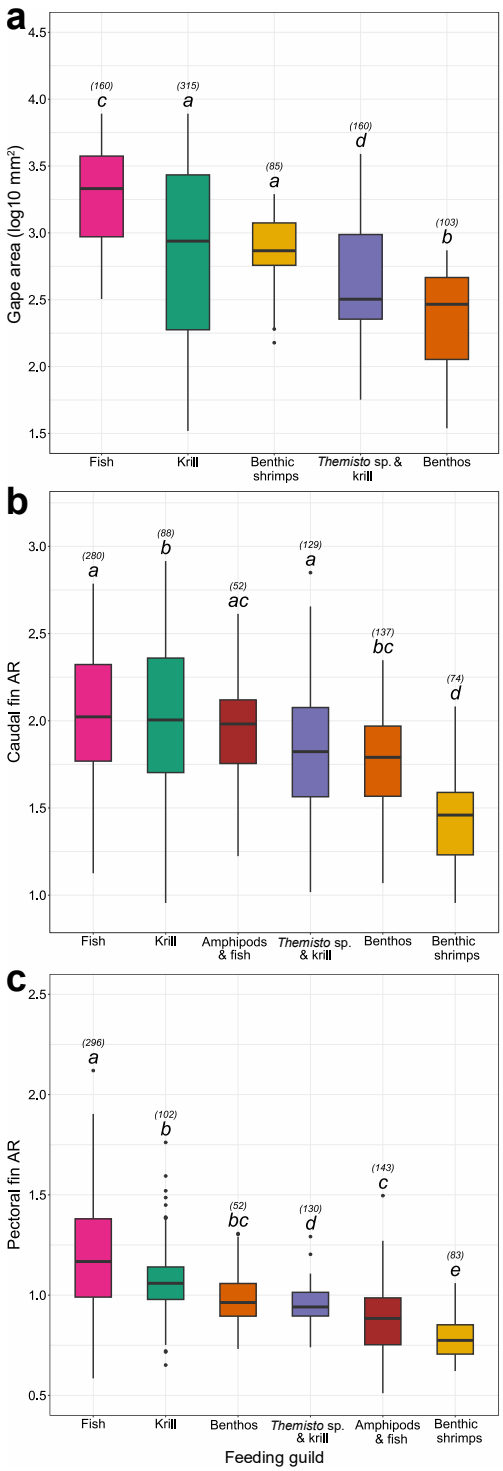

Figure 2.4: Boxplots displaying the distribution of absolute traits for each feeding guild: (a) gape area; (b) caudal fin aspect ratio (*AR*); (c) pectoral fin *AR*. Numbers in brackets represent sample sizes, letters indicate groupings assigned by a Dunn's test with Bonferroni correction (groups with a letter in common are not significantly different). Boxplots are organized in decreasing order of median trait value. Note the log scale in panel (a).

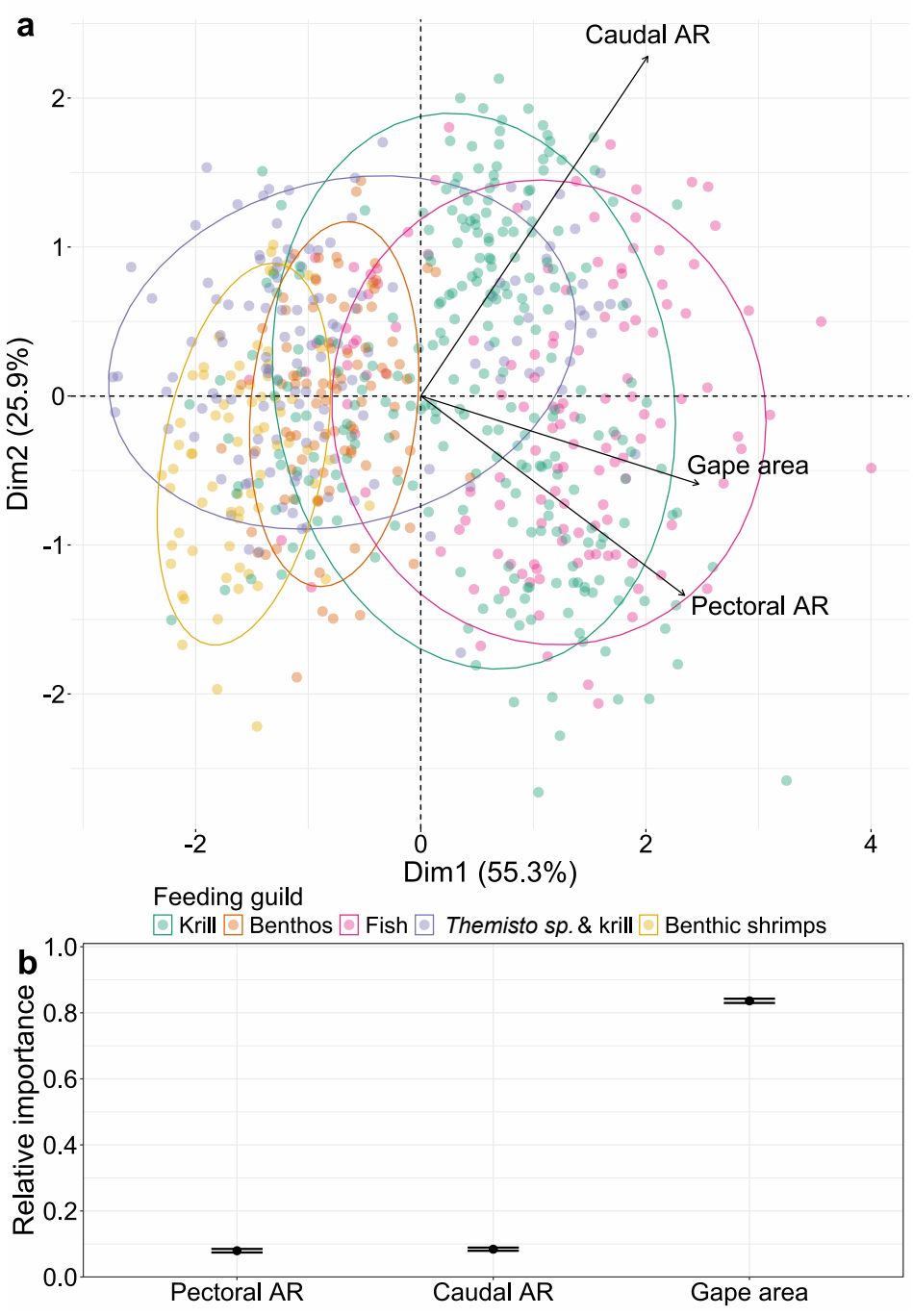

884

885 Figure 2.5: a) PCA plot of individual fish based on the length-standardised morphological
886 traits, coloured by feeding guild. Ellipses encompass 80% of the points from that guild; b)
887 relative importance of each length-standardised trait (as a proportion of the summed
888 importance of all traits) for classifying individuals into feeding guilds, as identified by the
889 Random Forest model. Error bars are the 95% confidence intervals from 100 cross-
890 validations of the model.

2.4 Discussion

We investigated the role of morphological traits in driving prey selection at the community level, providing insight into the partitioning of energy flows across species and size classes of demersal fish. Such a trait-based understanding of trophic interactions can ultimately be used to model community structure and function (Kiørboe et al. 2018) and could thus elucidate how future environmental change will alter the structure and stability of food webs.

Our analyses suggest that members of this community display differing levels of dietary specialisation, with the diets of some groups dominated by specific taxa while others are clearly more opportunistic and generalist. The feeding relationships we observed are supported by previous dietary research in the region (e.g. McKenna 1991; Reid et al. 2007; Targett 1981; Clarke et al. 2008; Main et al. 2009; Hollyman et al. 2021), indicating that we successfully described the broad summer dietary niches of the studied fish. There can, however, be interannual variability in diets (e.g. Main et al. 2009, Hollyman et al. 2021), possibly driven by changes in krill availability, and it is notable that the %IRI of krill in *C. gunnari* diets in 2023 (the collection year for this study) was the third highest in 14 years of data (see Figure A2). Thus, our data may represent a situation in which krill were more readily available to the demersal fish community than usual. Overall, the utilisation of krill by all feeding guilds highlights the key role this group plays in maintaining energy flow within Southern Ocean food webs. Demersal fish are themselves a major dietary component of albatrosses, petrels, gentoo penguins, and Antarctic fur seals (Hill et al. 2005; Reid et al. 2005; Waluda et al. 2017), indicating that these fish are a key link between krill and many top predators in the Southern Ocean.

2.4.1 Size-based feeding

Average prey mass increased with predator mass, with a consistent scaling across all feeding guilds regardless of prey type, suggesting strong size-structuring. Previous research has shown that predator-prey size scaling relationships vary with diet type, as piscivores exhibit positive allometric relationships but benthic invertivores have no significant change in prey size with predator size (Dunic and Baum 2017). In contrast, our results support the generalisability of predator-prey size relationships across feeding guilds, suggesting that such allometric scaling could be applied more broadly to predict feeding interactions. Further work will be required to determine whether the contrast with Dunic and Baum (2017) is down to any differences in the available prey field and/or the behaviour of the focal fish species. The

variation in the intercepts of the relationship between predator size and prey size for different feeding guilds may reflect differences in the levels of dietary specialisation of their constituent members. Surprisingly, the 'fish feeders' had the smallest intercept, which could be due to their generalist diets consisting of a broad range of prey sizes including numerous very small prey items in addition to fewer large fish prey. As fish grow, their minimum prey sizes often increase less steeply than their maximum prey sizes, resulting in a broadening of their trophic niche, which may be the case for members of this guild (Scharf et al. 2000). In contrast, the apparent high dependence of the 'krill feeders' on such a relatively large-bodied prey, with minor contributions from other prey groups, may lead to a low trophic niche breadth which ultimately drives the higher intercept for this feeding guild. There were also some ontogenetic changes in prey selection, e.g. *C. aceratus* switched from a mixture of krill, *Themisto* sp., and limited fish consumption to a fish-dominated diet as they became larger, while *G. gibberifrons* moved from small and relatively immobile taxa like bivalves, polychaetes, annelids, and gastropods to more mobile, large isopods as they grew. These shifts indicate that these fish are potentially gape limited at smaller sizes or that their foraging behaviour changes as they grow.

2.4.2 Functional traits and feeding guilds

We found that some easily measured morphological traits can be used to distinguish feeding guilds. Gape area was the best predictor of guild membership, and 'fish feeders' generally had the largest gapes, reflecting the influence of gape limitation on the diets of fish. One krill-feeding species, the icefish *P. georgianus*, had absolute and standardised gape areas of similar or even greater dimensions to those of 'fish feeders', which suggests that prey selection by this species is not driven solely by gape limitation. Thus, the combination of multiple traits is important in determining trophic niches in ecological communities. It has been proposed that the elongated head, non-protractile jaw, and large gape of channichthyids including *P. georgianus* facilitates a ram feeding mode (Bansode et al. 2014), and this might aid zooplanktivores that feed on swarming prey as they can efficiently capture many prey items simultaneously. The diets of larger *P. georgianus* also contained some fish and both *P. georgianus* and *C. aceratus* ('fish feeder') are morphologically very similar, which indicates that there may be further factors driving prey selection in these species. At the other end of the scale, the 'benthos feeders' had the smallest absolute and relative gape areas of all the feeding guilds. Possession of a relatively small mouth aperture correlates inversely with flow velocity (Wainwright et al. 2007) and may benefit these fish which likely use suction feeding

to capture benthic epi- and infauna. Interestingly, *L. larseni* had an extremely small gape area despite being a member of the 'krill feeders' guild, which normally utilise large mouths to consume many prey items simultaneously. This suggests that *L. larseni* may target individual krill despite their sub-optimal trait configuration, highlighting the adaptability of the demersal fish community to incorporate such ubiquitous, high energy content prey in their diet.

The fin *AR*s measured across this community are quite low for fish in general (Sambilay 1990). This reflects the demersal nature of these fish, as low *AR* typically corresponds with lower swimming efficiency but higher manoeuvrability at low speeds, suited to fish that inhabit benthic environments (Bridge et al. 2016; Pauly 1989). Despite the narrow range of *AR* values, it was possible to distinguish some species and feeding guilds based on this trait. For example, *C. gunnari* are known to feed pelagically, which may explain their relatively high caudal *AR* as this facilitates sustained swimming (Higham 2007). Similarly, the high pectoral fin *AR* of the 'fish feeders' likely aids in capturing mobile prey, providing greater potential for efficient, lift-based swimming (Pauly 1989; Bridge et al. 2016). The extremely low fin *AR* observed for the 'benthic shrimp feeders' may be closely tied to the ecology of their main prey (mysids and the decapods *Notocrangon spp.* and *Chorismus spp.*), which spend much of their time either partially buried in substrate or perched on sponges (Gutt et al. 2004). Low pectoral fin *AR,* representing greater manoeuvrability and stability at low speeds (Higham 2007), may provide this group with the mobility required to position themselves rapidly and accurately in relation to these individual prey items. Additionally, malacostracan crustaceans including shrimps are capable of rapid 'tail-flip' antipredator escape responses (Arnott et al. 1998), therefore the high acceleration potential provided by very low caudal *AR* may allow the 'benthic shrimp feeders' to strike and capture their prey before they are able to flee. The remaining guilds are more difficult to distinguish by their fin morphology alone, suggesting either that similar swimming capabilities are required for feeding on krill, amphipods, and benthic taxa, or that their fin morphology is not tied strongly to their diet.

2.4.3 Further considerations

While our simple morphological traits proved useful for differentiating some feeding guilds, we also conclude that there is a significant region of shared trait space between certain guilds. In particular, the 'krill feeders' guild displayed a broad range of morphologies which overlapped with all other guilds, suggesting that krill were readily available to fish regardless of their morphology and behaviour. *Euphausia superba* is traditionally considered a pelagic species which spends most of its time in epipelagic waters, but there is evidence that krill-

benthos interactions are common, with large krill swarms often observed close to the seabed and krill found in the diet of strictly benthic species like the benthic skate *Amblyraja georgiana* (Schmidt et al. 2011; Main and Collins 2011). Plasticity in krill behaviour may mean they act as both a swarming prey in the water column for bentho-pelagic predators to feed on and also come into contact with the epibenthos where they become available to benthic feeders. The combination of such widespread accessibility and the high energetic value and general abundance of krill makes them a suitable prey item for fish displaying a wide variety of trait configurations. This further highlights the key role of krill within Southern Ocean food webs, indicating that they effectively bridge the ecological niches otherwise imposed by longer-term morphological evolution.

The density and availability of krill to shelf predators around South Georgia varies interannually (Fielding et al. 2014) and, as noted above, availability may have been high during sampling for the current study. Competition theory holds that niche partitioning should increase as resources become limited, with predators focusing on the prey they are best suited to exploit, thereby promoting coexistence (Schoener 1982). The link between morphology and diet might therefore become clearer in periods of krill scarcity when levels of dietary segregation within the groundfish community may increase as species match their longer-term evolutionary niches. Continued monitoring of diets across the whole demersal community, including over different seasons, would provide insight into such competitive dynamics and could reveal temporal shifts in the importance of different prey taxa. For example, amphipods such as *T. gaudichaudii* are widely consumed by Southern Ocean fish, squid, seabirds, and marine mammals (Padovani et al. 2012; Havermans et al. 2019), and our results highlight their role in supplementing the diets of many demersal species around South Georgia. These amphipod taxa might therefore provide an alternative resource for demersal fish around South Georgia during periods of low krill availability, although the extent to which they could support the total energy requirements of the groundfish community requires further study (Kock et al. 1994).

Further studies on the links between morphological traits and diet will help elucidate the evolutionary constraints on prey selection. The traits used in this study represent broad and easily measurable morphological features expected to influence feeding, but there are likely to be further fine-scale morphological features that could be investigated in future studies. For example, jaw length is linked to stealth and jaw closing speed and may therefore influence prey selection (Ferry et al. 2015), mouth position relates to feeding mode and

habitat association (Helfman et al. 2023), and gill raker morphology determines feeding mode and minimum prey size (Macnuson and Heitz 1971). Ultimately, predator-prey interactions are determined by the combination of traits exhibited by both predator and prey individuals, including mobility, body size, physical and chemical defences, camouflage, visual acuity, feeding method, and habitat association (Spitz et al. 2014; Weigel and Bonsdorff 2018). It will therefore be important to consider the traits of prey alongside those of their predators when further investigating the drivers of feeding interactions. Detailed predator-prey trait matching could also facilitate analyses of the drivers of predation at the individual level by capturing the fine-scale variation in trait space across predator diets. By describing the distribution of traits across the available prey assemblage it is also possible to investigate how environmental change alters the suitability of the prey field for different predators (Weigel and Bonsdorff 2018), which will be a powerful tool for predicting the ecological consequences of climate change.

2.4.4 Conclusion

Ongoing ecological changes, including shifting distributions of key prey like Antarctic krill, may result in the re-organisation of marine communities. This study provides a baseline understanding of how morphological traits underlie the ecology of Southern Ocean demersal fish. Continued investigation of the links between functional traits and prey selection will aid the production of generalisable community models to answer questions regarding trophic dynamics in marine food webs and the implications of abiotic change.

3 Trophic structuring of modularity alters energy flow through marine food webs

Published in *Frontiers in Marine Science* (https://doi.org/10.3389/fmars.2022.1046150)

Abstract

Food web interactions govern how ecosystems respond to climate change and biodiversity loss. Modularity, where subgroups of species interact more often with each other than with species outside their subgroup, is a key structural feature which has been linked to food web stability. We sought to address the lack of understanding of how modularity varies among ecosystems by comparing the structure of four highly resolved marine food webs and the importance of functional traits for predicting module membership. Modules in two offshore networks were partitioned largely by trophic level, creating an interdependence among them, whereas modules in two semi-enclosed bays were generally separated into energy channels with less trophic separation and containing distinct basal resources, providing greater redundancy in the flow of energy through the network. Foraging habitat and mobility predicted module membership in all networks, whilst body mass and foraging strategy also differentiated modules in the offshore and bay ecosystems, respectively. Environmental heterogeneity may be a key factor driving the differences in modularity and the relative importance of functional traits for predicting module membership. Our results indicate that, in addition to overall network modularity, the trophic structure of modules within food webs should be considered when making inferences about ecosystem stability.

3.1 Introduction

The current global rate of species extinctions is unprecedented (Ceballos et al. 2015), and there is concern that biodiversity loss will reduce ecosystem functioning and services (Schmid et al. 2009; Tilman et al. 2014). Species interaction networks are key to understanding the ecosystem-level consequences of biodiversity loss, with certain network structures helping to limit the spread of perturbations through the ecosystem (Bruder et al. 2019; Clark et al. 2020). Food webs provide tractable representations of species interactions and thereby allow us to compare the key structural features of communities that may confer stability (Rooney and McCann 2012; Ives and Carpenter 2007). One such stabilising feature is modularity, which is the presence of subgroups (modules) of species that interact often or strongly with one-another but have few or weak connections to species outside their subgroup

(Krause et al. 2003). Modularity is believed to enhance food web stability by restricting the propagation of extinctions after a perturbation, thus buffering the wider network against disruption (Thébault and Fontaine 2010; Stouffer and Bascompte 2011). While common network-level properties, such as connectance or mean trophic level, are scale-dependent (Wood et al. 2015; Galiana et al. 2021), modularity is uncorrelated with species richness (Rivera-Hutinel et al. 2012; Montoya et al. 2015), facilitating structural comparisons across networks. Studies of modularity to date have generally quantified modularity in single food webs and with a variety of underlying methods, which precludes direct comparison of results across ecosystems (e.g., Rezende et al. 2009; D'Alelio et al. 2019). Assessing modularity in networks with different species assemblages would help to identify generalisable patterns in the distribution of modules, providing insight into the underlying drivers of stability.

Physical and environmental variables play a key role in determining food web structure, with habitat heterogeneity shown to increase network complexity and niche availability (Tews et al. 2004; Kortsch et al. 2019). The diversity of ecological niches and refuges present in intertidal and coastal regions may therefore increase modularity compared with more uniform offshore areas. Differences in environmental factors such as temperature and depth may also drive structural contrasts between ecosystems (Gibert 2019; López-López et al. 2021). For example, the historically stable temperatures of Antarctic waters and their relative biotic isolation from other oceans (Murphy et al. 2007; Morley et al. 2020), might lead to less modular networks compared to lower latitudes.

Functional traits provide a framework for describing community structure, as the match between consumer and resource traits determines the distribution of feeding interactions (Bartomeus et al. 2016). A key trait underlying trophic interactions in marine systems is body size, and the relative size of consumers to their resources has been recognised as a potentially key determinant of species organisation into modules (Rezende et al. 2009; Gravel et al. 2013). The consumer-resource body mass ratio generally declines with increasing consumer size due to the higher energy demands of larger organisms, which leads to a greater reliance on proportionally larger prey (Arim et al. 2007). As larger organisms usually occur higher in the food web, the result is a negative relationship between consumer trophic level and consumer-resource body mass ratio: a macroecological pattern which is consistently found in different food webs (Jonsson et al. 2005; Tucker and Rogers 2014). This indicates that body size could also determine the distribution of modules across trophic levels. Previous research has suggested that the level of diet contiguity in the food web may determine modularity,

with modules in some networks displaying trophic clustering such that they encompass a relatively limited range of trophic levels and have low overlap of trophic levels between modules (Guimera et al. 2010; Kortsch et al. 2015). Other traits may also play an important role, with foraging habitat determining the spatial distribution of species and thus their likelihood of interacting (Rezende et al. 2009; Kortsch et al. 2019). Mobility and feeding mode also contribute to the trophic role of species within networks, by determining their activity levels and the types of resources they consume (Lazzaro et al. 2009; Gilabert et al. 2019). In fact, it has been proposed that modules in some networks represent semi-isolated energy channels, whereby energy flows from a distinct set of basal resources to an assemblage of higher consumers with a particular set of functional traits (Gauzens et al. 2015; Rodriguez et al. 2022). Clearly, despite the consensus that modularity acts to stabilise food webs, there are contrasting viewpoints on what the key determinants of modularity are and how modules are distributed within communities.

In this study, we compared the modular structure of the four most highly resolved marine food webs currently available. We quantified how differences in their spatial distribution and constituent taxonomic groups translate into the organisation of modules and the relative importance of functional traits for predicting module membership. Our primary research objectives were 1) to determine whether there are differences in the organisation of modules between networks; 2) to identify which functional traits can be used to predict the species that are included in each module.

3.2 Materials and methods

3.2.1 Study systems

Based on a review of marine food webs in the GATEWAy (Brose et al. 2019) and ECOWeB (Cohen 2010) databases and the wider literature, we identified four systems in which the overwhelming majority of nodes were highly resolved to genus or species level (excluding a handful of cryptic taxa and basal groups such as sediment and detritus). Aggregation of taxa in the other networks could mask potential modules and introduce methodological biases (Krause et al. 2003), so they were not considered here. The four chosen food webs represent a range of locations from the high Antarctic (Weddell Sea), and (sub)Antarctic (Scotia Sea), to temperate (Lough Hyne) and Arctic (Kongsfjorden). The networks differ in their size (number of nodes and links), spatial extent (including depth), and functional groups (Table 3.1). The Scotia Sea food web was obtained from the British Antarctic Survey's UK Polar

Data Centre (López-López et al. 2021), while the remaining webs were extracted from the GATEWAy database (Brose et al. 2019). Each of these networks was compiled through a combination of direct observation and diet analysis of organisms within the focal ecosystem, and wider literature research to characterise the diet of organisms in other regions or for closely related taxa. Following Grilli et al. (2016), we removed cannibalistic links in order to focus on interspecific interactions.

Table 3.1: Characteristics of the four study systems. SS = Scotia Sea, WS = Weddell Sea, LH = Lough Hyne, KO = Kongsfjorden.

Name	**Nodes**	**Links**	**Approximate latitude (°N)**	**Approximate extent (km^2)**	**Min to max bottom depth (m)**	**Ecosystem type**	**Constituent functional groups**
SS	228	10,827	-57.0	1.5×10^6	>1,000 to >3,000	Offshore	Pelagic (excluding birds and mammals), benthos excluded
WS	490	15,987	-76.0	2×10^5	200 to 500	Offshore	Pelagic (including birds and mammals), benthos
LH	340	5,012	51.5	0.5	0 to 50	Coastal bay	Pelagic (including birds and mammals), benthos, intertidal
KO	260	1,590	79.0	209	0 to 400	Coastal bay	Pelagic (including birds and mammals), benthos, intertidal

3.2.2 Module identification

The modularity of each food web was calculated with a Simulated Annealing algorithm using the '*netcarto'* function in the R package '*rnetcarto*' (Doulcier and Stouffer 2015). This

algorithm uses a probabilistic procedure whereby nodes are initially partitioned into arbitrary modules and then iteratively moved into different modules until the maximum modularity is obtained (Guimerà and Nunes Amaral 2005; Chen et al. 2014). Modularity ranges from -1 to +1, with negative and positive values indicating a less and more modular structure than expected at random, respectively (Newman and Girvan 2004; Newman 2006). One hundred simulations were conducted per network to assess the variability in outputs resulting from the stochastic component of the algorithm.

3.2.3 Functional traits

Eight functional traits were selected to investigate the partitioning of species into modules (Table 3.2). These traits were chosen because they could be easily identified and generalised across all species in the four ecosystems. For each species, body mass estimates were derived from the original food web studies, and the remaining trait values were assigned based on data obtained via literature review, assessment of images, and diet compositions.

Table 3.2: Functional traits identified for each species in the four food webs. See Appendix B1: Supplementary methods and results for more details.

Trait	**Description**
Body mass	Species averages from field measurements and literature, $\log_{10}$ transformed
Foraging habitat	Physical space in which organisms forage. Categories vary due to environmental differences between food webs. Scotia Sea: epipelagic, mesopelagic, bathypelagic. Weddell Sea: epipelagic, meso/benthopelagic, benthic. Lough Hyne and Kongsfjorden: pelagic, benthic, intertidal.
Mobility	A scale of increasing mobility: sessile; passive drifter; crawler; use of swimming appendages; jet propulsion; lift-based swimming.
Prey-capture strategy	A scale based on how actively the species captures prey: primary producer; passive capture; ambush predator; active suspension/detritus feeder; active searcher/hunter
Prey-capture appendages	Binary, presence or absence of external appendages which could be reasonably considered to play a role in prey grasping and manipulation.
Body robustness	A scale of body type, from fragile to robust: gelatinous; soft-tissue with no internal skeleton; soft-tissue with internal skeleton; external carapace; external hard shell
Spines	Binary, presence or absence of defensive spines
Translucency	Binary, used to distinguish species that are clearly see-through (e.g. most gelatinous zooplankton, some amphipods) from those which are not (e.g. crabs, fish)

3.2.4 Statistical analysis

All analyses were conducted in R 4.1.0 (R Core Team, 2021). Differences in the modular structure of each network were investigated by comparing the distribution of node-level metrics (prey averaged trophic level, body mass, generality, vulnerability, and omnivory) across modules. The data did not conform to normality and homogeneity of residuals, and so non-parametric Kruskal-Wallis tests were performed followed by post-hoc Dunn tests with a Bonferroni correction.

We used Random Forest (RF) models to investigate the relative roles of the functional traits in explaining the modular structure of each network. The RF model is a machine learning classification tool which uses bootstraps of the data to predict observations and provide a measure of the relative importance of predictor variables (Cutler et al. 2007). A benefit of RF models is that they make no prior assumptions about the distribution of response or predictor variables and can handle datasets containing multiple data types (Cutler et al. 2007). We implemented the conditional RF algorithm using the '*cforest*' function in the R package '*party*' (Hothorn et al. 2005), which relies on a conditional inference framework and is unbiased in cases where predictors have a highly variable number of categories or are correlated (Strobl et al. 2007; Strobl et al. 2008). For each food web, we implemented a cross-validation approach by randomly sub-sampling 70% of the data for model calibration and then making predictions from the remaining 30%. This process was repeated 20 times to give an indication of the variability in the classification accuracy and relative importance of each functional trait. The predictive ability of the models was assessed using the average True Skill Statistic (TSS), which represents the proportion of successful predictions versus false predictions, with values of 0 and 1 indicating completely random and perfect predictions, respectively (Allouche et al. 2006).

To further investigate the role of body size (specifically, whether size-structured feeding is related to modularity), we used analysis of covariance (ANCOVA) to test the relationship between consumer-resource body mass ratio and consumer trophic level, while distinguishing between trophic links occurring within or between different modules. The average consumer-resource body mass ratio of each consumer species was used as the dependent variable to avoid any confounding effects resulting from the fact that some consumers had many resources while others had very few. The main and interactive effects of consumer trophic level and link position (within or between modules) were the explanatory variables. Weighted Generalised

Least Squares models were used, with an exponential variance structure by trophic level to account for heterogeneity in the model residuals.

3.3 Results

The Scotia Sea network represents a pelagic system, dominated by phytoplankton, gelatinous zooplankton, crustaceans, and fish, while benthic taxa are excluded due to the lack of available information on benthic communities. The Weddell Sea has a similar functional group composition, though it also includes many benthic species including sessile sponges, mobile detritivores, and demersal fish, in addition to incorporating mammals and seabirds. Both Lough Hyne and Kongsfjorden include a variety of benthic, intertidal and pelagic species, including macroalgae, sponges, crustaceans, and fish, in addition to seabirds and mammals. The Weddell Sea, Lough Hyne and Kongsfjorden food webs have similar maximum trophic levels (5.1, 4.6 and 4.8, respectively), while the Scotia Sea has a maximum trophic level of 6.1. The trophic distribution of species is similar in the Weddell Sea, Lough Hyne and Kongsfjorden, with most species found between trophic levels 2 and 4, while in the Scotia Sea, species are distributed quite evenly between trophic levels 2 and 5 (Figure 3.1a). The trophic distribution of body masses is similar in all networks, with larger organisms found at higher trophic levels (Figure 3.1b).

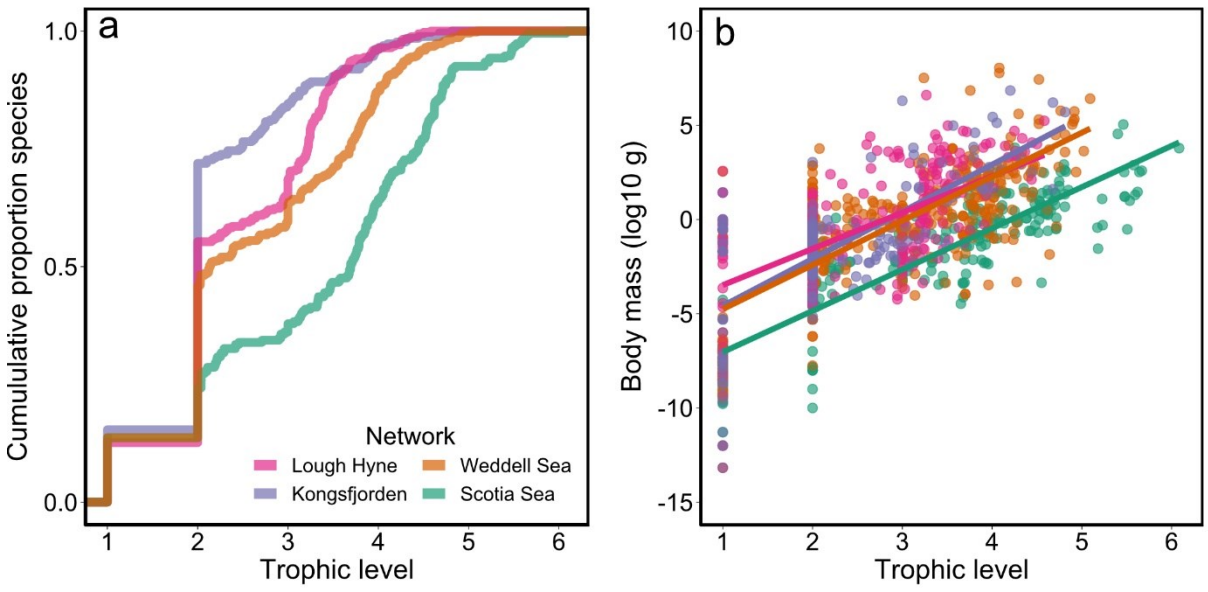

Figure 3.1: Plots of (a) the cumulative proportion of species across trophic levels, and (b) the distribution of body masses at each trophic level, coloured by network.

3.3.1 Module identification

Modularity was significantly different between all four food webs ($X^2_{(8)} = 374.80$, $p < 0.001$; Dunn's test: $p < 0.001$). Three modules were identified in the Scotia Sea and Weddell Sea networks (Modularity = 0.157 ± 0.007 and 0.319 ± 0.002, respectively), while five were found in Lough Hyne and Kongsfjorden (Modularity = 0.404 ± 0.009 and 0.496 ± 0.005, respectively) (Figure 3.2). Energy flow between modules in the Scotia Sea and Weddell Sea was generally one-sided, with the majority of links between any pair of modules flowing in the same direction, whereas flows were more two-sided in Lough Hyne and Kongsfjorden (Figure 3.2). These results were deemed to be representative of the 100 Simulated Annealing runs, with at least 95% of within-module interactions found to be consistent across runs in each network (see Appendix B1: Supplementary methods and results for details of the Simulated Annealing result selection process and robustness).

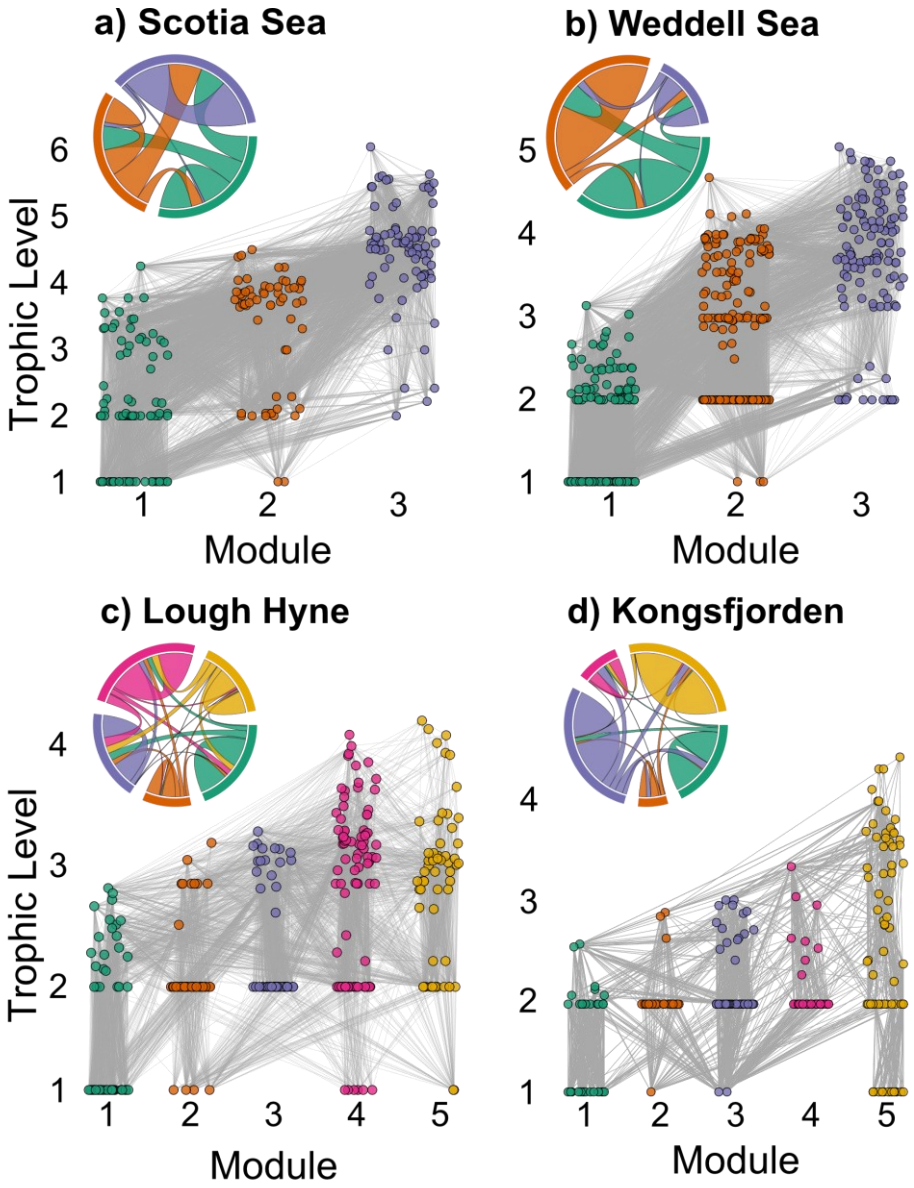

Figure 3.2: Modular structure of the four studied food webs: (a) Scotia Sea; (b) Weddell Sea; (c) Lough Hyne; (d) Kongsfjorden. Networks are plotted with nodes coloured and positioned along the x- and y-axes according to module and trophic level, respectively. Inset chord diagrams display the distribution of interactions within and between modules, with chord thickness proportional to the number of links and colour indicating the source module of the interactions.

Some of the networks displayed similarities in the distribution of species across modules. In both the Scotia Sea and Weddell Sea there was a basal module that contained most (>90%) of the basal resources, being made up largely of epipelagic phytoplankton and crustaceans, and a top predator module that was made up primarily of fish and squid (in addition to marine mammals and seabirds in the Weddell Sea) (Figure 3.3a-b). The main difference between these

networks was the remaining module, which was composed primarily of gelatinous organisms and crustaceans in the Scotia Sea and benthic taxa such as echinoderms, sponges, and bryozoans in the Weddell Sea (Figure 3.3a-b). In both Lough Hyne and Kongsfjorden, basal resources were present in four out of five modules. In both networks there was a macrophyte module consisting largely of seaweeds and sessile algae and a module containing many benthic and intertidal amphipods, while fishes were distributed across all modules (Figure 3.3c-d). Both food webs contained a benthic consumer module consisting mainly of gastropods, crustaceans, and worms, and a sessile filter-feeding module composed mostly of sponges and bryozoans in Lough Hyne and of bivalves and barnacles in Kongsfjorden (Figure 3.3c-d). The final module in both networks was largely made up of bentho-pelagic organisms (Figure 3.3c-d).

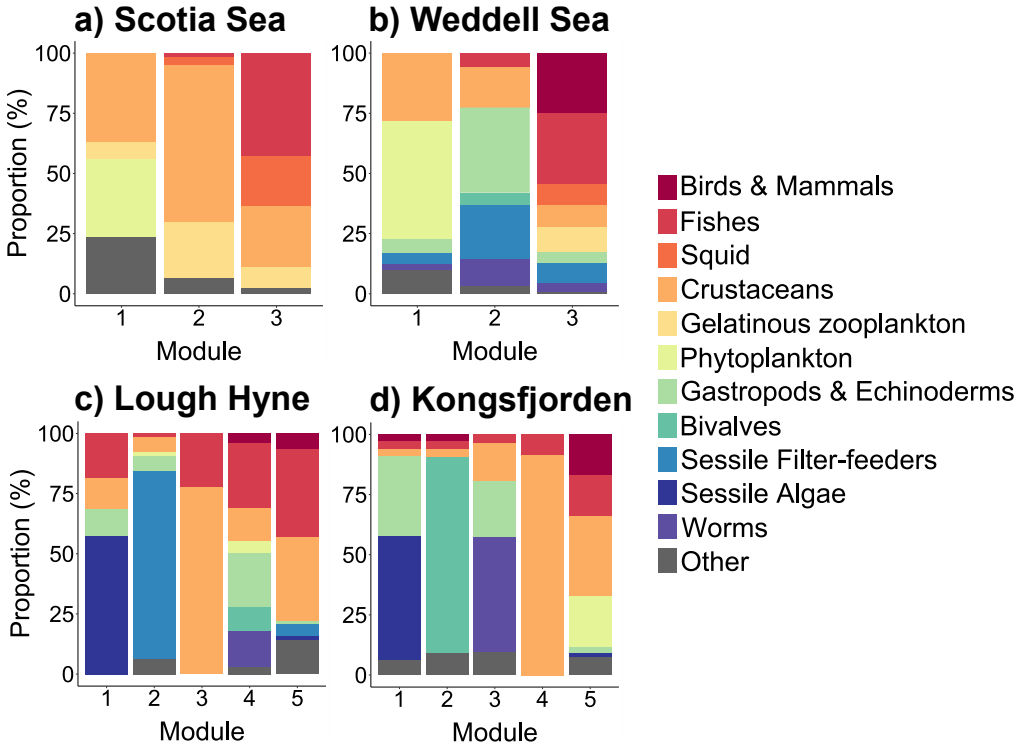

Figure 3.3: The relative proportion of different taxonomic groups within each module in the four food webs: (a) Scotia Sea; (b) Weddell Sea; (c) Lough Hyne; (d) Kongsfjorden. Species were initially grouped by taxonomy and then groups with few individuals were either combined (if they had similar ecology) or were assigned to the group "Other".

3.3.2 Module topology

There was a significant difference in trophic level between modules in each of the food webs (Scotia Sea: $X^2_{(2)} = 147.16$, $p < 0.001$; Weddell Sea: $X^2_{(2)} = 192.56$, $p < 0.001$; Lough Hyne, $X^2_{(4)} = 86.643$, $p < 0.001$; Kongsfjorden, $X^2_{(4)} = 16.57$, $p = 0.002$; Figure 3.4). In the Scotia Sea and Weddell Sea, trophic level was significantly different among all three modules (Dunn's

test: $p < 0.001$), while in Lough Hyne and Kongsfjorden significant differences were only found between certain module pairs. The mean difference in trophic level between all possible species pairs which belong to separate modules was greater in the Scotia Sea (1.62, SE = 0.009) and Weddell Sea (1.43, SE = 0.004) than in Lough Hyne (0.70, SE = 0.004) and Kongsfjorden (0.44, SE = 0.005), and this pattern was retained after accounting for the effects of the differing number of modules and maximum trophic level in each network (Appendix B1). This highlights the greater trophic clustering of modules that is present in the Scotia Sea and Weddell Sea compared with Lough Hyne and Kongsfjorden. A comparison of the distribution of trophic levels for each module across all Simulated Annealing runs suggested that these results are robust to changes in the number of modules or distribution of nodes between modules (Appendix B1). Results for the other node-level metrics (i.e. generality, vulnerability, and omnivory) generally reflect the distribution of modules across trophic levels in these networks, with clear differences between modules for the Scotia Sea and Weddell Sea, but not for Lough Hyne and Kongsfjorden (Figure B1-B5).

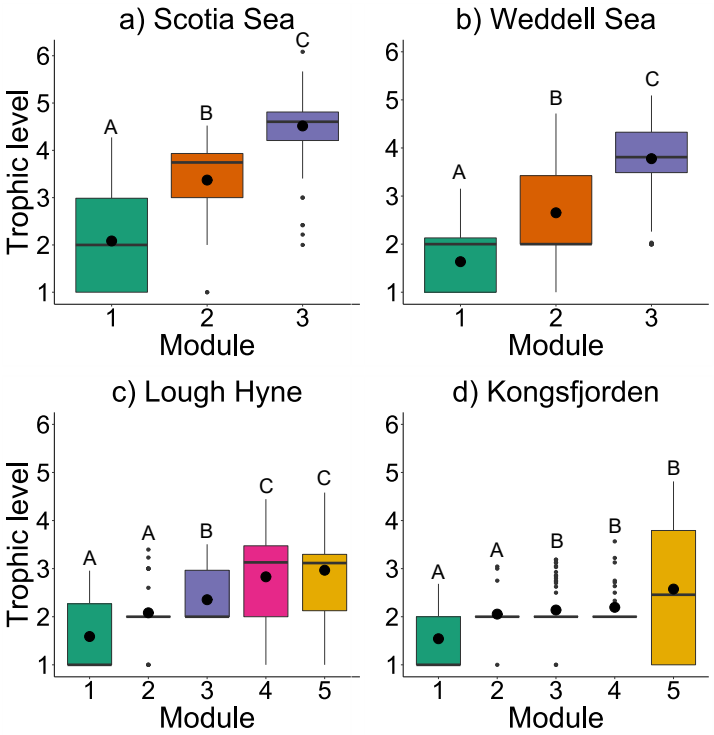

Figure 3.4: Boxplots of prey-averaged trophic level across modules within each network: (a) Scotia Sea; (b) Weddell Sea; (c) Lough Hyne; (d) Kongsfjorden. Large black points indicate the mean, thick horizontal lines represent the median, boxes indicate the interquartile range, whiskers are 1.5 × the interquartile range, and outliers beyond this range are indicated as small black points. Boxes not sharing a common letter are significantly different from one another using a Dunn's test ($p < 0.05$).

3.3.3 Functional traits

The Random Forest models performed well at predicting module membership from the functional traits, as evidenced by their high TSS scores (>0.56; Figure 3.5). Body mass was a key trait for predicting module membership in the Scotia Sea, accounting for ~30% of overall importance, followed by habitat, mobility, feeding appendages, and translucency, which all had similar values of importance (Figure 3.5a). In the Weddell Sea, mobility and habitat together accounted for almost 60% of importance, and body mass was also valuable (~13% of importance, Figure 3.5b). In Lough Hyne and Kongsfjorden, mobility, capture strategy and habitat accounted for ~60% of the total importance, while body mass represented <10% of overall importance (Figure 3.5c-d).

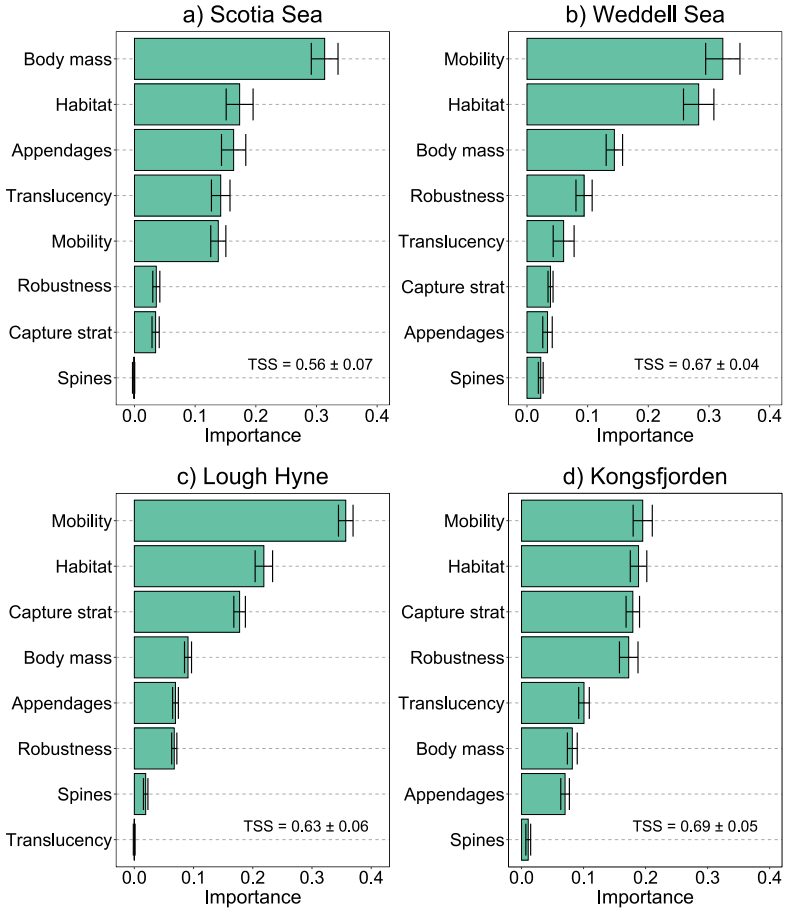

Figure 3.5: Relative importance of each functional trait (as a proportion of the summed importance of all traits) for classifying species into modules, as identified by Random Forest models for each network: (a) Scotia Sea; (b) Weddell Sea; (c) Lough Hyne; (d) Kongsfjorden. Error bars are the 95% confidence intervals resulting from 20 cross-validations of the importance of each trait. True Skill Statistics (TSS) values indicate the predictive performance of the model.

The importance of body mass in the Scotia Sea and Weddell Sea RF models is reflected in the distribution of sizes across modules. There was a significant difference in body mass among all modules in the Scotia Sea ($X^2_{(2)} = 113.75$, $p < 0.001$; Figure 3.6a) and Weddell Sea ($X^2_{(2)} = 191.09$, $p < 0.001$; Figure 3.6b). While the distribution of body masses was also significantly different between some modules in Lough Hyne and Kongsfjorden ($X^2_{(4)} = 27.634$, $p < 0.001$, and $X^2_{(4)} = 32.414$, $p < 0.001$, respectively), modules were not as obviously separated according to body mass as in the other webs (Figure 3.6c-d), which also reflects the results of the RF models. A comparison of the distribution of body mass values in each module across all Simulated Annealing runs suggested that these results are robust to changes in the number of modules or distribution of nodes between modules (Appendix B1). See Figure B6-B12 for a description of the distribution of the remaining traits across modules in each network.

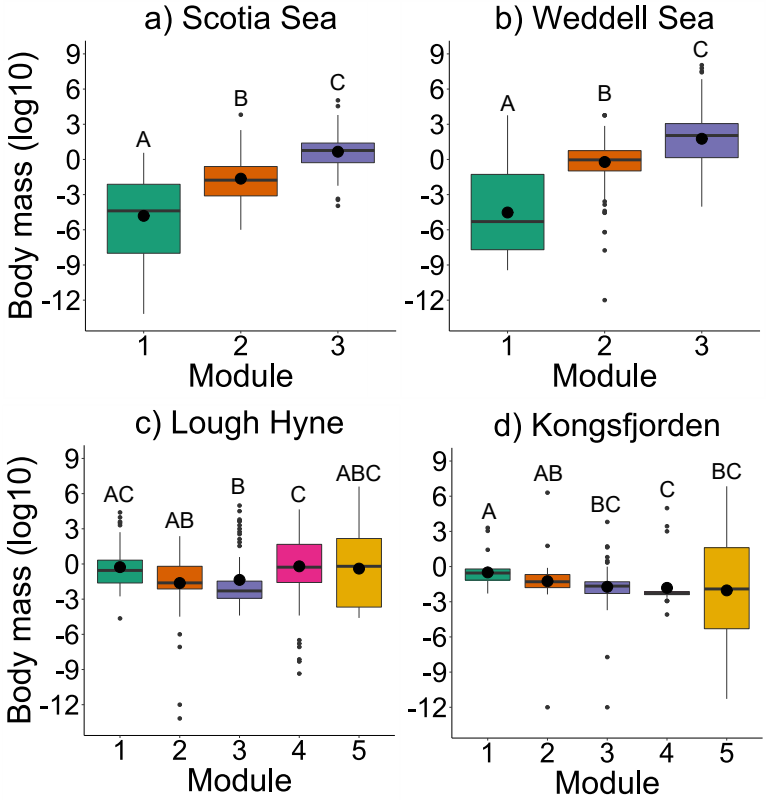

Figure 3.6: Boxplots of body mass across modules within each network: (a) Scotia Sea; (b) Weddell Sea; (c) Lough Hyne; (d) Kongsfjorden. Large black points indicate the mean, thick horizontal lines represent the median, boxes indicate the interquartile range, whiskers are 1.5 × the interquartile range, and outliers beyond this range are indicated as small black points. Boxes not sharing a common letter are significantly different from one another using a Dunn test ($p < 0.05$).

There were some key differences in the distribution of consumer-resource body mass ratios among networks (Figure 3.7). There was a significant interaction between consumer trophic level and link position in the Scotia Sea ($F_{1,338} = 29.76$, $p < 0.001$) and Weddell Sea ($F_{1,643} = 44.53$, $p < 0.001$). In both, consumer-resource body mass ratio declined more steeply with consumer trophic level for interactions within modules than for interactions between modules (Scotia Sea: within, $p < 0.001$, $r^2 = 0.35$; between: $p = 0.807$; Weddell Sea: within, $p < 0.001$, $r^2 = 0.50$; between, $p < 0.001$) (Figure 3.7a-b). In contrast, no significant interaction between consumer trophic level and link position was observed in Lough Hyne ($F_{1,447} = 0.01$, $p = 0.919$) or Kongsfjorden ($F_{1,326} = 0.39$, $p = 0.531$). Instead, consumer-resource body mass ratio declined significantly with increasing consumer trophic level regardless of link position in both Lough Hyne ($F_{1,449} = 106.80$, $p < 0.001$, $r^2 = 0.20$) and Kongsfjorden ($F_{1,328} = 142.66$, $p < 0.001$, $r^2 = 0.27$; Figure 3.7c-d).

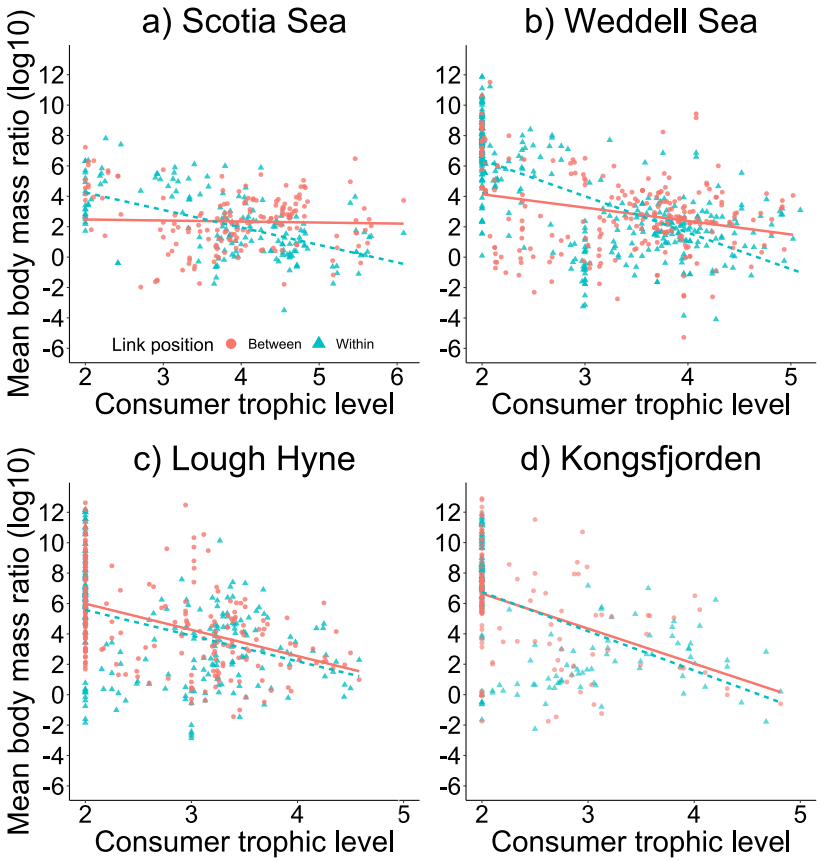

Figure 3.7: Average body mass ratio of every consumer to each of its resources, plotted against the trophic level of the consumer, for each network: (a) Scotia Sea; (b) Weddell Sea; (c) Lough Hyne; (d) Kongsfjorden. Point shape and colour indicate whether the focal interaction occurred among species within the same module, or between modules. There was an interactive effect of consumer trophic level and link position on consumer-resource body mass ratio for the Scotia Sea (within: $y = 6.62 – 1.17x$, $p < 0.001$, $r2 = 0.35$; between: $y = 2.48 – 0.04x$, $p = 0.807$, $r2 = 0.01$) and Weddell Sea (within: $y = 11.77 – 2.59x$, $p < 0.001$, $r2 = 0.50$; between: $y = 5.27 – 0.70x$, $p < 0.001$, $r2 = 0.10$). There was only a significant main effect of consumer trophic level on consumer-resource body mass ratio for Lough Hyne ($y = 9.22 – 1.71x$, $p < 0.001$, $r2 = 0.20$) and Kongsfjorden ($y = 11.64 – 2.47x$, $p < 0.001$, $r2 = 0.27$).

3.4 Discussion

This study provides insight into the patterns and drivers of modularity in marine food webs. We found two distinct ways in which modules were organised: (1) a strong differentiation by trophic level in the Weddell Sea and Scotia Sea, matching the trophic clustering of modularity described for other food webs (Guimera et al. 2010; Kortsch et al. 2015); and (2) multiple modules spanning from distinct basal resources to higher trophic levels in Lough Hyne and

Kongsfjorden, resembling the description of modules as energy channels (Gauzens et al. 2015; Zhao et al. 2017). Our results also confirm the importance of body mass and foraging habitat for determining modularity (Krause et al. 2003; Rezende et al. 2009), whilst highlighting the added importance of mobility and prey capture strategy. The strong size-structuring of modules in the Weddell Sea and Scotia Sea leads to shallower trends in consumer-resource body mass ratios with consumer trophic level for interactions between modules than those within modules. This represents a disruption to the macroecological pattern of declining consumer-resource body mass ratios with consumer trophic level observed in many food webs (Jonsson 2014; Tucker and Rogers 2014), suggesting that feeding interactions between modules are occurring at sub-optimal size ratios. In contrast, Lough Hyne and Kongsfjorden display weak size-structuring and show a declining relationship between consumer-resource body mass ratios and consumer trophic level both for interactions occurring within and between modules. Our results suggest contrasting mechanisms underlying the structure of marine food webs in different regions, which may affect their stability in the face of global change.

3.4.1 Drivers of structural differences

Strong spatial and temporal variability in abiotic conditions, such as temperature, desiccation, and salinity, can drive differentiation of ecological niches and patterns of species zonation, particularly in intertidal ecosystems (Gingold et al. 2010; Kraan et al. 2013; Gallucci et al. 2020). Intertidal and benthic community composition is also shaped by habitat heterogeneity, which determines the distribution of traits such as mobility and feeding mode (Pacheco et al. 2011; Buhl-Mortensen et al. 2012; Srinivas et al. 2020). In contrast, offshore ecosystems are generally considered less complex with major structuring environmental gradients (e.g. light, temperature, pressure) changing predictably with depth (López-López et al. 2021), and may therefore display stronger size-structuring of trophic interactions. As the breadth of available niches increases with environmental, habitat, and resource heterogeneity, food webs may become more modular and separated into distinct energy channels. In highly heterogeneous environments, module membership may therefore be determined primarily by traits specific to the environmental niche, such as prey capture strategy and mobility, rather than by more general structuring factors such as body mass. Below, we explore this hypothesis in the context of our focal food webs.

The Scotia Sea network represents a pelagic oceanic ecosystem, and the Weddell Sea network represents a deep shelf system incorporating both pelagic and benthic shelf species. The

offshore nature of these networks means that basal resources are limited largely to phytoplankton and detritus, with both networks excluding the pronounced heterogeneity of the intertidal zone. The Antarctic Circumpolar Current also provides these Southern Ocean ecosystems with relatively stable and predictable oceanographic conditions (Murphy et al. 2007; Morley et al. 2020), which might help to drive the similarity in modular organisation. Both ecosystems experience a high degree of connectivity, with large-scale diurnal vertical migrations in the Scotia Sea and strong bentho-pelagic coupling in the Weddell Sea (Piatkowski et al. 1994; La Mesa et al. 2019; Pineda-Metz 2020). This may result in a stronger interdependence between modules in both ecosystems, as the deeper top-predator modules rely on the energy generated in the near-surface basal resource modules, linked via the diurnal migrators or bentho-pelagic couplers. This might reduce the influence of factors like habitat heterogeneity and prey capture strategy, with depth-based foraging habitat and size-based prey-handling constraints becoming the primary factors structuring modularity in both networks. The additional importance of mobility in the Weddell Sea largely reflects the distinct locomotory methods used in the different modules, i.e., sessile or crawling organisms in the benthic module, drifting phytoplankton and primary consumers with appendages in the epipelagic basal module, and mobile swimmers in the top predator module.

In contrast, Lough Hyne and Kongsfjorden are semi-enclosed coastal ecosystems which encompass both the intertidal and subtidal zones and experience high environmental variability. Kongsfjorden is subject to significant seasonal inputs of terrestrial nutrients (Calleja et al. 2017; Retelletti Brogi et al. 2019), and experiences strong gradients in turbidity, temperature, and salinity due to glacial inputs and influxes from the West Spitsbergen Current (Hop et al. 2002; Calleja et al. 2017). As a result, there are significant differences in community composition and abundance at different locations within the fjord (Hop et al. 2002; Calleja et al. 2017). Lough Hyne experiences high terrestrial nutrient loads (Jessop et al. 2011), in addition to significant pH gradients, high variability in water temperature, and seasonal hypoxia at depth (Bell 2002; Sullivan et al. 2014), which are also likely to drive spatial contrasts in community structure. The presence of the physically complex and variable intertidal zone, and the fluctuating environmental conditions may promote the differentiation of ecological niches. This could drive the diversity of energy channels centred around different types of basal resources, supporting species with a mix of foraging behaviours, mobilities, and habitat traits (Gauzens et al. 2015; Rodriguez et al. 2022).

3.4.2 Implications for food web stability

Modules partially isolate sections of the food web from one another, and thereby reduce the propagation of perturbations and maintain the functioning of the wider network (Stouffer and Bascompte 2011). Previous studies have used overall network modularity to make inferences regarding their stability and functioning (e.g., Stouffer and Bascompte 2011; Grilli et al. 2016; D'Alelio et al. 2019), but there has been little consideration of how the positioning of modules across trophic levels might alter stability. Our results suggest that, in networks with strong trophic clustering of modules, inter-module energy flows will be key to maintaining consumer populations and providing top-down regulation. Any perturbation affecting species in one module will have consequent effects on those in other modules, thus undermining the potential stabilising effect of modularity. The trophic clustering of modules also has implications for stabilising consumer-resource mass ratios, which are generally greatest near the base of the food web and decrease at higher trophic levels (Jonsson 2014; Tucker and Rogers 2014). This is because larger consumers need to consume larger prey to maximise energy intake and handling efficiency, such that optimal prey size gets closer to the size of the predator as its trophic level increases (Costa 2009). We found this pattern only exists for interactions within modules in networks that exhibit strong trophic (size) structuring of modularity, while many interactions between modules may be allometrically sub-optimal. For example, a predator in a lower-level module may be too small to handle prey from a higher-level module, while prey in lower-level modules may be too small to provide enough energy for predators in higher-level modules. This may reduce the redundancy of alternative pathways for energy flow in the food web by constraining consumers largely to within-module prey choices. Furthermore, the allometric scaling of metabolism and consumption rates means that consumer-resource body mass ratios can determine the strength of trophic interactions (Emmerson and Raffaelli 2004; Vucic-Pestic et al. 2010). An environmental perturbation which results in prey loss from a given module may therefore have a strong destabilising effect as predators are forced to feed on sub-optimal prey sizes to compensate, thereby also disrupting the distribution of strong and weak interactions within the food web.

In contrast, food webs with modules that represent semi-isolated food chains may be more robust to perturbations, as species extinctions in a given module will not impact the supply of energy to species in other modules. This structure maintains the negative relationship between consumer-resource mass ratio and consumer trophic level, regardless of whether consumers interact with resources within or between modules, because such modules encompass species

at a broad range of trophic levels and body masses. This means consumers are allometrically unconstrained in their ability to feed on species in different modules and may be able to adapt their feeding behaviour in response to perturbations within their own module. For example, while the loss of key basal resources from an individual module could have detrimental consequences for the specialised primary consumers in that module, higher predators may be able to maintain sufficient energy intake by feeding on species from other modules. This is analogous to fast and slow energy channels coupled by mobile predators, which promote stability by generating asynchronously fluctuating resources that dampen variation in consumer populations (Rooney et al. 2008; McCann and Rooney 2009). The stabilising effect of modular energy channels could be tested by simulating food webs with different distributions of modules and running analyses such as sequential node deletions to compare the relative effects of overall modularity and module distribution on network robustness (Dunne et al. 2004). It is important that such analyses incorporate link weighting and indirect effects such as population dynamics to avoid the underestimation of secondary extinctions (Zhao et al. 2016).

3.4.3 Further considerations

We explored the potential mechanisms underlying the modular structure of marine food webs, but more highly resolved networks across a range of ecosystem types are necessary to generalise our results. While most nodes were resolved to the genus or species level, a small minority of basal and consumer groups in each network were subject to greater aggregation. It has previously been suggested that certain topological metrics such as linkage density and mean chain length are sensitive to the level of aggregation employed, though there has been no explicit investigation of the effects on modularity (Martinez 1993). However, it has also been demonstrated that there is no consistent relationship between species richness and modularity at different scales (Montoya et al. 2015); This suggests that slight underestimations of the number of species (and links) resulting from species aggregation are unlikely to have a material impact on the resulting modular structure of our focal networks.

A further unknown is the effect of different data compilation approaches on network structure. Each of the focal food webs was compiled using species- and region -specific diet information, but also broader literature sources spanning variable taxonomic and spatial resolutions, which increases the level of uncertainty over some interactions. However, modularity has been found to be relatively robust to variation in sampling effort (Rivera-Hutinel et al. 2012), and each of the focal ecosystems has been subject to extensive long-term sampling whereby the ecology of

most constituent species is well understood. The underlying core species list and structure of each of our focal networks is therefore likely to be robust to minor variation in the distribution and number of interactions and nodes. We encourage researchers to provide information regarding the number of data sources used to determine the diet composition of each species and some indication of sampling completeness (e.g. yield-effort curves), and to ensure minimal and comparable levels of taxonomic aggregation, as these efforts will facilitate the assessment of the comparability of network structures (Martinez 1993; Gauzens et al. 2013). While network size alone does not drive modularity (Rivera-Hutinel et al. 2012; Montoya et al. 2015), contrasts between our study datasets may have arisen from a combination of natural and arbitrary differences in the scale at which the network is considered. In this study, the two offshore food webs had arbitrary differences in their boundaries and constituent species (e.g. omission of the sea floor, marine mammals, and seabirds in the Scotia Sea), but their modular structure was still consistent, which provides some confidence in our ability to detect overarching trends despite methodological differences. Food web modules have been found to represent distinct functional groups (i.e. groups of species with similar ecological functions such as pollination, herbivory, predation etc.; Montoya et al. 2015). Therefore, there is a risk that omitting species with certain characteristics when describing food webs means we only capture part of the processes structuring ecosystems, and that our perception of modularity or stability is influenced by the scale at which the network is considered. This is a topic which merits further investigation and should certainly be discussed when comparing networks.

3.4.4 Conclusion

This study provides insight into the underlying drivers of modularity in marine food webs through the comparison of multiple highly resolved networks. Modules in relatively stable offshore environments appear to be structured largely by body mass, while those in more heterogeneous coastal and intertidal settings are organised according to the broader diversity of ecological niches and feeding modes. The resulting differences in modular structure (i.e. trophic clustering of modules versus differentiation into energy channels) could underpin ecosystem responses to species loss and other perturbations and suggest that traditional modularity metrics do not fully represent the stability of food webs. Further testing of the link between the distribution of modules and the degree of network robustness (e.g., using simulated networks and species extinction scenarios) will ensure that we continue to make progress towards gaining a comprehensive understanding of the underlying determinants of network stability.

4 Temperature alters the predator-prey size relationships and size-selectivity of Southern Ocean fish.

Published in *Nature Communications* (https://doi.org/10.1038/s41467-024-48279-0)

Abstract

A primary response of many marine ectotherms to warming is a reduction in body size, to lower the metabolic costs associated with higher temperatures. The impact of such changes on ecosystem dynamics and stability will depend on the resulting changes to community size-structure, but few studies have investigated how temperature affects the relative size of predators and their prey in natural systems. We utilise >3,700 prey size measurements from ten Southern Ocean lanternfish species sampled across >10° of latitude to investigate how temperature influences predator-prey size relationships and size-selective feeding. As temperature increased, we show that predators became closer in size to their prey, which was primarily associated with a decline in predator size and an increase in the relative abundance of intermediate-sized prey. The potential implications of these changes include reduced top-down control of prey populations and a reduction in the diversity of predator-prey interactions. Both factors could reduce the stability of community dynamics and ecosystem resistance to perturbations under ocean warming.

4.1 Introduction

Global warming represents a major threat to the structure and functioning of ecosystems. One possible consequence of rising temperatures is a decrease in body size across many species and communities (Daufresne et al. 2009). At the individual level, warming alters the physiology of organisms and is likely to reduce body sizes within populations as organisms attempt to maintain metabolic functioning (Daufresne et al. 2009; Deutsch et al. 2022). At the community level, warming may alter assembly processes through environmental filtering, competition, or trophic interactions, which may result in communities dominated by smaller-bodied species (Daufresne et al. 2009; Rutterford et al. 2023). The subsequent impacts on population abundances and species interactions can drive changes to structure and functioning at the ecosystem scale (Brierley and Kingsford 2009). Aquatic ectotherms such as fish are particularly susceptible to temperature-induced reductions in body size, due to the lower rates of oxygen diffusion in water and the energetic costs associated with maintaining water flow over surfaces (Forster et al. 2012). Additionally, gape limited feeding means that

many fish species display ontogenetic changes in prey selection, with larger predators consuming larger, more energetically valuable prey (Scharf et al. 2000; Sánchez-Hernández et al. 2019). Declines in prey size with warming may therefore reduce the rates of energy acquisition by larger predators, resulting in reduced fish growth and smaller overall body sizes within populations (Queiros et al. 2024). Furthermore, such altered prey size distributions may favour smaller-sized predator species, providing them with a competitive advantage and thereby shifting the fish community composition towards smaller body sizes (Gjoni et al. 2023). Evidence from the last interglacial period suggests that fish communities experienced declining body size in response to warmer conditions (Agiadi et al. 2022; Salvatteci et al. 2022), and the average size of contemporary fish is expected to show a similar pattern under the current rate of global warming (Cheung et al. 2013). However, there is currently little understanding of how these changes will impact the structure and stability of marine ecosystems.

Body mass is a key life-history trait which determines factors such as consumption rates, handling times, and gape size (Petchey et al. 2008; Potapov et al. 2019). As such, body mass provides an important link between individual physiology and food web structure and is therefore often used to parameterise models of population dynamics and energy flow within ecosystems (Boit et al. 2012; Martinez 2020). In the marine environment, predators are generally larger than their prey, and the predator-prey mass ratio (PPMR) is a good predictor of trophic interactions. For example, allometric diet breadth models accurately predict who eats who in aquatic ecosystems (Petchey et al. 2008), whilst declines in PPMR typically result in lower per capita interaction strengths as predators are able to gain the same amount of energy by consuming fewer large prey (Brose et al. 2006). At the community level, larger ectotherms may decline in size more rapidly than smaller ectotherms with warming as a result of their reduced surface area to body mass ratio and the associated challenge of maintaining a higher metabolic rate (Forster et al. 2012; Petrik et al. 2020). This is particularly true for the marine environment, where larger fish and invertebrates display the strongest temperature-size responses (Lavin et al. 2022). If warming causes a greater decline in the size of ectotherm predators relative to that of their smaller prey (i.e. changes in community size structure), the average PPMR might decrease, with consequences for interaction strengths and thus energy flow through marine ecosystems.

The physiological basis for temperature effects on PPMR at the community level may be complicated by behavioural responses to environmental change. For example, predators may

select for more nutritious (larger) prey in an effort to increase per capita energy intake under energetically stressful conditions, thus reducing their PPMR (Lemoine et al. 2013; O'Gorman et al. 2016). Alternatively, predators might feed in a more density-dependent manner, consuming a greater proportion of abundant but relatively smaller prey and thereby increasing PPMR. Importantly, behavioural responses are unlikely to be uniform across predator body sizes, given the different dietary niches of small and large organisms and their differential susceptibility to warming. Previous research has identified variable size-dependent relationships between PPMR and temperature, such that both systematic increases (Dobashi et al. 2018) and decreases (Gibert and Delong 2014) to per capita interaction strength are possible.

It is clear we still have limited understanding of how temperature-driven changes in body size may alter community-level feeding relationships, and it is vital to address this knowledge gap if we are to predict ecosystem responses to warming. This is particularly true for the Southern Ocean, which is experiencing widespread environmental changes including rapid regional warming in areas such as the western Antarctic Peninsula (Meredith and King 2005) and northern Scotia Sea (Whitehouse et al. 2008). The Southern Ocean supports a diverse array of higher predator populations including seabirds, seals, penguins, and whales, with a food web largely centred around krill (particularly *Euphausia superba*) (Hill et al. 2006). However, it is expected that krill will shift their distribution southward in response to ocean warming (Atkinson et al. 2019), with potentially drastic consequences for many regional predator populations unless other suitable prey are available (Klein et al. 2018). Previous research has identified mesopelagic lanternfish (Family Myctophidae, hereafter myctophids) as one such potential alternative resource, due to their extremely high biomass and their role in supporting energy flow to higher predators including seals and penguins during periods of low krill availability (McCormack et al. 2021b). Additionally, myctophids themselves are major generalist consumers of prey including krill, amphipods and copepods, and therefore exert significant influence over food web dynamics (McCormack et al. 2020). Myctophids are strongly size distributed in the Southern Ocean, with smaller species and individuals found at lower (warmer) latitudes (Saunders and Tarling 2018), and they display clear size-selectivity in their feeding (Cherel et al. 2010; Saunders et al. 2019). Warming may therefore alter the size distribution of myctophids and the size relationships between these predators and their prey, and it is important that we understand what these likely changes will be in order to model ecosystem responses.

In this study, we assessed the relationship between temperature and the relative sizes of myctophids and their prey using a dataset of 1,576 stomachs and 3,707 prey size measurements from ten myctophid species sampled across >10° of latitude in the Southern Ocean (Figure 4.1). We hypothesised that myctophids would exhibit a decline in PPMR with increasing temperature, due to (1) a greater decrease in the size of these predators versus their prey, and/or (2) predators selecting for larger prey as temperature increases.

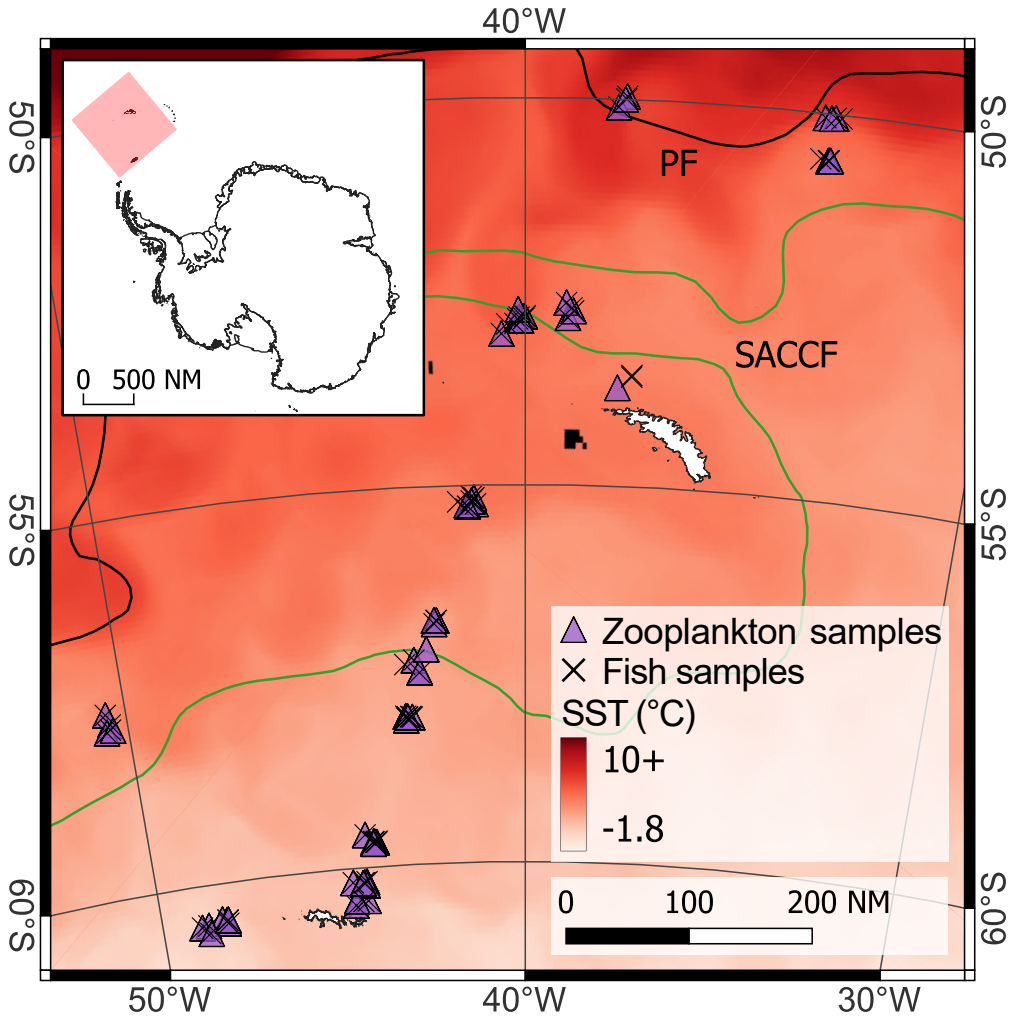

Figure 4.1: Map of the study region displaying the locations of myctophid (black crosses) and zooplankton (purple triangles) sampling stations. The interannual average position of key oceanic fronts are also displayed (PF = Polar front; SACCF = Southern Antarctic Circumpolar Current front). Temperature data represents the mean value from 15th March – 15th April 2009 from the Copernicus Global Ocean Physics Reanalysis (GLORYS12) (Jean-Michel et al. 2021). Map projection is WGS84/Antarctic Polar Stereographic.Black fill represents missing temperature data. Map produced using QGIS 3.28 Firenze.

4.2 Materials and methods

All data used in this study were collected following standard protocols and ethic approval from the British Antarctic Survey and the Environmental Protocol (1991) of the Antarctic Treaty.

4.2.1 Fish sampling

Myctophids were collected during three research surveys conducted in austral spring (JR161, Oct-Dec 2006), summer (JR177, Jan-Feb 2008) and autumn (JR200, Mar-Apr 2009) in the Scotia Sea in the Atlantic sector of the Southern Ocean. Fish were sampled at stations across a transect spanning the entire Scotia Sea, from the Antarctic Polar Front to the sea ice zone. The exact location of these stations varied between cruises but was similar across years, with a broad latitudinal range sampled during each cruise (Figure C1-C2). Sampling was conducted using a depth-stratified 25 m^2 rectangular mid-water trawl net (RMT25), deployed at depth ranges of 0-200, 200-400, 400-700, and 700-1000 m (Figure 4.1). The nets had a cod end mesh size of 5 mm. Hauls were conducted during both light and dark conditions in spring and summer, but only darkness during autumn, due to a reduced daylight period.

Fish were processed on-board and identified to species level where possible, with standard length (SL) measured to the nearest millimetre. A random subsample of 25 fish per species (or all individuals in the case of small catches) were set aside for stomach dissection. These stomach samples were then frozen at -20 °C for later laboratory analysis, where the stomach contents were thawed and identified to the lowest taxonomic level possible. For each stomach, the number of individuals and average weight of each prey taxon was recorded using a motion compensated balance. The resulting datasets can be accessed via the UK Polar Data Centre (Collins et al. 2020; Belcher et al. 2019).

For this study, fish SL was converted to mass in grams using species-specific length-weight equations from the British Antarctic Survey's long-term records (Table C1) for those individuals which did not have empty stomachs. This was done for ten species (see Table C1), while data for a further two species were omitted due to very low sample sizes (n = 7 for *Gymnoscopelus opisthopterus*, n = 1 for *G. piabilis*). The final datasets used in this study consisted of 3,707 prey records from 1,576 fish stomachs (Table C2), in addition to a larger set of fish body size estimates from 6,143 individuals (the majority without stomach content data; Table C3) and species-specific abundance estimates for each sampling location.

4.2.2 Zooplankton sampling

Macrozooplankton samples were collected from RMT25 nets, while mesozooplankton were sampled using paired Bongo nets (mesh size 50 μm), which were deployed to a depth of 400 m during daylight hours (Ward et al. 2012; Tarling et al. 2012a; Tarling et al. 2012b). Zooplankton samples were preserved in 4% formalin with seawater and analysed in the laboratory, with taxa identified to the lowest possible taxonomic resolution. The total wet weight (g) was calculated for each macrozooplankton taxon using a motion compensated balance and divided by the number of individuals to estimate the mean body mass for each taxon. Mesozooplankton taxa were assigned an average dry mass (DM, mg) from published sources, which were converted to wet mass (WM, g) using general DM to WM conversion factors in Atkinson et al. (2012). Abundance values for macro- and mesozooplankton (standardised to individuals m^{-2}) were calculated using the estimated area sampled by the nets. Copepods dominated the zooplankton community by abundance, constituting over 70% of total density on average across hauls, followed by polychaetes and chaetognaths and, to a lesser extent, pteropods and ostracods (Table C4). The original zooplankton data are as presented in (Tarling et al. 2012a) and can be accessed from the UK Polar Data Centre (Ward et al. 2020).

4.2.3 Environmental covariates

We extracted daily sea-surface temperature (SST) values for the coordinates of each station from the 1/12° gridded Copernicus Global Ocean Physics Reanalysis product GLORYS12V1 (Jean-Michel et al. 2021). To investigate the consistency of results at depth, we also extracted modelled temperature data from the GLORYS12V1 ~1062m depth bin, which is the closest match to the lower depth limit of the trawls. Temperature data were averaged for the 30 days prior to and including the day of sampling. To identify the potential influence of local productivity on myctophid feeding relationships, we also extracted surface chlorophyll-a (Chl-a) values from the Copernicus-GlobColour dataset, which has a spatial resolution of 4x4 km (Garnesson et al. 2019). As with the temperature data, daily Chl-a values at each station were averaged for the 30 days prior to and including the day of sampling. See Figure C3 for an overview of the relationship between temperature and latitude. The remaining methods refer to analyses involving SST but see Supplementary Information for an overview of the results of modelling with temperature at depth. We did not consider the effects of spatial heterogeneity in fishing effort as there is currently no targeted myctophid fishery in the Southern Ocean. Fish constitute the majority of bycatch by the winter krill fishery in the

Scotia Sea but appear to consist predominantly of members of the Channichthyidae and Nototheniidae (Krafft et al. 2023). Overall annual average bycatch weights across all bycatch taxa (0.1-51.3 tonnes) are low compared to the estimated biomass of mesopelagic fish in the Scotia Sea (~4.5 million tonnes) and would therefore be expected to have negligible impact on community structure (Krafft et al. 2023).

4.2.4 Statistical analyses

Linear mixed models (LMMs) were used to investigate the relationship between the environmental variables and multiple metrics related to myctophids and their prey, using the predator-prey body size dataset. PPMR was calculated as the body mass of each fish predator (g) divided by the abundance-weighted average prey mass (g) in its stomach. LMMs were fitted using the function 'lme' in the package 'nlme' (Pinheiro et al. 2023) with either PPMR, predator body mass, or abundance-weighted mean prey body mass as response variables (each subject to $\log_{10}$ transformation to meet the assumptions of normality, homogeneity, and independence of residuals). No strong collinearity was identified between SST and chl-a (Spearman's rho: -0.077, $p = 0.002$), therefore these were both entered as explanatory variables in the same model, including their interaction term. Model selection was then conducted to identify the best specification of fixed effects (SST and Chl-a) and random effects (nesting the variables 'year' and 'predator species'). The use of weighted variance structures to account for heterogeneity in residual variance by year or species was also investigated during model selection. The absence of spatial autocorrelation in model residuals was confirmed using Moran's I, therefore autocorrelation structures were not included in the models. The best model was determined by AIC comparison and visual diagnostics (heteroscedasticity and normality of residuals). All models incorporated a combined constant variance structure to account for heteroscedasticity in the errors within both year and predator species. The final selected models all included a random intercept for year and a random slope for SST by predator species. Chl-a had no significant main or interactive effects on the response variables and was therefore omitted from further analyses. See Table C5-C11 for an overview of the model selection process and Moran's I results for these models.

The selectivity of predators for different prey sizes was estimated by fitting kernel density distributions to the prey body masses identified in predator stomachs (realised distribution) and to the comparable range of prey body masses sampled from the environment (environmental distribution) (Gauzens et al. 2024). The environmental distribution represents the expected predator diet if feeding is based solely on density-dependent foraging, while the

realised distribution generally represents the combination of such neutral processes and the active selection for specific prey sizes (Gauzens et al. 2024). This approach assumes that the diets of these predators are generalist and primarily size-constrained, which is supported by previous studies of Southern Ocean myctophid diets (Cherel et al. 2010; Saunders et al. 2019). Using the ratio of the realised and environmental distributions, a preference distribution can be calculated, representing the selectivity of predators for different prey sizes. To link the predator diets to the distribution of potential prey sizes in the environment, we grouped predators and zooplankton samples which were collected in the same area and within a few days of one-another, resulting in a total of 24 separate sampling locations spanning the study region. Within these groups, we then aggregated predators from the same species into size-classes of $10^{0.05}$ g to ensure that enough prey were present in the combined diets to reliably estimate a density distribution, whilst ensuring there were enough data points for later analysis (n = 164). The final size classes ranged from $10^{-0.525}$ = 0.30 g to $10^{1.575}$ = 37.58 g. For each aggregation, an average temperature was estimated from the constituent stations. We used the mean value of the preference distribution for each size class to represent the average preferred prey size of predators at each temperature. We then used a LMM to investigate the relationship between preferred prey size and the interaction between temperature and predator size-class, following the same approach to model specification and selection as described above. The final model included random intercepts for year and predator species, and a combined variance structure for year and predator species (see Table C12-C13 for an overview of the model selection process).

To differentiate the potential individual-level and community-level mechanisms underlying trends in body size with temperature, we also conducted analyses of predator body size and community composition using a larger dataset of individual body sizes and species abundance estimates (n = 6,143). We fitted a Generalised Least Squares (GLS) regression model of species diversity (Shannon–Wiener (log e) diversity index) as a function of SST and Chl-a to investigate whether there was any change in community structure with environmental conditions. For this analysis, densities of each species caught during each haul were estimated by multiplying counts by the product of the distance towed multiplied by the nominal net mouth area (25 m^2), and then standardised to values of individuals per 1,000 m^{-3}. A square-root transformation was then applied to the density estimates to reduce the weighting of dominant species. An LMM was fitted to the relationship between body mass and the interaction between SST and Chl-a at the community level, before linear models of

body size and SST were fitted for each predator species individually, to identify whether community-level trends in size with temperature were present at the population level. The optimal model structure for each species-level analysis varied, and very low but statistically significant levels of spatial autocorrelation were identified for a small number of species and dealt with by incorporating spatial autocorrelation functions. See Table C14-C22 for model selection of the optimal variance weighting, random and fixed effects structures, Moran's I test results and implemented autocorrelation structures, and model outputs.

4.3 Results and discussion

PPMR declined by ~11% per °C increase in sea surface temperature (SST), associated with a significant decline in predator body size at a rate of ~6% per °C and no coherent trend in the mean body size of prey in the diet (Figure 4.2; Table 4.1). Chlorophyll *a* was initially used as a further explanatory variable but it was not significant in any model and was therefore excluded during model selection (Table C5-C11). The same general results were found when temperature at ~1000m (the estimated maximum of myctophid depth distributions) was considered instead of SST (Figure C4, Table C23Table C30). A similar decline in predator body size was also found when using a larger dataset of fish body masses (n = 6,143, the majority without stomach content data; Figure C5, Table C14-C16). In all, seven of the ten myctophid species also displayed significant declines in size with increasing temperature (Figure C6, Table C17-C19). Together, these results suggest that the decline in PPMR is associated with a greater decrease in the size of these predators relative to their prey as temperature increases.

The effect of declining PPMR on interaction strengths will depend on the interactive effects of temperature and body mass on metabolism and consumption (Kratina et al. 2022), making it difficult to predict the consequences for ecosystem stability. It has previously been found that temperature alters the directionality and shape of the relationship between PPMR and predator attack rate and prey handling time, with low PPMR destabilising community dynamics under warming due to elevated predation rates at low prey density (Kratina et al. 2022). Additionally, when declines in body mass under warming are restricted to isolated trophic levels, community stability is expected to be reduced (Sentis et al. 2017), possibly due to lower top-down control of prey populations (Shackell et al. 2010). However, while the reduced ingestion efficiencies and higher metabolic costs associated with higher temperatures are expected to make predator populations increasingly vulnerable to starvation, this effect is exacerbated under high PPMRs (Rall et al. 2009), therefore the observed decline in predator

size with warming may in fact provide a buffer against population crashes. Ultimately, the effects of warming and PPMR on the strength of interactions will depend on factors including predator and prey identity, predator body size, and thermal tolerance. Further investigations of the combined effects of temperature and PPMR on interaction strengths will be important for determining the possible consequences of altered size-structuring of predator-prey interactions for the stability of ecological communities. This could be facilitated through the application of ecosystem flux or dynamical population models (Gauzens et al. 2019; Sohlström et al. 2021).

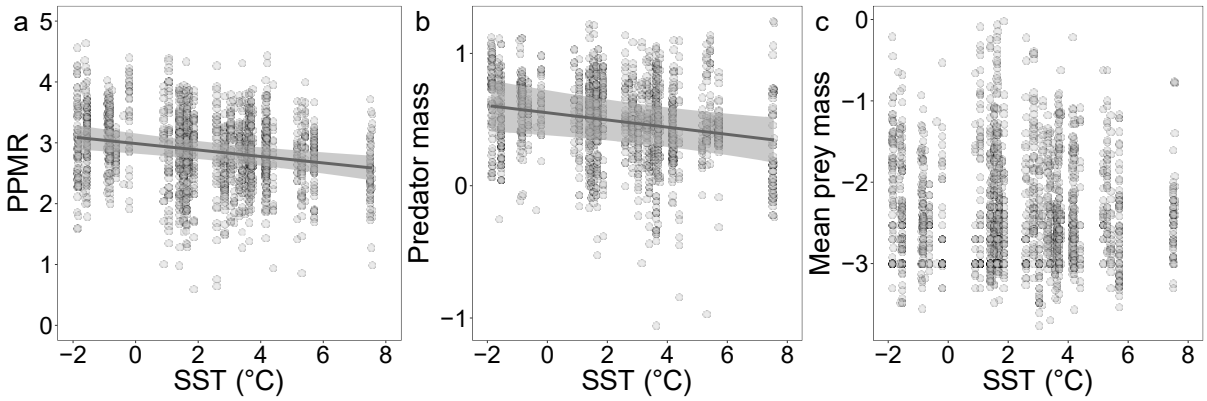

Figure 4.2: Effects of temperature on predator and prey body mass. (a) partial residual plot from a linear mixed model of the effect of sea-surface temperature (SST) on prey-averaged predator-prey mass ratio (PPMR); (b) partial residual plot from a linear mixed model of the effect of SST on predator body mass; (c) scatterplot of the relationship between SST and abundance-weighted average prey mass in predator stomachs. Y-axis values are in $\log_{10}$ g. Lines represent predicted values at each SST. Shading represents 95% confidence intervals.

Table 4.1: Model statistics for the effect of temperature on predator and prey body masses. Output from linear mixed models with predator-prey mass ratio (PPMR), predator body mass and abundance-weighted average prey body mass in predator stomachs as response variables (all $\log_{10}$). SST represents sea-surface temperature. R^2m and R^2c represent the Nakagawa's marginal and conditional model R^2 values, respectively.

Model	Coefficient	Estimate	SE	DF	t-value	p-value
PPMR	Intercept	2.988	0.085	1550	35.251	<0.0001
	SST	-0.053	0.015	1550	-3.601	0.0003
$R^2m = 0.049$, $R^2c = 0.493$						
Predator body mass	Intercept	0.552	0.087	1550	6.346	<0.0001
	SST	-0.027	0.011	1550	-2.482	0.0132
$R^2m = 0.024$, $R^2c = 0.978$						
Mean prey body mass	Intercept	-2.371	0.069	1551	-34.249	<0.0001
$R^2m < 0.001$, $R^2c = 0.455$						

The observed decline in predator size with increasing temperature fits the wider expectation that a primary response of ectotherm vertebrates, including Southern Ocean myctophids, to warming should involve a reduction in individual body size and shifts in overall community size structure (Deutsch et al. 2022; Rubalcaba et al. 2020). Declines in size at the individual level are thought to facilitate continued persistence with warming by minimising the extent to which metabolic rate must increase to match the greater energetic demands of the environment (Riemer et al. 2018). Changes in community size structure may also be the result of a combination of physiological and competitive processes which result in species of a certain size range becoming dominant (Gjoni et al. 2023). There was a significant increase in Shannon diversity of the myctophid community with increasing SST, associated with a shift in species abundances from communities dominated by a few large-bodied species (e.g. *Electrona antarctica*) at cold high latitudes to a more even distribution of abundances in the more northerly warmer regions (Figure C7, Table C20-C22), as previously documented (Collins et al. 2012). This indicates that the link between temperature and body size at the community level may be driven in part by community assembly processes which select for species of different sizes as it becomes warmer, e.g. smaller predators are able to outcompete larger ones under the altered prey size distribution and relatively lower metabolic demands. However, our analyses of the relationship between body mass and SST at the population level

also revealed significant declines in size with increasing temperature for many of the myctophid species, both for large-bodied taxa such as *E. antarctica* and for small species like *Krefftichthys. anderssoni* (Figure C6, Table C17-C19). The observed trends at the community level therefore are not explained by community assembly processes alone, but also by temperature effects on populations, likely mediated by physiological responses to warming.

Under both moderate and high emissions scenarios, Antarctic waters are expected to become increasingly favourable for smaller, sub-Antarctic myctophid species, likely altering community diversity and size structure (Freer et al. 2019). Such changes may reduce their suitability as prey for predators such as penguins and seals, with knock-on effects on these higher predator populations and food web dynamics (Murphy et al. 2007). Additionally, many myctophid species display size-selective feeding, with a switch from euphausiids and fish to smaller copepods as their body size decreases (Saunders et al. 2019). Thus, a reduction in the average size of myctophids may alter the diversity and size distribution of the prey community as predation rates on different species change (Rudolf 2012; Ives et al. 2004). Furthermore, smaller species are generally expected to have fewer feeding interactions across a more restricted range of trophic levels, which could alter the distribution of energy flow by reducing network complexity and trophic redundancy (Brose et al. 2017).

To investigate the evidence for size-selective feeding behaviour that could further underlie the decline in PPMR with temperature, we conducted an analysis of dietary size preferences for prey in the environment in relation to predator body size class and temperature (see Methods). Predator size and SST had a significant interactive effect on preferred prey size, with small predators feeding on relatively larger prey and large predators feeding on relatively smaller prey in warmer regions (Figure 4.3a; Table 4.2). This partially supports hypothesis 2, that predators will select for larger prey in warmer environments, but not for the largest fish. This result may be explained by an increase in the relative abundance of intermediate prey sizes within the range of body masses commonly consumed by the fish (Figure 4.3b).

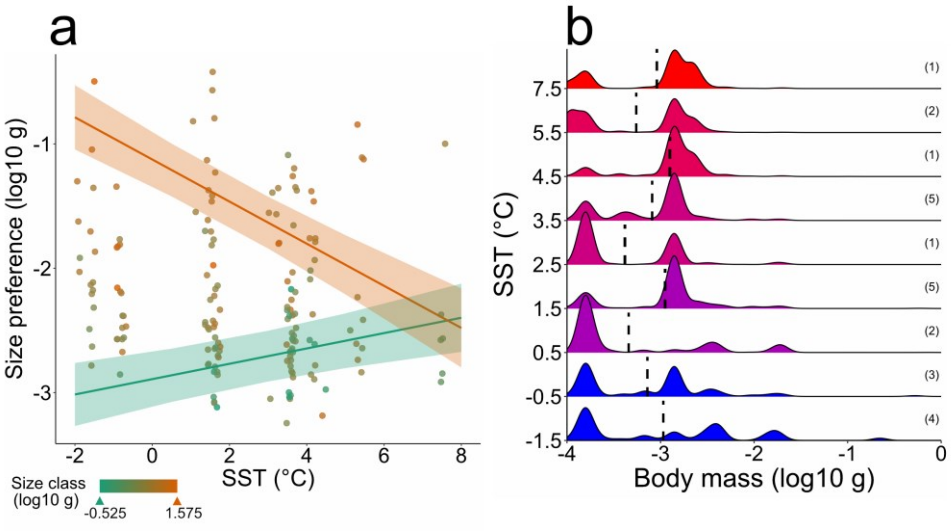

Figure 4.3: Predicted interactive effect of SST and fish size class on myctophid average preferred prey size. Lines represent predicted values at each SST, for the largest and smallest predator size classes. Shading represents 95% confidence intervals. Points are coloured according to size class, jittered slightly for clarity. (b) Density plots of zooplankton body mass distribution in the environment within size range commonly consumed by the myctophids, grouped into 1 °C temperature bins. Dashed lines represent abundance-weighted average body mass. Y-axis indicates central temperature value for each bin. Values in brackets indicate number of hauls. Note: in panel b, large prey sizes (above approx. −2 $\log_{10}$ g) are present at all temperatures but extremely low abundance relative to smaller organisms prevents them from being visible.

Table 4.2: Model statistics for the effect of temperature on predatory size preferences. Output from a linear mixed effects model with mean preferred prey size ($\log_{10}$) as the response variable and sea-surface temperature (SST) and predator size class ($\log_{10}$) as explanatory variables. R^2m and R^2c represent the marginal and conditional model R^2 values, respectively.

Coefficient	*Estimate*	*SE*	*DF*	*t-value*	*p*
Intercept	-2.460	0.194	139	-12.673	<0.0001
SST	0.006	0.021	139	0.295	0.7681
Size class	0.848	0.109	139	7.795	<0.0001
SST*Size class	-0.110	0.031	139	-3.483	0.00071
R^2m = 0.298, R^2c = 0.801					

Our results suggest that temperature influences the size-structuring of feeding relationships within the Southern Ocean mid-trophic community through a combination of density-dependence and active selection. Under colder conditions, large predators appear to select for relatively abundant, large, energetically valuable prey while small predators feed on small prey. Under warmer conditions, the shift in the distribution of suitable prey sizes towards intermediate body masses restricts the feeding behaviour of large predators and forces them to feed sub-optimally on smaller prey while small predators actively select for these abundant intermediate prey sizes, possibly because they provide greater per capita energy intake. This reduction in prey size diversity could constrain the foraging niches of smaller and larger predators, increasing competition and, under the general expectation that food web complexity promotes predator population stability (Petchey 2000), potentially destabilising predator-prey dynamics. Larger predators may also be forced to feed on prey that are smaller than their optimal foraging niche, thus preventing them from meeting their higher energetic demands under warmer conditions. These changes in size-selectivity may also explain the increasing prevalence of smaller myctophid species in warmer regions (Figure C7), as they can capitalise on the available prey field and outcompete their larger counterparts. The increasing dominance of smaller myctophids, which feed preferentially on larger prey in warmer regions, is likely to drive the observed decline in overall PPMR across the predator community. Thus, we suggest that the observed patterns in myctophid size and foraging with temperature are likely to be the result of a combination of interacting processes acting at both the population and community levels, and we encourage further efforts to disentangle them. Overall, our results highlight the importance of considering the size structuring of biotic interactions and plasticity of size-based foraging behaviour when investigating the possible consequences of environmental change for community structure and composition.

We investigated a temperature gradient across a large spatial scale (>10° of latitude) rather than directly testing the effects of temperature change over time. Such temporal changes are difficult to investigate in-situ, but mesocosm experiments could provide insight into how rapid warming affects species body sizes and biotic interactions. However, the results of such studies primarily relate to the plastic responses of individuals over the short-term, which may differ from the adaptive responses of populations to sustained gradual warming over the multi-decadal timescales that are relevant to ongoing climate change. In contrast, given the historically stable temperatures of the Southern Ocean (Morley et al. 2020), our space-for-time substitution represents the long-term eco-evolutionary adaptation of predator and prey

communities. One potential caveat of our approach was the use of sea-surface temperatures to represent the environmental conditions experienced by the myctophids, as temperatures at depth may differ from those at the surface. Indeed, while a positive relationship between latitude and temperature is still apparent at approximately 1,000m depth, the trend is weaker than at the surface (Figure C5). When substituting SST with the temperature at depth in our analyses, however, the results are consistent (Figure C4, Table C23-C30), suggesting that the observed relationships hold across the depth range that myctophids are thought to inhabit.

As our oceans continue to warm, significant changes to the size structuring of marine communities are likely to occur in many regions, and the use of dietary preference analyses such as this will be useful for disentangling the interactive effects of behaviour and physiology on the feeding ecology of key species and functional groups. Myctophids are one of the most abundant fish families globally and a major component of many pelagic food webs, from the poles to the tropics (Morley et al. 2020; Chaudhary et al. 2021). The insights gained in this study therefore have relevance for other open ocean systems, including those near the equator where warming is expected to drive strong declines in body size and changes to the distribution of many mesopelagic species (Chaudhary et al. 2021; Lefort et al. 2015). Changes in species composition with temperature may also alter community PPMR in unexpected ways, as it has previously been found that the relationship between individual body mass and PPMR varies between taxa, due to factors such as morphology and feeding strategy (Reum et al. 2019). It will therefore be important to expand these analyses to other regions and taxa to provide an overview of the generality of the observed relationships.

Rising metabolic costs and oxygen limitation resulting from ocean warming are expected to drive declines in the body size distribution of many marine ectotherms (Deutsch et al. 2022; Forster et al. 2012), and we sought here to investigate the potential consequences for the size-structuring of species interactions. Using an extensive dataset spanning a large latitudinal range, we have shown that increasing temperature is associated with changes in body mass and dietary size-selectivity across Southern Ocean myctophids, a key component of pelagic food webs, resulting in predator communities that are closer in size to their prey. As a result, warming might alter prey population dynamics and reduce top-down control, potentially reducing community stability. The shift in predator-prey size relationships could also drive a reduction in the diversity of predator-prey interactions and a loss of redundancy within ecological networks, which may reduce their resistance to perturbations. The trends identified in this study provide a basis for mechanistic models to investigate the potential consequences

of warming scenarios for the structure of biotic interactions and the stability of ecosystems. Efforts to investigate these relationships in other regions and for other taxa will aid the search for macroecological patterns that can be used to predict ecosystem responses to climate change.

5 Trade-offs between the recovery of Southern Ocean baleen whales and conservation of their competitors

In preparation for *PNAS*

Abstract

The historical over-exploitation of Southern Ocean baleen whales is thought to have resulted in the reorganization of food webs and the expansion of competitor populations such as seals and penguins. Many whale populations are now recovering, leading to uncertainty for the impact this will have on their krill-feeding competitors, which are themselves a focus of conservation efforts. We used a circumpolar suite of standardized regional Ecopath models to explore the potential ecological trade-offs associated with increases in baleen whale populations. There was variation in the capacity of ecosystems to support increases in whale consumption while also sustaining competitor populations at close to their contemporary estimates. Under median estimates of daily krill consumption by baleen whales, only limited increases in whale biomass were possible without major reductions in competitor populations, although the impacts of whale population recovery would be mitigated under plausible future increases in primary production. We identified that the level of unexploited production by whale prey, alongside the degree of dietary overlap between whales and their competitors, are associated with the ecosystem capacity to support whale population increases and could be used to guide decision-making in relation to the implementation of regional conservation actions. Ultimately, it must be recognized that contemporary and future Southern Ocean ecosystems may have reduced capacity to sustain higher trophic levels, resulting in strong trade-offs between conservation objectives.

5.1 Introduction

Southern Ocean ecosystems are complex and diverse, supporting a variety of vital services including provisioning, biogeochemical processes and nutrient cycling (Cavanagh et al. 2021). Many species there are unique and endemic, with large populations of marine mammals and seabirds sustained by a variety of mid-trophic taxa ranging from copepods to Antarctic krill (*Euphausia superba*) and highly abundant demersal and pelagic fish (Queirós et al. 2024). Over the past two centuries, however, Southern Ocean ecosystems have been considerably impacted by anthropogenic activities including the exploitation of seals and whales and the more recent harvesting of finfish and Antarctic krill (Miller 1991; Kock et al.

2007). Climate change is also affecting the Southern Ocean, with regional warming and shifts in sea ice extent and duration, which could negatively impact the distributions and population dynamics of species such as krill and emperor penguins (*Aptenodytes forsteri*) (Auger et al. 2021; Meredith et al. 2019; Fretwell et al. 2023). Widespread increases in productivity are also predicted for various regions, but shifts in the phytoplankton community size structure may have negative consequences for ecosystem function by driving changes in the composition of zooplankton communities, with a dominance of salps resulting in reduced efficiency of energy transfer to higher predators (Kawaguchi et al. 2024; Pinkerton et al. 2021; Queirós et al. 2024). If we are to implement effective management strategies, it is imperative that we understand the implications of past and future ecological shifts and the possible trade-offs that may be required to achieve conservation goals.

The exploitation of baleen whales during the 20th century represents possibly the most extensive human impact on Southern Ocean ecosystems to date, resulting in the severe depletion of many species including blue (*Balaenoptera musculus*), humpback (*Megaptera novaeangliae*), fin (*B. physalus*) and sei (*B. borealis*) whales (Christensen 2006; Mori and Butterworth 2006). These predators exert significant top-down control over Antarctic krill, zooplankton and fish populations (Tulloch et al. 2019; Bury et al. 2024), and the rapid decline of the whales will almost certainly have altered energy flow through regional food webs. For example, the release of Antarctic krill from whale predation is hypothesised to have resulted in a krill biomass 'surplus' which was then rapidly consumed by other predators including seals and penguins, increasing their populations (Laws 1977). Ecological modelling has provided some limited support for this hypothesis, although this is dependent on relatively high and stable levels of primary productivity (Surma et al. 2014). The contemporary average total Antarctic krill biomass in the Southern Ocean is estimated to be below 400 million tonnes (Atkinson et al. 2009; Kawaguchi et al. 2024), far lower than the 600-900 million tonnes estimated to be required to sustain unexploited baleen whale populations (Smetacek and Duarte 2008; Surma et al. 2014). Such high Antarctic krill biomass may historically have been sustained by elevated primary production driven by biological nutrient cycling, as whales fertilized surface waters with limiting elements such as iron and thereby promoted krill population growth (Nicol et al. 2010; Ratnarajah et al. 2016). The viability of such whale-driven surface fertilization for sustaining Antarctic krill populations is, however, unclear (Maldonado et al. 2016), and observed regional declines in the biomass of Antarctic

krill over the 20th century may have been driven more by temperature-related changes in spawning habitat quality (Yang et al. 2020; Atkinson et al. 2022).

Since the ongoing moratorium on commercial whaling began in 1985, some whale populations have begun to recover but many remain well below their estimated pre-exploitation levels and there is a widespread desire to see further whale biomass recovery (Zerbini et al. 2019; Tulloch et al. 2019; Calderan et al. 2020; IWC 2024). It is unclear, however, whether contemporary Southern Ocean ecosystems can support large increases in baleen whale populations. A key uncertainty is the extent to which population recovery might come at the expense of competitor groups for krill such as seals, penguins and fish, which may have experienced competitive release as a result of whaling. Newly revised estimates of baleen whale daily consumption rates, which may in fact be up to three times greater than previously thought (Savoca et al. 2021), suggest that the extent of this potential release may also have been greater than previously assumed. Such high consumption rates mean the influence that these whales exert over key prey such as Antarctic krill is also very high, and, under limited prey availability, their population recovery may therefore require particularly large compensatory decreases in competitor populations. Two core objectives of the international convention governing conservation in the Southern Ocean are to maintain the ecological relationships between species and restore depleted populations (Constable 2011). Given the likely competitive relationships between higher trophic level groups, these objectives may well be in conflict if the goal is to conserve Southern Ocean ecosystems as they are now whilst also restoring whale populations. It is therefore important that we explore the possible implications of baleen whale population recovery for the dynamics of their competitors. This will provide insight into the likely conservation outcomes that are feasible under future conditions and could help guide regional management actions.

Food web models provide a tool for understanding how the structure and dynamics of regional ecosystems might respond to press perturbations such as sustained changes in the abundance of certain taxa (Montoya et al. 2009). In particular, the Ecopath framework is often used to model the structure of trophic interactions and energy flow in aquatic food webs, which can be used to test management scenarios or explore the effects of environmental changes (Christensen and Walters 2004; Heymans et al. 2016). Ecopath models have been developed for a variety of locations around the Southern Ocean, ranging from subantarctic areas such as South Georgia and the Prince Edward Islands to high latitude regions like the Antarctic Peninsula and Ross Sea (McCormack et al. 2021a). This suite of

models represents a powerful resource for exploring regional similarities and contrasts in ecosystem structure and function (Hill et al. 2021). In this study, we use six regional Ecopath food web models in conjunction with a novel objective balancing approach to explore the potential ecological trade-offs resulting from the recovery of Southern Ocean baleen whale populations. Our analysis incorporates the full range of plausible whale prey consumption rates, and assesses the compensatory changes in system productivity required, which might result from a combination of climate change and whale-mediated nutrient recycling. Using the Ecopath framework allows us to explore some of the possible mechanisms underlying the capacity of different models to support increased whale populations. A key parameter in Ecopath models is the ecotrophic efficiency (*EE*) of each group, which ranges from zero to one and represents the extent to which their biomass production is consumed within the system, with lower values indicating greater 'spare' production which could potentially support increases in consumption. As a result, models with generally low *EE*s for baleen whale prey groups might be expected to have a greater capacity to support increases in baleen whale consumption without affecting other functional groups, when compared with models that have generally high *EE*s. Additionally, the degree of overlap in the consumption of prey groups by baleen whales and their competitors could also determine the capacity of the model to support increases in whale consumption. If the competitive overlap in prey consumption is high, we expect to see a greater degree of negative coupling between populations of whales and their competitor groups, as increases in consumption by whales require relatively larger compensatory changes in competitor biomasses.

In this study, we implemented two scenarios to investigate the possible consequences of baleen whale population recovery. Firstly, we explored the capacity of contemporary food webs to support increasing whale populations by estimating the consequences for competitors in the absence of compensatory changes in system productivity. This also included an investigation of the influence of different whale prey consumption estimates on the rates of competitor biomass change. Secondly, we explored the levels of system productivity that are necessary to support increased whale populations while maintaining contemporary competitor populations.

5.2 Materials and methods

5.2.1 Modelling framework

This study makes use of the Ecopath modelling framework, which is used to construct food web models that meet the assumption of mass-balance, whereby the energy outputs of a group do not exceed their inputs (Christensen and Walters 2004). As discussed in chapter 1, Ecopath models represent a specific time period (often a year), with nodes in the food web representing single life stages, species or, more commonly, aggregated functional groups. The key parameters required are the biomass (*B*), diet composition by weight (*DC*), production per unit biomass (*P/B*), consumption per unit biomass (*Q/B*), and assimilation efficiency (AE) of each group, although parameters representing biomass accumulation rates, fishery catches and discards, and migration rates can also be supplied (Christensen and Walters 2004). These form the basis of linear equations describing the production of each group in terms of their other parameters and those of their consumers. A key parameter which is often an output of Ecopath models is the ecotrophic efficiency (*EE*), representing the proportion of the production of each group that is used in the system. Values range from zero (limited to top predators that are not fished) to one (100% of production is consumed by other groups in the model).

The initial parameterisation often results in an unbalanced model, and *EE* values greater than one can be used to identify problematic groups with mortality rates that cannot be sustained by production rates. The most common method of balancing an Ecopath model involves an iterative process of manual adjustments to group parameters, focussed on unbalanced groups and their consumers, until balance is achieved (Heymans et al. 2016). Often, the main parameter that is adjusted is the diet composition as this is often the most uncertain, followed by biomass and energetic rates (*P/B* and *Q/B*). This process can be time-consuming with many unbalanced groups and may be subjective as the choice of groups and parameters to adjust, and the magnitude and direction of those adjustments ultimately depend on the ecological understanding and decisions of the modeller. The balancing process must therefore be extremely well documented if the results are to be reproducible, and can be aided by following thermodynamic principles such as ensuring that the growth efficiencies (*GE*) of groups fall within expected values (Heymans et al. 2016). To reduce the subjectivity of the balancing process and facilitate the generation of multiple versions of the same model to account for parameter uncertainties, efforts have been made to develop various automated balancing algorithms. These range from using the built-in Ecopath Monte-Carlo routine to

randomly generate alternative balanced parameter sets from a single balanced input model (Steenbeek et al. 2018), conducting an exhaustive random search of possible parameter combinations that generate a thermodynamically viable (but not necessarily balanced) model (Aydin et al. 2005), and making targeted adjustments to unbalanced groups to 'push' the model into balance (though this method was removed after Ecopath version 5.1) (Kavanagh et al. 2004). These methods all rely on a data 'pedigree' approach, whereby the uncertainties around parameter estimates are quantified and used to put bounds on the range of possible values (Heymans et al. 2016).

In this study, we needed to generate a large ensemble of balanced models from a set of initial unbalanced input models. This meant that the approaches of Steenbeck et al. (2018) (which uses a balanced input model) and Aydin et al. (2005) (which generates thermodynamically viable, but not necessarily balanced parameters sets) were not suitable. However, the approach of Kavanagh et al. (2004), whereby targeted adjustments are made solely to groups out of balance, was also undesirable as it fails to incorporate uncertainty around the parameters for balanced groups. As a result, we developed a bespoke balancing algorithm and used this to generate 1000 versions of each regional model, to explore the effects of perturbation across a range of plausible alternative model parameterisations (see Model balancing).

Our analytical approach in this study involved a number of sequential steps, from the standardisation and balancing of a set of published models to the implementation of perturbation scenarios. The major steps are conceptualised in Figure 5.1 and detailed below.

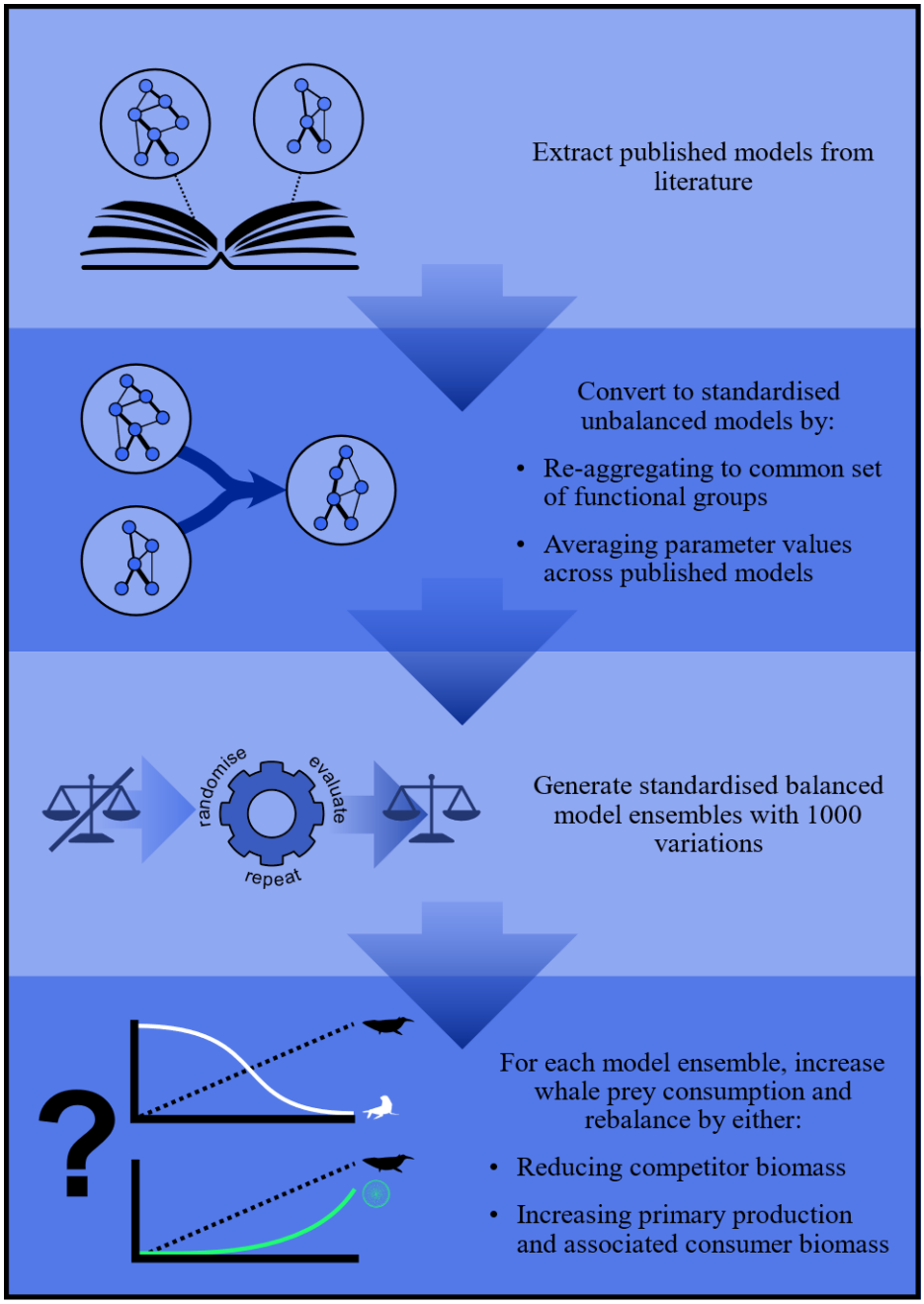

Figure 5.1: Conceptual diagram illustrating the main steps that make up the methods and analyses in this study.

5.2.2 Regional Ecopath models

We selected six published Ecopath-type food web models, each developed independently by a different group of researchers and representing a different region of the Southern Ocean: The South Georgia shelf (SG; Hill et al. 2012); Ross Sea (RS; Pinkerton and Bradford-Grieve 2010); Prince Edward Islands (PE; Gurney et al. 2014); Kerguelen Plateau (KP; Subramaniam et al. 2019); Prydz Bay (PB; McCormack et al. 2020); and West Antarctic Peninsula (AP; Dahood et al. 2019). The model locations are mapped in Figure 5.2 and an

overview of the key characteristics of each model is provided in Table 5.1. Each of these models represents the feeding interactions between a set of functional groups (either individual species or aggregates based on taxonomy, size or other aspects of their ecology), and provides the key parameters necessary to estimate energy flows within the system.

Table 5.1: Key characteristics of each of the six published Ecopath models used in this study.

Region	**South Georgia (SG)**	**West Antarctic Peninsula (AP)**	**Ross Sea (RS)**	**Prince Edward Islands (PE)**	**Kerguelen Plateau (KP)**	**Prydz Bay (PB)**
Ocean basin	South Atlantic	South Atlantic	Pacific	Indian	Indian	Indian
Latitudinal group	Subantarctic	Antarctic	Antarctic	Subantarctic	Subantarctic	Antarctic
Ecosystem type	Island shelf	Continental shelf	Continental shelf	Island shelf	Island shelf	Continental shelf
Extent	Shelf area between coastline and 1000m depth contour. Approximately 55°S, 36°W	CCAMLR Statistical Subarea 48.1 (approximately 60-70°S and 50-70°W)	Shelf area between 160°W and 170°E, from 3000m depth contour to permanent ice shelf	200NM radius with centre at 46°46′S, 37°51′E	Between 45-56°S and 60-80°E	From 60°S to the Antarctic continent, and 60-90°E
Area ($km^{2)}$	45,530	630,279	637,000	431,014	1,720,348	1,433,028
Biomass units	Grams wet mass km^{-2} y^{-1}	Grams wet mass km^{-2} y^{-1}	Grams carbon m^{-2} y^{-1}	Grams wet mass km^{-2} y^{-1}	Grams wet mass km^{-2} y^{-1}	Grams wet mass km^{-2} y^{-1}
Modelling purpose	Identify data inconsistencies. Investigate the trophic roles of krill and copepods. Explore future scenarios of reduced krill abundance.	Describe dynamics of monitored and declining species. Evaluate how sea-ice cover explains variations in species biomasses.	Describe food web structure excluding current commercial fisheries.	Guide decision-making around ecosystem management. Separate models generated to represent ecosystem state in 1960s, 1908s and 2000s	Expansion of existing model (Subramaniam et al. 2019) to include Heard and McDonald Islands. Provide an overview of ecosystem structure for the entire plateau including fisheries.	Identify energy pathways through mesopelagic groups (fish, krill, squid). Identify keystone species. Explore the ecosystem implications of future climate scenarios.
Modelling period	2000-2010	Nominally 1996, with biomass data from 1992-2002	1990-2000	Various, but 2000s model used here	1990s-2000s	Period around 2016
***N* functional groups**	31	35	38	37	28	28
***N* baleen whale groups**	1	4	2	0	1	2
Published model versions	Parameters: Balanced and unbalanced Diets: Balanced and unbalanced	Parameters: Balanced Diets: Balanced and unbalanced	Parameters: Balanced and unbalanced Diets: Balanced and unbalanced	Parameters: unbalanced Diets: Balanced and unbalanced	Parameters: Balanced and unbalanced Diets: Balanced	Parameters: Balanced and unbalanced Diets: Balanced and unbalanced
Degree of system closure	External feeding by some predators represented by additional functional groups	Closed system	Export of production represented for migratory mammals	Closed system	Closed system	Closed system

5.2.3 Model standardisation

A key issue when using multiple models from disparate sources is that many of the assumptions and decisions made when compiling the associated data and structuring the models are dependent on the objectives of the study and preferences of the authors. This means that models are not necessarily directly comparable, as they may include differences in the number of functional groups and levels of functional group aggregation and in the approach taken to estimate energetic parameters, which may influence their outputs (Pinnegar et al. 2005; Heymans et al. 2016). Standardising the energetic parameters and the number and identity of functional groups between models is therefore a key step in comparing different models (Hill et al. 2021). The following subsections describe how model standardisation was conducted in this study.

Standardisation of units

Five of the selected models expressed biomass in units of wet mass (gWM $m^{-2}y^{-1}$) while one (RS) used units of organic carbon (gC $m^{-2}y^{-1}$). To standardize the model units, we converted the RS model to gWM $m^{-2}y^{-1}$ using literature-derived conversion factors for the major functional groups (Table D1). The biomass of each group was scaled using the relevant conversion factor, while *P/B* is unitless and therefore does not need conversion. *Q/B* was converted following the equation:

$$\frac{Q}{B_{W,i}} = \frac{\sum_{z=1}^{n} Q_{C,i,z} / CF_z}{B_{C,i}/CF_i}$$

where $Q/B_{W,i}$ represents the *Q/B* of group i in wet mass, $Q_{C,i,z}$ represents the consumption of prey z by predator i in carbon mass, $B_{C,i}$ represents the biomass of predator i in carbon mass, and CF_i and CF_z are the conversion factors for the predator and prey, respectively.

The diet composition of each predator was converted from proportion carbon to proportion wet weight of each prey consumed using the equation:

$$D_{W,i,z} = \frac{Q_{C,i,z}/CF_z}{\sum_{z=1}^{n} Q_{C,i,z} / CF_z}$$

whereby $D_{W,i,z}$ is the proportional contribution in wet weight units of prey z to the diet of predator i. The diet of each predator is expressed in terms of consumption ($Q_{W,i,z}$) by multiplying the diet matrix ($D_{W,i,z}$) by the consumption parameter Q of the predator:

$$Q_{W,i,z} = D_{W,i,z} \times \frac{Q}{B_{W,i}} \times B_{W,i}$$

Re-aggregation of functional groups

Where possible, we combined existing groups in each model to generate a subset of comparable groups, but in some cases, groups were disaggregated to ensure that our new set of models all explicitly represented the same key groups (see Appendix D1 for a detailed description of the reaggregation steps applied to each functional group). Our final aggregation scheme included 21 functional groups overall, though not all of these were included in each model (Table D2). We retained a few regional contrasts representing genuine ecological differences in the groups present between models (e.g. presence of sea ice algae in high-latitude models, absence of Antarctic krill in low-latitude eastern Antarctic models). Four of the original models explicitly included bacterial groups and we retained these but did not add bacterial groups to models which did not already include them, to avoid introducing further subjectivity through our decisions surrounding the parameterisation of this group.

Diets were reaggregated following Hill et al. (2021) by expressing the diet of each consumer in terms of their reaggregated prey groups, calculating a consumption-weighted average for each prey item across the constituent consumers, and then rescaling the resulting values to sum to one. We opted to use the balanced diet matrices for this as, in some cases, the unbalanced matrices were missing important prey groups from the diets of some consumers, which caused unwanted behaviour during the later balancing process. The SG model incorporated off-shelf (beyond the model boundary) feeding by some groups, which we removed to improve standardisation between models. To do so, we redistributed the diet composition of affected consumers across their relevant on-shelf prey groups. We also reduced the biomass of these consumers appropriately to reflect the reduction in available energy from solely on-shelf feeding. As a result, our model for SG represents the ecosystem structure, including top predator populations, that can be supported by on-shelf feeding alone. The published RS model incorporates export of migratory mammal production, representing emigration of individuals, but for the purposes of consistency with the other models we omitted these export parameters to model this as a closed system.

Representation of baleen whales

We modelled baleen whales as three functional groups: humpback whales, minke whales and "other baleen whales". These groups were determined primarily based on their diets as,

2195 across models, humpbacks and minkes consumed a greater proportion of fish compared to the
2196 remaining whales which are more dependent on krill and other zooplankton. Humpback and
2197 minke whales also display some ecological differences in foraging, the former preferring
2198 open-ocean regions and the latter often feeding in the sea-ice zone (Bombosch et al. 2014),
2199 therefore these groups were kept separate. One model (PE) did not include any baleen
2200 whales, and another (KP) only included southern right whales and fin whales. In both cases,
2201 the exclusion of other whale species was due to their low contemporary occurrence in the
2202 model regions (Gurney et al. 2014; Subramaniam et al. 2020). The missing whale groups
2203 were added to these models but represented initially with negligible biomass to minimise the
2204 impact of this addition on the structure of the initial models. The addition of new whale
2205 groups to these models required the estimation of relevant diet matrices. To ensure that the
2206 initial consumptive impact of whale groups was comparable between models, we averaged
2207 the diets of each baleen whale group across models where such diet information was
2208 available and used the resulting averages as inputs across all models. The only exception to
2209 this was our treatment of krill. Antarctic krill were absent from two models (PE and KP –
2210 these only included 'other krill'), which meant that simply applying an average whale diet
2211 across models was not appropriate. Instead, to apply a consistent approach to diet
2212 standardisation which accounted for fundamental differences in prey distributions, we
2213 combined Antarctic krill and 'other krill' into a single group in each model, conducted our
2214 averaging, and then split these groups apart in proportion to their relative biomass in each
2215 model. This meant that the overall proportion of krill in whale diets was the same across
2216 models, but the relative proportion of each krill group varied based on their underlying
2217 biomass estimates for the relevant model regions (Table D3).

2218 Three of the original models included fishery takes: the KP model incorporated icefish and
2219 toothfish catches, the PE model included toothfish fishery, and the AP model incorporated
2220 krill fishery landings. The SG model does not incorporate fishery removals despite there
2221 being commercial catches of fish and krill around the shelf, as these removals are estimated
2222 to represent only 1% and 7% of input production estimates for these groups (Hill et al. 2012).
2223 For consistency, we excluded all fisheries catches and by-catch from models.

2224 *Standardisation of rate parameters*

2225 To standardise the input energetic parameters (*P/B* and *Q/B*) of each aggregate group, we
2226 averaged the values for each relevant reaggregated functional group across all models for

which an independent estimate was available. Where possible, we used the unbalanced parameter estimates for these calculations, to minimise the potential influence of changes to these input parameters made by the respective model authors during the balancing process. The exception to this was the AP model for which only balanced biomass and rate parameter estimates were available.

5.2.4 Catch-derived estimates of plausible whale biomass

We used catch records from the International Whaling Commission (IWC) to generate region-specific upper estimates of plausible biomass for each whale group (henceforth 'limit biomass'). These data provide information on species and length of whales caught during the 20th century, at spatial resolutions ranging from the nearest degree to the nearest minute or only approximate to the nearest 5- or 10-degree grid cell, depending on the expedition.

To estimate an upper limit to the total biomass of whales in each model, we aggregated catches for each whale group within a 1000km buffer around each study region (Figure D1). This assumes that all individuals within this buffer are capable of spending time in the model area, which is a reasonable assumption for such wide-ranging animals. To estimate the biomass of each whale group, we first converted length records to mass using published length-weight relationships for each species (Lockyer 1976). We assumed that each whale group spends only part of the year feeding in each region, given their migratory nature. Some models (RS, PB and KP) already provide estimates of residence time, while for the others we assumed a 90-day feeding period in the region which, according to Savoca et al. (2021), represents the lower limit of the most likely annual feeding period for individuals. By combining the total biomass, residence time and the spatial area of the model regions, we estimated the annual biomass per unit area for each whale group in each model. By adding the contemporary values from the models, we identified an upper estimate of plausible pre-exploitation whale biomass for each model region. These steps are illustrated in the following equation:

$$B_{pre,i} = \frac{\sum_{i=1}^{n} B_{catch,i} \times t_i}{area} + B_{current,i}$$

Where $B_{pre,i}$ is the upper estimate of plausible pre-exploitation annual biomass density (tonnes) for baleen whale group i, $B_{catch,i}$ is the biomass (tonnes) of group i caught in the 1000km buffer, t_i is the proportion of the year that whale group i spends in the model region,

area is the area of the model in km^2, and $B_{current,i}$ is the biomass (tonnes) per unit area of whale group *i* already estimated for the published model.

5.2.5 Estimates of baleen whale Q/B

We calculated a range of *Q/B* estimates for each whale group using the information contained in Savoca et al. (2021). For the minimum estimates, we used the constants and metabolic exponents from previous studies, provided in Savoca et al. (2021) (Table D4), combined with average body masses for each whale group from Greenspoon et al. (2023) to calculate an average *Q/B* for each whale group, assuming a 90-day feeding period (applied to all model regions for consistency) (Table D5). We opted to estimate these using the 'prior' parameter values in Savoca et al. (2021) because they represent a consistent approach which establishes a lower bound on whale consumption rates. These *Q/B* values will henceforth be referred to as the 'baseline' *Q/B* values.

We then used the lower, median and upper estimates of daily rations estimated by Savoca et al. (2021) combined with the average whale body masses, again assuming a 90-day feeding period, to calculate higher *Q/B* values for later perturbation analyses (Table D5).

5.2.6 Model balancing

To standardise the balancing process across regional models and to explore the effects of perturbation across a range of plausible alternative model parameterisations, we developed a bespoke balancing algorithm and used this to generate 1000 versions of each regional model. The algorithm employs an automated iterative stepwise approach to optimise the set of parameter values to achieve balance, and the method is explained in detail in Appendix D1, with a general overview provided here. The algorithm randomly varies *B, P/B, Q/B, GE* and *DC* to search the parameter space for parameter combinations that satisfy balance criteria (all *EEs* equal to or below 1), while ensuring that values remain within defined confidence intervals (Table D6). One exception is that the whale *Q/B* values were fixed to the baseline estimates calculated for each group, to ensure that the initial consumptive impact of whales per unit biomass was standardised across models. Assimilation efficiencies were fixed for all groups, using values obtained from Pinkerton and Bradford-Grieve (2010). At each step, the new parameter set is evaluated using an objective function (the sum of *EE* for all groups out of balance). A record of the 'best' model (lowest objective function) is updated throughout, until either a balanced parameter set is identified, or the algorithm has reached a specified number of steps (we set this to 2000 but more can be used, although this increases runtime).

In the latter case, the algorithm then switches to targeted, generally small, adjustments to biomasses and diets to nudge the model towards balance, much like the approach of Kavanagh et al. (2004). These adjustments are focussed on the group most out of balance, and their most influential predator (i.e. the one with the greatest consumption of the prey group). Once a balanced model is found, the biomass values for each group are checked, and the model is rejected if any biomass values fall outside their specified confidence intervals.

In some cases, the balancing process resulted in skews in the distribution of some balanced parameters across model runs, particularly for *P/B* (often right-skewed) and *Q/B* (often left-skewed) (Figure D2-D7). These skews were generally consistent between regional models, suggesting no obvious model bias. There were also some differences in the distribution of EE values across groups, but these were not consistent between models (Figure D8-D9).

5.2.7 Perturbation scenarios

Our perturbation scenarios explored the effects of increasing whale prey consumption (*Q*) on either competitor biomasses or on system-level primary productivity demand. As *Q* is simply the combination of *B* and *Q/B*, it was possible to set an upper plausible limit on *Q* by combining the whale limit biomass with the upper *Q/B* estimate from Savoca et al. (2021). This range of *Q* values encompasses all plausible scenarios of increased biomass and revised understanding of consumption rates. This also meant that we could convert any given *Q* into a different *B* based on the relevant *Q/B* estimate we wanted to apply, allowing us to determine the effect of the revised daily consumption rate estimates on the capacity to support more whales.

Scenario 1: Compensatory changes in competitor populations

In this scenario, we explored the compensatory decreases in the aggregate biomass of key higher-trophic competitors (marine mammals, birds, fish, and squid) required to facilitate increases in baleen whale *Q* up to the plausible limit without changes to lower trophic levels. We also identified the Q that could be supported by each model at a specific threshold of total competitor biomass. For this we used a threshold of 75% of initial competitor biomass, as this has previously been identified as a suitable boundary for the ecosystem-based management of the Southern Ocean (Watters et al. 2013). To implement this scenario, we increased the whale *Q* in each model version in a stepwise manner for a range of values up to the maximum suggested by the relevant regional limit biomass and the upper *Q/B* estimates. At each step in the process, any prey groups that were pushed out of balance ($EE > 1$) were identified. The

biomasses of the competitor groups that fed on these prey groups were then reduced by small amounts in proportion to their predatory impact until balance was achieved. This process continued until the plausible limit on baleen whale *Q* was reached or until the biomass of all competitor groups had been reduced to below one percent of their starting values.

To investigate the possible drivers of any variation in the capacity of regional models to sustain increases in whale *Q*, we calculated two different metrics. The first was the production-weighted average *EE* across all whale prey groups, which describes the spare capacity that each model has to support further consumption by whales without requiring compensatory changes to competitor biomasses. The second was a modified version of the Schoener dietary overlap index (Schoener 1970), using the normalised summed consumption of each prey group by baleen whales compared to that of their competitors, to capture the degree of competition between baleen whales and their competitors:

$$C = 1 - \frac{1}{2}(\sum|P_{x,i} - P_{y,i}|)$$

where C is the Schoener index, P_{xi} is the consumption of diet item i as a proportion of total prey consumption by group x (all baleen whales), and $P_{y,i}$ is the consumption of diet item i as a proportion of total prey consumption by group y (all whale competitors).

To identify how these metrics indicate the capacity of models to sustain increases in whale *Q*, we estimated the slope of the average relationship between competitor biomass proportion and whale *Q* across the 1000 runs within each regional model ensemble. For consistency between models and to capture the most linear part of the relationship we used the section between 80% and 20% of competitor biomass. We used a Pearson's correlation to identify the association between the slope of each model average and the average *EE* or Schoener index across each of the regional model ensembles.

Scenario 2: Lower-trophic changes required to support baleen whale recovery and competitor populations

This scenario followed a similar approach to the previous one, but this time the biomasses of higher trophic level competitors (marine mammals and birds) were fixed, and the biomasses of baleen whale prey and other lower trophic level groups were increased if their EE rose above 1, to compensate for higher predation. We focussed on the relative change in primary production required, as a measure of the total system productivity needed to support these potential future ecosystems.

5.3 Results

5.3.1 Initial balanced model ensembles

There was some regional variation in the average consumptive flows for the baleen whale prey and competitor groups. Krill made up a large proportion of total flows in the SG, AP, PB and RS models, while other zooplankton contributed more to total consumptive flows in the PE and KP models (Figure 5.2). The sources of consumptive flows to higher predators (marine mammals and seabirds) were quite varied in the SG, AP, PB and RS models, but were dominated by flows from squid and fish in the PE and KP models (Figure 5.2).

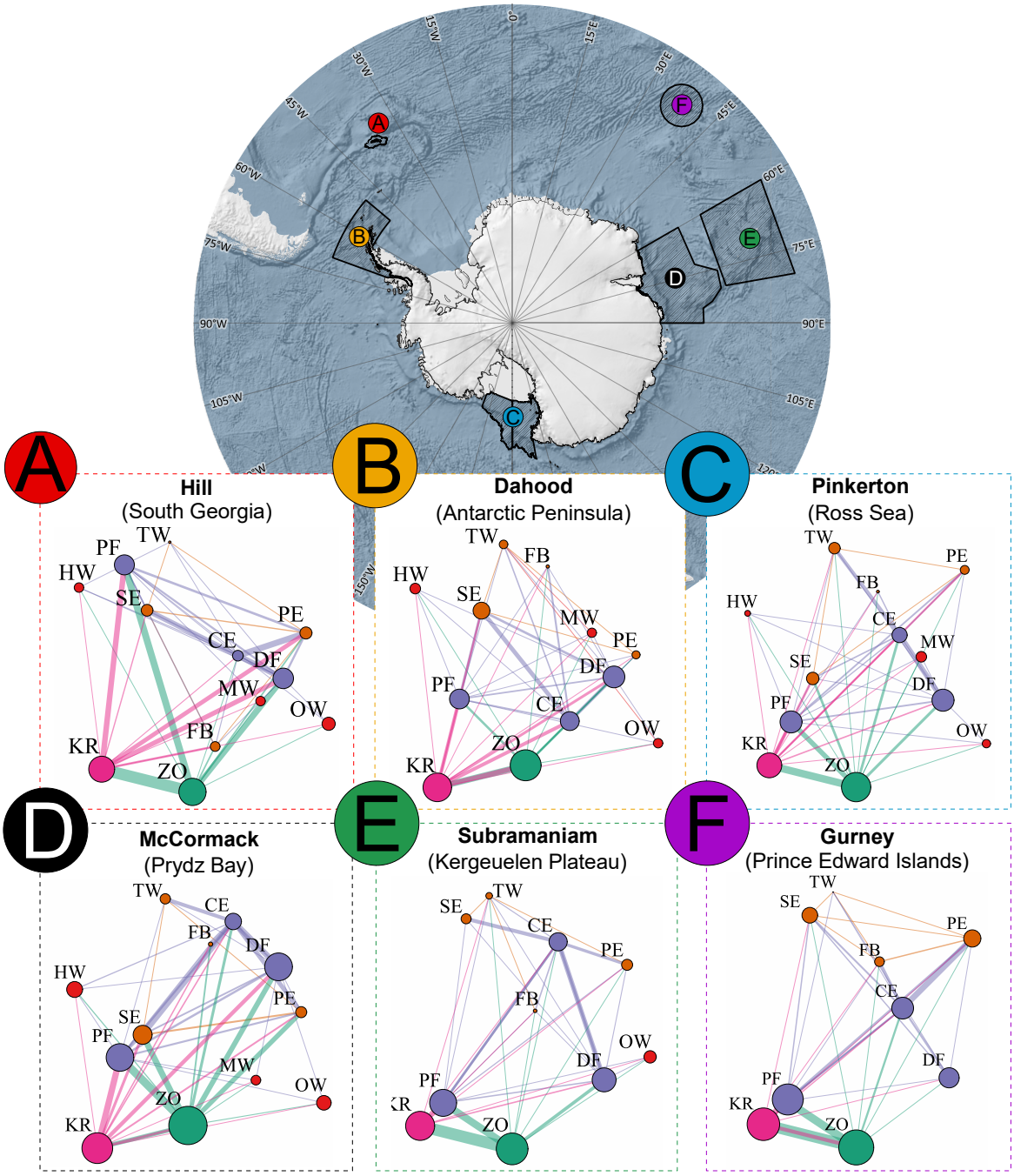

Figure 5.2: Spatial distribution of the models. Inset network diagrams display the log-transformed consumptive flows between whales, their prey groups and their main competitors, averaged across model ensembles. Node and link size are proportional to biomass and consumption, respectively (not comparable between panels). Nodes are arranged evenly aong the vertical axis by rank order of their trophic level, coloured by the main groupings (red: baleen whales, orange: marine mammals and seabirds, purple: fish and squid, pink: krill, green: zooplankton). TW = toothed whales; HW = humpback whales; MW = minke whales; OW = other baleen whales; SE = seals; PE = penguins; FB = flying birds; PF = pelagic fish; DF = demersal fish; CE = cephalopods; KR = krill; ZO = zooplankton.

When comparing the models based on the combination of their production-weighted average EEs and Schoener index, there appeared to be three primary groupings of models: Group 1 (PB, PE and RS) had low Schoener index and high *EE;* Group 2 (SG and KP) had high Schoener index and low *EE*; Group 3 (AP) had a low Schoener index and low *EE* (Figure 5.3; Table D5).

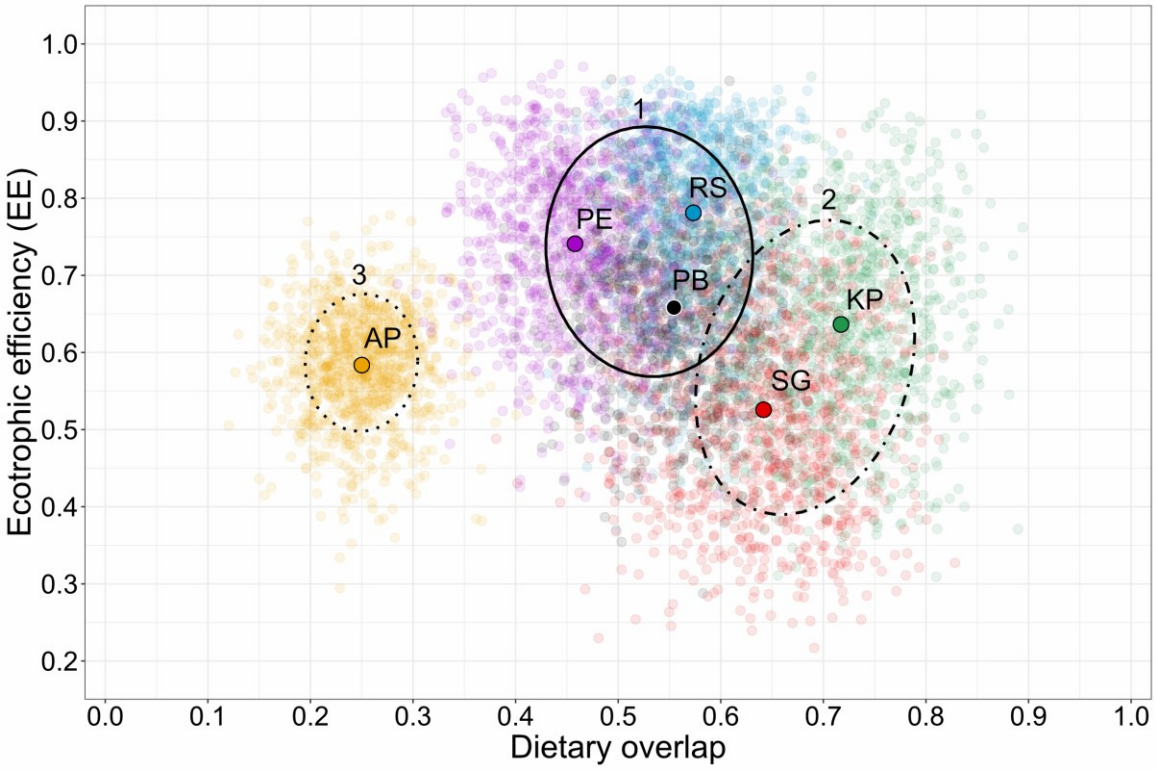

Figure 5.3: Relationship between production-weighted average ecotrophic efficiency (*EE*) of all baleen whale prey groups and the overall dietary overlap between baleen whales and their competitors. Points are coloured by model region, with small points indicating the position of individual model runs and larger points representing their average. Ellipses represent one standard deviation around the three qualitative groupings, identified by numbers on the plot. The initial balanced PE model included no whale biomass therefore the dietary overlap was calculated by adding a negligible biomass to the model.

5.3.2 Catch-derived total whale biomass

There was considerable variation in the upper bound on plausible biomass for baleen whales in each model region. The SG model had the largest value (75.45 t km^{-2} y^{-1}), more than twenty times higher than that of the other models, which ranged between 1.04 and 3.62 t km^{-2} y^{-1} (Table D6). This also represented the greatest proportional increase compared to initial whale biomass amongst the six models (262 times compared to between 18 and 80 times in

the other models) (Table D7). There were also changes in the group composition of baleen whale biomass between the initial unbalanced published model inputs and in the catch-derived limit biomass for the corresponding regions. In particular, humpback and minke whales made up the majority of baleen whale biomass in the initial inputs of the AP, PB and RS models, but 'Other baleen whales' dominated the catch in all models (Figure D10).

5.3.3 Perturbation scenarios

Scenario 1: Compensatory changes in competitor populations

There were large differences in the capacity of each regional model to support increased whale consumption (*Q*). The model groupings identified based on the combination of their averaged EE and Schoener index (Figure 5.3) were clearly linked to differences in the average slopes of the relationship between competitor biomass and whale *Q*. The models with low Schoener index and high *EE* (PB, RS, PE) experienced the most rapid decrease in relative competitor biomass with increasing whale *Q*, followed by those with high Schoener index and low *EE* (KP, SG), while the AP (low Schoener index, low *EE*) was able to support large whale Q increases while also retaining competitor biomass (Figure 5.4a). Of these two parameters, there was a stronger correlation between *EE* and the slope of competitor biomass ($r = -0.61$) than for the Schoener index ($r = -0.16$) (Figure 5.4b & c). It should be noted that neither of these correlations were significant ($p>0.05$), likely due to the small sample size ($n = 6$ models).

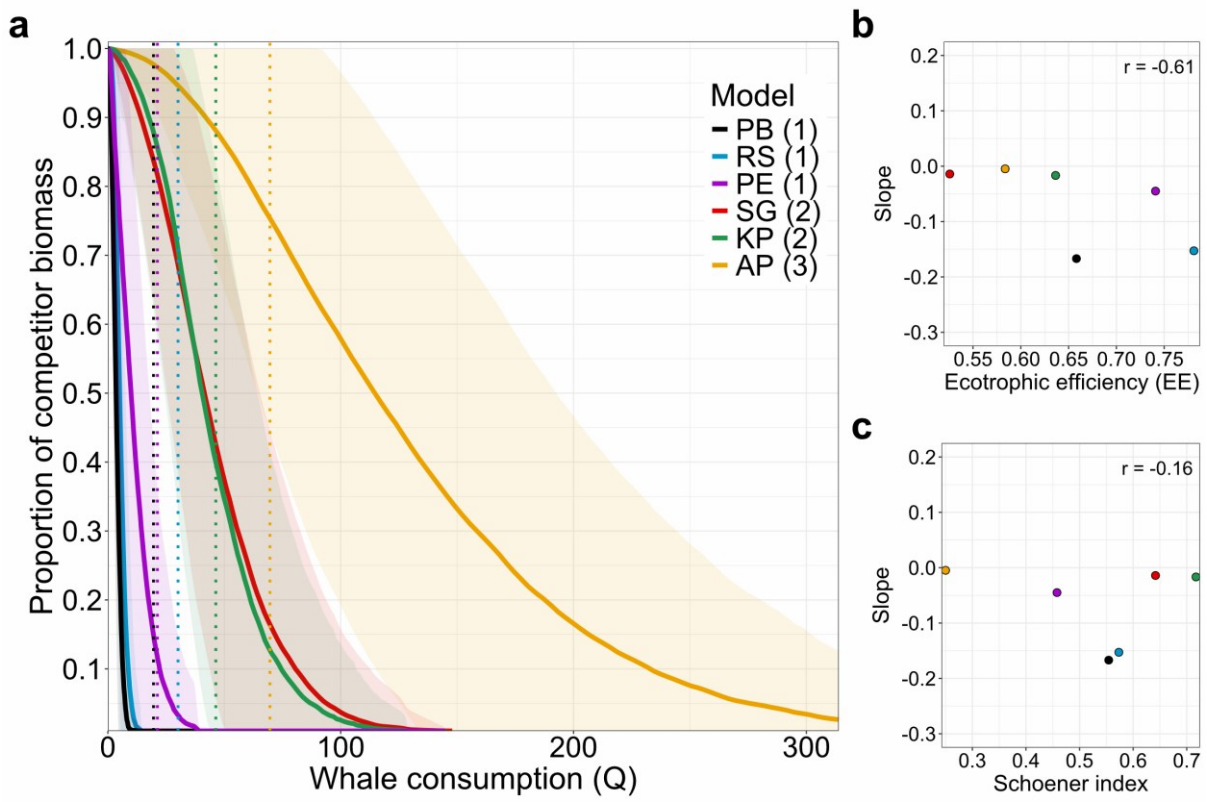

Figure 5.4: a) Average relationship between competitor biomass proportion and whale consumption ($Q\ t\ km^2y^{-1}$) for each of the model ensembles. Solid lines indicate model averages, shading indicates standard deviation. Vertical dashed lines identify the upper whale Q identified for each of the model regions (not shown for the SG model because this was beyond the x axis scale). Numbers in brackets represent the groupings of the models by the combination of their production-weighted ecotrophic efficiency (*EE*) and Schoener index; b) association between the slope of each model average in panel a) and the production-weighted mean *EE* of baleen whale prey; c) association between the slope of each model average in panel a) and the Schoener diet overlap index between baleen whales and their competitors.

Across models, the use of different *Q/B* estimates had a large impact on the increases in whale biomass that were possible. Under the baseline *Q/B* estimates, and while conserving the majority (99%) of competitor biomass, baleen whale biomass could be increased between 1.52x (PB) and 159.35x (KP) (Figure D11, Table D8). If conserving only 75% of competitor biomass, the average increases in baleen whale biomass were substantially higher, ranging from 12.40x in the PB model to 865.62x in the KP model (Figure D11, Table D8). Using the median *Q/B* estimates based on Savoca et al. (2021), on average only two of the models (KP and RS) were capable of supporting any additional whale biomass while maintaining competitor biomass at above 99% of initial values (Figure D11, Table D9). At the competitor

biomass threshold of 75% of starting values, the relative increases in baleen whale biomass were far more conserved than under the baseline *Q/B* estimates, ranging from 1.17x (PB) to 79.92x (KP) on average (Figure D11, Table D9). Using the upper *Q/B* estimates, the possibility for baleen whale biomass increases was even more restricted (Table D9). Within each model ensemble, there was high variability in competitor responses across model runs (Figure D12).

Increases in whale *Q* had different impacts on the biomasses of individual competitor groups in each model. Of the higher trophic competitors, seals experienced particularly rapid biomass declines in the AP and PB models, while penguins were especially impacted in the SG and RS models (Figure D12). Within the lower trophic competitors, the biomass of demersal fish declined particularly rapidly in the SG, PB, RS and AP models, while, in contrast, pelagic fish were the most strongly affected across all competitor groups in the PE and KP models (Figure D12).

Scenario 2: Lower-trophic changes required to support baleen whale recovery and competitor populations

The relative increases in primary productivity required to support the limit baleen whale consumption were relatively modest in the AP and KP models (0.32% and 0.39%, respectively; Figure 5.5a & b), but considerably larger in the RS, PB and PE models (ranging from 11.08% to 18.61%) (Figure 5.5c-e; Table D10). The SG model required extremely large increases in primary production (575.97%; Figure 5.5f). Based on a linear estimation of the slope of the average relationship between whale Q and primary production in each model, we estimated that a unit increase in whale Q ($t\ km^2\ y^{-1}$) required relative increases in primary production ranging from 0.005% (AP) to 0.565% (RS) (Table D11).

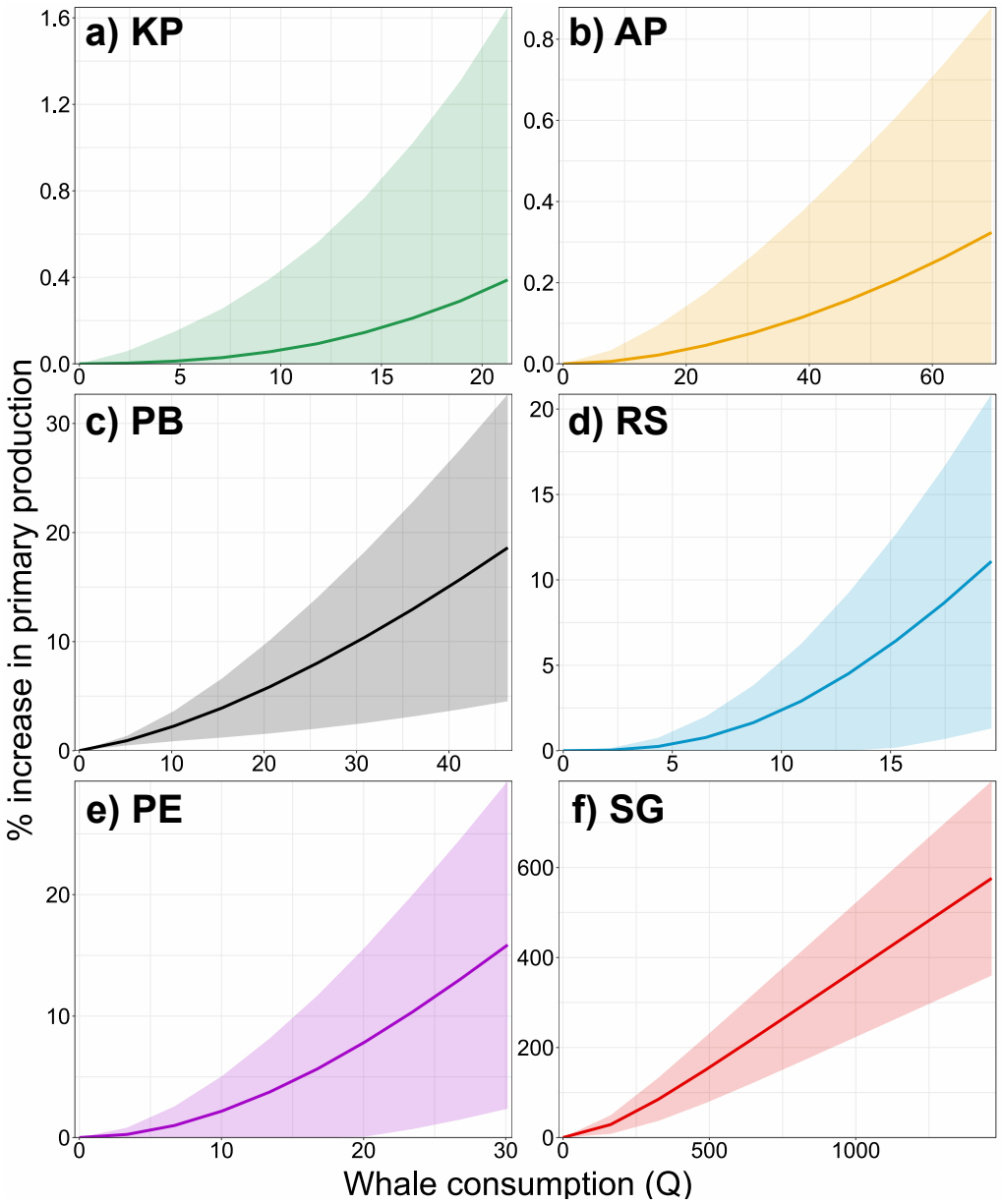

Figure 5.5: Relative changes in annual primary production ($t\ km^2\ y^{-1}$) required to support increases in total whale consumption ($Q\ t\ km^2\ y^{-1}$) if lower trophic level biomasses are increased to support increases in whale Q while competitor biomasses are fixed. Solid lines indicate model averages, shading indicates standard deviation. The maximum value on the x-axis represents the upper bound on plausible baleen whale consumption (Q). Note varying axis scales.

5.4 Discussion

Commercial whaling during the 19th and 20th centuries drove massive declines in baleen whale populations within the Southern Ocean, and thus impacted wider ecosystem structure (Christensen 2006; Mori and Butterworth 2006). The recovery of these populations could

therefore have major impacts on the population trajectories of other important competitors such as seals, penguins and fish. In this study we identified the compensatory changes to competitor populations that would be necessary to support increases in whale consumption rates under contemporary conditions, and the bottom-up changes necessary to simultaneously achieve baleen whale population recovery and conservation of current competitor biomass. Our results highlight the importance of taking a holistic approach to the management and conservation of different competing populations.

Scenario 1: compensatory changes to competitor populations

We found that contemporary regional Southern Ocean food webs have some capacity to support increased baleen whale populations, but this was dependent on daily prey consumption estimates and may come at the expense of competitor populations. Previous modelling has also found increases in global baleen whale populations to have strong indirect impacts on populations of other higher trophic groups including seals and seabirds (Ruzicka et al. 2013). Five-fold increases in consumption by baleen whales were found to cause declines in top predator production of up to 29%, and twenty-fold increases in baleen whale consumption required significant (up to 73%) reductions in production by competitor populations (Ruzicka et al. 2013). Under more recent estimates of higher baleen whale daily consumption rates (Savoca et al. 2021), the competitive impact of whales may be elevated. This is because values of *Q/B* (the annual prey consumption per unit biomass) determine the relationship between *Q* (consumption) and *B* (biomass), with a given *Q* value representing ever smaller *B* as *Q/B* increases. In consequence, at high *Q/B* values, the whale *Q* thresholds at which competitor populations begin to decline will be reached at comparatively lower whale *B* than at low *Q/B* values. We found that, when using revised *Q/B* values based on median daily consumption estimates in Savoca et al. (2021) and conserving 75% of total competitor biomass (representing changes that are potentially reversible within two or three decades; CCAMLR 2008; Watters et al. 2013), increases in whale biomass were highly constrained (only around 9% of the values possible under baseline *Q/B* estimates; Table D9). In four of the six models this represented only a fraction (from 2.5% to 26%) of the plausible limit biomass, although the remaining two models (AP and KP) could still sustain the full upper bound on whale biomass. Under higher prey consumption estimates the capacity of food webs to support larger whale populations was even more constrained (Table D9). Overall, these results support the conclusions of Ruzicka et al. (2013) that whale recovery will have large impacts on competitor populations. It should be noted that there are various

other factors that might modify these relationships, such as the degree of flexibility in competitor diets and the competitive hierarchies between competitors and whales, which are discussed further in a later section.

While our use of ensemble averages suggests a smooth and relatively consistent relationship between whale *Q* and competitor biomass, individual model runs displayed much more sudden inflection points along the *Q* scale, leading to rapid competitor biomass declines (Figure D12). Most models exhibited a phase of no change in competitor biomass, likely due to spare consumptive capacity of prey groups (i.e. low EE) which provided an initial buffer against the increases in whale *Q*. This was generally followed by a phase of gradual competitor biomass decline as the spare consumptive capacity of whale prey is used up and biomass adjustments are spread across multiple competitor groups based on their relative *Q/B* and degree of dietary overlap with whales. Finally, most model runs displayed a sudden changepoint after which competitor biomasses rapidly declined to zero. As the individual competitor populations are reduced, their overall consumptive impact on a given prey relative to the total consumption of that prey by other groups becomes smaller, and therefore relatively greater reductions in biomass are required to counteract the increased consumption by baleen whales. Individual competitor populations will eventually become so small they cannot be further adjusted, and the remaining competitor groups then must be subject to relatively greater biomass adjustments to account for this. This is compounded by the fact that the last remaining competitor groups are likely to be those with relatively low *Q/B* (as they will have had the least impact on whale prey groups and will therefore have been reduced the least in the previous phase), and therefore each unit of *Q* removed to balance the impact of more whales will represent a relatively greater biomass. It would be worth investigating whether the drivers of these abrupt transitions in the models actually exist in nature. It is also likely that other factors such as competitive hierarchies, dietary flexibility and population depensation would modify these relationships by determining the relative impacts of increased consumption by whales on each competitor group (Barlow et al. 2002; Abrams 2010; Liermann and Hilborn 2001), and their effects should be investigated.

Scenario 2: Bottom-up changes to support baleen whales and competitors

There was considerable variation in the total primary production required to support the limit whale biomass and contemporary competitor populations in each model. In particular, the SG model needed extremely large increases in primary production (>500%), likely because the

extensive whale catches that occurred within the 1000km buffer, coupled with the small modelled spatial area, generated very high estimates of biomass per unit area (Figure D1). The shelf waters around South Georgia are highly productive and considered a biodiversity hotspot (Hogg et al. 2011), which may have driven some of the highest densities of baleen whales on the planet (Richardson et al. 2012). However, some of the models with comparatively small plausible upper whale biomass estimates (e.g. RS, PB and PE) also needed a substantial rise in primary production (up to 19%) to support whale population increases without adverse effects on competitors. These models also displayed the steepest competitor biomass declines in Scenario 1, highlighting the link between apparent sensitivity to whale recovery and the magnitude of changes in bottom-up forcing needed to mitigate negative impacts.

The role of baleen whales in nutrient cycling in the ocean is still poorly understood, and likely to vary by geographical location, ecosystem productivity and whale community composition (Gilbert et al. 2023). In nutrient-limited sub-tropical calving grounds, unexploited blue whale populations increased primary productivity by up to 15% compared to the average for subtropical waters (Roman et al. 2014). In the Southern Ocean, where trace metals such as iron are the primary limiting factor for phytoplankton growth the iron excreted by unexploited whale populations could represent around 12% of the average contemporary iron content in Southern Ocean surface waters (Ratnarajah et al. 2014; Nicol et al. 2010). This could have stimulated higher levels of primary productivity, possibly up to 11% greater across the Southern Ocean under high whale consumption rate estimates (Savoca et al. 2021). This value is at the lower end of the increases we estimated to be required to support the upper plausible bound on whale consumption in the three models that were most sensitive to baleen whale population recovery (PB, RS and PE), and far below the values required by the SG model. Our results therefore suggest that, across the Southern Ocean, whale-driven nutrient cycling alone is unlikely to be sufficient to fully mitigate impacts of whale recovery on other higher trophic levels.

Predicted future changes in primary production are highly uncertain, and there will likely be considerable regional variation in trends. Overall, increases in temperature and irradiance, combined with shallowing of mixed layer depths, are expected to drive increased primary productivity across the Southern Ocean (Henley et al. 2020; Kaufman et al. 2017). Increases in net primary production may be 50% or more in some high latitude regions by the end of the century, with more modest increases (up to 30%) elsewhere (Steinacher et al. 2010; Fu et

al. 2016; Fisher et al. 2024), although a study on the Ross Sea predicted more limited increases in primary productivity of 5% by 2050, and up to 14% by 2100 (Kaufman et al. 2017). Overall, it seems plausible that future increases in primary production will be sufficient to mitigate at least some of the negative impacts of baleen whale population recovery identified in our models (except SG), particularly if there is an additive effect of elevated whale nutrient-cycling. This will, however, also depend on the nature of potential changes in primary producer composition as this will determine their suitability for sustaining whale prey populations (discussed further below).

Regional differences

There were regional differences in model capacity to support increases in baleen whale *Q*. These distinctions could result from both arbitrary differences between models (so-called model 'personality') and true ecological differences (Hill et al. 2021). While it is beyond the scope of this study to definitively distinguish the relative influence of each of these factors, we made significant efforts to ensure the comparability of the models used. By standardising functional group composition and energetic parameters, we removed some of the possible inter-model variation that might result from decisions made during the original model construction process. Additionally, our use of a novel automated balancing algorithm facilitated the construction of model sets encompassing a range of plausible balanced parameter sets for each regional model, thus allowing us to explore uncertainty around model structure. By analysing a suite of runs from a variety of regional models, we were able to explore a broad set of ecologically viable scenarios representing the multitude of potential responses that Southern Ocean ecosystems might display in future.

Models were grouped based on their combination of average whale prey *EE* and whale-competitor diet overlap (Schoener's index), and these groupings matched the general order of steepness of the model average slopes of competitor biomass decline with increasing whale *Q* (Scenario 1). A group's *EE* inversely relates to the spare production available for additional consumption, therefore low values suggest a greater capacity for increasing consumption without pushing the prey group out of balance, and vice-versa (Christensen and Walters 2004). As a consequence, the model runs with higher average prey *EE* generally had less capacity to support additional whale *Q* without compensation by competitors. This is because increases in *Q* promptly drive prey groups out of balance, resulting in compensatory declines in competitor biomass. Since a large proportion of model runs start with high prey *EE*s, the

inflection points at which competitor biomasses decline generally take place over a small range of whale *Q* values, leading to steeper average slopes.

Whilst the *EE*s are dependent on the combination of model parameters adjusted during the balancing process, some of the differences in the distribution of *EE* values between regions could represent genuine ecological contrasts. The efficiencies of lower- and mid-trophic groups are often assumed to be close to one, suggesting that most of their production is directly utilized within the modelled ecosystem (Heymans et al. 2016). However, while predation mortality is a major driver of lower-trophic population dynamics, other sources of mortality (e.g. environmental conditions and food availability) can be considerable for organisms such as zooplankton, and advection by currents could reduce the proportion of production that is consumed by predators within the system (Tang et al. 2014; Hirst and Kiørboe 2002). It is therefore plausible for lower *EE* values to exist for these groups, and differences between models could reflect the influence of these local processes. Additionally, model parameters are based on data collected over multiple years and forced to meet equilibrium assumptions and may encompass considerable variability in production at lower trophic levels (Plagányi and Butterworth 2004). Temporal variability in local abundances generally declines with trophic level (Siqueira et al. 2024), so populations of higher trophic consumers with relatively low-fecundity, such as marine mammals and birds, are unlikely to respond rapidly enough to changes in lower-trophic biomass to fully exploit any temporary surpluses in production. As a result, *EE*s for some prey groups may display inter-annual variation which could differ significantly between regions.

Given the strong correlation between *EE* and the apparent capacity of models to cope with sustained press perturbations like whale population increases (Figure 4b & c), an improved understanding of the processes underlying the local sources of mortality of key prey groups would aid managers in targeting management and conservation actions. Gaining this understanding will require the integration of biological and physical data across relatively fine spatial but broad temporal scales. Identifying the processes driving natural mortality will also be key to predicting possible climate-driven changes in population dynamics and would aid our understanding of how ecosystems will change in future (Plagányi et al. 2022).

The distinction between two model groupings (SG and KP vs AP) was largely due to the degree of dietary overlap between whales and their competitors. We adjusted competitor biomasses in proportion to their relative importance as consumers of each unbalanced prey

group until balance was achieved and, as a result, in models where prey consumption by whales and competitors is more similar (high overlap), a unit increase in whale *Q* will need to be compensated for by relatively greater reductions in competitor biomass. Differences in dietary overlap may be due to genuine ecological contrasts, as the relative importance of krill, other euphausiids and pelagic fish in the diets of higher predators varies geographically (McCormack et al. 2021b), and we observed contrasts in the distribution of consumptive flows across our balanced suite of models which appear to broadly match these trends. In consequence, different competitor groups were most impacted by increases in whale *Q*, with seals and penguins declining most rapidly in regions with high reliance on Antarctic krill and pelagic fish strongly impacted in regions which are more heavily dependent on other groups such as *Thysanoessa macrura* (Wallis et al. 2019). Further studies of regional similarities and differences in diets will better resolve the degree of dietary overlap between baleen whales and other higher-trophic groups, thereby providing greater insight into the likely capacity of ecosystems to cope with future population changes.

It would be valuable to further explore the relative effects of EE, dietary overlap and other potential factors (e.g. competitor group identity, biomass distribution and *Q/B*) on model capacity, to develop robust metrics which can be used to predict model responses to change. This could be explored further using suites of smaller (simpler) models with systematic differences in their parameters, with the shapes of competitor biomass responses to whale *Q* increases investigated on an individual group and model basis rather than as an aggregate. Doing so might reveal interactive effects of different parameters on the overall model capacity to support whale population increases.

Further considerations:

Our study represents an initial effort to explore the potential impacts of baleen whale population recoveries on ecosystem structure. There are several additional factors which could influence the relationship between the population trajectories of whales and their competitors.

The expansion of krill fisheries and establishment of new fisheries for groups like mesopelagic fishes could reduce their availability for predators (Meyer et al. 2020; Fjeld et al. 2023). Environmental changes such as warming, sea ice loss, and changes to the production and composition of phytoplankton communities, could also alter the production of key prey (e.g. krill) and modify energy flow to higher trophic levels (Kawaguchi et al. 2024; Swadling

et al. 2023; Thomalla et al. 2023). Behavioural changes in groups such as Antarctic krill might alter the density and distribution of swarms (Kawaguchi et al. 2024), reducing feeding opportunities and elevating competition between whales and other groups. These anthropogenic and environmental changes could therefore impact the capacity of regional ecosystems to sustain whale population increases with minimal effects on competitors.

Some competitor groups may have more flexible diets than others, making them better able to mitigate the impacts associated with greater competitive pressure from larger whale populations. For example, groups such as crabeater seals and chinstrap penguins are highly dependent on krill while others such as Weddell seals, fur seals and gentoo penguins have quite generalist and flexible diets according to the available prey field (Wege et al. 2021; McMahon et al. 2019; Reisinger et al. 2018).

Differences in the competitive ability of whales and competitor groups may also influence the trade-offs between whale consumption and competitor biomass. Groups that are higher in the competitive hierarchy, perhaps due to greater foraging ability (Barlow et al. 2002), may be less impacted by increasing baleen whale populations because they will be able to outcompete other groups and maintain necessary energy intake, while their competitors may experience rapid declines. Additionally, while we explored the effects of increased whale biomasses on other groups, competition can also have strong effects on whales themselves (Ruzicka et al. 2013). Previous modelling suggests that increased competition for Antarctic krill (between baleen whales and other groups, and between whale species themselves) could strongly limit whale population recoveries (Tulloch et al. 2019).

It is also important to consider whether changes in primary production are associated with shifts in the composition of phytoplankton communities, as these may influence the capacity for future primary productivity to mitigate the ecosystem effects of whale recovery. Sea ice changes, warming, and increases in stratification and irradiation, may result in large diatoms being replaced by smaller flagellates and other groups in regions such as the sea ice zone, while more open ocean regions could experience the opposite trend due to increasing iron flux and atmospheric cloudiness (Henley et al. 2020; Krumhardt et al. 2022). In regions which experience declining diatom abundance and concurrent increases in populations of smaller phytoplankton, the efficiency of energy flow to higher trophic levels may be reduced (Krumhardt et al. 2022; Hunt et al. 2021). Additionally, some of the drivers of increased primary productivity (loss of sea ice, increases in temperature) are expected to negatively

impact groups such as Antarctic krill (Flores et al. 2012). The combination of warming and shifts in phytoplankton community composition towards smaller, less energetically valuable species may also increase the abundance of salps (*Salpa thompsoni*) which can outcompete krill, resulting in fundamental changes to food web structure that could negatively impact energy supply to higher trophic levels (Pauli et al. 2021; Pietzsch et al. 2023).

Overall, the capacity of Southern Ocean food webs to support both increased whale populations and contemporary competitor biomass will depend on a variety of interacting factors, and it would be valuable to include these in future modelling studies to explore the full suite of uncertainty around the potential for, and consequences of, baleen whale population recovery.

Implications for management

Anthropogenic and environmental changes have altered Southern Ocean ecosystems, creating challenges for certain management and conservation goals. Here, we have shown that the full recovery of baleen whale populations in the Southern Ocean is likely to result in strong trade-offs between conservation objectives. The absolute magnitude of compensatory changes in competitor populations, and the points along the pathway of whale recovery at which they will occur remain uncertain and are probably region-specific. We identified that the levels of unexploited production by whale prey and the degree of dietary overlap between whales and their competitors may play an important role in the capacity of food webs to sustain whale population increases with minimal wider ecosystem impacts. Additionally, baleen whale consumption rates strongly influence the relative impact of whale population increases on food webs. Future changes in primary productivity due to environmental drivers and whale-driven nutrient cycling, could potentially mitigate the ecosystem impacts of whale recovery. Future efforts to better resolve these factors will improve our understanding of likely regional ecosystem responses and aid management decisions. Ultimately, policymakers seeking to implement management and conservation strategies (e.g. fishery catch limits and marine protected areas) will need to integrate information regarding both the inherent capacity of ecosystems to support whale population increases (i.e. model structure) and the likelihood of beneficial environmental changes (e.g. production and composition of phytoplankton communities).

6 General discussion

Food webs are the framework upon which much of modern ecological research is built, providing insight into many aspects of ecology ranging from the drivers of individual population dynamics to the broader patterning of biodiversity and the impacts of global change on ecosystem functioning (Layman et al. 2015). The Antarctic is a particularly important focus of food web research, as the historically stable conditions and the physiological adaptations and high stenothermy of many species make Southern Ocean ecosystems especially vulnerable to changes such as warming and sea ice loss (Queirós et al. 2024). Given the central role that the Southern Ocean plays within the wider earth system, it is important that we improve our understanding of the structural properties of regional food webs and how these influence their resilience to environmental and ecological change (Murphy et al. 2012). This thesis explored some key aspects of the structure of Southern Ocean food webs and their responses to change. Chapters 2 and 3 used functional traits to explain trophic structure at different scales, from the distribution of feeding links at the community level to the organisation of a key stabilising substructure, modularity, at the level of entire food webs. Chapter 4 then investigated how temperature alters the size-structuring of trophic interactions, which is a key aspect of marine food webs. Finally, chapter 5 explored the range of possible responses of Southern Ocean ecosystems to a key ecological perturbation, the recovery of baleen whales. Below, I discuss the primary contributions of each chapter to our knowledge of food webs in the Southern Ocean and beyond and explore some of the further avenues which could be taken to improve our understanding of each topic. I then finish by summarising some of the major future directions that I see for food web research in general, based on the themes covered in this thesis.

6.1 Chapter contributions

6.1.1 Chapter 2: Morphological traits distinguish feeding guilds in a Southern Ocean fish community.

Chapter 2 determined the ecomorphology of demersal fish around South Georgia by first classifying species and size classes into feeding guilds using stomach contents data and then using morphological traits to predict feeding guild membership. This approach is well-established, having been used to study a number of fish communities in freshwater and marine systems across temperate and tropical regions, particularly reefs (e.g. Ramírez et al. 2015; Winkler et al. 2017; Podder et al. 2021; Albouy et al. 2011). Within the Southern

Ocean, however, only one study has combined morphological analyses with direct dietary observations in this manner, focussing on ten species of the family Artedidraconidae in the Weddell Sea and identifying links between their ecological niches and their sensory capability and mouth morphology (Lombarte et al. 2003).

My investigation of the South Georgia demersal fish community encompassed three taxonomic families (Channichthyidae, Nototheniidae and Bathydraconidae) and a large sample size, thereby providing a substantial contribution to our understanding of the associations between functional traits and ecology in Southern Ocean communities. I showed that a small number of simple, easily measurable traits can successfully capture most of the broad dietary niches present across much of the community, providing insight into the drivers of trophic interactions. This is an approach that could be applied to other Southern Ocean communities to improve our understanding of the drivers of food web structure. The ecology of demersal fish has been comprehensively studied around many regions of the Southern Ocean encompassing a diversity of bioregions (e.g. Wang et al. 2024; Cousins and Priede 2012; Baena et al. 2023) but the influence of functional traits has not yet been explored for these communities. It would be interesting to investigate how spatial contrasts in factors such as prey species assemblages, benthopelagic coupling or abiotic forcing (such as between low and high latitudes or east and west- Antarctic regions) relate to differences in the association between morphological traits and trophic niches. This could be facilitated by the routine sampling of diets and associated standard morphological traits such as mouth size and shape, fin morphology, body shape and gill structure across ecological communities during scientific and fishery expeditions.

Chapter 2 also highlights the possibility to identify broad dietary niches based on morphology, which could be useful for combining species into functional groups to develop better-resolved ecosystem models in data-poor environments (Ladds et al. 2018; Albouy et al. 2011). A focus on traits rather than taxonomy also provides a framework for determining how environmental and biotic filtering drive functional diversity (Green et al. 2022). Within marine taxa, body size is the most commonly measured trait, likely due to its major role in structuring marine food webs and the relative ease with which it can be measured (Green et al. 2022; Potapov et al. 2019). However, as shown in this chapter, other morphological traits reflecting feeding mode and mobility can also provide insight into the drivers of niche partitioning and should therefore be included in trait-based studies. It must also be recognized that, while morphological traits provide an extremely useful basis for investigating

community ecology, their use alone may not be sufficient to fully explain trophic structure. For example, the widespread distribution of krill feeders across morphological niche space could reflect a degree of trophic plasticity which is not linked obviously to morphology, and it will be important to consider further context such as general prey availability and abiotic factors. The wide range of morphologies exhibited by krill feeders could also suggest that krill possess certain traits which allow fish to feed outside their evolutionary morphological niches. These traits might include their high energy content and often widespread distribution across pelagic and benthic habitats, which make them an accessible and energetically efficient prey item for predators displaying a range of feeding modes, habitats and mobilities. This emphasizes the importance of considering both predator and prey characteristics when exploring the functional trait basis of trophic interactions (Wootton et al. 2023; Laigle et al. 2017). Within the Southern Ocean, trait-based approaches are still rare (McCormack et al. 2021a) and it will be important to determine the distribution of functional traits across more components of the ecosystem, as this would allow us to compare the positions of different species in multi-dimensional trait space and could help elucidate key differences which map onto their roles within food webs.

It is possible that ongoing environmental change around South Georgia will drive shifts in the distribution of species and broader community composition, particularly under the loss of key groups such as Antarctic krill (Kawaguchi et al. 2024; Whitehouse et al. 2008). There are still several unanswered questions regarding the structure of the South Georgia food web, most crucial being the distribution of feeding interactions in response to interannual variation in the local abundance of krill, as this could provide insight into possible future ecosystem states. Chapter 2 therefore represents a baseline study of the position of the demersal fish community among ecological niche space which further work can build upon to describe how interannual changes in prey availability influence ecomorphological niche partitioning. In particular, it would be interesting to investigate how changes in the relative abundance of different prey and demersal fish species affect the abundance-weighted diversity of traits within multivariate space (e.g. Liu et al. 2019), as this would provide insight into the potential impacts of future ecological change for functional diversity.

6.1.2 Chapter 3: Trophic structuring of modularity alters energy flow through marine food webs

The presence of modules within ecological networks is well established but investigations of this structure and links to functional traits remain quite limited, with previous studies

generally using a small set of traits (e.g. body size, foraging habitat and interaction type) to explain module membership (Kortsch et al. 2015; Rezende et al. 2009; Montoya et al. 2015). Within the Southern Ocean, there has been comparatively little effort to explore the basic food web theory which has dominated research in other regions, including the presence of modules and relevance of species traits (McCormack et al. 2021a). My work in chapter 3 therefore provides much needed insight into how functional traits underly the structure of Southern Ocean food webs. I conducted an extensive review of a broad range of both predator and prey characteristics for each species within multiple food webs, encompassing size, foraging behaviour, motility and defensive traits, amongst others. This dataset represents a valuable resource for further studies wishing to use these food webs to investigate how functional traits relate to network structure. Many of the traits could also be transferred to similar species in other regions, making this dataset useful beyond the focal models for investigating topics such as environmental filtering and the drivers of niche partitioning.

Modules can be structured by trophic level, whereby modules encompass relatively distinct groupings of trophic levels and form a hierarchy from the base of the food web to higher predators (Kortsch et al. 2019; Rezende et al. 2009; Guimera et al. 2010), or by energy channel, whereby modules partition food webs into trophic chains running from low to high trophic levels, often encompassing discrete basal resources (Gauzens et al. 2015; Zhao et al. 2017; Rodriguez et al. 2022). Previous studies have analysed individual networks exhibiting varying levels of taxonomic aggregation and have used a variety of methods to determine modularity, making it difficult to determine whether differences in module structure between studies are due to genuine ecological contrasts or methodological factors (Gauzens et al. 2013). In contrast, I used four food webs selected specifically for their high taxonomic resolution and employed a consistent method for determining modularity, making direct comparisons possible. A key finding was that module structuring is not consistent, with the 'trophic level' structure identified in two food webs while the remainder displayed the 'energy channel' structure. The relative importance of functional traits for predicting module membership also differed, with body mass found to be key in the food webs with structuring by trophic level, and feeding strategy important for the energy channel structure, while mobility and habitat were important across all networks. I explained these differences in terms of the levels of environmental heterogeneity inherent in each of the modelled systems, as this can strongly modify network structure including modularity (Kortsch et al. 2019). I proposed that networks in more homogenous ocean environments have reduced niche

diversity at lower basal levels, being centered primarily on phytoplankton, and are therefore structured largely by body mass, which is thought to be a primary driver of marine food web structure in general (Petchey et al. 2008; Rall et al. 2012; Potapov et al. 2019). In systems subject to stronger environmental gradients and variability, the heterogeneity of available habitat and basal resources could drive a diversity of trophic niches resulting in more specialized modules encompassing energy channels. These results are analogous to the *habitat heterogeneity hypothesis* (Thompson and Townsend 2005), whereby more varied habitats provide a greater diversity of niches and resources, supporting a greater diversity of species (or in this case, energy channels).

This research highlights key aspects regarding the use of functional traits and investigations of modularity that require further consideration. Firstly, underlying abiotic factors may modify the relative importance of different functional traits for determining network organisation. This means that a set of traits that provides good predictions of network structure in one region may not be so useful in another, and the environmental gradients influencing trait distributions will need to be considered before one can use traits to make generalised predictions of ecosystem structure. This calls for more investigation of the links between functional trait diversity (and identity) and environmental factors. If generalisable rules can be established (e.g. greater basal resource heterogeneity results in greater differentiation in feeding behaviours and therefore a stronger effect of feeding mode on network structure), then it will be possible to tailor trait-based approaches to specific ecosystems, improving predictive accuracy.

Secondly, rather than focusing solely on the absolute value of modularity, researchers should also investigate the structuring of modules in relation to trophic levels, as this could be particularly important for stability. Modularity reduces the overall connectivity within the network, thereby limiting the propagation of extinctions (Stouffer and Bascompte 2011), but in cases where modules are arranged largely by trophic level, perturbations within lower modules might still cascade up to higher modules. Two networks with similar values of modularity but different modular arrangement may therefore have quite different capacity to cope with species loss. This could be evaluated with formal stability analyses using theoretical food webs with standardized characteristics such as network size and complexity. Expanding these analyses to more real food webs will require the development of a greater number of highly resolved networks across a suite of environmental gradients. A systematic effort to sample and describe the structure of food webs to the highest taxonomic resolution

possible across a variety of habitats and environmental conditions would therefore be extremely valuable. This would aid in the search for generalisable network structures and could highlight regions of the Southern Ocean which may be more susceptible to environmental and ecological perturbations. It would also be useful to extend such food web analyses to quantitative networks, as the inclusion of interaction weights can greatly alter structural inferences (Banašek-Richter et al. 2009). The construction of quantitative networks is data-intensive, but recent developments make it possible to determine interaction strengths and energy fluxes based on relatively straightforward information such as body size, foraging behaviour and metabolic type (Marina et al. 2024; Gauzens et al. 2019), which should facilitate their adoption more widely within the Southern Ocean modelling community. It will still however be important to ground truth these estimates of energy flow with direct measurements of parameters such as consumer dietary preferences, metabolic rates and assimilation efficiencies (Jochum et al. 2021), as factors such as the distribution of interactions and the plasticity of metabolic rates can greatly alter the efficiency of energy flow and the magnitude of predicted energy fluxes (Kordas et al. 2022; Jochum and Eisenhauer 2022).

6.1.3 Chapter 4: Temperature alters the predator-prey size relationships and size-selectivity of Southern Ocean fish

Chapter 4 targeted our lack of knowledge regarding how predator-prey mass ratios (PPMR) change with temperature, by investigating how the relative sizes of mesopelagic myctophid fish and their zooplankton prey vary across a large latitudinal temperature gradient in the Southern Ocean. This is of particular interest as marine ecosystems are strongly size-structured and the relative size of predators to their prey has been used to successfully predict the distribution and even the strength of trophic interactions (Petchey et al. 2008; Bideault et al. 2019; Emmerson and Raffaelli 2004). Changes in the distribution of body sizes across trophic levels could therefore alter the flows of energy within food webs, with implications for ecosystem functioning.

By combining dietary and environmental prey size distributions it was possible to estimate the ‘preferred PPMR’, which distinguishes density-dependent and active prey selection by the fish (Tsai et al. 2016). This revealed some of the mechanisms underlying foraging by these fish under different temperatures. In particular, decreases in the average body size of fish (due to compositional changes and intra-specific declines in size) and shifts in the size distribution of zooplankton towards intermediate individuals acted together to reduce community-level

PPMR. These results could be used to better inform the parameterization of predictive size-based models of food web dynamics, which often assume a fixed PPMR when assigning trophic interactions and may therefore fail to account for environmentally-driven shifts in prey selection (Andersen et al. 2016; Tsai et al. 2016).

As illustrated by Gauzens et al. (2024), shifts in foraging behaviour and size-selectivity can be maladaptive, with important consequences for the persistence of communities under perturbations. It is therefore vital that we continue to investigate how environmental and ecological changes alter feeding preferences across taxa. It would also be interesting to further investigate the mechanisms that could be underlying the shifts in size selection by these myctophids from an energetic perspective. Previous research has shown that, in sardines, energy expenditure is influenced not only by warming but also by the size of prey available; if prey are small, sardines feed by continuous filtration which is more energy intensive than the particle feeding method employed when prey are larger, resulting in much higher energy expenditure (Queiros et al. 2024). Feeding trials of myctophids under different prey size treatments might reveal similar changes in foraging behaviour, providing further insight into the factors driving prey selection and energetics within this community.

As discussed in chapter 1, the impacts of climate change on populations may be driven as much by changes to species interactions as by direct environmental effects on organisms themselves (Ockendon et al. 2014). Chapter 4 only focussed on one (albeit important) component of Southern Ocean ecosystems, and the investigation of the impact of temperature on trophic interactions should be extended to other groups including zooplankton. Experiments have been conducted on groups such as Antarctic krill and amphipods to identify the effects of temperature on metabolic rates, growth, feeding rates and mortality (Michael et al. 2021; Saba et al. 2021; Schram et al. 2016), and it would be worthwhile to extend such experiments to include investigations of how temperature influences their prey selection (both in terms of species identity and size). Gaining this understanding for a wide range of functional groups within the Southern Ocean will greatly improve our capacity to predict how climate change may reorganize ecosystems.

Given the link between PPMR and interaction strengths (Bideault et al. 2019; Emmerson and Raffaelli 2004), the community-level decline in PPMR identified in chapter 4 might represent a change in community stability. The relationship between PPMR and interaction strength in this community could be tested by measuring the densities of prey under different predator

conditions in mesocosms (as in O'Gorman et al. 2010 and Emmerson and Raffaelli 2004), with different combinations of predator and prey size across multiple components of the food web. This information could then be used to parameterise population dynamics models (e.g. Gauzens et al. 2024; Bideault et al. 2019) to formally test the implications of changes in size structure (i.e. interaction strengths) for different facets of stability such as population variability and robustness.

6.1.4 Chapter 5: Trade-offs between the recovery of Southern Ocean baleen whales and conservation of their competitors

Chapter 5 provides important insights into how whale population recovery may impact Southern Ocean ecosystems, which will be a key issue for policymakers wanting to implement appropriate conservation measures under climate change. Various studies have concluded that whaling had major effects on prey and competitor abundances and overall food web dynamics (Laws 1977; Surma et al. 2014), but less attention has been drawn to the possible ecological consequences of whale population recoveries. By generating a broad suite of regional model structures, it was possible to identify some structural metrics which might be important indicators of the capacity for ecosystems to support increased whale biomass. Such indicator metrics are a key management tool for monitoring ecosystem health and resilience (Keramidas et al. 2023; Flensborg et al. 2023), and will aid the management and conservation of Southern Ocean ecosystems (Ruckelshaus et al. 2008). The analyses in this chapter focused primarily on broad responses averaged across competitor groups and model runs. There is therefore scope to further explore how the relationship between the focal metrics and model capacity varies at the individual model and functional group level and in relation to other factors (e.g. the distribution of biomass and *Q/B* values across competitor groups, or the *EE* distributions across whale prey groups). This would improve our understanding of the drivers of regional differences in ecosystem responses to whale population increases and provide greater insight into the reliability of different indicators of ecosystem resilience.

There is also scope to further investigate the factors determining regional ecosystem responses to whale recovery. Regular monitoring of the composition and diets of a range of functional groups across different regions and environmental conditions would increase our understanding of the spatial and temporal variability of trophic interactions. This would improve our ability to accurately model regional contrasts in ecosystem structure and incorporate the influence of dietary flexibility into predictions. Techniques such as DNA

metabarcoding of environmental samples and stomach contents or scats could prove extremely useful for monitoring food web structure and exploring spatial differences, as they provide a relatively cost-effective way of identifying marine community composition and monitoring trophic interactions across time and space (Canals et al. 2024). This could be facilitated through the routine collection of samples from fishing vessels, which has been found to be a very effective way of reconstructing food webs in exploited areas (Cicala et al. 2024). Tourist cruise vessels, which make extensive journeys across much of the Southern Ocean every year (McCarthy et al. 2022), are also a useful platform for conducting routine sampling of communities. Even the simple collection of surface water samples, such as through continuous plankton recorders (CPRs), would improve the monitoring of zooplankton and phytoplankton community composition across environmental gradients. The widespread adoption of CPR devices on tourist cruise vessels would greatly increase the coverage of existing datasets such as the SCAR Southern Ocean Continuous Plankton Recorder (SO-CPR) Survey, which is currently based primarily on samples from research and fishing vessels (Hosie et al. 2003). This would provide insight into questions such as the likelihood of regional changes in phytoplankton composition and production which mitigate baleen whale population increases in different regions.

The balancing algorithm developed for this chapter helps address a primary limitation of the Ecopath with Ecosim (EwE) framework, which has been the lack of capabilities to incorporate parameter uncertainty during the modelling process (Steenbeek et al. 2018). The ability to generate plausible balanced parameter sets from an initial highly unbalanced model is valuable, as current existing EwE uncertainty plugins (e.g. ‘Ecosampler’) work with input models that are at, or close to, balance (Steenbeek et al. 2018), while other methods generate unbalanced models which then need testing to ensure they are thermodynamically viable (Whitehouse and Aydin 2020). The issue of model standardization, which was addressed in this chapter, applies more broadly to all comparative modeling studies across the Southern Ocean and beyond, as many network metrics are sensitive to model structure (Heymans et al. 2016). Efforts to identify further indicators of ecosystem resilience must therefore ensure that models are directly comparable. The approach to model standardization and balancing taken in chapter 5 could be applied to many other comparative questions within the Southern Ocean including the effects of species loss or environmental regime shifts, aiding our ability to identify regional contrasts in food web structure and responses to change.

This chapter made heavy use of *Rpath*, the R implementation of EwE (Lucey et al. 2020). The development of this package is exciting as it introduces a whole range of flexibility for modellers to ask questions that perhaps are not fully suited to the original EwE framework. For example, *Rpath* has been used to implement feedback mechanisms between an operating model and external assessment model to evaluate fishery management strategies (Lucey et al. 2021). The package has also facilitated the incorporation of temperature-dependent energetic demands and metabolic costs into mass-balance models, which is a big step towards the development of robust predictions of the impacts of warming on species and ecosystem processes (Heinichen et al. 2022). These applications of *Rpath* will be extremely valuable for exploring management and conservation strategies in the Southern Ocean, where the EwE framework is relied on heavily (McCormack et al. 2021a).

6.2 Future Directions

This thesis touched upon a broad range of themes relating to different aspects of the organization and dynamics of Southern Ocean food webs, at a variety of spatial and ecological scales. However, there are some common threads regarding the future directions in which I see the research field heading, both within the Southern Ocean and more generally.

6.2.1 Using functional traits to explain and predict food web structure

Functional traits clearly represent a valuable framework for explaining and predicting the current structure of food webs and will likely become increasingly popular for predicting the future effects of environmental change and shifting community compositions. Recent developments will aid the application of the trait-based approach; in particular, machine learning tools can be a powerful method for reconstructing changes in ecosystem properties from past records and predicting the structure of past and future networks from functional traits (Brown et al. 2023; Pichler et al. 2020; Fricke et al. 2022). Additionally, the development of AI-driven algorithms to extract ecological information from literature (e.g. Gougherty and Clipp 2024) will greatly aid trait-based food web research. I imagine that similar tools could also be developed to predict the occurrence of certain traits based on taxonomy by disentangling the relative effects of environmental variables and phylogeny on trait expression (Sanchez-Martinez et al. 2024), which would make it easier to compile trait information for poorly studied species and regions. It is also important to recognise that trophic interactions are highly multidimensional, made up of multiple component steps (e.g. prey identification, capture, consumption) during which the probability of success is

determined by a variety of different traits and abiotic factors (Wootton et al. 2023). Considering the matching between interactions and functional traits in a more fine-scale, modular manner will facilitate the quantification and comparison of the relative influence of different traits, component steps and abiotic factors, and improve the prediction of network structure and dynamics (Wootton et al. 2023).

Overall, only a minority of studies have used functional traits to make predictions of the impacts of global change on ecological communities (Green et al. 2022). As this becomes more of a research focus, it is likely that the demand for extensive and well-resolved trait data will increase. As previously discussed, body size is a key trait which is easily measurable and has been used to successfully predict trophic interactions (Petchey et al. 2008). However, as shown in this thesis and in previous studies (e.g. Brose et al. 2019; Morales-Castilla et al. 2015; Laigle et al. 2017; Rezende et al. 2009; Jacob et al. 2011), a variety of other traits including habitat association, mobility, feeding mode, and other behavioural and physiological characteristics can also play major roles in determining whether organisms interact. A key recommendation is therefore that we further develop datasets of functional traits, expanding them to encompass more species and aspects of organismal ecology, and to explicitly consider the various component steps involved in trophic interactions. Trait databases already exist for many regions and taxonomic groups (for example this thesis made heavy use of resources such as Brun et al. 2017, Degen and Faulwetter 2019 and MarLIN 2006) but many data gaps remain, particularly for Southern Ocean taxa (Degen et al. 2018). I would therefore encourage researchers to consider what traits they can easily measure for their study organisms to further add value and support trait-based research. Doing so will allow us to build upon existing tools such as the Allometric Diet Breadth Model (Petchey et al. 2008), improving our ability to predict food web structure. A danger here is that, without some degree of standardization and coordination between researchers, the resulting suite of trait databases may not be fully comparable or compatible between studies, limiting their utility. This subject is neatly summarized in Keller et al. (2023), along with relevant guidelines to avoid these issues. I would add that it is also worth considering which traits should be prioritized (e.g. those which provide the most explanatory power for predicting trophic interactions or those which are most strongly tied to important ecosystem functions, rather than simply being the easiest to measure) as this will avoid wasting research effort and resources on identifying traits which have little practical use. Of course, the identification of priority traits will require significant effort itself, but could be initially achieved by

theoretical modelling and small-scale experimental or mesocosm studies before being applied more widely.

6.2.2 Understanding temporal and spatial variability in food web structure

A common theme amongst my chapters, and indeed from much of my wider reading, has been the need to identify how trophic interactions and network structure differ over space and time. This will provide insight into the drivers of variation in community assembly, including environmental filtering and coexistence mechanisms (Pellissier et al. 2018), and will help predict the consequences of environmental and ecological change. An increasing number of studies have focused on how food web structure differs geographically (e.g. Pellissier et al. 2018; Frelat et al. 2022; Kortsch et al. 2019; Gauzens et al. 2020), and temporally (e.g. Griffith et al. 2019; Olivier et al. 2019; Kortsch et al. 2021; Frelat et al. 2022), but this aspect of food web research remains understudied, particularly in the Southern Ocean where sampling is logistically limited by its overall remoteness and the inhospitableness of winter months (Van De Putte et al. 2021). The Southern Ocean has a variety of strong environmental gradients, including sea temperature, sea ice concentration and productivity (Deppeler and Davidson 2017; Morley et al. 2010; Pinkerton et al. 2021), and the impact of these factors on community structure and dynamics should be explored. Additionally, in highly seasonal environments such as polar regions, winter processes can have a strong influence on summer ecosystem dynamics, and indirect interactions between seasonally migrant and resident species can be important (Hutchison et al. 2020). Within Antarctic benthic communities in particular, seasonal sea ice break-up has been found to strongly alter food web structure, resulting in simpler, more vulnerable networks (Rossi et al. 2019; Caputi et al. 2020). This suggests that temporal changes may be a particularly fruitful topic of food web research within the Southern Ocean.

I would recommend that efforts are made to construct a greater number of highly resolved and comparable food web models in a systematic manner across different global regions, and to put in place appropriate monitoring plans to facilitate the investigation of temporal changes in structure. Given the logistical constraints that apply in the Southern Ocean, it may be necessary to select a small number of sampling sites encompassing different bioregions which can be sampled regularly enough to develop time series of community composition and associated network structure and dynamics. These could target some key CCAMLR Marine Protected Area (MPA) planning domains (Teschke et al. 2021), thereby providing important baselines for ongoing monitoring of the effectiveness of current and future MPAs.

As shown by (Frelat et al. 2022), spatio-temporal monitoring of food web structure can be facilitated through the generation of a 'metaweb' of potential trophic interactions, which can then be resampled based on species abundances to generate spatial and temporal snapshots of network structure in a relatively straightforward manner. I would also argue that, in addition to simply describing how the distribution of trophic interactions differs across environmental gradients and over time, it is important that we move past mere correlative studies and begin to model the mechanisms linking changing network structure to its drivers. This is discussed further below.

6.2.3 Using bioenergetics to gain mechanistic understanding of food web dynamics

To accurately forecast the impacts of environmental change for ecological communities and ecosystem functioning, we will need to understand the mechanisms linking biotic and abiotic factors to population dynamics, communities and overall ecosystem processes. This could be addressed through the bioenergetics approach, which explicitly considers the physiological and behavioural responses of organisms and accounts for the variety of indirect effects and non-linear responses which will result from changing environmental and ecological conditions (Rose et al. 2024). Energy is a relevant currency across all scales of spatial, temporal and ecological organisation, from individual cells to entire ecosystems, therefore focussing on energy flow provides a tractable basis for investigating links between different levels of biological organisation (Carlisle 2000). In particular, methods such as Dynamic Energy Budget (DEB) modelling can be used to predict both inter- and intra-specific variation in energy and mass fluxes in response to changing environments (Rose et al. 2024; Nisbet et al. 2012). DEB modelling is a highly generalisable approach which can be applied to any animal to predict its intake and utilisation of energy and relate metabolic processes to physiological performance and thus wider population dynamics and ecosystem processes (Nisbet et al. 2012). This allows researchers to investigate how abiotic conditions and food availability affect organismal growth, feeding and reproduction (Pouvreau et al. 2006; Agüera et al. 2017; van der Meer et al. 2020; Teixeira et al. 2014). This approach can be scaled up to entire ecosystems (van der Meer et al. 2022), and integrating it into broader food web modelling will allow us to mechanistically understand and predict how communities respond to change.

The field of food web ecology is increasingly recognising the value of bioenergetic approaches for tracking energy flux and studying the dynamics of multi-species assemblages. A number of tools based upon bioenergetics and metabolic theory have been developed for

different platforms (e.g. Gauzens et al. 2019; Gauzens et al. 2023; Delmas et al. 2017), and used to ask questions such as how environmental change impacts ecosystem function and stability (Polazzo et al. 2023), how physiological plasticity influences ecosystem impacts of warming (Kordas et al. 2022), and what the interactive effects of multiple stressors are on patterns of energy flux (Wang et al. 2023). As previously discussed, the inclusion of temperature-dependent bioenergetics within the EwE framework has provided further insight into the potential effects of warming on biomass production within marine ecosystems (Heinichen et al. 2022). The flux-based approach has also revealed how trophic redundancy can mitigate the impacts of warming on total energy flow within food webs (Nelson et al. 2020). As these bioenergetic approaches are largely based on theory and generalisable relationships, they could be well suited to locations such as the Southern Ocean where the observational and experimental data required to parameterise more complex dynamic models are scarce (McCormack et al. 2021a; Murphy et al. 2012). It will, however, be important to consider whether some of the characteristics of many Southern Ocean taxa, e.g. stenothermy, mean they do not adhere to theoretical relationships. This emphasises the need to further investigate the fundamental rates of different Southern Ocean taxa and how they respond to environmental changes such as warming. Given that the rate of physiological process can vary between individuals and there may be intra-specific variability in physiological and behavioural responses to different stressors (Gårdmark and Huss 2020), bioenergetic approaches may be best suited to individual-based food webs which explicitly consider populations and size-classes rather than simply aggregating at the species or functional group level (Woodward et al. 2010; Gårdmark and Huss 2020).

6.2.4 Summary

The results of this thesis contribute to our growing understanding of the drivers of food web structure and the impacts of environmental change. While the focus of my chapters was primarily on the Southern Ocean, many of my conclusions are also relevant to the food web modelling field more broadly. In particular, I have provided insight into some of the core aspects of food web theory, namely the relationship between functional traits and the distribution of trophic interactions, the organisation of stabilising substructures, and the influence of the environment on size-based interactions. I see various avenues of research through which the food web field will advance in future. On the one hand, ‘more of the same’ (continued characterisation of diets and traits, and construction of networks across temporal and spatial scales and environmental gradients) will allow us to more robustly test the effects

of abiotic and biotic factors on food web structure and dynamics. On the other hand, I foresee that a shift towards flux-based approaches, and a focus on individual-based food webs and explicit consideration of dynamic consumers with flexible diets, offers the chance to gain more mechanistic understanding of the processes underlying the formation and maintenance of natural communities. I'm sure that cutting-edge developments such as super-computing, machine-learning and AI will open up further possibilities for modelling ecosystems – what a time to be a food web researcher!

References

Abrams, P. A. 2010. Implications of Flexible Foraging for Interspecific Interactions: Lessons from Simple Models. *Functional Ecology,* 24**,** 7-17.

Agiadi, K., Quillévéré, F., Nawrot, R., Sommeville, T., Coll, M., Koskeridou, E., Fietzke, J. & Zuschin, M. 2022. Palaeontological Evidence for Community-Level Decrease in Mesopelagic Fish Size During Pleistocene Climate Warming in the Eastern Mediterranean. *bioRxiv***,** 2022.10.04.510798.

Agüera, A., Ahn, I.-Y., Guillaumot, C. & Danis, B. 2017. A Dynamic Energy Budget (Deb) Model to Describe Laternula Elliptica (King, 1832) Seasonal Feeding and Metabolism. *PLOS ONE,* 12**,** e0183848.

Åkesson, A., Curtsdotter, A., Eklöf, A., Ebenman, B., Norberg, J. & Barabás, G. 2021. The Importance of Species Interactions in Eco-Evolutionary Community Dynamics under Climate Change. *Nature Communications,* 12.

Albouy, C., Guilhaumon, F., Villéger, S., Mouchet, M., Mercier, L., Culioli, J., Tomasini, J., Le Loc'h, F. & Mouillot, D. 2011. Predicting Trophic Guild and Diet Overlap from Functional Traits: Statistics, Opportunities and Limitations for Marine Ecology. *Marine Ecology Progress Series,* 436**,** 17-28.

Allouche, O., Tsoar, A. & Kadmon, R. 2006. Assessing the Accuracy of Species Distribution Models: Prevalence, Kappa and the True Skill Statistic (Tss). *Journal of Applied Ecology,* 43**,** 1223-1232.

Andersen, K. H., Jacobsen, N. S. & Farnsworth, K. D. 2016. The Theoretical Foundations for Size Spectrum Models of Fish Communities. *Canadian Journal of Fisheries and Aquatic Sciences,* 73**,** 575-588.

Arim, M., Bozinovic, F. & Marquet, P. A. 2007. On the Relationship between Trophic Position, Body Mass and Temperature: Reformulating the Energy Limitation Hypothesis. *Oikos,* 116**,** 1524-1530.

Arnott, S. A., Neil, D. M. & Ansell, A. D. 1998. Tail-Flip Mechanism and Size-Dependent Kinematics of Escape Swimming in the Brown Shrimp *Crangon Crangon*. *Journal of Experimental Biology,* 201**,** 1771-1784.

Atkinson, A., Hill, S. L., Pakhomov, E. A., Siegel, V., Reiss, C. S., Loeb, V. J., Steinberg, D. K., Schmidt, K., Tarling, G. A., Gerrish, L. & Sailley, S. F. 2019. Krill (Euphausia Superba) Distribution Contracts Southward During Rapid Regional Warming. *Nature Climate Change,* 9**,** 142-147.

Atkinson, A., Hill, S. L., Reiss, C. S., Pakhomov, E. A., Beaugrand, G., Tarling, G. A., Yang, G., Steinberg, D. K., Schmidt, K., Edwards, M., Rombola, E. & Perry, F. A. 2022. Stepping Stones Towards Antarctica: Switch to Southern Spawning Grounds Explains an Abrupt Range Shift in Krill. *Glob Chang Biol,* 28**,** 1359-1375.

Atkinson, A., Siegel, V., Pakhomov, E. A., Jessopp, M. J. & Loeb, V. 2009. A Re-Appraisal of the Total Biomass and Annual Production of Antarctic Krill. *Deep Sea Research Part I: Oceanographic Research Papers,* 56**,** 727-740.

Atkinson, A., Ward, P., Hunt, B. P. V., Pakhomov, E. A. & Hosie, G. W. 2012. An Overview of Southern Ocean Zooplankton Data: Abundance, Biomass, Feeding and Functional Relationships. *CCAMLR Science,* 19**,** 171 - 218.

Auger, M., Morrow, R., Kestenare, E., Sallée, J.-B. & Cowley, R. 2021. Southern Ocean in-Situ Temperature Trends over 25 Years Emerge from Interannual Variability. *Nature Communications,* 12.

Aydin, K. Y., Mcfarlane, G. A., King, J. R., Megrey, B. A. & Myers, K. W. 2005. Linking Oceanic Food Webs to Coastal Production and Growth Rates of Pacific Salmon (Oncorhynchus Spp.), Using Models on Three Scales. *Deep Sea Research Part II: Topical Studies in Oceanography,* 52**,** 757-780.

Bachiller, E. & Irigoien, X. 2013. Allometric Relations and Consequences for Feeding in Small Pelagic Fish in the Bay of Biscay. *ICES Journal of Marine Science,* 70**,** 232-243.

Baena, P., Santín, A., La Mesa, M., Riginella, E., Owsianowski, N., Gili, J.-M. & Ambroso, S. 2023. Are There Distribution Patterns and Population Structure Differences among Demersal Fish Species in Relation to Antarctic Benthic Communities? A Case Study in the Weddell Sea. *Polar Biology,* 46**,** 1069-1082.

Baines, M., Jackson, J. A., Fielding, S., Warwick-Evans, V., Reichelt, M., Lacey, C., Pinder, S. & Trathan, P. N. 2022. Ecological Interactions between Antarctic Krill (Euphausia Superba) and Baleen Whales in the South Sandwich Islands Region– Exploring Predator-Prey Biomass Ratios. *Deep Sea Research Part I: Oceanographic Research Papers,* 189**,** 103867.

Ballerini, T., Hofmann, E. E., Ainley, D. G., Daly, K., Marrari, M., Ribic, C. A., Smith, W. O. & Steele, J. H. 2014. Productivity and Linkages of the Food Web of the Southern Region of the Western Antarctic Peninsula Continental Shelf. *Progress in Oceanography,* 122**,** 10-29.

Banašek-Richter, C., Bersier, L.-F., Cattin, M.-F., Baltensperger, R., Gabriel, J.-P., Merz, Y., Ulanowicz, R. E., Tavares, A. F., Williams, D. D., Ruiter, P. C., Winemiller, K. O. & Naisbit, R. E. 2009. Complexity in Quantitative Food Webs. *Ecology,* 90**,** 1470-1477.

Bansode, M. A., Eastman, J. T. & Aronson, R. B. 2014. Feeding Biomechanics of Five Demersal Antarctic Fishes. *Polar Biology,* 37**,** 1835-1848.

Barlow, K., Boyd, I., Croxall, J., Reid, K., Staniland, I. & Brierley, A. 2002. Are Penguins and Seals in Competition for Antarctic Krill at South Georgia? *Marine Biology,* 140**,** 205-213.

Barnes, C. L., Beaudreau, A. H. & Yamada, R. N. 2021. The Role of Size in Trophic Niche Separation between Two Groundfish Predators in Alaskan Waters. *Marine and Coastal Fisheries,* 13**,** 69-84.

Barnes, D., Griffiths, H. & Kaiser, S. 2009. Geographic Range Shift Responses to Climate Change by Antarctic Benthos: Where We Should Look. *Marine Ecology Progress Series,* 393**,** 13-26.

Barr, A. W. 2018. Ecomorphology. *Methods in paleoecology* 339-349.

Bartomeus, I., Gravel, D., Tylianakis, J. M., Aizen, M. A., Dickie, I. A. & Bernard-Verdier, M. 2016. A Common Framework for Identifying Linkage Rules across Different Types of Interactions. *Functional Ecology,* 30**,** 1894-1903.

Belcher, A., Saunders, R. & Tarling, G. 2019. Length, Weight and Abundance Data of Fish Species Captured in Rmt-25 Net Surveys in the Scotia Sea, Southern Ocean in 2006, 2008, and 2009 (Version 1.0). . UK Polar Data Centre, Natural Environment Research Council, UK Research & Innovation.

Bell, J. J. 2002. Morphological Responses of a Cup Coral to Environmental Gradients. *Sarsia,* 87**,** 319-330.

Berlow, E. L., Navarrete, S. A., Briggs, C. J., Power, M. E. & Menge, B. A. 1999. Quantifying Variation in the Strengths of Species Interactions. *Ecology,* 80**,** 2206-2224.

Bideault, A., Loreau, M. & Gravel, D. 2019. Temperature Modifies Consumer-Resource Interaction Strength through Its Effects on Biological Rates and Body Mass. *Frontiers in Ecology and Evolution,* 7.

Biggs, C. R., Yeager, L. A., Bolser, D. G., Bonsell, C., Dichiera, A. M., Hou, Z., Keyser, S. R., Khursigara, A. J., Lu, K., Muth, A. F., Negrete, B. & Erisman, B. E. 2020. Does Functional Redundancy Affect Ecological Stability and Resilience? A Review and Meta-Analysis. *Ecosphere,* 11.

Biuw, M., Lindstrøm, U., Jackson, J. A., Baines, M., Kelly, N., Mccallum, G., Skaret, G. & Krafft, B. A. 2024. Estimated Summer Abundance and Krill Consumption of Fin Whales Throughout the Scotia Sea During the 2018/2019 Summer Season. *Scientific Reports,* 14.

Blanchard, J. L., Law, R., Castle, M. D. & Jennings, S. 2011. Coupled Energy Pathways and the Resilience of Size-Structured Food Webs. *Theoretical Ecology,* 4**,** 289-300.

Blowes, S. A., Supp, S. R., Antão, L. H., Bates, A., Bruelheide, H., Chase, J. M., Moyes, F., Magurran, A., Mcgill, B., Myers-Smith, I. H., Winter, M., Bjorkman, A. D., Bowler, D. E., Byrnes, J. E. K., Gonzalez, A., Hines, J., Isbell, F., Jones, H. P., Navarro, L. M., Thompson, P. L., Vellend, M., Waldock, C. & Dornelas, M. 2019. The Geography of Biodiversity Change in Marine and Terrestrial Assemblages. *Science,* 366**,** 339-345.

Boit, A., Martinez, N. D., Williams, R. J. & Gaedke, U. 2012. Mechanistic Theory and Modelling of Complex Food-Web Dynamics in Lake Constance. *Ecology Letters,* 15**,** 594-602.

Bombosch, A., Zitterbart, D. P., Van Opzeeland, I., Frickenhaus, S., Burkhardt, E., Wisz, M. S. & Boebel, O. 2014. Predictive Habitat Modelling of Humpback (Megaptera Novaeangliae) and Antarctic Minke (Balaenoptera Bonaerensis) Whales in the Southern

Ocean as a Planning Tool for Seismic Surveys. *Deep Sea Research Part I: Oceanographic Research Papers,* 91**,** 101-114.

Bonin, M., Dussault, C., Taillon, J., Lecomte, N. & Côté, S. D. 2020. Combining Stable Isotopes, Morphological, and Molecular Analyses to Reconstruct the Diet of Free-Ranging Consumers. *Ecology and Evolution,* 10**,** 6664-6676.

Bratbak, G. & Dundas, I. 1984. Bacterial Dry Matter Content and Biomass Estimations. *Applied and Environmental Microbiology,* 48**,** 755-757.

Bridge, T. C. L., Luiz, O. J., Coleman, R. R., Kane, C. N. & Kosaki, R. K. 2016. Ecological and Morphological Traits Predict Depth-Generalist Fishes on Coral Reefs. *Proceedings of the Royal Society B: Biological Sciences,* 283**,** 20152332.

Brierley, A. S. & Kingsford, M. J. 2009. Impacts of Climate Change on Marine Organisms and Ecosystems. *Current Biology,* 19**,** R602-R614.

Brose, U., Archambault, P., Barnes, A. D., Bersier, L.-F., Boy, T., Canning-Clode, J., Conti, E., Dias, M., Digel, C., Dissanayake, A., Flores, A. a. V., Fussmann, K., Gauzens, B., Gray, C., Häussler, J., Hirt, M. R., Jacob, U., Jochum, M., Kéfi, S., Mclaughlin, O., Macpherson, M. M., Latz, E., Layer-Dobra, K., Legagneux, P., Li, Y., Madeira, C., Martinez, N. D., Mendonça, V., Mulder, C., Navarrete, S. A., O'gorman, E. J., Ott, D., Paula, J., Perkins, D., Piechnik, D., Pokrovsky, I., Raffaelli, D., Rall, B. C., Rosenbaum, B., Ryser, R., Silva, A., Sohlström, E. H., Sokolova, N., Thompson, M. S. A., Thompson, R. M., Vermandele, F., Vinagre, C., Wang, S., Wefer, J. M., Williams, R. J., Wieters, E., Woodward, G. & Iles, A. C. 2019. Predator Traits Determine Food-Web Architecture across Ecosystems. *Nature Ecology & Evolution,* 3**,** 919-927.

Brose, U., Blanchard, J. L., Eklöf, A., Galiana, N., Hartvig, M., R. Hirt, M., Kalinkat, G., Nordström, M. C., O'gorman, E. J., Rall, B. C., Schneider, F. D., Thébault, E. & Jacob, U. 2017. Predicting the Consequences of Species Loss Using Size-Structured Biodiversity Approaches. *Biological Reviews,* 92**,** 684-697.

Brose, U., Williams, R. J. & Martinez, N. D. 2006. Allometric Scaling Enhances Stability in Complex Food Webs. *Ecology Letters,* 9**,** 1228-1236.

Brown, K. A., Bunting, M. J., Carvalho, F., De Bello, F., Mander, L., Marcisz, K., Mottl, O., Reitalu, T. & Svenning, J. C. 2023. Trait-Based Approaches as Ecological Time Machines: Developing Tools for Reconstructing Long-Term Variation in Ecosystems. *Functional Ecology,* 37**,** 2552-2569.

Bruder, A., Frainer, A., Rota, T. & Primicerio, R. 2019. The Importance of Ecological Networks in Multiple-Stressor Research and Management. *Frontiers in Environmental Science,* 7.

Brun, P., Payne, M. R. & Kiørboe, T. 2017. A Trait Database for Marine Copepods. *Earth Syst. Sci. Data,* 9**,** 99-113.

Buhl-Mortensen, L., Buhl-Mortensen, P., Dolan, M. F. J., Dannheim, J., Bellec, V. & Holte, B. 2012. Habitat Complexity and Bottom Fauna Composition at Different Scales on the Continental Shelf and Slope of Northern Norway. *Hydrobiologia,* 685**,** 191-219.

Bury, S. J., Peters, K. J., Sabadel, A. J. M., St John Glew, K., Trueman, C., Wunder, M. B., Cobain, M. R. D., Schmitt, N., Donnelly, D., Magozzi, S., Owen, K., Brown, J. C. S., Escobar-Flores, P., Constantine, R., O'driscoll, R. L., Double, M., Gales, N., Childerhouse, S. & Pinkerton, M. H. 2024. Southern Ocean Humpback Whale Trophic Ecology. I. Combining Multiple Stable Isotope Methods Elucidates Diet, Trophic Position and Foraging Areas. *Marine Ecology Progress Series,* 734**,** 123-155.

Calderan, S. V., Black, A., Branch, T. A., Collins, M. A., Kelly, N., Leaper, R., Lurcock, S., Miller, B. S., Moore, M., Olson, P. A., Širović, A., Wood, A. G. & Jackson, J. A. 2020. South Georgia Blue Whales Five Decades after the End of Whaling. *Endangered Species Research,* 43**,** 359-373.

Calleja, M. L., Kerhervé, P., Bourgeois, S., Kędra, M., Leynaert, A., Devred, E., Babin, M. & Morata, N. 2017. Effects of Increase Glacier Discharge on Phytoplankton Bloom Dynamics and Pelagic Geochemistry in a High Arctic Fjord. *Progress in Oceanography,* 159**,** 195-210.

Canals, O., Lanzén, A., Mendibil, I., Bachiller, E., Corrales, X., Andonegi, E., Cotano, U. & Rodríguez-Ezpeleta, N. 2024. Increasing Marine Trophic Web Knowledge through DNA Analyses of Fish Stomach Content: A Step Towards an Ecosystem-Based Approach to Fisheries Research. *Journal of Fish Biology,* n/a.

Caputi, S. S., Careddu, G., Calizza, E., Fiorentino, F., Maccapan, D., Rossi, L. & Costantini, M. L. 2020. Seasonal Food Web Dynamics in the Antarctic Benthos of Tethys Bay (Ross Sea): Implications for Biodiversity Persistence under Different Seasonal Sea-Ice Coverage. *Frontiers in Marine Science,* 7.

Carlig, E., Di Blasi, D., Ghigliotti, L., Pisano, E., Faimali, M., O'driscoll, R., Parker, S. & Vacchi, M. 2018. Diversification of Feeding Structures in Three Adult Antarctic Nototheniid Fish. *Polar Biology,* 41**,** 1707-1715.

Carlig, E., Di Blasi, D., Pisano, E., Vacchi, M., Santovito, G. & Ghigliotti, L. 2022. Ecomorphological Differentiation of Feeding Structures within the Antarctic Fish Species Flock Trematominae (Notothenioidei) from Terra Nova Bay (Ross Sea). *Journal of Marine Science and Engineering,* 10**,** 1876.

Carlisle, D. M. 2000. Bioenergetic Food Webs as a Means of Linking Toxicological Effects across Scales of Ecological Organization. *Journal of Aquatic Ecosystem Stress and Recovery,* 7**,** 155-165.

Carter, L., Mccave, I. N. & Williams, M. J. M. 2008. Chapter 4 Circulation and Water Masses of the Southern Ocean: A Review. *In:* Florindo, F. & Siegert, M. (eds.) *Developments in Earth and Environmental Sciences.* Elsevier.

Casaux, R. & Barrera-Oro, E. 2013. Dietary Overlap in Inshore Notothenioid Fish from the Danco Coast, Western Antarctic Peninsula. *Polar Research,* 32**,** 21319.

Cavanagh, R. D., Melbourne-Thomas, J., Grant, S. M., Barnes, D. K. A., Hughes, K. A., Halfter, S., Meredith, M. P., Murphy, E. J., Trebilco, R. & Hill, S. L. 2021. Future Risk for Southern Ocean Ecosystem Services under Climate Change. *Frontiers in Marine Science,* 7.

Ceballos, G., Ehrlich, P. R., Barnosky, A. D., García, A., Pringle, R. M. & Palmer, T. M. 2015. Accelerated Modern Human–Induced Species Losses: Entering the Sixth Mass Extinction. *Science Advances,* 1**,** e1400253.

Chapman, E. J., Byron, C. J., Lasley-Rasher, R., Lipsky, C., Stevens, J. R. & Peters, R. 2020. Effects of Climate Change on Coastal Ecosystem Food Webs: Implications for Aquaculture. *Marine Environmental Research,* 162**,** 105103.

Chaudhary, C., Richardson, A. J., Schoeman, D. S. & Costello, M. J. 2021. Global Warming Is Causing a More Pronounced Dip in Marine Species Richness around the Equator. *Proceedings of the National Academy of Sciences,* 118**,** e2015094118.

Chen, M., Kuzmin, K. & Szymanski, B. K. 2014. Community Detection Via Maximization of Modularity and Its Variants. *IEEE Transactions on Computational Social Systems,* 1**,** 46-65.

Cherel, Y., Fontaine, C., Richard, P. & Labatc, J.-P. 2010. Isotopic Niches and Trophic Levels of Myctophid Fishes and Their Predators in the Southern Ocean. *Limnology and Oceanography,* 55**,** 324-332.

Cherkasheva, A., Bracher, A., Melsheimer, C., Köberle, C., Gerdes, R., Nöthig, E. M., Bauerfeind, E. & Boetius, A. 2014. Influence of the Physical Environment on Polar Phytoplankton Blooms: A Case Study in the Fram Strait. *Journal of Marine Systems,* 132**,** 196-207.

Cheung, W. W. L., Lam, V. W. Y. & Pauly, D. 2008. Modelling Present and Climate-Shifted Distribution of Marine Fishes and Invertebrates.

Cheung, W. W. L., Sarmiento, J. L., Dunne, J., Frölicher, T. L., Lam, V. W. Y., Deng Palomares, M. L., Watson, R. & Pauly, D. 2013. Shrinking of Fishes Exacerbates Impacts of Global Ocean Changes on Marine Ecosystems. *Nature Climate Change,* 3**,** 254-258.

Christensen, B. 1996. Predator Foraging Capabilities and Prey Antipredator Behaviours: Pre- Versus Postcapture Constraints on Size-Dependent Predator-Prey Interactions. *Oikos,* 76**,** 368-380.

Christensen, L. B. 2006. Marine Mammal Populations: Reconstructing Historical Abundances at the Global Scale. *Fisheries Centre research reports,* 14.

Christensen, V. & Walters, C. J. 2004. Ecopath with Ecosim: Methods, Capabilities and Limitations. *Ecological Modelling,* 172**,** 109-139.

Cicala, D., Maiello, G., Fiorentino, F., Garofalo, G., Massi, D., Sbrana, A., Mariani, S., D'alessandro, S., Stefani, M., Perrodin, L. & Russo, T. 2024. Spatial Analysis of Demersal Food Webs through Integration of Edna Metabarcoding with Fishing Activities. *Frontiers in Marine Science,* 10.

Cirtwill, A. R. & Eklöf, A. 2018. Feeding Environment and Other Traits Shape Species' Roles in Marine Food Webs. *Ecology Letters,* 21**,** 875-884.

Clark, J. S., Scher, C. L. & Swift, M. 2020. The Emergent Interactions That Govern Biodiversity Change. *Proceedings of the National Academy of Sciences,* 117**,** 17074-17083.

Clarke, S., Reid, W. D. K., Collins, M. A. & Belchier, M. 2008. Biology and Distribution of South Georgia Icefish (Pseudochaenichthys Georgianus) around South Georgia and Shag Rocks. *Antarctic Science,* 20**,** 343-353.

Coghlan, A. R., Blanchard, J. L., Wotherspoon, S., Stuart-Smith, R. D., Edgar, G. J., Barrett, N. & Audzijonyte, A. 2024. Mean Reef Fish Body Size Decreases Towards Warmer Waters. *Ecology Letters,* 27.

Cohen, J. E. 2010. Ecologists' Co-Operative Web Bank. Version 1.1. Machine-Readable Database of Food Webs. New York: The Rockefeller University.

Cohen, J. E., Jonsson, T. & Carpenter, S. R. 2003. Ecological Community Description Using the Food Web, Species Abundance, and Body Size. *Proceedings of the National Academy of Sciences,* 100**,** 1781-1786.

Coll, M., Palomera, I., Tudela, S. & Sardà, F. 2006. Trophic Flows, Ecosystem Structure and Fishing Impacts in the South Catalan Sea, Northwestern Mediterranean. *Journal of Marine Systems,* 59**,** 63-96.

Collins, M., Shreeve, R., Stowasser, G., Foster, E. & Saunders, R. 2020. Conventional Stomachs Contents Data for Mesopelagic Fish Collected from the Scotia Sea between 2004-2009 (Version 1.0). UK Polar Data Centre, Natural Environment Research Council, UK Research & Innovation.

Collins, M. A., Stowasser, G., Fielding, S., Shreeve, R., Xavier, J. C., Venables, H. J., Enderlein, P., Cherel, Y. & Van De Putte, A. 2012. Latitudinal and Bathymetric Patterns in the Distribution and Abundance of Mesopelagic Fish in the Scotia Sea. *Deep Sea Research Part II: Topical Studies in Oceanography,* 59-60**,** 189-198.

Constable, A. J. 2011. Lessons from Ccamlr on the Implementation of the Ecosystem Approach to Managing Fisheries. *Fish and Fisheries,* 12**,** 138-151.

Convey, P., Bindschadler, R., Di Prisco, G., Fahrbach, E., Gutt, J., Hodgson, D. A., Mayewski, P. A., Summerhayes, C. P. & Turner, J. 2009. Antarctic Climate Change and the Environment. *Antarctic Science,* 21**,** 541-563.

Cooley, S., Schoeman, D., Bopp, L., Boyd, P., Donner, S., Ghebrehiwet, D. Y., Ito, S.-I., Kiessling, W., Martinetto, P., Ojea, E., Racault, M.-F., Rost, B. & M., S.-M. 2022. Oceans and Coastal Ecosystems and Their Services. *Climate Change 2022 – Impacts, Adaptation and Vulnerability. Contribution of Working Group Ii to the Sixth Assessment Report of the Intergovernmental Panel on Climate Change*

Costa, G. C. 2009. Predator Size, Prey Size, and Dietary Niche Breadth Relationships in Marine Predators. *Ecology,* 90**,** 2014 - 2019.

Costello, C., Cao, L., Gelcich, S., Cisneros-Mata, M. Á., Free, C. M., Froehlich, H. E., Golden, C. D., Ishimura, G., Maier, J., Macadam-Somer, I., Mangin, T., Melnychuk, M. C., Miyahara, M., De Moor, C. L., Naylor, R., Nøstbakken, L., Ojea, E., O'reilly, E.,

Parma, A. M., Plantinga, A. J., Thilsted, S. H. & Lubchenco, J. 2020. The Future of Food from the Sea. *Nature,* 588**,** 95-100.

Cousins, N. J. & Priede, I. G. 2012. Abyssal Demersal Fish Fauna Composition in Two Contrasting Productivity Regions of the Crozet Plateau, Southern Indian Ocean. *Deep Sea Research Part I: Oceanographic Research Papers,* 64**,** 71-77.

Crespo, E. A., Pedraza, S. N., Dans, S. L., Svendsen, G. M., Degrati, M. & Coscarella, M. A. 2019. The Southwestern Atlantic Southern Right Whale, <I>Eubalaena Australis</I>, Population Is Growing but at a Decelerated Rate. *Marine Mammal Science,* 35**,** 93-107.

Cutler, D. R., Edwards, T. C., Beard, K. H., Cutler, A., Hess, K. T., Gibson, J. & Lawler, J. J. 2007. Random Forests for Classification in Ecology. *Ecology,* 88**,** 2783-2792.

D'alelio, D., Hay Mele, B., Libralato, S., Ribera D'alcala, M. & Jordan, F. 2019. Rewiring and Indirect Effects Underpin Modularity Reshuffling in a Marine Food Web under Environmental Shifts. *Ecol Evol,* 9**,** 11631-11646.

Dahood, A., Watters, G. M. & De Mutsert, K. 2019. Using Sea-Ice to Calibrate a Dynamic Trophic Model for the Western Antarctic Peninsula. *PLoS One,* 14**,** e0214814.

Daufresne, M., Lengfellner, K. & Sommer, U. 2009. Global Warming Benefits the Small in Aquatic Ecosystems. *Proc Natl Acad Sci U S A,* 106**,** 12788-93.

Degen, R., Aune, M., Bluhm, B. A., Cassidy, C., Kędra, M., Kraan, C., Vandepitte, L., Włodarska-Kowalczuk, M., Zhulay, I., Albano, P. G., Bremner, J., Grebmeier, J. M., Link, H., Morata, N., Nordström, M. C., Shojaei, M. G., Sutton, L. & Zuschin, M. 2018. Trait-Based Approaches in Rapidly Changing Ecosystems: A Roadmap to the Future Polar Oceans. *Ecological Indicators,* 91**,** 722-736.

Degen, R. & Faulwetter, S. 2019. The Arctic Traits Database – a Repository of Arctic Benthic Invertebrate Traits. *Earth Syst. Sci. Data,* 11**,** 301-322.

Delmas, E., Brose, U., Gravel, D., Stouffer, D. B. & Poisot, T. 2017. Simulations of Biomass Dynamics in Community Food Webs. *Methods in Ecology and Evolution,* 8**,** 881-886.

Deppeler, S. L. & Davidson, A. T. 2017. Southern Ocean Phytoplankton in a Changing Climate. *Frontiers in Marine Science,* 4.

Deutsch, C., Penn, J. L., Verberk, W. C. E. P., Inomura, K., Endress, M.-G. & Payne, J. L. 2022. Impact of Warming on Aquatic Body Sizes Explained by Metabolic Scaling from Microbes to Macrofauna. *Proceedings of the National Academy of Sciences,* 119.

Dobashi, T., Iida, M. & Takemoto, K. 2018. Decomposing the Effects of Ocean Environments on Predator–Prey Body-Size Relationships in Food Webs. *Royal Society Open Science,* 5**,** 180707.

Doulcier, G. & Stouffer, D. 2015. Rnetcarto: Fast Network Modularity and Roles Computation by Simulated Annealing. *R package version 0.2.4.*

Dunic, J. C. & Baum, J. K. 2017. Size Structuring and Allometric Scaling Relationships in Coral Reef Fishes. *Journal of Animal Ecology,* 86**,** 577-589.

Dunne, J., Williams, R. & Martinez, N. 2004. Network Structure and Robustness of Marine Food Webs. *Marine Ecology Progress Series,* 273**,** 291-302.

Eastman, J. T. 2004. The Nature of the Diversity of Antarctic Fishes. *Polar Biology,* 28**,** 93-107.

Emmerson, M. C. & Raffaelli, D. 2004. Predator-Prey Body Size, Interaction Strength and the Stability of a Real Food Web. *Journal of Animal Ecology,* 73**,** 399-409.

Eskuche-Keith, P., Hill, S. L., Hollyman, P., Taylor, M. L. & O'gorman, E. J. 2023. Trophic Structuring of Modularity Alters Energy Flow through Marine Food Webs. *Frontiers in Marine Science,* 9.

Eskuche-Keith, P., Hill, S. L., López-López, L., Rosenbaum, B., Saunders, R. A., Tarling, G. A. & O'gorman, E. J. 2024. Temperature Alters the Predator-Prey Size Relationships and Size-Selectivity of Southern Ocean Fish. *Nature Communications,* 15.

Ferry, L. A., Paig-Tran, E. M. & Gibb, A. C. 2015. Suction, Ram, and Biting: Deviations and Limitations to the Capture of Aquatic Prey. *Integr Comp Biol,* 55**,** 97-109.

Fielding, S., Watkins, J. L., Trathan, P. N., Enderlein, P., Waluda, C. M., Stowasser, G., Tarling, G. A. & Murphy, E. J. 2014. Interannual Variability in Antarctic Krill (Euphausia Superba) Density at South Georgia, Southern Ocean: 1997–2013. *ICES Journal of Marine Science,* 71**,** 2578-2588.

Finlay, B. J. & Uhlig, G. 1981. Calorific and Carbon Values of Marine and Freshwater Protozoa. *Helgoländer Meeresuntersuchungen,* 34**,** 401-412.

Fisher, B. J., Poulton, A. J., Meredith, M. P., Baldry, K., Schofield, O. & Henley, S. F. 2024. Biogeochemistry of Climate Driven Shifts in Southern Ocean Primary Producers. Copernicus GmbH.

Fjeld, K., Tiller, R., Grimaldo, E., Grimsmo, L. & Standal, I.-B. 2023. Mesopelagics–New Gold Rush or Castle in the Sky? *Marine Policy,* 147.

Flensborg, L. C., Maureaud, A. A., Bravo, D. N. & Lindegren, M. 2023. An Indicator-Based Approach for Assessing Marine Ecosystem Resilience. *ICES Journal of Marine Science,* 80**,** 1487-1499.

Flores, H., Atkinson, A., Kawaguchi, S., Krafft, B., Milinevsky, G., Nicol, S., Reiss, C., Tarling, G., Werner, R., Bravo Rebolledo, E., Cirelli, V., Cuzin-Roudy, J., Fielding, S., Van Franeker, J., Groeneveld, J., Haraldsson, M., Lombana, A., Marschoff, E., Meyer, B., Pakhomov, E., Van De Putte, A., Rombolá, E., Schmidt, K., Siegel, V., Teschke, M., Tonkes, H., Toullec, J., Trathan, P., Tremblay, N. & Werner, T. 2012. Impact of Climate Change on Antarctic Krill. *Marine Ecology Progress Series,* 458**,** 1-19.

Forget, N. L., Duplisea, D. E., Sardenne, F. & Mckindsey, C. W. 2020. Using Qualitative Network Models to Assess the Influence of Mussel Culture on Ecosystem Dynamics. *Ecological Modelling,* 430.

Forster, J., Hirst, A. G. & Atkinson, D. 2012. Warming-Induced Reductions in Body Size Are Greater in Aquatic Than Terrestrial Species. *Proceedings of the National Academy of Sciences,* 109**,** 19310-19314.

Freer, J. J., Tarling, G. A., Collins, M. A., Partridge, J. C. & Genner, M. J. 2019. Predicting Future Distributions of Lanternfish, a Significant Ecological Resource within the Southern Ocean. *Diversity and Distributions*.

Frelat, R., Kortsch, S., Kröncke, I., Neumann, H., Nordström, M. C., Olivier, P. E. N. & Sell, A. F. 2022. Food Web Structure and Community Composition: A Comparison across Space and Time in the North Sea. *Ecography,* 2022.

Fretwell, P. T., Boutet, A. & Ratcliffe, N. 2023. Record Low 2022 Antarctic Sea Ice Led to Catastrophic Breeding Failure of Emperor Penguins. *Communications Earth & Environment,* 4.

Fricke, E. C., Hsieh, C., Middleton, O., Gorczynski, D., Cappello, C. D., Sanisidro, O., Rowan, J., Svenning, J.-C. & Beaudrot, L. 2022. Collapse of Terrestrial Mammal Food Webs since the Late Pleistocene. *Science,* 377**,** 1008-1011.

Fu, W., Randerson, J. T. & Moore, J. K. 2016. Climate Change Impacts on Net Primary Production (Npp) and Export Production (Ep) Regulated by Increasing Stratification and Phytoplankton Community Structure in the Cmip5 Models. *Biogeosciences,* 13**,** 5151-5170.

Galiana, N., Barros, C., Braga, J., Ficetola, G. F., Maiorano, L., Thuiller, W., Montoya, J. M. & Lurgi, M. 2021. The Spatial Scaling of Food Web Structure across European Biogeographical Regions. *Ecography,* 44**,** 653-664.

Gallucci, F., A. Christofoletti, R., Fonseca, G. & M. Dias, G. 2020. The Effects of Habitat Heterogeneity at Distinct Spatial Scales on Hard-Bottom-Associated Communities. *Diversity,* 12**,** 39.

Gårdmark, A. & Huss, M. 2020. Individual Variation and Interactions Explain Food Web Responses to Global Warming. *Philos Trans R Soc Lond B Biol Sci,* 375**,** 20190449.

Garnesson, P., Mangin, A., Fanton D'andon, O., Demaria, J. & Bretagnon, M. 2019. The Cmems Globcolour Chlorophyll a Product Based on Satellite Observation: Multi-Sensor Merging and Flagging Strategies. *Ocean Science,* 15**,** 819-830.

Gauzens, B., Barnes, A., Giling, D. P., Hines, J., Jochum, M., Lefcheck, J. S., Rosenbaum, B., Wang, S. & Brose, U. 2019. Fluxweb : An R Package to Easily Estimate Energy Fluxes in Food Webs. *Methods in Ecology and Evolution,* 10**,** 270-279.

Gauzens, B., Brose, U., Delmas, E. & Berti, E. 2023. Atnr: Allometric Trophic Network Models in R. *Methods in Ecology and Evolution,* 14**,** 2766-2773.

Gauzens, B., Legendre, S., Lazzaro, X. & Lacroix, G. 2013. Food-Web Aggregation, Methodological and Functional Issues. *Oikos,* 122**,** 1606-1615.

Gauzens, B., Rall, B. C., Mendonça, V., Vinagre, C. & Brose, U. 2020. Biodiversity of Intertidal Food Webs in Response to Warming across Latitudes. *Nature Climate Change,* 10**,** 264-269.

Gauzens, B., Rosenbaum, B., Kalinkat, G., Boy, T., Jochum, M., Kortsch, S., O'gorman, E. J. & Brose, U. 2024. Flexible Foraging Behaviour Increases Predator Vulnerability to Climate Change. *Nature Climate Change,* 14**,** 387-392.

Gauzens, B., Thebault, E., Lacroix, G. & Legendre, S. 2015. Trophic Groups and Modules: Two Levels of Group Detection in Food Webs. *J R Soc Interface,* 12.

Gibb, H., Stoklosa, J., Warton, D. I., Brown, A. M., Andrew, N. R. & Cunningham, S. A. 2015. Does Morphology Predict Trophic Position and Habitat Use of Ant Species and Assemblages? *Oecologia,* 177**,** 519-531.

Gibert, J. P. 2019. Temperature Directly and Indirectly Influences Food Web Structure. *Scientific Reports,* 9.

Gibert, J. P. & Delong, J. P. 2014. Temperature Alters Food Web Body-Size Structure. *Biology Letters,* 10**,** 20140473.

Gilabert, O. R., Navia, A. F., De La Cruz-Agüero, G., Molinero, J. C., Sommer, U. & Scotti, M. 2019. Body Size and Mobility Explain Species Centralities in the Gulf of California Food Web. *Community Ecology,* 20**,** 149-160.

Gilbert, L., Jeanniard-Du-Dot, T., Authier, M., Chouvelon, T. & Spitz, J. 2023. Composition of Cetacean Communities Worldwide Shapes Their Contribution to Ocean Nutrient Cycling. *Nature Communications,* 14.

Gillooly, J. F. 2000. Effect of Body Size and Temperature on Generation Time in Zooplankton. *Journal of Plankton Research,* 22**,** 241-251.

Gingold, R., Mundo-Ocampo, M., Holovachov, O. & Rocha-Olivares, A. 2010. The Role of Habitat Heterogeneity in Structuring the Community of Intertidal Free-Living Marine Nematodes. *Marine Biology,* 157**,** 1741-1753.

Gissi, E., Manea, E., Mazaris, A. D., Fraschetti, S., Almpanidou, V., Bevilacqua, S., Coll, M., Guarnieri, G., Lloret-Lloret, E., Pascual, M., Petza, D., Rilov, G., Schonwald, M., Stelzenmüller, V. & Katsanevakis, S. 2021. A Review of the Combined Effects of Climate Change and Other Local Human Stressors on the Marine Environment. *Science of The Total Environment,* 755**,** 142564.

Gjoni, V., Glazier, D. S., Wesner, J. S., Ibelings, B. W. & Thomas, M. K. 2023. Temperature, Resources and Predation Interact to Shape Phytoplankton Size–Abundance Relationships at a Continental Scale. *Global Ecology and Biogeography,* 32**,** 2006-2016.

Gogina, M., Zettler, A. & Zettler, M. L. 2022. Weight-to-Weight Conversion Factors for Benthic Macrofauna: Recent Measurements from the Baltic and the North Seas. *Earth System Science Data,* 14**,** 1-4.

Gougherty, A. V. & Clipp, H. L. 2024. Testing the Reliability of an Ai-Based Large Language Model to Extract Ecological Information from the Scientific Literature. *npj Biodiversity,* 3.

Gravel, D., Albouy, C. & Thuiller, W. 2016. The Meaning of Functional Trait Composition of Food Webs for Ecosystem Functioning. *Philosophical Transactions of the Royal Society B: Biological Sciences,* 371**,** 20150268.

Gravel, D., Poisot, T., Albouy, C., Velez, L. & Mouillot, D. 2013. Inferring Food Web Structure from Predator-Prey Body Size Relationships. *Methods in Ecology and Evolution,* 4**,** 1083-1090.

Green, S. J., Brookson, C. B., Hardy, N. A. & Crowder, L. B. 2022. Trait-Based Approaches to Global Change Ecology: Moving from Description to Prediction. *Proceedings of the Royal Society B: Biological Sciences,* 289.

Greenspoon, L., Krieger, E., Sender, R., Rosenberg, Y., Bar-On, Y. M., Moran, U., Antman, T., Meiri, S., Roll, U., Noor, E. & Milo, R. 2023. The Global Biomass of Wild Mammals. *Proceedings of the National Academy of Sciences,* 120.

Griffith, G. P., Hop, H., Vihtakari, M., Wold, A., Kalhagen, K. & Gabrielsen, G. W. 2019. Ecological Resilience of Arctic Marine Food Webs to Climate Change. *Nature Climate Change,* 9**,** 868-872.

Grilli, J., Rogers, T. & Allesina, S. 2016. Modularity and Stability in Ecological Communities. *Nature Communications,* 7**,** 12031.

Guimerà, R. & Nunes Amaral, L. A. 2005. Functional Cartography of Complex Metabolic Networks. *Nature,* 433**,** 895-900.

Guimera, R., Stouffer, D. B., Sales-Pardo, M., Leicht, E. A. & Newman, M. E. J. 2010. Origin of Compartmentalization in Food Webs. *Ecology,* 91**,** 2941-2951.

Gurney, L. J., Pakhomov, E. A. & Christensen, V. 2014. An Ecosystem Model of the Prince Edward Island Archipelago. *Ecological Modelling,* 294**,** 117-136.

Gutt, J., Alvaro, M. C., Barco, A., Böhmer, A., Bracher, A., David, B., De Ridder, C., Dorschel, B., Eléaume, M., Janussen, D., Kersken, D., López-González, P. J., Martínez-Baraldés, I., Schröder, M., Segelken-Voigt, A. & Teixidó, N. 2016. Macroepibenthic Communities at the Tip of the Antarctic Peninsula, an Ecological Survey at Different Spatial Scales. *Polar Biology,* 39**,** 829-849.

Hatton, I. A., Heneghan, R. F., Bar-On, Y. M. & Galbraith, E. D. 2021. The Global Ocean Size Spectrum from Bacteria to Whales. *Science Advances,* 7**,** eabh3732.

Havermans, C., Auel, H., Hagen, W., Held, C., Ensor, N. S. & A. Tarling, G. 2019. Predatory Zooplankton on the Move: Themisto Amphipods in High-Latitude Marine Pelagic Food Webs. Elsevier.

He, X., Liang, J., Zeng, G., Yuan, Y. & Li, X. 2019. The Effects of Interaction between Climate Change and Land-Use/Cover Change on Biodiversity-Related Ecosystem Services. *Global Challenges,* 3**,** 1800095.

Heinichen, M., Mcmanus, M. C., Lucey, S. M., Aydin, K., Humphries, A., Innes-Gold, A. & Collie, J. 2022. Incorporating Temperature-Dependent Fish Bioenergetics into a Narragansett Bay Food Web Model. *Ecological Modelling,* 466**,** 109911.

Helfman, G. S., Collette, B. B., Facey, D. E. & Bowen, B. W. 2023. *The Diversity of Fishes: Biology, Evolution and Ecology*, John Wiley & Sons Ltd.

Henley, S. F., Cavan, E. L., Fawcett, S. E., Kerr, R., Monteiro, T., Sherrell, R. M., Bowie, A. R., Boyd, P. W., Barnes, D. K. A., Schloss, I. R., Marshall, T., Flynn, R. & Smith, S. 2020. Changing Biogeochemistry of the Southern Ocean and Its Ecosystem Implications. *Frontiers in Marine Science,* 7.

Heymans, J. J., Coll, M., Libralato, S., Morissette, L. & Christensen, V. 2014. Global Patterns in Ecological Indicators of Marine Food Webs: A Modelling Approach. *PLoS ONE,* 9**,** e95845.

Heymans, J. J., Coll, M., Link, J. S., Mackinson, S., Steenbeek, J., Walters, C. & Christensen, V. 2016. Best Practice in Ecopath with Ecosim Food-Web Models for Ecosystem-Based Management. *Ecological Modelling,* 331**,** 173-184.

Higham, T. E. 2007. The Integration of Locomotion and Prey Capture in Vertebrates: Morphology, Behavior, and Performance. *Integrative and Comparative Biology,* 47**,** 82-95.

Hill, S. L., Keeble, K., Atkinson, A. & Murphy, E. J. 2012. A Foodweb Model to Explore Uncertainties in the South Georgia Shelf Pelagic Ecosystem. *Deep Sea Research Part II: Topical Studies in Oceanography,* 59-60**,** 237-252.

Hill, S. L., Murphy, E. J., Reid, K., Trathan, P. N. & Constable, A. J. 2006. Modelling Southern Ocean Ecosystems: Krill, the Food-Web, and the Impacts of Harvesting. *Biological Reviews,* 81**,** 581.

Hill, S. L., Pinkerton, M. H., Ballerini, T., Cavan, E. L., Gurney, L. J., Martins, I. & Xavier, J. C. 2021. Robust Model-Based Indicators of Regional Differences in Food-Web Structure in the Southern Ocean. *Journal of Marine Systems,* 220.

Hill, S. L., Reid, K. & North, A. W. 2005. Recruitment of Mackerel Icefish (Champsocephalus Gunnari) at South Georgia Indicated by Predator Diets and Its Relationship with Sea Surface Temperature. *Canadian Journal of Fisheries and Aquatic Sciences,* 62**,** 2530-2537.

Hines, J., Ebeling, A., Barnes, A. D., Brose, U., Scherber, C., Scheu, S., Tscharntke, T., Weisser, W. W., Giling, D. P., Klein, A. M. & Eisenhauer, N. 2019. Mapping Change in Biodiversity and Ecosystem Function Research: Food Webs Foster Integration of Experiments and Science Policy. *Mechanisms Underlying the Relationship between Biodiversity and Ecosystem Function.*

Hirst, A. G. & Kiørboe, T. 2002. Mortality of Marine Planktonic Copepods: Global Rates and Patterns. *Marine Ecology Progress Series,* 230**,** 195-209.

Hobson, E., S. 1979. Interactions between Piscivorous Fishes and Their Prey. *Predator-prey systems in fisheries management***,** 231-242.

Hogg, O. T., Barnes, D. K. A. & Griffiths, H. J. 2011. Highly Diverse, Poorly Studied and Uniquely Threatened by Climate Change: An Assessment of Marine Biodiversity on South Georgia's Continental Shelf. *PLoS ONE,* 6**,** e19795.

Hollyman, P., Hill S.L., Gunn C., Keith P., Rodriguez, B. & Collins, M. A. 2023. Report of the Uk Groundfish Survey at South Georgia (Ccamlr Subarea 48.3) in February 2023. CCAMLR WG-FSA 2023/45.

Hollyman, P. R., Hill, S. L., Laptikhovsky, V. V., Belchier, M., Gregory, S., Clement, A. & Collins, M. A. 2021. A Long Road to Recovery: Dynamics and Ecology of the Marbled Rockcod (Notothenia Rossii, Family: Nototheniidae) at South Georgia, 50 Years after Overexploitation. *ICES Journal of Marine Science*.

Hop, H., Pearson, T., Hegseth, E. N., Kovacs, K. M., Wiencke, C., Kwasniewski, S., Eiane, K., Mehlum, F., Gulliksen, B., Wlodarska-Kowalczuk, M., Lydersen, C., Weslawski, J. M., Cochrane, S., Gabrielsen, G. W., Leakey, R. J. G., Lønne, O. J., Zajaczkowski, M., Falk-Petersen, S., Kendall, M., Wängberg, S.-Å., Bischof, K., Voronkov, A. Y., Kovaltchouk, N. A., Wiktor, J., Poltermann, M., Prisco, G. D., Papucci, C. & Gerland, S. 2002. The Marine Ecosystem of Kongsfjorden, Svalbard. *Polar Research,* 21**,** 167-208.

Horn, S. & De La Vega, C. 2016. Relationships between Fresh Weight, Dry Weight, Ash Free Dry Weight, Carbon and Nitrogen Content for Selected Vertebrates. *Journal of Experimental Marine Biology and Ecology,* 481**,** 41-48.

Horswill, C., Jackson, J. A., Medeiros, R., Nowell, R. W., Trathan, P. N. & O'connell, T. C. 2018. Minimising the Limitations of Using Dietary Analysis to Assess Foodweb Changes by Combining Multiple Techniques. *Ecological Indicators,* 94**,** 218-225.

Hosie, G. W., Fukuchi, M. & Kawaguchi, S. 2003. Development of the Southern Ocean Continuous Plankton Recorder Survey. *Progress in Oceanography,* 58**,** 263-283.

Hothorn, T., Bühlmann, P., Dudoit, S., Molinaro, A. & Van Der Laan, M. J. 2005. Survival Ensembles. *Biostatistics,* 7**,** 355-373.

Hucke-Gaete, R., Osman, L. P., Moreno, C. A. & Torres, D. 2004. Examining Natural Population Growth from near Extinction: The Case of the Antarctic Fur Seal at the South Shetlands, Antarctica. *Polar Biology,* 27**,** 304-311.

Hunt, B. P., Pakhomov, E. A. & Williams, R. 2011. Comparative Analysis of the 1980s and 2004 Macrozooplankton Composition and Distribution in the Vicinity of Kerguelen and Heard Islands: Seasonal Cycles and Oceanographic Forcing of Long-Term Change. *The Kerguelen plateau: marine ecosystem and fisheries,* 35**,** 79-92.

Hunt, B. P. V., Espinasse, B., Pakhomov, E. A., Cherel, Y., Cotté, C., Delegrange, A. & Henschke, N. 2021. Pelagic Food Web Structure in High Nutrient Low Chlorophyll (Hnlc) and Naturally Iron Fertilized Waters in the Kerguelen Islands Region, Southern Ocean. *Journal of Marine Systems,* 224**,** 103625.

Hutchison, C., Guichard, F., Legagneux, P., Gauthier, G., Bêty, J., Berteaux, D., Fauteux, D. & Gravel, D. 2020. Seasonal Food Webs with Migrations: Multi-Season Models Reveal Indirect Species Interactions in the Canadian Arctic Tundra. *Philosophical*

Transactions of the Royal Society A: Mathematical, Physical and Engineering Sciences, 378**,** 20190354.

Ikeda, T. 2016. Routine Metabolic Rates of Pelagic Marine Fishes and Cephalopods as a Function of Body Mass, Habitat Temperature and Habitat Depth. *Journal of Experimental Marine Biology and Ecology,* 480**,** 74-86.

Ives, A. R., Cardinale, B. J. & Snyder, W. E. 2004. A Synthesis of Subdisciplines: Predator-Prey Interactions, and Biodiversity and Ecosystem Functioning. *Ecology Letters,* 8**,** 102-116.

Ives, A. R. & Carpenter, S. R. 2007. Stability and Diversity of Ecosystems. *Science,* 317**,** 58-61.

Iwc. 2024. *Population Status* [Online]. International Whaling Commission. Available: https://iwc.int/about-whales/population-status [Accessed].

Jacob, U., Thierry, A., Brose, U., Arntz, W. E., Berg, S., Brey, T., Fetzer, I., Jonsson, T., Mintenbeck, K., Möllmann, C., Petchey, O. L., Riede, J. O. & Dunne, J. A. 2011. The Role of Body Size in Complex Food Webs. *The Role of Body Size in Multispecies Systems.*

Jacquet, C., Gounand, I. & Altermatt, F. 2020. How Pulse Disturbances Shape Size-Abundance Pyramids. *Ecology Letters,* 23**,** 1014-1023.

Janis, C. M. & Carrano, M. 1991. Scaling of Reproductive Turnover in Archosaurs and Mammals: Why Are Large Terrestrial Mammals So Rare? *Annales Zoologici Fennici,* 28**,** 201-216.

Jean-Michel, L., Eric, G., Romain, B.-B., Gilles, G., Angélique, M., Marie, D., Clément, B., Mathieu, H., Olivier, L. G., Charly, R., Tony, C., Charles-Emmanuel, T., Florent, G., Giovanni, R., Mounir, B., Yann, D. & Pierre-Yves, L. T. 2021. The Copernicus Global 1/12° Oceanic and Sea Ice Glorys12 Reanalysis. *Frontiers in Earth Science,* 9.

Jennings, S., Pinnegar, J. K., Polunin, N. V. C. & Boon, T. W. 2001. Weak Cross-Species Relationships between Body Size and Trophic Level Belie Powerful Size-Based Trophic Structuring in Fish Communities. *Journal of Animal Ecology,* 70**,** 934-944.

Jessop, M., Mcallen, R., O'halloran, J. & Kelly, T. 2011. Nutrient and Ecosystem Dynamics in Ireland's Only Marine Nature Reserve (Neidin). *EPA STRIVE Programme 2007–2013.* Environmental Protection Agency.

Jochum, M., Barnes, A. D., Brose, U., Gauzens, B., Sünnemann, M., Amyntas, A. & Eisenhauer, N. 2021. For Flux's Sake: General Considerations for Energy-Flux Calculations in Ecological Communities. *Ecology and Evolution,* 11**,** 12948-12969.

Jochum, M. & Eisenhauer, N. 2022. Out of the Dark: Using Energy Flux to Connect above- and Belowground Communities and Ecosystem Functioning. *European Journal of Soil Science,* 73.

Jonsson, T. 2014. Trophic Links and the Relationship between Predator and Prey Body Sizes in Food Webs. *Community Ecology,* 15**,** 54-64.

Jonsson, T., Berg, S., Pimenov, A., Palmer, C. & Emmerson, M. 2015. The Reliability of R_{50} as a Measure of Vulnerability of Food Webs to Sequential Species Deletions. *Oikos,* 124**,** 446-457.

Jonsson, T., Cohen, J. E. & Carpenter, S. R. 2005. Food Webs, Body Size, and Species Abundance in Ecological Community Description. *Advances in Ecological Research,* 36**,** 1-84.

Jonsson, T. & Ebenman, B. 1998. Effects of Predator–Prey Body Size Ratios on the Stability of Food Chains. *Journal of Theoretical Biology,* 193**,** 407-417.

Kaufman, D. E., Friedrichs, M. a. M., Smith, W. O., Hofmann, E. E., Dinniman, M. S. & Hemmings, J. C. P. 2017. Climate Change Impacts on Southern Ross Sea Phytoplankton Composition, Productivity, and Export. *Journal of Geophysical Research: Oceans,* 122**,** 2339-2359.

Kavanagh, P., Newlands, N., Christensen, V. & Pauly, D. 2004. Automated Parameter Optimization for Ecopath Ecosystem Models. *Ecological Modelling,* 172**,** 141-149.

Kawaguchi, S., Atkinson, A., Bahlburg, D., Bernard, K. S., Cavan, E. L., Cox, M. J., Hill, S. L., Meyer, B. & Veytia, D. 2024. Climate Change Impacts on Antarctic Krill Behaviour and Population Dynamics. *Nature Reviews Earth & Environment,* 5**,** 43-58.

Keller, A., Ankenbrand, M. J., Bruelheide, H., Dekeyzer, S., Enquist, B. J., Erfanian, M. B., Falster, D. S., Gallagher, R. V., Hammock, J., Kattge, J., Leonhardt, S. D., Madin, J. S., Maitner, B., Neyret, M., Onstein, R. E., Pearse, W. D., Poelen, J. H., Salguero-Gomez, R., Schneider, F. D., Tóth, A. B. & Penone, C. 2023. Ten (Mostly) Simple Rules to Future-Proof Trait Data in Ecological and Evolutionary Sciences. *Methods in Ecology and Evolution,* 14**,** 444-458.

Keramidas, I., Dimarchopoulou, D., Ofir, E., Scotti, M., Tsikliras, A. C. & Gal, G. 2023. Ecotrophic Perspective in Fisheries Management: A Review of Ecopath with Ecosim Models in European Marine Ecosystems. *Frontiers in Marine Science,* 10.

Kiørboe, T. 2013. Zooplankton Body Composition. *Limnology and Oceanography,* 58**,** 1843-1850.

Kiørboe, T., Visser, A., Andersen, K. H. & Browman, H. 2018. A Trait-Based Approach to Ocean Ecology. *ICES Journal of Marine Science,* 75**,** 1849-1863.

Klein, E. S., Hill, S. L., Hinke, J. T., Phillips, T. & Watters, G. M. 2018. Impacts of Rising Sea Temperature on Krill Increase Risks for Predators in the Scotia Sea. *PLOS ONE,* 13**,** e0191011.

Kock, K.-H., Reid, K., Croxall, J. & Nicol, S. 2007. Fisheries in the Southern Ocean: An Ecosystem Approach. *Philosophical Transactions of the Royal Society B: Biological Sciences,* 362**,** 2333-2349.

Kock, K., H.,, Barrera-Oro, E., Belchier, M., Collins, M. A., Duhamel, G., Hanchet, S., Pshenichnov, L., Welsford, D. & Williams, R. 2012. The Role of Fish as Predators of Krill (Euphausia Superba) and Other Pelagic Resources in the Southern Ocean. *CCAMLR Science,* 19**,** 115-169.

Kock, K. H., Wilhelms, S., Everson, I. & Gröger, J. 1994. Variations in the Diet Composition and Feeding Intensity of Mackerel Icefish Champsocephalus Gunnari at South Georgia (Antarctic). *Marine Ecology Progress Series,* 108**,** 43-57.

Kordas, R. L., Pawar, S., Kontopoulos, D.-G., Woodward, G. & O'gorman, E. J. 2022. Metabolic Plasticity Can Amplify Ecosystem Responses to Global Warming. *Nature Communications,* 13.

Kortsch, S., Frelat, R., Pecuchet, L., Olivier, P., Putnis, I., Bonsdorff, E., Ojaveer, H., Jurgensone, I., Strāķe, S., Rubene, G., Krūze, Ē. & Nordström, M. C. 2021. Disentangling Temporal Food Web Dynamics Facilitates Understanding of Ecosystem Functioning. *Journal of Animal Ecology,* 90**,** 1205-1216.

Kortsch, S., Primicerio, R., Aschan, M., Lind, S., Dolgov, A. V. & Planque, B. 2019. Food-Web Structure Varies Along Environmental Gradients in a High-Latitude Marine Ecosystem. *Ecography,* 42**,** 295-308.

Kortsch, S., Primicerio, R., Fossheim, M., Dolgov, A. V. & Aschan, M. 2015. Climate Change Alters the Structure of Arctic Marine Food Webs Due to Poleward Shifts of Boreal Generalists. *Proceedings of the Royal Society B: Biological Sciences,* 282**,** 20151546.

Kouwenberg, J. H. M., Razouls, C. & Desreumaux, N. 2014. Chapter 6.6. Southern Ocean Pelagic Copepods. *In:* De Broyer C., Koubbi P., Griffiths H.J., Raymond B., Udekem D'acoz C. D', Van De Putte A.P., Danis B., David B., Grant S., Gutt J., Held C., Hosie G., Huettmann F., Post A. & Y., R.-C. (eds.) *Biogeographic Atlas of the Southern Ocean.* Cambridge: Scientific Committee on Antarctic Research.

Kraan, C., Aarts, G., Piersma, T. & Dormann, C. F. 2013. Temporal Variability of Ecological Niches: A Study on Intertidal Macrobenthic Fauna. *Oikos,* 122**,** 754-760.

Krafft, B. A., Lowther, A. & Krag, L. A. 2023. Bycatch in the Antarctic Krill (<I>Euphausia Superba</I>) Trawl Fishery. *Fisheries Management and Ecology,* 30**,** 154-160.

Kratina, P., Lecraw, R. M., Ingram, T. & Anholt, B. R. 2012. Stability and Persistence of Food Webs with Omnivory: Is There a General Pattern? *Ecosphere,* 3**,** 1-18.

Kratina, P., Rosenbaum, B., Gallo, B., Horas, E. L. & O'gorman, E. J. 2022. The Combined Effects of Warming and Body Size on the Stability of Predator-Prey Interactions. *Frontiers in Ecology and Evolution,* 9.

Krause, A. E., Frank, K. A., Mason, D. M., Ulanowicz, R. E. & Taylor, W. W. 2003. Compartments Revealed in Food-Web Structure. *Nature,* 426**,** 282-285.

Krumhardt, K. M., Long, M. C., Sylvester, Z. T. & Petrik, C. M. 2022. Climate Drivers of Southern Ocean Phytoplankton Community Composition and Potential Impacts on Higher Trophic Levels. *Frontiers in Marine Science,* 9.

La Mesa, M. & Eastman, J. T. 2011. Antarctic Silverfish: Life Strategies of a Key Species in the High-Antarctic Ecosystem. *Fish and Fisheries,* 13**,** 241-266.

La Mesa, M., Piepenburg, D., Pineda-Metz, S. E. A., Riginella, E. & Eastman, J. T. 2019. Spatial Distribution and Habitat Preferences of Demersal Fish Assemblages in the Southeastern Weddell Sea (Southern Ocean). *Polar Biology,* 42**,** 1025-1040.

Ladds, M. A., Sibanda, N., Arnold, R. & Dunn, M. R. 2018. Creating Functional Groups of Marine Fish from Categorical Traits. *PeerJ,* 6**,** e5795.

Laigle, I., Aubin, I., Digel, C., Brose, U., Boulangeat, I. & Gravel, D. 2017. Species Traits as Drivers of Food Web Structure. *Oikos,* 127**,** 316-326.

Lavin, C. P., Gordó-Vilaseca, C., Stephenson, F., Shi, Z. & Costello, M. J. 2022. Warmer Temperature Decreases the Maximum Length of Six Species of Marine Fishes, Crustacean, and Squid in New Zealand. *Environmental Biology of Fishes*.

Laws, R. M. 1977. Seals and Whales of the Southern Ocean. *Philosophical Transactions of the Royal Society of London. B, Biological Sciences,* 279**,** 81-96.

Layman, C. A., Giery, S. T., Buhler, S., Rossi, R., Penland, T., Henson, M. N., Bogdanoff, A. K., Cove, M. V., Irizarry, A. D., Schalk, C. M. & Archer, S. K. 2015. A Primer on the History of Food Web Ecology: Fundamental Contributions of Fourteen Researchers. *Food Webs,* 4**,** 14-24.

Lazzaro, X., Lacroix, G., Gauzens, B., Gignoux, J. & Legendre, S. 2009. Predator Foraging Behaviour Drives Food-Web Topological Structure. *Journal of Animal Ecology,* 78**,** 1307-1317.

Lefort, S., Aumont, O., Bopp, L., Arsouze, T., Gehlen, M. & Maury, O. 2015. Spatial and Body-Size Dependent Response of Marine Pelagic Communities to Projected Global Climate Change. *Global Change Biology,* 21**,** 154-164.

Lemoine, N. P., Drews, W. A., Burkepile, D. E. & Parker, J. D. 2013. Increased Temperature Alters Feeding Behavior of a Generalist Herbivore. *Oikos,* 122**,** 1669-1678.

Liermann & Hilborn 2001. Depensation: Evidence, Models and Implications. *Fish and Fisheries,* 2**,** 33-58.

Liu, K., Lin, H., He, X., Huang, Y., Li, Z., Lin, J., Mou, J., Zhang, S., Lin, L., Wang, J. & Sun, J. 2019. Functional Trait Composition and Diversity Patterns of Marine Macrobenthos across the Arctic Bering Sea. *Ecological Indicators,* 102**,** 673-685.

Lleonart, J., Salat, J. & Torres, G. J. 2000. Removing Allometric Effects of Body Size in Morphological Analysis. *J Theor Biol,* 205**,** 85-93.

Lockyer, C. 1976. Body Weights of Some Species of Large Whales. *ICES Journal of Marine Science,* 36**,** 259-273.

Lombarte, A., Olaso, I. & Bozzano, A. 2003. Ecomorphological Trends in the Artedidraconidae (Pisces: Perciformes: Notothenioidei) of the Weddell Sea. *Antarctic Science,* 15**,** 211-218.

López-López, L., Genner, M. J., Tarling, G. A., Saunders, R. A. & O'gorman, E. J. 2021. Ecological Networks in the Scotia Sea: Structural Changes across Latitude and Depth. *Ecosystems*.

Lucey, S. M., Aydin, K. Y., Gaichas, S. K., Cadrin, S. X., Fay, G., Fogarty, M. J. & Punt, A. 2021. Evaluating Fishery Management Strategies Using an Ecosystem Model as an Operating Model. *Fisheries Research,* 234**,** 105780.

Lucey, S. M., Gaichas, S. K. & Aydin, K. Y. 2020. Conducting Reproducible Ecosystem Modeling Using the Open Source Mass Balance Model Rpath. *Ecological Modelling,* 427**,** 109057.

Luiz, O. J., Crook, D. A., Kennard, M. J., Olden, J. D., Saunders, T. M., Douglas, M. M., Wedd, D. & King, A. J. 2019. Does a Bigger Mouth Make You Fatter? Linking Intraspecific Gape Variability to Body Condition of a Tropical Predatory Fish. *Oecologia,* 191**,** 579-585.

Macnuson, J. J. & Heitz, J. G. 1971. Gill Raker Apparatus and Food Selectivity among Mackerels, Tunas, and Dolphins. *Fishery Bulletin,* 69.

Main, C. E. & Collins, M. A. 2011. Diet of the Antarctic Starry Skate Amblyraja Georgiana (Rajidae, Chondrichthyes) at South Georgia (Southern Ocean). *Polar Biology,* 34**,** 389-396.

Main, C. E., Collins, M. A., Mitchell, R. & Belchier, M. 2009. Identifying Patterns in the Diet of Mackerel Icefish (Champsocephalus Gunnari) at South Georgia Using Bootstrapped Confidence Intervals of a Dietary Index. *Polar Biology,* 32**,** 569-581.

Maldonado, M. T., Surma, S. & Pakhomov, E. A. 2016. Southern Ocean Biological Iron Cycling in the Pre-Whaling and Present Ecosystems. *Philosophical Transactions of the Royal Society A: Mathematical, Physical and Engineering Sciences,* 374**,** 20150292.

Marina, T. I., Salinas, V., Cordone, G., Campana, G., Moreira, E., Deregibus, D., Torre, L., Sahade, R., Tatián, M., Barrera Oro, E., De Troch, M., Doyle, S., Quartino, M. L., Saravia, L. A. & Momo, F. R. 2018. The Food Web of Potter Cove (Antarctica): Complexity, Structure and Function. *Estuarine, Coastal and Shelf Science,* 200**,** 141-151.

Marina, T. I., Saravia, L. A. & Kortsch, S. 2024. New Insights into the Weddell Sea Ecosystem Applying a Quantitative Network Approach. *Ocean Science,* 20**,** 141-153.

MarLIN 2006. Biotic - Biological Traits Information Catalogue. Marine Biological Association of the United Kingdom. Available from <www.marlin.ac.uk/biotic>.

Martinez, N. D. 1993. Effects of Resolution on Food Web Structure. *Oikos,* 66**,** 403-412.

Martinez, N. D. 2020. Allometric Trophic Networks from Individuals to Socio-Ecosystems: Consumer–Resource Theory of the Ecological Elephant in the Room. *Frontiers in Ecology and Evolution,* 8.

Massom, R. A. & Stammerjohn, S. E. 2010. Antarctic Sea Ice Change and Variability – Physical and Ecological Implications. *Polar Science,* 4**,** 149-186.

Matsuoka, K., Skoglund, A., Roth, G., De Pomereu, J., Griffiths, H., Headland, R., Herried, B., Katsumata, K., Le Brocq, A., Licht, K., Morgan, F., Neff, P. D., Ritz, C., Scheinert, M., Tamura, T., Van De Putte, A., Van Den Broeke, M., Von Deschwanden, A., Deschamps-Berger, C., Van Liefferinge, B., Tronstad, S. & Melvær, Y. 2021. Quantarctica, an Integrated Mapping Environment for Antarctica, the Southern Ocean, and Sub-Antarctic Islands. *Environmental Modelling & Software,* 140**,** 105015.

May, R. M. 1973. *Stability and Complexity in Model Ecosystems*, Princeton University Press.

Mccann, K. & Hastings, A. 1997. Re–Evaluating the Omnivory–Stability Relationship in Food Webs. *Proceedings of the Royal Society of London. Series B: Biological Sciences,* 264**,** 1249-1254.

Mccann, K., Hastings, A. & Huxel, G. R. 1998. Weak Trophic Interactions and the Balance of Nature. *Nature,* 395**,** 794-798.

Mccann, K. S. 2000. The Diversity–Stability Debate. *Nature,* 405**,** 228-233.

Mccann, K. S., Rasmussen, J. B. & Umbanhowar, J. 2005. The Dynamics of Spatially Coupled Food Webs. *Ecology Letters,* 8**,** 513-523.

Mccann, K. S. & Rooney, N. 2009. The More Food Webs Change, the More They Stay the Same. *Philosophical Transactions of the Royal Society B: Biological Sciences,* 364**,** 1789-1801.

Mccarthy, A. H., Peck, L. S. & Aldridge, D. C. 2022. Ship Traffic Connects Antarctica's Fragile Coasts to Worldwide Ecosystems. *Proceedings of the National Academy of Sciences,* 119**,** e2110303118.

Mccormack, S. A., Melbourne-Thomas, J., Trebilco, R., Blanchard, J. L. & Constable, A. 2020. Alternative Energy Pathways in Southern Ocean Food Webs: Insights from a Balanced Model of Prydz Bay, Antarctica. *Deep Sea Research Part II: Topical Studies in Oceanography,* 174.

Mccormack, S. A., Melbourne-Thomas, J., Trebilco, R., , Griffith, G., Hill, S. L., Hoover, C., Johnston, N. M., Marina, T. I., Murphy, E. J., Pakhomov, E. A. & Pinkerton, M. 2021a. Southern Ocean Food Web Modelling: Progress, Prognoses, and Future Priorities for Research and Policy Makers. *Frontiers in Ecology and Evolution***,** 626.

Mccormack, S. A., Melbourne-Thomas, J., Trebilco, R., Blanchard, J. L., Raymond, B. & Constable, A. 2021b. Decades of Dietary Data Demonstrate Regional Food Web Structures in the Southern Ocean. *Ecology and Evolution,* 11**,** 227-241.

Mckenna, J. E. 1991. Trophic Relationships within the Antarctic Demersal Fish Community of South Georgia Island. *Fishery Bulletin,* 89**,** 643-654.

Mcmahon, K. W., Michelson, C. I., Hart, T., Mccarthy, M. D., Patterson, W. P. & Polito, M. J. 2019. Divergent Trophic Responses of Sympatric Penguin Species to Historic Anthropogenic Exploitation and Recent Climate Change. *Proceedings of the National Academy of Sciences,* 116**,** 25721-25727.

Melbourne-Thomas, J., Constable, A., Wotherspoon, S. & Raymond, B. 2013. Testing Paradigms of Ecosystem Change under Climate Warming in Antarctica. *PLoS ONE,* 8**,** e55093.

Meredith, M., Sommerkorn, M., Cassotta, S., Derksen, C., Ekaykin, A., Hollowed, A., Kofinas, G., Mackintosh, A., Melbourne-Thomas, J., Muelbert, M. M. C., Ottersen, G., Pritchard, H. & Schuur, E. a. G. 2019. Polar Regions. *In:* PöRtner H.-O., Roberts, D. C., Masson-Delmotte, V., Zhai, P., Tignor, M., Poloczanska, E., Mintenbeck, K., AlegríA, A., Nicolai, M., Okem, A., Petzold, J., Rama, B. & Weyer, N. M. (eds.) *Ipcc Special Report on the Ocean and Cryosphere in a Changing Climate.* Cambridge, UK and New York, NY, USA: Cambridge University Press.

Meredith, M. P. & King, J. C. 2005. Rapid Climate Change in the Ocean West of the Antarctic Peninsula During the Second Half of the 20th Century. *Geophysical Research Letters,* 32**,** n/a-n/a.

Meyer, B., Atkinson, A., Bernard, K. S., Brierley, A. S., Driscoll, R., Hill, S. L., Marschoff, E., Maschette, D., Perry, F. A., Reiss, C. S., Rombolá, E., Tarling, G. A., Thorpe, S. E., Trathan, P. N., Zhu, G. & Kawaguchi, S. 2020. Successful Ecosystem-Based Management of Antarctic Krill Should Address Uncertainties in Krill Recruitment, Behaviour and Ecological Adaptation. *Communications Earth & Environment,* 1.

Michael, K., Suberg, L. A., Wessels, W., Kawaguchi, S. & Meyer, B. 2021. Facing Southern Ocean Warming: Temperature Effects on Whole Animal Performance of Antarctic Krill (Euphausia Superba). *Zoology,* 146**,** 125910.

Miller, D. G. M. 1991. Exploitation of Antarctic Marine Living Resources: A Brief History and a Possible Approach to Managing the Krill Fishery. *South African Journal of Marine Science,* 10**,** 321-339.

Mintenbeck, K. 2017. Impacts of Climate Change on the Southern Ocean. *Climate Change Impacts on Fisheries and Aquaculture.*

Montoya, D., Yallop, M. L. & Memmott, J. 2015. Functional Group Diversity Increases with Modularity in Complex Food Webs. *Nature Communications,* 6**,** 7379.

Montoya, J. M., Woodward, G., Emmerson, M. C. & Sole, R. V. 2009. Press Perturbations and Indirect Effects in Real Food Webs. *Ecology,* 90**,** 2426-33.

Morales-Castilla, I., Matias, M. G., Gravel, D. & Araujo, M. B. 2015. Inferring Biotic Interactions from Proxies. *Trends Ecol Evol,* 30**,** 347-56.

Mori, M. & Butterworth, D. S. 2006. A First Step Towards Modelling the Krill–Predator Dynamics of the Antarctic Ecosystem. *CCAMLR Science,* 13**,** 217-277.

Morley, S. A., Abele, D., Barnes, D. K. A., Cárdenas, C. A., Cotté, C., Gutt, J., Henley, S. F., Höfer, J., Hughes, K. A., Martin, S. M., Moffat, C., Raphael, M., Stammerjohn, S. E., Suckling, C. C., Tulloch, V. J. D., Waller, C. L. & Constable, A. J. 2020. Global Drivers on Southern Ocean Ecosystems: Changing Physical Environments and Anthropogenic Pressures in an Earth System. *Frontiers in Marine Science,* 7.

Morley, S. A., Belchier, M., Sands, C., Barnes, D. K. A. & Peck, L. S. 2014. Geographic Isolation and Physiological Mechanisms Underpinning Species Distributions at the Range Limit Hotspot of South Georgia. *Reviews in Fish Biology and Fisheries,* 24**,** 485-492.

Morley, S. A., Griffiths, H. J., Barnes, D. K. A. & Peck, L. S. 2010. South Georgia: A Key Location for Linking Physiological Capacity to Distributional Changes in Response to Climate Change. *Antarctic Science,* 22**,** 774-781.

Mougi, A. 2018. Spatial Compartmentation and Food Web Stability. *Scientific Reports,* 8.

Murphy, E. J., Cavanagh, R. D., Hofmann, E. E., Hill, S. L., Constable, A. J., Costa, D. P., Pinkerton, M. H., Johnston, N. M., Trathan, P. N., Klinck, J. M., Wolf-Gladrow, D. A., Daly, K. L., Maury, O. & Doney, S. C. 2012. Developing Integrated Models of Southern Ocean Food Webs: Including Ecological Complexity, Accounting for Uncertainty and the Importance of Scale. *Progress in Oceanography,* 102**,** 74-92.

Murphy, E. J., Watkins, J. L., Trathan, P. N., Reid, K., Meredith, M. P., Thorpe, S. E., Johnston, N. M., Clarke, A., Tarling, G. A., Collins, M. A., Forcada, J., Shreeve, R. S., Atkinson, A., Korb, R., Whitehouse, M. J., Ward, P., Rodhouse, P. G., Enderlein, P., Hirst, A. G., Martin, A. R., Hill, S. L., Staniland, I. J., Pond, D. W., Briggs, D. R., Cunningham, N. J. & Fleming, A. H. 2007. Spatial and Temporal Operation of the Scotia Sea Ecosystem: A Review of Large-Scale Links in a Krill Centred Food Web. *Philosophical Transactions of the Royal Society B: Biological Sciences,* 362**,** 113-148.

Nelson, D., Benstead, J. P., Huryn, A. D., Cross, W. F., Hood, J. M., Johnson, P. W., Junker, J. R., Gíslason, G. M. & Ólafsson, J. S. 2020. Thermal Niche Diversity and Trophic Redundancy Drive Neutral Effects of Warming on Energy Flux through a Stream Food Web. *Ecology,* 101**,** e02952.

Newbold, T. 2018. Future Effects of Climate and Land-Use Change on Terrestrial Vertebrate Community Diversity under Different Scenarios. *Proceedings of the Royal Society B: Biological Sciences,* 285**,** 20180792.

Newman, M. E. 2006. Modularity and Community Structure in Networks. *PNAS,* 103**,** 8577-8582.

Newman, M. E. & Girvan, M. 2004. Finding and Evaluating Community Structure in Networks. *Phys Rev E Stat Nonlin Soft Matter Phys,* 69**,** 026113.

Nicol, S., Bowie, A., Jarman, S., Lannuzel, D., Meiners, K. M. & Van Der Merwe, P. 2010. Southern Ocean Iron Fertilization by Baleen Whales and Antarctic Krill. *Fish and Fisheries,* 11**,** 203-209.

Nielsen, J. M., Clare, E. L., Hayden, B., Brett, M. T. & Kratina, P. 2017. Diet Tracing in Ecology: Method Comparison and Selection. *Methods in Ecology and Evolution,* 9**,** 278-291.

Nikolaou, A. & Katsanevakis, S. 2023. Marine Extinctions and Their Drivers. *Regional Environmental Change,* 23.

Nisbet, R. M., Jusup, M., Klanjscek, T. & Pecquerie, L. 2012. Integrating Dynamic Energy Budget (Deb) Theory with Traditional Bioenergetic Models. *Journal of Experimental Biology,* 215**,** 892-902.

Niu, J., Huss, M., Vasemägi, A. & Gårdmark, A. 2023. Decades of Warming Alters Maturation and Reproductive Investment in Fish. *Ecosphere,* 14.

O'connor, M. I., Piehler, M. F., Leech, D. M., Anton, A. & Bruno, J. F. 2009. Warming and Resource Availability Shift Food Web Structure and Metabolism. *PLoS Biology,* 7**,** e1000178.

O'gorman, E. J. & Emmerson, M. C. 2009. Perturbations to Trophic Interactions and the Stability of Complex Food Webs. *Proceedings of the National Academy of Sciences,* 106**,** 13393-13398.

O'gorman, E. J. & Emmerson, M. C. 2010. Manipulating Interaction Strengths and the Consequences for Trivariate Patterns in a Marine Food Web. *Advances in Ecological Research,* 42**,** 301-419.

O'gorman, E. J., Ólafsson, Ó. P., Demars, B. O. L., Friberg, N., Guðbergsson, G., Hannesdóttir, E. R., Jackson, M. C., Johansson, L. S., Mclaughlin, Ó. B., Ólafsson, J. S., Woodward, G. & Gíslason, G. M. 2016. Temperature Effects on Fish Production across a Natural Thermal Gradient. *Global Change Biology,* 22**,** 3206-3220.

O'gorman, E. J., Jacob, U., Jonsson, T. & Emmerson, M. C. 2010. Interaction Strength, Food Web Topology and the Relative Importance of Species in Food Webs. *Journal of Animal Ecology,* 79**,** 682-692.

O'gorman, E. J., Petchey, O. L., Faulkner, K. J., Gallo, B., Gordon, T. a. C., Neto-Cerejeira, J., Ólafsson, J. S., Pichler, D. E., Thompson, M. S. A. & Woodward, G. 2019. A Simple Model Predicts How Warming Simplifies Wild Food Webs. *Nature Climate Change,* 9**,** 611-616.

O'gorman, E. J., Zhao, L., Pichler, D. E., Adams, G., Friberg, N., Björn, Seeney, A., Zhang, H., Reuman, D. C. & Woodward, G. 2017. Unexpected Changes in Community Size Structure in a Natural Warming Experiment. *Nature Climate Change,* 7**,** 659-663.

Ockendon, N., Baker, D. J., Carr, J. A., White, E. C., Almond, R. E. A., Amano, T., Bertram, E., Bradbury, R. B., Bradley, C., Butchart, S. H. M., Doswald, N., Foden, W., Gill, D. J. C., Green, R. E., Sutherland, W. J., Tanner, E. V. J. & Pearce-Higgins, J. W. 2014. Mechanisms Underpinning Climatic Impacts on Natural Populations: Altered Species Interactions Are More Important Than Direct Effects. *Global Change Biology,* 20**,** 2221-2229.

Ojeda, F. P. 1986. Morphological Characterization of the Alimentary Tract of Antarctic Fishes and Its Relation to Feeding Habits. *Polar Biology,* 5**,** 125-128.

Olden, J. D., Leroy Poff, N., Douglas, M. R., Douglas, M. E. & Fausch, K. D. 2004. Ecological and Evolutionary Consequences of Biotic Homogenization. *Trends Ecol Evol,* 19**,** 18-24.

Olivier, P., Frelat, R., Bonsdorff, E., Kortsch, S., Kröncke, I., Möllmann, C., Neumann, H., Sell, A. F. & Nordström, M. C. 2019. Exploring the Temporal Variability of a Food Web Using Long-Term Biomonitoring Data. *Ecography,* 42**,** 2107-2121.

Pacheco, A. S., González, M. T., Bremner, J., Oliva, M., Heilmayer, O., Laudien, J. & Riascos, J. M. 2011. Functional Diversity of Marine Macrobenthic Communities from Sublittoral Soft-Sediment Habitats Off Northern Chile. *Helgoland Marine Research,* 65**,** 413-424.

Padovani, L. N., Viñas, M. D., Sánchez, F. & Mianzan, H. 2012. Amphipod-Supported Food Web: Themisto Gaudichaudii, a Key Food Resource for Fishes in the Southern Patagonian Shelf. *Journal of Sea Research,* 67**,** 85-90.

Paine, R. T. 1992. Food-Web Analysis through Field Measurement of Per Capita Interaction Strength. *Nature,* 355**,** 73-75.

Park, J., Kuzminov, F. I., Bailleul, B., Yang, E. J., Lee, S., Falkowski, P. G. & Gorbunov, M. Y. 2017. Light Availability Rather Than Fe Controls the Magnitude of Massive Phytoplankton Bloom in the Amundsen Sea Polynyas, Antarctica. *Limnology and Oceanography,* 62**,** 2260-2276.

Parkinson, C. L. 2019. A 40-Y Record Reveals Gradual Antarctic Sea Ice Increases Followed by Decreases at Rates Far Exceeding the Rates Seen in the Arctic. *Proceedings of the National Academy of Sciences,* 116**,** 14414-14423.

Pauli, N.-C., Metfies, K., Pakhomov, E. A., Neuhaus, S., Graeve, M., Wenta, P., Flintrop, C. M., Badewien, T. H., Iversen, M. H. & Meyer, B. 2021. Selective Feeding in Southern Ocean Key Grazers—Diet Composition of Krill and Salps. *Communications Biology,* 4.

Pauly, D. 1989. Food Consumption by Tropical and Temperate Fish Populations: Some Generalizations. *Journal of Fish Biology,* 35**,** 11-20.

Peck, L. S., Morley, S. A., Richard, J. & Clark, M. S. 2014. Acclimation and Thermal Tolerance in Antarctic Marine Ectotherms. *Journal of Experimental Biology,* 217**,** 16-22.

Pellissier, L., Albouy, C., Bascompte, J., Farwig, N., Graham, C., Loreau, M., Maglianesi, M. A., Melián, C. J., Pitteloud, C., Roslin, T., Rohr, R., Saavedra, S., Thuiller, W., Woodward, G., Zimmermann, N. E. & Gravel, D. 2018. Comparing Species Interaction Networks Along Environmental Gradients. *Biological Reviews,* 93**,** 785-800.

Pérez-Matus, A., Ospina-Alvarez, A., Camus, P., Carrasco, S., Fernandez, M., Gelcich, S., Godoy, N., Ojeda, F., Pardo, L., Rozbaczylo, N., Subida, M., Thiel, M., Wieters, E. & Navarrete, S. 2017. Temperate Rocky Subtidal Reef Community Reveals Human Impacts across the Entire Food Web. *Marine Ecology Progress Series,* 567**,** 1-16.

Petchey, O. L. 2000. Prey Diversity, Prey Composition, and Predator Population Dynamics in Experimental Microcosms. *J Anim Ecol,* 69**,** 874-882.

Petchey, O. L., Beckerman, A. P., Riede, J. O. & Warren, P. H. 2008. Size, Foraging, and Food Web Structure. *Proceedings of the National Academy of Sciences,* 105**,** 4191-4196.

Petrik, C. M., Stock, C. A., Andersen, K. H., Van Denderen, P. D. & Watson, J. R. 2020. Large Pelagic Fish Are Most Sensitive to Climate Change Despite Pelagification of Ocean Food Webs. *Frontiers in Marine Science,* 7.

Piatkowski, U., Rodhouse, P. G., White, M. G., Bone, D. G. & Symon, C. 1994. Nekton Community of the Scotia Sea as Sampled by the Rmt 25 During Austral Summer. *marine Ecology Progress Series,* 112**,** 13-28.

Pichler, M., Boreux, V., Klein, A. M., Schleuning, M. & Hartig, F. 2020. Machine Learning Algorithms to Infer Trait-Matching and Predict Species Interactions in Ecological Networks. *Methods in Ecology and Evolution,* 11**,** 281-293.

Pietzsch, B. W., Schmidt, A., Groeneveld, J., Bahlburg, D., Meyer, B. & Berger, U. 2023. The Impact of Salps (Salpa Thompsoni) on the Antarctic Krill Population (Euphausia Superba): An Individual-Based Modelling Study. *Ecological Processes,* 12.

Pigot, A. L., Trisos, C. H. & Tobias, J. A. 2016. Functional Traits Reveal the Expansion and Packing of Ecological Niche Space Underlying an Elevational Diversity Gradient in Passerine Birds. *Proceedings of the Royal Society B: Biological Sciences,* 283**,** 20152013.

Pineda-Metz, S. E. A. 2020. Benthos-Pelagos Interconnectivity: Antarctic Shelf Examples. Springer International Publishing.

Pineda Metz, S. E. 2019. *Benthic Communities of the Weddell Sea: Past, Present and Future.*

Pinheiro, J., Bates, D. & Team, R. C. 2023. Nlme: Linear and Nonlinear Mixed Effects Models. R Package Version 3.1-162. https://CRAN.R-project.org/package=nlme.

Pinkas, L., Oliphant, M. S. & Iverson, I. L. K. 1970. Food Habits of Albacore, Bluefin Tuna, and Bonito in California Waters. *Fish Bulletin 152*.

Pinkerton, M. & Bradford-Grieve, J. M. 2010. A Balanced Model of the Food Web of the Ross Sea, Antarctica. *CCAMLR Science,* 17**,** 1-31.

Pinkerton, M. H., Boyd, P. W., Deppeler, S., Hayward, A., Höfer, J. & Moreau, S. 2021. Evidence for the Impact of Climate Change on Primary Producers in the Southern Ocean. *Frontiers in Ecology and Evolution,* 9.

Pinkerton, M. H. & Bradford-Grieve, J. M. 2014. Characterizing Foodweb Structure to Identify Potential Ecosystem Effects of Fishing in the Ross Sea, Antarctica. *ICES Journal of Marine Science,* 71**,** 1542-1553.

Pinnegar, J. K., Blanchard, J. L., Mackinson, S., Scott, R. D. & Duplisea, D. E. 2005. Aggregation and Removal of Weak-Links in Food-Web Models: System Stability and Recovery from Disturbance. *Ecological Modelling,* 184**,** 229-248.

Plagányi, É. E., Blamey, L. K., Rogers, J. G. D. & Tulloch, V. J. D. 2022. Playing the Detective: Using Multispecies Approaches to Estimate Natural Mortality Rates. *Fisheries Research,* 249.

Plagányi, É. E. & Butterworth, D. S. 2004. A Critical Look at the Potential of Ecopath with Ecosim to Assist in Practical Fisheries Management. *African Journal of Marine Science,* 26**,** 261-287.

Podder, A., Panja, S., Chaudhuri, A., Roy, A., Biswas, M. & Homechaudhuri, S. 2021. Patterns of Morphological Traits Shaping the Feeding Guilds in the Intertidal Mudflat Fishes of the Indian Sundarbans. *Journal of Fish Biology,* 99**,** 1010-1031.

Polazzo, F., Hermann, M., Crettaz-Minaglia, M. & Rico, A. 2023. Impacts of Extreme Climatic Events on Trophic Network Complexity and Multidimensional Stability. *Ecology,* 104.

Post, D. M. 2002. The Long and Short of Food-Chain Length. *Trends in Ecology & Evolution,* 17**,** 269-277.

Potapov, A. M., Brose, U., Scheu, S. & Tiunov, A. V. 2019. Trophic Position of Consumers and Size Structure of Food Webs across Aquatic and Terrestrial Ecosystems. *Am Nat,* 194**,** 823-839.

Pouvreau, S., Bourles, Y., Lefebvre, S., Gangnery, A. & Alunno-Bruscia, M. 2006. Application of a Dynamic Energy Budget Model to the Pacific Oyster, Crassostrea Gigas, Reared under Various Environmental Conditions. *Journal of Sea Research,* 56**,** 156-167.

Queirós, J. P., Borras-Chavez, R., Friscourt, N., Groß, J., Lewis, C. B., Mergard, G. & O'brien, K. 2024. Southern Ocean Food-Webs and Climate Change: A Short Review and Future Directions. *PLOS Climate,* 3**,** e0000358.

Queiros, Q., Mckenzie, D. J., Dutto, G., Killen, S., Saraux, C. & Schull, Q. 2024. Fish Shrinking, Energy Balance and Climate Change. *Science of The Total Environment,* 906**,** 167310.

Quetin, L. B., Ross, R. M., Fritsen, C. H. & Vernet, M. 2007. Ecological Responses of Antarctic Krill to Environmental Variability: Can We Predict the Future? *Antarctic Science,* 19**,** 253-266.

Rall, B. C., Brose, U., Hartvig, M., Kalinkat, G., Schwarzmüller, F., Vucic-Pestic, O. & Petchey, O. L. 2012. Universal Temperature and Body-Mass Scaling of Feeding Rates. *Philosophical Transactions of the Royal Society B: Biological Sciences,* 367**,** 2923-2934.

Rall, B. C., Vucic-Pestic, O., Ehnes, R. B., Emmerson, M. & Brose, U. 2009. Temperature, Predator-Prey Interaction Strength and Population Stability. *Global Change Biology,* 16**,** 2145-2157.

Ramírez, F., Davenport, T. L. & Mojica, J. I. 2015. Dietary–Morphological Relationships of Nineteen Fish Species from an Amazonian Terra Firme Blackwater Stream in Colombia. *Limnologica,* 52**,** 89-102.

Ratnarajah, L., Bowie, A. R., Lannuzel, D., Meiners, K. M. & Nicol, S. 2014. The Biogeochemical Role of Baleen Whales and Krill in Southern Ocean Nutrient Cycling. *PLoS ONE,* 9**,** e114067.

Ratnarajah, L., Melbourne-Thomas, J., Marzloff, M. P., Lannuzel, D., Meiners, K. M., Chever, F., Nicol, S. & Bowie, A. R. 2016. A Preliminary Model of Iron Fertilisation by Baleen Whales and Antarctic Krill in the Southern Ocean: Sensitivity of Primary Productivity Estimates to Parameter Uncertainty. *Ecological Modelling,* 320**,** 203-212.

R Core Team 2023. R: Language and Environment for Statistical Computing. *R Foundation for Statistical Computing, Vienna, Austria.* https://www.R-project.org/.

Reid, K., Hill, S. L., Diniz, T. C. D. & Collins, M. A. 2005. Mackerel Icefish Champsocephalus Gunnari in the Diet of Upper Trophic Level Predators at South Georgia: Implications for Fisheries Management. *Marine Ecology Progress Series,* 305**,** 153-161.

Reid, W. D. K., Clarke, S., Collins, M. A. & Belchier, M. 2007. Distribution and Ecology of Chaenocephalus Aceratus (Channichthyidae) around South Georgia and Shag Rocks (Southern Ocean). *Polar Biology,* 30**,** 1523-1533.

Reisinger, R. R., Landman, M., Mgibantaka, N., Smale, M. J., Bester, M. N., De Bruyn, P. J. N. & Pistorius, P. A. 2018. Overlap and Temporal Variation in the Diets of Sympatric Antarctic and Subantarctic Fur Seals (Arctocephalus Spp.) at Marion Island, Prince Edward Islands. *Polar Research,* 37**,** 1451142.

Retelletti Brogi, S., Jung, J. Y., Ha, S. Y. & Hur, J. 2019. Seasonal Differences in Dissolved Organic Matter Properties and Sources in an Arctic Fjord: Implications for Future Conditions. *Sci Total Environ,* 694**,** 133740.

Reum, J. C. P., Holsman, K. K., Aydin, K. Y., Blanchard, J. L. & Jennings, S. 2019. Energetically Relevant Predator-Prey Body Mass Ratios and Their Relationship with Predator Body Size. *Ecology and Evolution,* 9**,** 201-211.

Rezende, E. L., Albert, E. M., Fortuna, M. A. & Bascompte, J. 2009. Compartments in a Marine Food Web Associated with Phylogeny, Body Mass, and Habitat Structure. *Ecol Lett,* 12**,** 779-88.

Richardson, J., Wood, A. G., Neil, A., Nowacek, D. & Moore, M. 2012. Changes in Distribution, Relative Abundance, and Species Composition of Large Whales around South Georgia from Opportunistic Sightings: 1992 to 2011. *Endangered Species Research,* 19**,** 149-156.

Riemer, K., Anderson-Teixeira, K. J., Smith, F. A., Harris, D. J. & Ernest, S. K. M. 2018. Body Size Shifts Influence Effects of Increasing Temperatures on Ectotherm Metabolism. *Global Ecology and Biogeography,* 27**,** 958-967.

Rivera-Hutinel, A., Bustamante, R. O., Marín, V. H. & Medel, R. 2012. Effects of Sampling Completeness on the Structure of Plant–Pollinator Networks. *Ecology,* 93**,** 1593-1603.

Rodriguez, I. D., Marina, T. I., Schloss, I. R. & Saravia, L. A. 2022. Marine Food Webs Are More Complex but Less Stable in Sub-Antarctic (Beagle Channel, Argentina) Than in Antarctic (Potter Cove, Antarctic Peninsula) Regions. *Mar Environ Res,* 174**,** 105561.

Roman, J., Estes, J. A., Morissette, L., Smith, C., Costa, D., Mccarthy, J., Nation, J., Nicol, S., Pershing, A. & Smetacek, V. 2014. Whales as Marine Ecosystem Engineers. *Frontiers in Ecology and the Environment,* 12**,** 377-385.

Rooney, N. & Mccann, K. S. 2012. Integrating Food Web Diversity, Structure and Stability. *Trends in Ecology & Evolution,* 27**,** 40-46.

Rooney, N., Mccann, K. S. & Moore, J. C. 2008. A Landscape Theory for Food Web Architecture. *Ecology Letters,* 11**,** 867-881.

Rose, K. A., Holsman, K., Nye, J. A., Markowitz, E. H., Banha, T. N., Bueno-Pardo, J., Deslauriers, D., Fulton, E. A., Huebert, K. B. & Huret, M. 2024. Advancing Bioenergetics-Based Modeling to Improve Climate Change Projections of Marine Ecosystems. *Marine Ecology Progress Series,* 732**,** 193-221.

Rossi, L., Sporta Caputi, S., Calizza, E., Careddu, G., Oliverio, M., Schiaparelli, S. & Costantini, M. L. 2019. Antarctic Food Web Architecture under Varying Dynamics of Sea Ice Cover. *Scientific Reports,* 9.

Rubalcaba, J. G., Verberk, W. C. E. P., Hendriks, A. J., Saris, B. & Woods, H. A. 2020. Oxygen Limitation May Affect the Temperature and Size Dependence of Metabolism in Aquatic Ectotherms. *Proceedings of the National Academy of Sciences,* 117**,** 31963-31968.

Ruckelshaus, M., Klinger, T., Knowlton, N. & Demaster, D. P. 2008. Marine Ecosystem-Based Management in Practice: Scientific and Governance Challenges. *BioScience,* 58**,** 53-63.

Rudolf, V. H. W. 2012. Seasonal Shifts in Predator Body Size Diversity and Trophic Interactions in Size-Structured Predator-Prey Systems. *Journal of Animal Ecology,* 81**,** 524-532.

Rutterford, L. A., Simpson, S. D., Bogstad, B., Devine, J. A. & Genner, M. J. 2023. Sea Temperature Is the Primary Driver of Recent and Predicted Fish Community Structure across Northeast Atlantic Shelf Seas. *Global Change Biology,* 29**,** 2510-2521.

Ruzicka, J. J., Steele, J. H., Ballerini, T., Gaichas, S. K. & Ainley, D. G. 2013. Dividing up the Pie: Whales, Fish, and Humans as Competitors. *Progress in Oceanography,* 116**,** 207-219.

Saba, G., Bockus, A., Shaw, C. & Seibel, B. 2021. Combined Effects of Ocean Acidification and Elevated Temperature on Feeding, Growth, and Physiological Processes of Antarctic Krill Euphausia Superba. *Marine Ecology Progress Series,* 665**,** 1-18.

Salvatteci, R., Schneider, R. R., Galbraith, E., Field, D., Blanz, T., Bauersachs, T., Crosta, X., Martinez, P., Echevin, V., Scholz, F. & Bertrand, A. 2022. Smaller Fish Species in a Warm and Oxygen-Poor Humboldt Current System. *Science,* 375**,** 101-104.

Sambilay, V. C. 1990. Interrelationships between Swimming Speed, Caudal Fin Aspect Ratio and Body Length of Fishes. *Fishbyte,* 8**,** 16-20.

Sánchez-Hernández, J., Nunn, A. D., Adams, C. E. & Amundsen, P.-A. 2019. Causes and Consequences of Ontogenetic Dietary Shifts: A Global Synthesis Using Fish Models. *Biological Reviews,* 94**,** 539-554.

Sanchez-Martinez, P., Ackerly, D. D., Martínez-Vilalta, J., Mencuccini, M., Dexter, K. G. & Dawson, T. E. 2024. A Framework to Study and Predict Functional Trait Syndromes Using Phylogenetic and Environmental Data. *Methods in Ecology and Evolution,* 15**,** 666-681.

Saunders, R. A., Collins, M. A., Shreeve, R., Ward, P., Stowasser, G., Hill, S. L. & Tarling, G. A. 2018. Seasonal Variation in the Predatory Impact of Myctophids on Zooplankton in the Scotia Sea (Southern Ocean). *Progress in Oceanography,* 168**,** 123-144.

Saunders, R. A., Hill, S. L., Tarling, G. A. & Murphy, E. J. 2019. Myctophid Fish (Family Myctophidae) Are Central Consumers in the Food Web of the Scotia Sea (Southern Ocean). *Frontiers in Marine Science,* 6.

Saunders, R. A. & Tarling, G. A. 2018. Southern Ocean Mesopelagic Fish Comply with Bergmann's Rule. *The American Naturalist,* 191**,** 343-351.

Savoca, M. S., Czapanskiy, M. F., Kahane-Rapport, S. R., Gough, W. T., Fahlbusch, J. A., Bierlich, K. C., Segre, P. S., Di Clemente, J., Penry, G. S., Wiley, D. N., Calambokidis, J., Nowacek, D. P., Johnston, D. W., Pyenson, N. D., Friedlaender, A. S., Hazen, E. L. & Goldbogen, J. A. 2021. Baleen Whale Prey Consumption Based on High-Resolution Foraging Measurements. *Nature,* 599**,** 85-90.

Scharf, F. S., Juanes, F. & Rountree, R. A. 2000. Predator Size-Prey Size Relationships of Marine Fish Predators: Interspecific Variation and Effects of Ontogeny and Body Size on Trophic-Niche Breadth. *Marine Ecology Progress Series,* 208**,** 229-248.

Schmid, B., Balvanera, P., Cardinale, B. J., Godbold, J., Pfisterer, A. B., Raffaelli, D., Solan, M. & Srivastava, D. S. 2009. Consequences of Species Loss for Ecosystem Functioning: Meta-Analyses of Data from Biodiversity Experiments. *In:* Shahid Naeem, D. E. B., Andy Hector, Michel Loreau, Charles Perrings (ed.) *Biodiversity, Ecosystem Functioning, and Human Wellbeing: An Ecological and Economic Perspective.* Oxford Scholarship Online: Oxford University Press.

Schmidt, K., Atkinson, A., Steigenberger, S., Fielding, S., Lindsay, M. C. M., Pond, D. W., Tarling, G. A., Klevjer, T. A., Allen, C. S., Nicol, S. & Achterberg, E. P. 2011. Seabed Foraging by Antarctic Krill: Implications for Stock Assessment, Bentho-Pelagic Coupling, and the Vertical Transfer of Iron. *Limnology and Oceanography,* 56**,** 1411-1428.

Schoener, T. W. 1970. Nonsynchronous Spatial Overlap of Lizards in Patchy Habitats. *Ecology,* 51**,** 408-418.

Schoener, T. W. 1982. The Controversy over Interspecific Competition: Despite Spirited Criticism, Competition Continues to Occupy a Major Domain in Ecological Thought. *American Naturalist,* 70**,** 586-595.

Schram, J., Schoenrock, K., Mcclintock, J., Amsler, C. & Angus, R. 2016. Seawater Acidification More Than Warming Presents a Challenge for Two Antarctic Macroalgal-Associated Amphipods. *Marine Ecology Progress Series,* 554**,** 81-97.

Schuckel, S., Sell, A. F., Kroncke, I. & Reiss, H. 2012. Diet Overlap among Flatfish Species in the Southern North Sea. *J Fish Biol,* 80**,** 2571-94.

Sentis, A., Binzer, A. & Boukal, D. S. 2017. Temperature-Size Responses Alter Food Chain Persistence across Environmental Gradients. *Ecology Letters,* 20**,** 852-862.

Shackell, N. L., Frank, K. T., Fisher, J. a. D., Petrie, B. & Leggett, W. C. 2010. Decline in Top Predator Body Size and Changing Climate Alter Trophic Structure in an Oceanic Ecosystem. *Proceedings of the Royal Society B: Biological Sciences,* 277**,** 1353-1360.

Sheehy, J. M., Taylor, N. L., Zwerschke, N., Collar, M., Morgan, V. & Merayo, E. 2022. Review of Evaluation and Valuation Methods for Cetacean Regulation and Maintenance Ecosystem Services with the Joint Cetacean Protocol Data. *Frontiers in Marine Science,* 9.

Siqueira, T., Hawkins, C. P., Olden, J. D., Tonkin, J., Comte, L., Saito, V. S., Anderson, T. L., Barbosa, G. P., Bonada, N. & Bonecker, C. C. 2024. Understanding Temporal Variability across Trophic Levels and Spatial Scales in Freshwater Ecosystems. *Ecology,* 105**,** e4219.

Smetacek, V. & Duarte, C. M. 2008. *Impacts of Global Warming on Polar Ecosystems.*

Sohlström, E. H., Archer, L. C., Gallo, B., Jochum, M., Kordas, R. L., Rall, B. C., Rosenbaum, B. & O'gorman, E. J. 2021. Thermal Acclimation Increases the Stability of a Predator–Prey Interaction in Warmer Environments. *Global Change Biology,* 27**,** 3765-3778.

Spitz, J., Ridoux, V. & Brind'amour, A. 2014. Let's Go Beyond Taxonomy in Diet Description: Testing a Trait-Based Approach to Prey–Predator Relationships. *Journal of Animal Ecology,* 83**,** 1137-1148.

Srinivas, T., Sukumaran, S., Neetu, S. & Ramesh Babu, K. 2020. Diversity and Functional Patterns of Benthic Amphipods in the Coralline Intertidal Zones of a Marine National Park, India. *Frontiers in Marine Science,* 7.

Stachowicz, J. J., Bruno, J. F. & Duffy, J. E. 2007. Understanding the Effects of Marine Biodiversity on Communities and Ecosystems. *Annual Review of Ecology, Evolution, and Systematics,* 38**,** 739-766.

Stearns, S. C. 1983. The Influence of Size and Phylogeny on Patterns of Covariation among Life-History Traits in the Mammals. *Oikos,* 41**,** 173-187.

Steenbeek, J., Corrales, X., Platts, M. & Coll, M. 2018. Ecosampler: A New Approach to Assessing Parameter Uncertainty in Ecopath with Ecosim. *SoftwareX,* 7**,** 198-204.

Steinacher, M., Joos, F., Frölicher, T. L., Bopp, L., Cadule, P., Cocco, V., Doney, S. C., Gehlen, M., Lindsay, K., Moore, J. K., Schneider, B. & Segschneider, J. 2010. Projected

21st Century Decrease in Marine Productivity: A Multi-Model Analysis. *Biogeosciences,* 7**,** 979-1005.

Stock, A., Murray, C. C., Gregr, E. J., Steenbeek, J., Woodburn, E., Micheli, F., Christensen, V. & Chan, K. M. A. 2023. Exploring Multiple Stressor Effects with Ecopath, Ecosim, and Ecospace: Research Designs, Modeling Techniques, and Future Directions. *Science of The Total Environment,* 869**,** 161719.

Stouffer, D. B. & Bascompte, J. 2011. Compartmentalization Increases Food-Web Persistence. *Proc Natl Acad Sci U S A,* 108**,** 3648-52.

Strobl, C., Boulesteix, A.-L., Kneib, T., Augustin, T. & Zeileis, A. 2008. Conditional Variable Importance for Random Forests. *BMC Bioinformatics,* 9**,** 307.

Strobl, C., Boulesteix, A.-L., Zeileis, A. & Hothorn, T. 2007. Bias in Random Forest Variable Importance Measures: Illustrations, Sources and a Solution. *BMC Bioinformatics,* 8**,** 25.

Subramaniam, R. C., Corney, S. P., Swadling, K. M. & Melbourne-Thomas, J. 2020. Exploring Ecosystem Structure and Function of the Northern Kerguelen Plateau Using a Mass-Balanced Food Web Model. *Deep Sea Research Part II: Topical Studies in Oceanography,* 174.

Subramaniam, R. C., Pinkerton, Matt H.,, Melbourne-Thomas, J., Corney, S. P., Swadling, K. M. & Pruvost, P. 2019. A Mass-Balanced Ecosystem Model for the Kerguelen Plateau. *HAL open science*.

Sullivan, T., Byrne, C., Harman, L., Davenport, J., Mcallen, R. & Regan, F. 2014. Determination of Spatial and Temporal Variability of Ph and Dissolved Oxygen Concentrations in a Seasonally Hypoxic Semi-Enclosed Marine Basin Using Continuous Monitoring. *Anal. Methods,* 6**,** 5489-5497.

Surma, S., Pakhomov, E. A. & Pitcher, T. J. 2014. Effects of Whaling on the Structure of the Southern Ocean Food Web: Insights on the "Krill Surplus" from Ecosystem Modelling. *PLoS One,* 9**,** e114978.

Swadling, K. M., Constable, A. J., Fraser, A. D., Massom, R. A., Borup, M. D., Ghigliotti, L., Granata, A., Guglielmo, L., Johnston, N. M., Kawaguchi, S., Kennedy, F., Kiko, R., Koubbi, P., Makabe, R., Martin, A., Mcminn, A., Moteki, M., Pakhomov, E. A., Peeken, I., Reimer, J., Reid, P., Ryan, K. G., Vacchi, M., Virtue, P., Weldrick, C. K., Wongpan, P. & Wotherspoon, S. J. 2023. Biological Responses to Change in Antarctic Sea Ice Habitats. *Frontiers in Ecology and Evolution,* 10.

Tang, K. W., Gladyshev, M. I., Dubovskaya, O. P., Kirillin, G. & Grossart, H.-P. 2014. Zooplankton Carcasses and Non-Predatory Mortality in Freshwater and Inland Sea Environments. *Journal of Plankton Research,* 36**,** 597-612.

Targett, T. E. 1981. Trophic Ecology and Structure of Coastal Antarctic Fish Communities. *Marine Ecology Progress Series,* 4**,** 243-263.

Tarling, G. A., Stowasser, G., Ward, P., Poulton, A. J., Zhou, M., Venables, H. J., Mcgill, R. a. R. & Murphy, E. J. 2012a. Seasonal Trophic Structure of the Scotia Sea Pelagic

Ecosystem Considered through Biomass Spectra and Stable Isotope Analysis. *Deep Sea Research Part II: Topical Studies in Oceanography,* 59-60**,** 222-236.

Tarling, G. A., Ward, P., Atkinson, A., Collins, M. A. & Murphy, E. J. 2012b. Discovery 2010: Spatial and Temporal Variability in a Dynamic Polar Ecosystem. *Deep Sea Research Part II: Topical Studies in Oceanography,* 59-60**,** 1-13.

Team, R. C. 2023. R: Language and Environment for Statistical Computing. *R Foundation for Statistical Computing, Vienna, Austria.* https://www.R-project.org/.

Teixeira, C. M. G. L., Sousa, T., Marques, G. M., Domingos, T. & Kooijman, S. a. L. M. 2014. A New Perspective on the Growth Pattern of the Wandering Albatross (Diomedea Exulans) through Deb Theory. *Journal of Sea Research,* 94**,** 117-127.

Teng, J. & Mccann, K. S. 2004. Dynamics of Compartmented and Reticulate Food Webs in Relation to Energetic Flows. *The American Naturalist,* 164**,** 85-100.

Teschke, K., Brtnik, P., Hain, S., Herata, H., Liebschner, A., Pehlke, H. & Brey, T. 2021. Planning Marine Protected Areas under the Ccamlr Regime–the Case of the Weddell Sea (Antarctica). *Marine Policy,* 124**,** 104370.

Tews, J., Brose, U., Grimm, V., Tielbörger, K., Wichmann, M. C., Schwager, M. & Jeltsch, F. 2004. Animal Species Diversity Driven by Habitat Heterogeneity/Diversity: The Importance of Keystone Structures. *Journal of Biogeography,* 31**,** 79-92.

Thébault, E. & Fontaine, C. 2010. Stability of Ecological Communities and the Architecture of Mutualistic and Trophic Networks. *Science,* 329**,** 853-856.

Thomalla, S. J., Nicholson, S.-A., Ryan-Keogh, T. J. & Smith, M. E. 2023. Widespread Changes in Southern Ocean Phytoplankton Blooms Linked to Climate Drivers. *Nature Climate Change,* 13**,** 975-984.

Thomas, K. N., Gower, D. J., Bell, R. C., Fujita, M. K., Schott, R. K. & Streicher, J. W. 2020. Eye Size and Investment in Frogs and Toads Correlate with Adult Habitat, Activity Pattern and Breeding Ecology. *Proceedings of the Royal Society B: Biological Sciences,* 287**,** 20201393.

Thomas, P. G. & Green, K. 1988. Distribution of Euphausia Crystallorophias within Prydz Bay and Its Importance to the Inshore Marine Ecosystem. *Polar Biology,* 8**,** 327-331.

Thompson, R. M., Brose, U., Dunne, J. A., Hall, R. O., Hladyz, S., Kitching, R. L., Martinez, N. D., Rantala, H., Romanuk, T. N., Stouffer, D. B. & Tylianakis, J. M. 2012. Food Webs: Reconciling the Structure and Function of Biodiversity. *Trends in Ecology & Evolution,* 27**,** 689-697.

Thompson, R. M. & Townsend, C. R. 2005. Energy Availability, Spatial Heterogeneity and Ecosystem Size Predict Food-Web Structure in Streams. *Oikos,* 108**,** 137-148.

Tilman, D. & Downing, J. A. 1994. Biodiversity and Stability in Grasslands. *Nature,* 367**,** 363-365.

Tilman, D., Isbell, F. & Cowles, J. M. 2014. Biodiversity and Ecosystem Functioning. *Annual Review of Ecology, Evolution, and Systematics,* 45**,** 471-493.

Tilman, D., Reich, P. B. & Knops, J. M. H. 2006. Biodiversity and Ecosystem Stability in a Decade-Long Grassland Experiment. *Nature,* 441**,** 629-632.

Townsend, C. R., Begon, M. & Harper, J. L. 2008. *Essentials of Ecology*, Blackwell publishing.

Trathan, P. N. & Hill, S. L. 2016. The Importance of Krill Predation in the Southern Ocean. *In:* Siegel, V. (ed.) *Biology and Ecology of Antarctic Krill.* Cham: Springer International Publishing.

Tsai, C. H., Hsieh, C. H. & Nakazawa, T. 2016. Predator–Prey Mass Ratio Revisited: Does Preference of Relative Prey Body Size Depend on Individual Predator Size? *Functional Ecology,* 30**,** 1979-1987.

Tucker, M. A. & Rogers, T. L. 2014. Examining Predator–Prey Body Size, Trophic Level and Body Mass across Marine and Terrestrial Mammals. *Proceedings of the Royal Society B: Biological Sciences,* 281**,** 20142103.

Tulloch, V. J. D., Plaganyi, E. E., Brown, C., Richardson, A. J. & Matear, R. 2019. Future Recovery of Baleen Whales Is Imperiled by Climate Change. *Glob Chang Biol,* 25**,** 1263-1281.

Ullah, H., Nagelkerken, I., Goldenberg, S. U. & Fordham, D. A. 2018. Climate Change Could Drive Marine Food Web Collapse through Altered Trophic Flows and Cyanobacterial Proliferation. *PLOS Biology,* 16**,** e2003446.

Van De Putte, A. P., Griffiths, H. J., Brooks, C., Bricher, P., Sweetlove, M., Halfter, S. & Raymond, B. 2021. From Data to Marine Ecosystem Assessments of the Southern Ocean: Achievements, Challenges, and Lessons for the Future. *Frontiers in Marine Science,* 8.

Van Der Meer, J., Hin, V., Van Oort, P. & Van De Wolfshaar, K. E. 2022. A Simple Deb-Based Ecosystem Model. *Conservation Physiology,* 10.

Van Der Meer, J., Van Donk, S., Sotillo, A. & Lens, L. 2020. Predicting Post-Natal Energy Intake of Lesser Black-Backed Gull Chicks by Dynamic Energy Budget Modeling. *Ecological Modelling,* 423.

Violle, C., Navas, M.-L., Vile, D., Kazakou, E., Fortunel, C., Hummel, I. & Garnier, E. 2007. Let the Concept of Trait Be Functional! *Oikos,* 116**,** 882-892.

Voronina, N. M. 1998. Comparative Abundance and Distribution of Major Filter-Feeders in the Antarctic Pelagic Zone. *Journal of Marine Systems,* 17**,** 375-390.

Vucic-Pestic, O., Rall, B. C., Kalinkat, G. & Brose, U. 2010. Allometric Functional Response Model: Body Masses Constrain Interaction Strengths. *Journal of Animal Ecology,* 79**,** 249-256.

Wainwright, P., Carroll, A. M., Collar, D. C., Day, S. W., Higham, T. E. & Holzman, R. A. 2007. Suction Feeding Mechanics, Performance, and Diversity in Fishes. *Integr Comp Biol,* 47**,** 96-106.

Wallis, J. R., Kawaguchi, S., Matsuno, K. & Swadling, M. 2019. Big Things Come in Small Packages. Biomass Contribution of the Krill *Thysanoessa Macrura* to the Marine Ecosystem in the Kerguelen Plateau Region. *Second Kerguelen Plateau Symposium: marine ecosystem and fisheries***,** 55-58.

Waluda, C. M., Hill, S. L., Peat, H. J. & Trathan, P. N. 2017. Long-Term Variability in the Diet and Reproductive Performance of Penguins at Bird Island, South Georgia. *Marine Biology,* 164.

Wang, R., Zhang, R., Miao, X., Li, H., Song, P., Li, Y. & Lin, L. 2024. Demersal Fish Community in the near-Shelf Zone of the Cosmonaut Sea, Southern Ocean. *Diversity,* 16**,** 156.

Wang, T., Zhang, P., Molinos, J. G., Xie, J., Zhang, H., Wang, H., Xu, X., Wang, K., Feng, M. & Cheng, H. 2023. Interactions between Climate Warming, Herbicides, and Eutrophication in the Aquatic Food Web. *Journal of Environmental Management,* 345**,** 118753.

Ward-Campbell, B. M. S., Beamish, F. W. H. & Kongchaiya, C. 2005. Morphological Characteristics in Relation to Diet in Five Coexisting Thai Fish Species. *Journal of Fish Biology,* 67**,** 1266-1279.

Ward, P., Atkinson, A. & Tarling, G. 2012. Mesozooplankton Community Structure and Variability in the Scotia Sea: A Seasonal Comparison. *Deep Sea Research Part II: Topical Studies in Oceanography,* 59-60**,** 78-92.

Ward, P., Tarling, G., Shreeve, R. & Ten Hoopen, P. 2020. Epipelagic Mesozooplankton Distribution and Abundance in Southern Ocean Atlantic Sector and the North Atlantic and Arctic 1996-2013 (Version 1.0). . UK Polar Data Centre, Natural Environment Research Council, UK Research & Innovation. .

Watters, G. M., Hill, S. L., Hinke, J. T., Matthews, J. & Reid, K. 2013. Decision-Making for Ecosystem-Based Management: Evaluating Options for a Krill Fishery with an Ecosystem Dynamics Model. *Ecological Applications,* 23**,** 710-725.

Wege, M., Salas, L. & Larue, M. 2021. Ice Matters: Life-History Strategies of Two Antarctic Seals Dictate Climate Change Eventualities in the Weddell Sea. *Global Change Biology,* 27**,** 6252-6262.

Weigel, B. & Bonsdorff, E. 2018. Trait-Based Predation Suitability Offers Insight into Effects of Changing Prey Communities. *PeerJ,* 6**,** e5899.

Weiss, A. I., King, J. C., Lachlan-Cope, T. A. & Ladkin, R. S. 2012. Albedo of the Ice Covered Weddell and Bellingshausen Seas. *The Cryosphere,* 6**,** 479-491.

White, E. P., Ernest, S. K. M., Kerkhoff, A. J. & Enquist, B. J. 2007. Relationships between Body Size and Abundance in Ecology. *Trends in Ecology & Evolution,* 22**,** 323-330.

Whitehouse, G. A. & Aydin, K. Y. 2020. Assessing the Sensitivity of Three Alaska Marine Food Webs to Perturbations: An Example of Ecosim Simulations Using Rpath. *Ecological Modelling,* 429**,** 109074.

Whitehouse, M. J., Meredith, M. P., Rothery, P., Atkinson, A., Ward, P. & Korb, R. E. 2008. Rapid Warming of the Ocean around South Georgia, Southern Ocean, During the 20th Century: Forcings, Characteristics and Implications for Lower Trophic Levels. *Deep Sea Research Part I: Oceanographic Research Papers,* 55**,** 1218-1228.

Winkler, N. S., Paz-Goicoechea, M., Lamb, R. W. & Pérez-Matus, A. 2017. Diet Reveals Links between Morphology and Foraging in a Cryptic Temperate Reef Fish. *Ecology and Evolution,* 7**,** 11124-11134.

Wood, S. A., Russell, R., Hanson, D., Williams, R. J. & Dunne, J. A. 2015. Effects of Spatial Scale of Sampling on Food Web Structure. *Ecology and Evolution,* 5**,** 3769-3782.

Woodward, G., Blanchard, J., Lauridsen, R. B., Edwards, F. K., Jones, J. I., Figueroa, D., Warren, P. H. & Petchey, O. L. 2010. Chapter 6 - Individual-Based Food Webs: Species Identity, Body Size and Sampling Effects. *In:* Woodward, G. (ed.) *Advances in Ecological Research.* Academic Press.

Woodward, G., Ebenman, B., Emmerson, M., Montoya, J. M., Olesen, J. M., Valido, A. & Warren, P. H. 2005. Body Size in Ecological Networks. *Trends in Ecology & Evolution,* 20**,** 402-409.

Wootton, K. L., Curtsdotter, A., Roslin, T., Bommarco, R. & Jonsson, T. 2021. Towards a Modular Theory of Trophic Interactions. *Functional Ecology,* 37**,** 26-43.

Wootton, K. L. & Stouffer, D. B. 2016. Many Weak Interactions and Few Strong; Food-Web Feasibility Depends on the Combination of the Strength of Species' Interactions and Their Correct Arrangement. *Theoretical Ecology,* 9**,** 185-195.

Yachi, S. & Loreau, M. 1999. Biodiversity and Ecosystem Productivity in a Fluctuating Environment: The Insurance Hypothesis. *Proceedings of the National Academy of Sciences,* 96**,** 1463-1468.

Yang, G., Atkinson, A., Hill, S. L., Guglielmo, L., Granata, A. & Li, C. 2020. Changing Circumpolar Distributions and Isoscapes of Antarctic Krill: Indo-Pacific Habitat Refuges Counter Long-Term Degradation of the Atlantic Sector. *Limnology and Oceanography,* 66**,** 272-287.

Yang, G., Atkinson, A., Pakhomov, E. A., Hill, S. L. & Racault, M. F. 2022. Massive Circumpolar Biomass of Southern Ocean Zooplankton: Implications for Food Web Structure, Carbon Export, and Marine Spatial Planning. *Limnology and Oceanography,* 67**,** 2516-2530.

Zerbini, A. N., Adams, G., Best, J., Clapham, P. J., Jackson, J. A. & Punt, A. E. 2019. Assessing the Recovery of an Antarctic Predator from Historical Exploitation. *Royal Society Open Science,* 6**,** 190368.

Zhao, L., Zhang, H., O'gorman, E. J., Tian, W., Ma, A., Moore, J. C., Borrett, S. R. & Woodward, G. 2016. Weighting and Indirect Effects Identify Keystone Species in Food Webs. *Ecology Letters,* 19**,** 1032-1040.

Zhao, L., Zhang, H., Tian, W. & Xu, X. 2017. Identifying Compartments in Ecological Networks Based on Energy Channels. *Ecology and Evolution,* 8**,** 309-318.

Appendix A: Supplementary material for chapter 2

A1: Supplementary figures

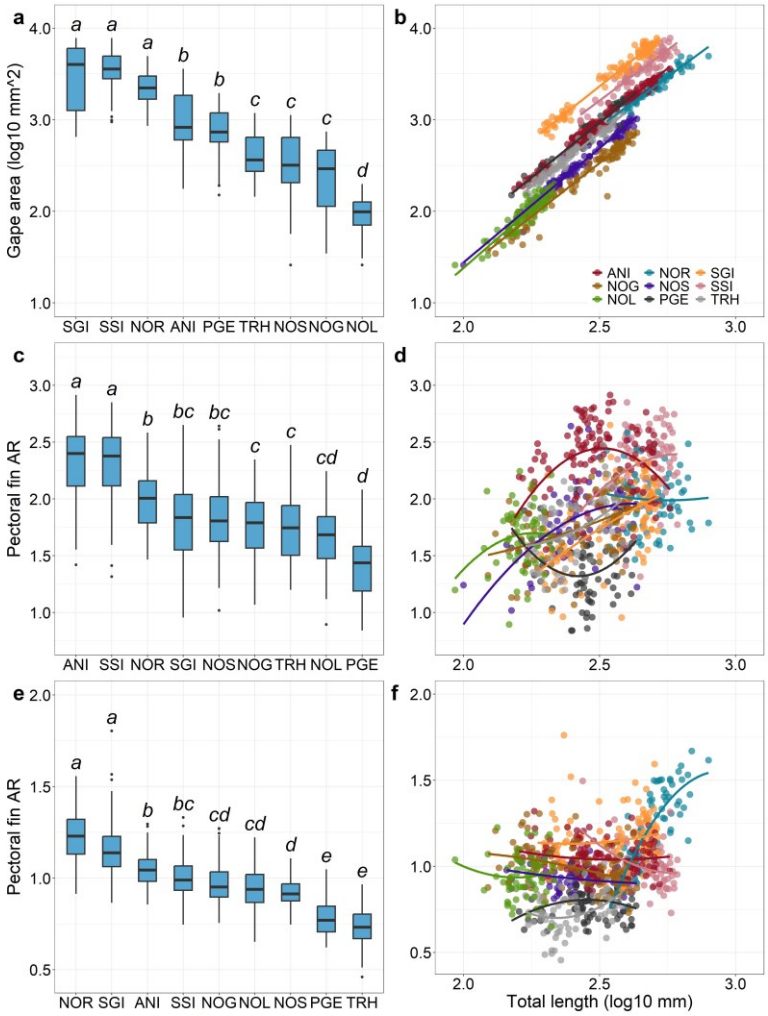

Figure A1: Panels a, c, and e are boxplots of the distribution of mouth gape area, caudal fin aspect ratio (*AR*) and pectoral fin AR, respectively, in 9 South Georgia demersal fish species. Boxplots are ordered by decreasing median value, with letters indicating groupings assigned by a Dunn's test with Bonferroni correction (groups with a letter in common are not significantly different). Panels b, d, and f display the relationship between total length and mouth gape area, caudal fin aspect ratio (*AR*) and pectoral fin *AR*, respectively. Regression lines represent first-order (panel b) and second-order (panels d and f) polynomial fits from linear regression models for each species. Species codes are: ANI, *Champsocephalus gunnari*; SSI, *Chaenocephalus aceratus*; SGI, *Pseudochaenichthys georgianus*; NOR, *Notothenia rossii*; TRH, *Trematomus hansoni*; NOS, *Lepidonotothen squamifrons*; NOL, *Lepidonotothen larseni*; NOG, *Gobionotothen gibberifrons*; PGE, *Parachaenichthys georgianus*.

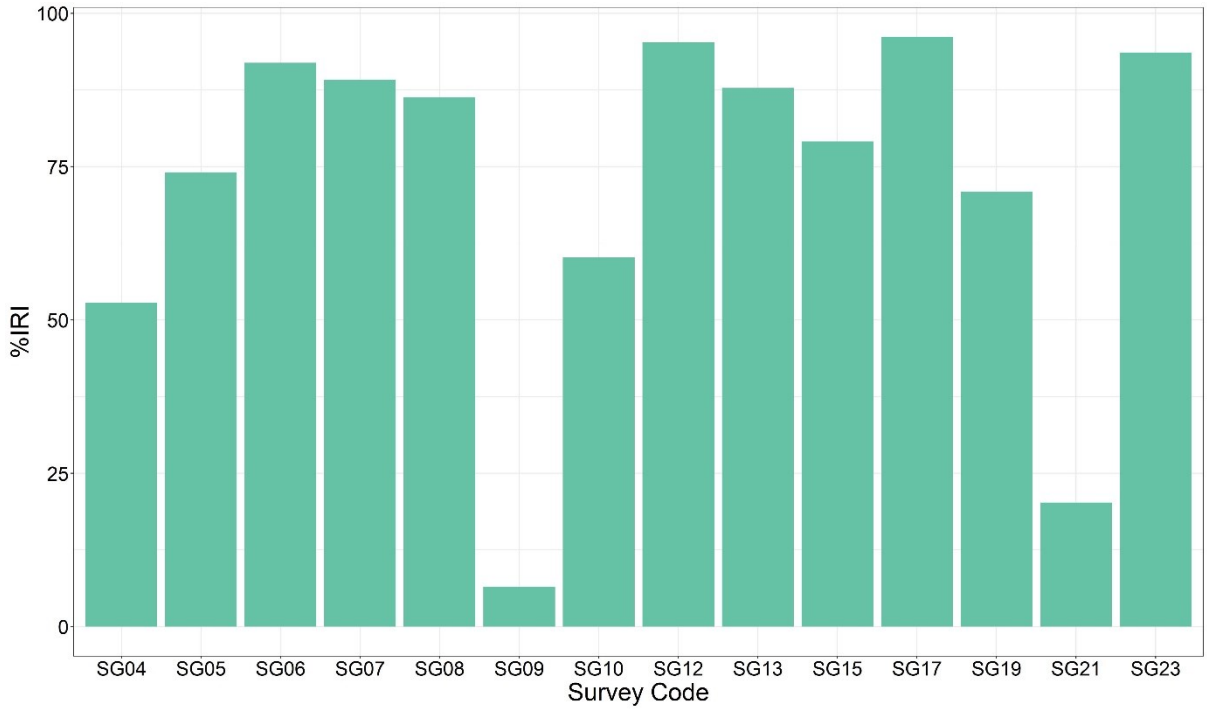

Figure A2: Barplot comparing the total percentage Index of Relative Importance (%IRI) of krill (all Euphausiidae) in the stomachs of Mackerel icefish (*Champsocephalus gunnari*) during each survey since 2004, including the values calculated from the 2023 data (SG23).

A2: Supplementary tables

Table A1: Packages and functions used during analyses:

Package	Reference	Usage
stats	R Core Team (2023)	Cluster analysis and PCA
factoextra	Kassambara & Mundt (2020)	PCA visualisation
vegan	Oksanen et al. (2022)	SIMPER analysis
nlme	Pinheiro et al. (2023)	Linear mixed effects modelling
FSA	Ogle, et al. (2023)	Dunn's tests
party	Hothorn et al. (2005)	Random Forest modelling
ggplot2	Wickham (2016)	Plotting
RColorBrewer	Neuwirth (2022)	Plotting
tidyverse	Wickham et al. (2019)	Data handling

Table A2: Outputs of SIMPER analysis with 99 permutations indicating the contribution of each prey group to the overall dissimilarities in diet composition (based on Index of Relative Importance, %IRI) between feeding guilds. 'Average' represents the contribution to average between-group dissimilarity, and 'SD' indicates the standard deviation of this contribution. The p-value indicates the probability of getting a larger or equal average contribution across the random permutations.

Krill feeders - Benthos feeders			
	Average	SD	p-value
Krill	0.1749	0.07372	0.84
Isopod	0.1008	0.06872	0.01
Misc. benthos	0.09615	0.01213	0.01
Fish	0.04096	0.06526	1
Themisto	0.03667	0.03613	0.99
Other amphipods	0.03464	0.02752	0.37
Mysid	0.00275	0.00329	1
Benthic shrimps	0	0	1
Krill feeders - Fish feeders			
	Average	SD	p-value
Krill	0.3945	0.07424	0.01
Fish	0.296	0.10198	0.01
Other amphipods	0.0556	0.0822	0.04
Themisto	0.0495	0.02517	1
Mysid	0.0268	0.04226	0.95
Isopod	0.0034	0.00416	1
Benthic shrimps	0.0006	0.00075	0.99
Misc. benthos	0.0001	0.00024	1
Krill feeders - *Themisto* & krill feeders			
	Average	SD	p-value
Krill	0.1966	0.07348	0.55
Themisto	0.1492	0.06747	0.01
Fish	0.0677	0.0739	1
Other amphipods	0.01775	0.03051	0.93
Misc. benthos	0.01188	0.0201	0.88
Isopod	0.00817	0.01385	0.84
Mysid	0.00311	0.00324	1
Benthic shrimps	0.00044	0.00076	0.99
Krill feeders - Benthic shrimp feeders			
	Average	SD	p-value
Krill	0.3911	0.07511	0.01
Benthic shrimps	0.2566	0.10619	0.01
Mysid	0.2018	0.07327	0.01
Fish	0.043	0.06098	1

Themisto	0.0317	0.04903	0.99
Other amphipods	0.0002	0.00023	1
Isopod	0	0.00003	1
Misc. benthos	0	0	1
Misc. benthos feeders - Fish feeders			
	Average	SD	p-value
Fish	0.3365	0.07915	0.01
Krill	0.2196	0.04635	0.29
Isopod	0.0974	0.0691	0.01
Misc. benthos	0.096	0.01217	0.01
Other amphipods	0.0625	0.06394	0.19
Themisto	0.03	0.02343	0.99
Mysid	0.0267	0.04271	0.79
Benthic shrimps	0.0006	0.00076	0.85
Misc. benthos feeders - *Themisto* & krill feeders			
	Average	SD	p-value
Themisto	0.16459	0.04883	0.01
Isopod	0.09264	0.0706	0.01
Misc. benthos	0.08427	0.02371	0.01
Fish	0.05016	0.07652	0.99
Krill	0.04143	0.02743	1
Other amphipods	0.03479	0.02771	0.46
Mysid	0.00205	0.00166	0.99
Benthic shrimps	0.00044	0.00077	0.86
Misc. benthos feeders - Benthic shrimp feeders			
	Average	SD	p-value
Benthic shrimps	0.25663	0.10869	0.01
Krill	0.21624	0.04803	0.28
Mysid	0.20207	0.0749	0.01
Isopod	0.10081	0.07034	0.01
Misc. benthos	0.09615	0.01241	0.01
Other amphipods	0.03444	0.02816	0.37
Themisto	0.01584	0.00382	0.98
Fish	0.00478	0.0015	1
Fish feeders - *Themisto* & krill feeders			
	Average	SD	p-value
Fish	0.28654	0.1093	0.01
Krill	0.1979	0.04622	0.61
Themisto	0.13458	0.05342	0.01
Other amphipods	0.0595	0.07484	0.06
Mysid	0.02678	0.0421	0.89
Misc. benthos	0.01184	0.02009	0.83
Isopod	0.00971	0.01173	0.78

Benthic shrimps	0.00074	0.00079	0.93
Fish feeders - Benthic shrimp feeders			
	Average	SD	p-value
Fish	0.3318	0.07917	0.01
Benthic shrimps	0.256	0.10658	0.01
Mysid	0.1771	0.08545	0.01
Other amphipods	0.0556	0.08279	0.21
Themisto	0.0459	0.02313	0.91
Krill	0.0398	0.02724	1
Isopod	0.0034	0.0042	0.94
Misc. benthos	0.0001	0.00024	0.99
Themisto & krill feeders - Benthic shrimp feeders			
	Average	SD	p-value
Benthic shrimps	0.2562	0.10692	0.01
Mysid	0.20156	0.07369	0.01
Krill	0.19455	0.04741	0.48
Themisto	0.18043	0.04869	0.01
Fish	0.04998	0.07353	0.99
Other amphipods	0.01773	0.03076	0.78
Misc. benthos	0.01188	0.02033	0.79
Isopod	0.00817	0.01401	0.77

Table A3: Model selection for optimum random effects and variance weighting structure for the linear mixed effects model describing the relationship between prey body mass (log_{10} g) and the predictors predator body mass (log_{10} g) and predator feeding guild plus their interaction. The final model structure selected based on Bayesian Information Criterion (BIC) and level of parsimony is highlighted in bold.

Random effects structure			Variance structure					BIC
None	~1 | Prey taxon	~ Predator mass | Prey taxon	varIdent(~1| Feeding group)	varIdent(~1| Prey taxon)	varFixed(~Predator mass)	varExp(~Predator mass)	varConst (~Predator mass)	
x								1419.92
	x							**1071.11**
		x						1080.51
			x					1080.09
				x				1092.52
			x	x				1110.26
					x			1055.98
						x		1060.82
							x	1066.71
			x		x			1076.93
			x			x		1080.49
			x				x	1086.63
				x	x			**1080.09**
				x		x		1085.93
				x			x	1092.23

Table A4: Model selection for optimum fixed effects structure for the linear mixed effects model describing the relationship between prey body mass (log_{10} g) and the predictors predator body mass (log_{10} g) and predator feeding guild. Each model includes the optimal random effects and variance weighting structure identified in Table A3. The most parsimonious model structure based on Bayesian Information Criterion (BIC) and retaining only significant fixed effects is highlighted in bold.

Fixed effects structure	BIC
Predator mass * Feeding guild	1054.76
Predator mass + Feeding guild	**1029.92**
Predator mass	1037.52
Feeding guild	1157.13
Null	1144.12

Table A5: Linear mixed effects model estimates of the relationship between prey mass and the additive combination of predator mass and feeding guild. The reference level is the krill-feeding guild.

Coefficient	Estimate	SE	df	t-value	p-value
Intercept	-1.245	0.215	599	-5.777	**<0.001**
Predator mass (log_{10} g)	0.562	0.045	599	12.471	**<0.001**
Benthos	-0.260	0.066	599	-3.921	**<0.001**
Fish	-0.414	0.080	599	-5.144	**<0.001**
Themisto and krill	-0.267	0.061	599	-4.389	**<0.001**
Benthic shrimps	-0.123	0.141	599	-0.868	0.386

Table A6: Results of Kruskal-Wallis tests of differences in the distribution of trait values between feeding guilds.

Trait	chi-squared	df	p-value
Gape area	224.47	4	<0.001
Caudal AR	171.54	4	<0.001
Pectoral AR	262.96	4	<0.001

Table A7: Results of pairwise Dunns tests with Bonferroni correction for differences in the distribution of traits between feeding guilds.

	Gape_area		*Caudal AR*		*Pectoral AR*	
Feeding guild pairing	Z	P.adj	Z	P.adj	Z	P.adj
Krill - Benthos	-8.486	<0.001	-4.994	<0.001	-4.631	<0.001
Krill - Fish	7.174	<0.001	2.184	0.289	-0.966	1
Krill – *Themisto* & krill	4.282	<0.001	3.897	<0.001	10.744	<0.001
Krill - Benthic shrimps	-0.311	1	-10.753	<0.001	-12.968	<0.001
Benthos - Fish	-13.138	<0.001	-6.174	<0.001	-3.370	0.008
Benthos - *Themisto* & krill	-4.334	<0.001	-1.493	1	4.340	<0.001
Benthos - Benthic shrimps	6.314	<0.001	-5.042	<0.001	-7.299	<0.001
Fish - *Themisto* & krill	9.947	<0.001	5.290	<0.001	8.486	<0.001
Fish - Benthic shrimps	-5.472	<0.001	-11.412	<0.001	-11.021	<0.001
Themisto & krill - Benthic shrimps	2.814	0.049	-6.926	<0.001	-3.743	0.002

Table A8: Axis loadings for a Principle Components Analysis (PCA) of the trait values for each individual fish.

Dimension	Eigenvalue	% variance	Cumulative % variance
PC1	1.660	55.327	55.327
PC2	0.778	25.928	81.256
PC3	0.562	18.745	100

Table A9: Variable loadings for a Principle Components Analysis (PCA) of the trait values for each individual fish.

Trait	PC1	PC2	PC3
Gape area	0.624	-0.218	-0.750
Caudal AR	0.510	0.842	0.179
Pectoral AR	0.592	-0.494	0.636

Supplementary references:

Hothorn, T., Bühlmann, P., Dudoit, S., Molinaro, A. & Van Der Laan, M. J. 2005. Survival Ensembles. Biostatistics, 7, 355-373.

Kassambara, A., Mundt, F. (2020). _factoextra: Extract and Visualize the Results of Multivariate Data Analyses. R package version 1.0.7, https://CRAN.R-project.org/package=factoextra.

Neuwirth E (2022). RColorBrewer: ColorBrewer Palettes. R package version 1.1-3, https://CRAN.R-project.org/package=RColorBrewer.

Ogle, D. H., Doll, J. C., Wheeler, A. P. & Dinno, A. 2023. Fsa: Simple Fisheries Stock Assessment Methods. R Package Version 0.9.4. https://CRAN.R-project.org/package=FSA.

Oksanen, J., Simpson G., Blanchet F., Kindt R., Legendre P., Minchin P., O'hara R., Solymos P., Stevens M., Szoecs E., Wagner H., Barbour M., Bedward M., Bolker B., Borcard D., Carvalho G., Chirico M., De Caceres M., Durand S., Evangelista H., Fitzjohn R., Friendly M., Furneaux B., Hannigan G., Hill M., Lahti L., Mcglinn D, Ouellette M., Ribeiro Cunha E., Smith T., Stier A., Ter Braak C. & J., W. 2022. Vegan: Community Ecology Package. R Package Version 2.6-4. https://CRAN.R-project.org/package=vegan

Pinheiro J., Bates D. & Team, R. C. 2023. Nlme: Linear and Nonlinear Mixed Effects Models. R Package Version 3.1-162. https://CRAN.R-project.org/package=nlme.

R Core Team 2023. R: Language and Environment for Statistical Computing. R Foundation for Statistical Computing, Vienna, Austria. https://www.R-project.org/.

Wickham, H. (2016). ggplot2: Elegant Graphics for Data Analysis. Springer-Verlag New York. ISBN 978-3-319-24277-4, https://ggplot2.tidyverse.org.

Wickham, H., Averick, M., Bryan, J., Chang, W., McGowan, L.D., François, R., Grolemund, G., Hayes, A., Henry, L., Hester, J., Kuhn, M., Pedersen, T.L., Miller, E., Bache, S.M., Müller, K., Ooms, J., Robinson, D., Seidel, D.P., Spinu, V., Takahashi, K., Vaughan, D., Wilke, C., Woo, K., Yutani, H. (2019). “Welcome to the tidyverse.” Journal of Open Source Software, 4(43), 1686. doi:10.21105/joss.01686, https://doi.org/10.21105/joss.01686.

Appendix B: Supplementary material for chapter 3

B1: Supplementary methods and results

Supplementary methods

Overview of functional traits.

Here we detail the functional traits compiled for this study, including a description of their ecological relevance and an overview of how they were coded for analyses.

Body mass data were already available for each food web, having been compiled through a combination of direct measurement in the field and the compilation of values from the literature (Brose et al. 2019 ; López-López et al. 2021). Upon inspection of the body mass data, a small number of discrepancies within and between the food webs were identified, and for consistency these were corrected using published mass data sources (see Supplementary Data). Values were then subject to log10 transformation for analyses.

Foraging habitat represents the physical space in which the organisms are primarily found, and therefore plays a role in determining which trophic interactions are feasible due to species overlap. Broad habitat categories were identified for each food web, and species were assigned to these based on literature review, with those found across multiple habitats assigned to a combined habitat category. For the Scotia Sea food web, three pelagic habitat categories ("epipelagic", "mesopelagic" and "benthopelagic") plus possible combinations of these ("epi-mesopelagic", "epi-meso-bathypelagic", "meso-bathypelagic") were taken from the original publication (López-López et al. 2021). In the Weddell Sea, habitats were assigned as "benthic", "lower pelagic" and "upper pelagic", in addition to the combinations of "upper and lower pelagic", "upper and lower pelagic and benthic", and "lower pelagic and benthic". For Lough Hyne and Kongsfjorden, habitats were assigned as "benthic", "intertidal" and "pelagic", in addition to "benthic and intertidal", "benthic and pelagic", "pelagic and intertidal", and "benthic, intertidal and pelagic", to reflect possible habitat overlaps.

Mobility represents the primary propulsive method used by each species, which will influence how likely predators and prey are to come into contact, and how easily consumers can capture resources or resources can evade their consumers. We assigned a scale of increasing mobility:

0 (sessile, attached); 1 (passive drifter, no substantial self-locomotion); 2 (crawler); 3 (swimming by cilia/flagella or appendages); 4 (jet propulsion); 5 (lift-based swimming).

Prey-capture strategy represents how active the predator is in capturing prey. The method employed will influence how likely different consumers and resources are to come into contact, and which types of resource can be consumed. We assigned a scale of increasing activity: 0 (Producer, no resource capture involved); 1 (Passive, no action by the consumer until after contact with resource has been made); 2 (Ambush, consumer is relatively inactive but selects and actively captures resources when in range); 3 (Active suspension/detritus feeder, displays limited activity such as pumping of water or sifting through sediment which may involve some locomotion, but prey selection occurs after contact); 4 (Active search, consumer moves actively searching for resources either as a browsing herbivore or hunting predator). In some cases, the primary capture strategy was not documented in the literature, in which case it was inferred from diet where possible (e.g., consumers of sessile prey must employ an active searching strategy).

Capture appendages represent any external appendage (i.e. tentacles/arms, legs) which could reasonably be considered to play a role in grasping and manipulating prey. Organisms which lack such appendages must engulf their prey to capture them. Cilia and flagella were not considered capture appendages due to their primary role in locomotion and producing simple feeding currents.

Body robustness represents the general body type of the organism, which will influence which consumers it has. We assigned a scale of increasing robustness: 0 (gelatinous); 1 (soft-bodied, no internal skeleton/shell); 2 (soft-bodied with internal skeleton/shell); 3 (external skeleton); 4 (external hard shell).

Spines are expected to deter certain consumers as they can cause physical damage and may make consumption difficult. The presence or absence of spines was determined based on image assessment. Spines were only considered present if their role could be confidently assigned to defence (e.g., rostral/dorsal spines in copepods and amphipods).

The translucency trait represents how visible organisms are within the water column and is expected to play a role in both prey capture and predator avoidance. This trait was assigned based on assessment of images.

Traits were assigned to all nodes except for difficult to define basal groups (detritus and sediment).

Robustness of module assignments

The stochastic element to the Simulated Annealing algorithm used to identify food web modules means the final results of different runs can vary both in terms of the number of modules identified and the partitioning of nodes between modules (i.e. the identity of species assigned to the same module could differ between runs). It was therefore important to ensure that the final modularity partition reported for each network was representative of the spread of results obtained across different runs of the algorithm. To select an appropriate result for each food web we first identified the number of modules in each Simulated Annealing output and then randomly selected a result displaying the most representative number of modules across the runs.

88% of runs for the Scotia Sea web identified three modules while the remaining 12% identified two modules, and 95% of runs for the Weddell Sea identified three modules while 5% identified four modules. A result with three modules was therefore randomly selected for these two webs. For Lough Hyne, 81% of runs identified five modules, and the remaining 19% found four, while for Kongsfjorden 83% of runs identified five, 16% identified four, and 1% identified six modules. A result with five modules was randomly selected for both networks.

The next step was to identify how consistent the partitioning of species into different modules in the selected result was across the remaining Simulated Annealing runs. We followed the methods of Rezende et al. (2009) in focusing on the distribution of interactions within modules. For each interacting species pair assigned to the same module in the chosen Simulated Annealing run, we calculated the number of times that pair co-occurred in a module across all the remaining runs. The results suggest that there is extremely low total variability in the module membership of interacting pairs, as the overwhelming majority of within-module interactions were consistent across runs: 96.6% in the Scotia Sea; 95.3% in the Weddell Sea; 99.2% in Lough Hyne; 99.5% in Kongsfjorden. These results support the robustness of the partitioning of the focal food webs by the Simulated Annealing algorithm.

Finally, we investigated the variability in trophic level (TL) and $\log_{10}$ body mass of each module for each network, across Simulated Annealing runs. For each run, we investigated the proportion of pairwise differences in the distribution of TL and body masses between modules

that were significant. The results of our randomly selected outputs were generally consistent with those of the remaining Simulated Annealing runs. In the Scotia Sea, the average proportion of significant pairwise differences was 94.0% (± 1.3% standard error) for TL, and 88.0% (± 2.6%) for body mass. In the Weddell Sea, these proportions were 99.0% (± 0.4%) for TL and 98.0% (± 0.7%) for mass. In Lough Hyne, the average proportion of significant pairwise differences was 72.0% (± 0.5%) for TL, and 31.0% (± 0.2%) for mass. For comparison, in the randomly chosen run, 70.0% of pairwise comparisons were significantly different for TL, while 30.0% were significantly different for mass. In Kongsfjorden, the values were 34.5% (± 1.0%) for TL and 45.1% (± 1.1%) for mass. In the randomly chosen run for this network, 30.0% of pairwise comparisons were significantly different for TL, while 40.0% were significantly different for mass. When plotting the average TL and body mass in each module for all the runs, the distribution of values in the randomly chosen run was generally consistent with the distribution of values from the other runs, though in a minority of cases, differences in the total number of modules or changes to the distribution of species across modules resulted in outliers (Figure B1 & B2.). These changes would be unlikely to alter the key findings of this study, as the overall pattern of modules in each network is maintained (modules in the Scotia Sea and Weddell Sea encompass distinct trophic clusters and body mass distributions while many of those in Lough Hyne and Kongsfjorden are not significantly different).

Supplementary results

Differences in trophic level variance within and between modules

A potential issue with comparing the mean difference in trophic level between modules in each network is that this metric could be sensitive to both the maximum trophic level of a given network and the number of modules identified. We therefore calculated two metrics; the variance in trophic level for all pairwise combinations of species from the same module (within-variance), and the variance in trophic level for all pairwise combinations of species from separate modules (between-variance). The ratio of the within-variance and between-variance provides a metric that is independent of network size and maximum trophic level and describes the organisation of modules: larger values indicate that modules encompass a wide range of trophic levels but have a large overlap with one-another; smaller values indicate that modules have less overlap in trophic levels. The results using this metric support the conclusions drawn using the mean trophic level differences: modules in the Scotia Sea and

Weddell Sea food webs have lower values than those in Lough Hyne and Kongsfjorden (0.49, SE = 0.001 and 0.58, SE = 0.001 versus 0.90, SE = 0.001 and 1.26, SE = 0.001, respectively).

Distribution of node metrics across modules

There is a significant decline in average vulnerability from modules 1 to 3 in both the Scotia Sea and Weddell Sea food webs (Figure B3). This likely results from the organisation of modules by trophic level, as organisms occupying the highest trophic levels (i.e. those in module 3) are the least vulnerable as they have relatively few predators. Similarly, the increase in omnivory with trophic level in both networks also fits with the organisation of modules by trophic level, as species found higher in the feeding hierarchy have a greater variety of organisms of different trophic levels available to feed upon (Thompson et al. (2007; Figure B4). The contrast in the change in generality across modules in these two networks (an increase in the Scotia Sea and a decrease in the Weddell Sea; Figure B5) suggests that top predators in the Scotia Sea feed on a greater number of prey species than those lower in the food web, while the inverse is true of top predators in the Weddell Sea. It is not clear what the underlying driver(s) of this difference in the level of dietary specialisation of higher predators in the two networks might be, but it is interesting that despite these contrasts both food webs display very similar structuring of modularity by trophic levels. In the Lough Hyne and Kongsfjorden food webs there is a lack of consistent differences in these node-level metrics across modules. This fits the description of modules in these networks as semi-isolated energy channels, as most modules contain an assemblage of species centred around distinct basal resources and therefore are not structured by trophic level in the same way as those in the Scotia Sea and Weddell Sea.

B2: Supplementary figures

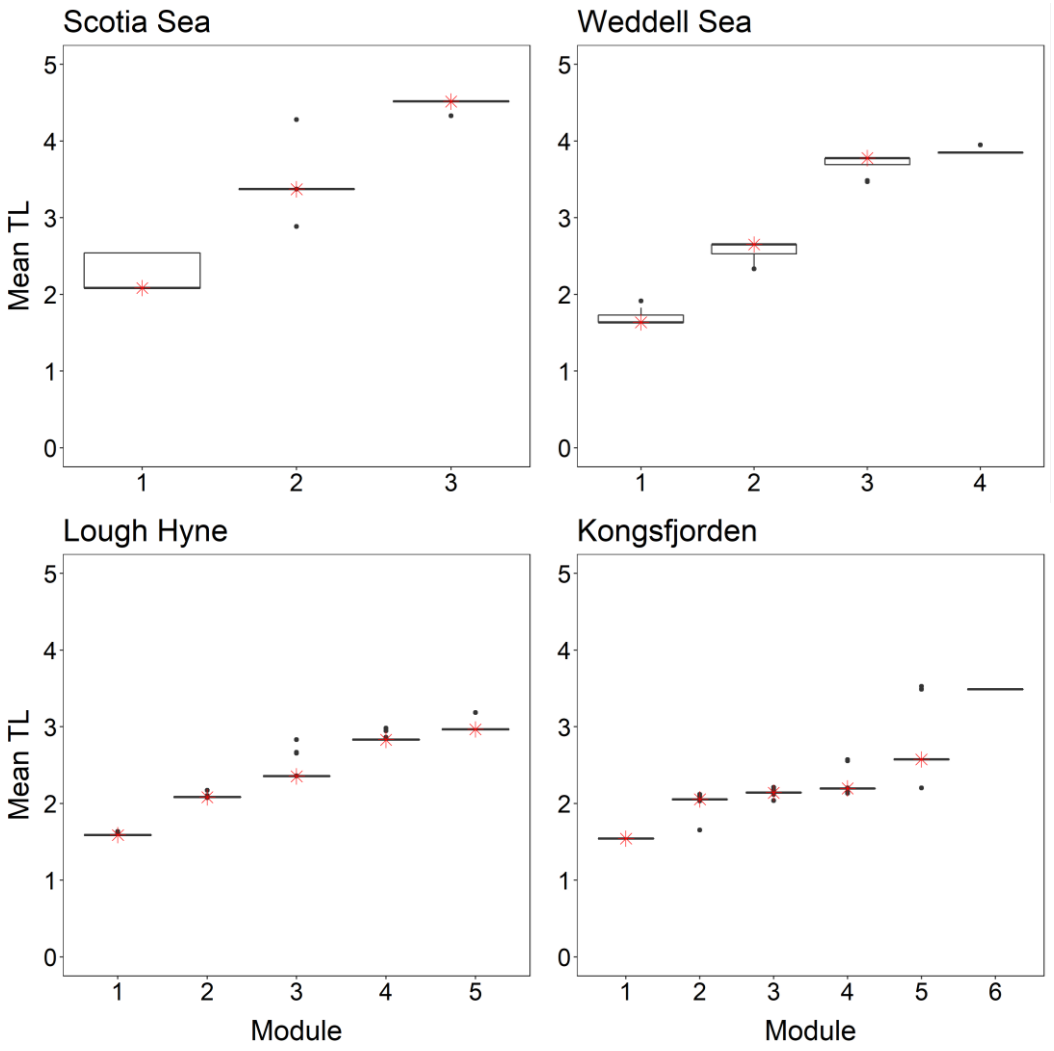

Figure B1: The distribution of mean trophic level of each module across all runs of the Simulated Annealing algorithm for each network. Red stars indicate the values for the randomly selected outputs used in later analyses. Note that the Weddell Sea had 4 modules in only 5% of runs, whilst Kongsfjorden had 6 modules in only 1% of runs

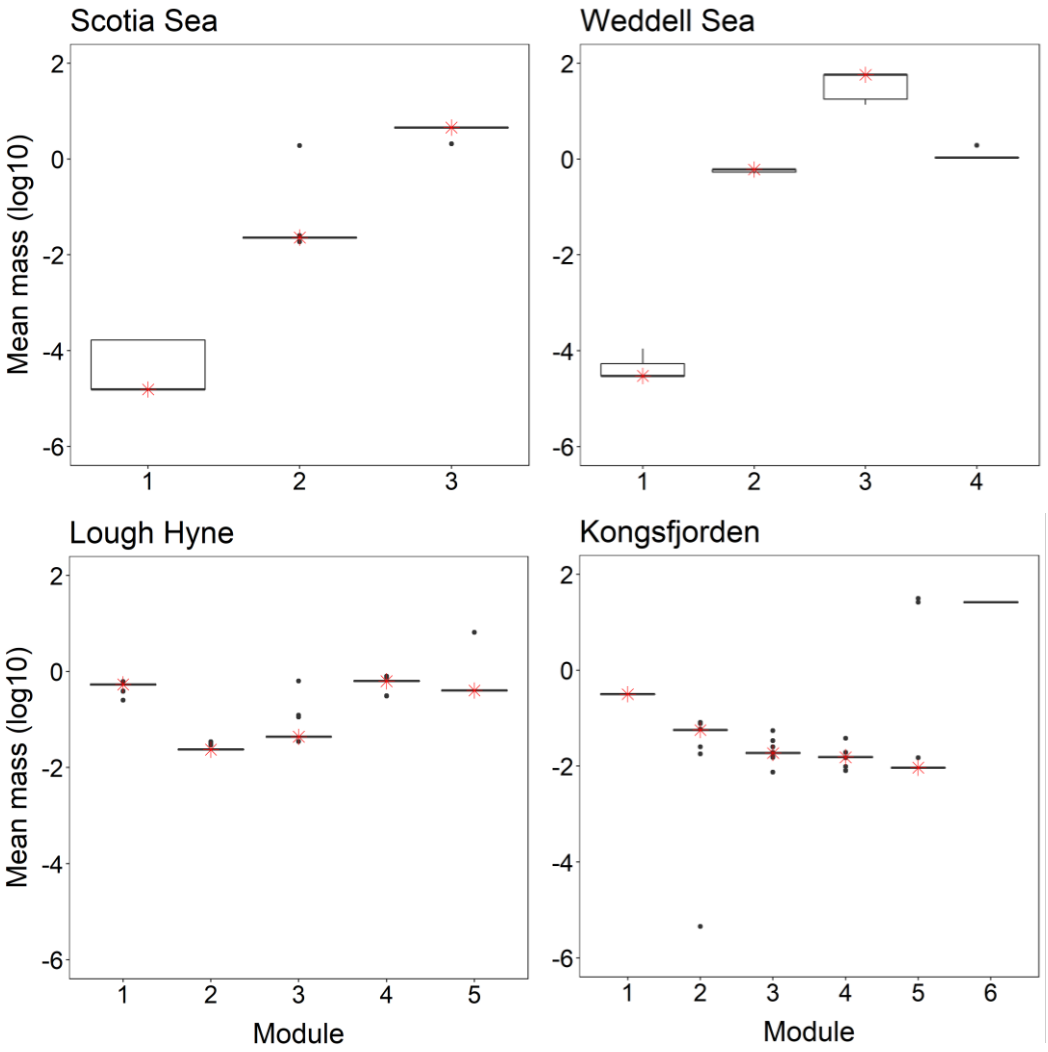

Figure B2: The distribution of mean body mass of each module across all runs of the Simulated Annealing algorithm for each network. Red stars indicate the values for the randomly selected outputs used in later analyses. Note that the Weddell Sea had 4 modules in only 5% of runs, whilst Kongsfjorden had 6 modules in only 1% of runs

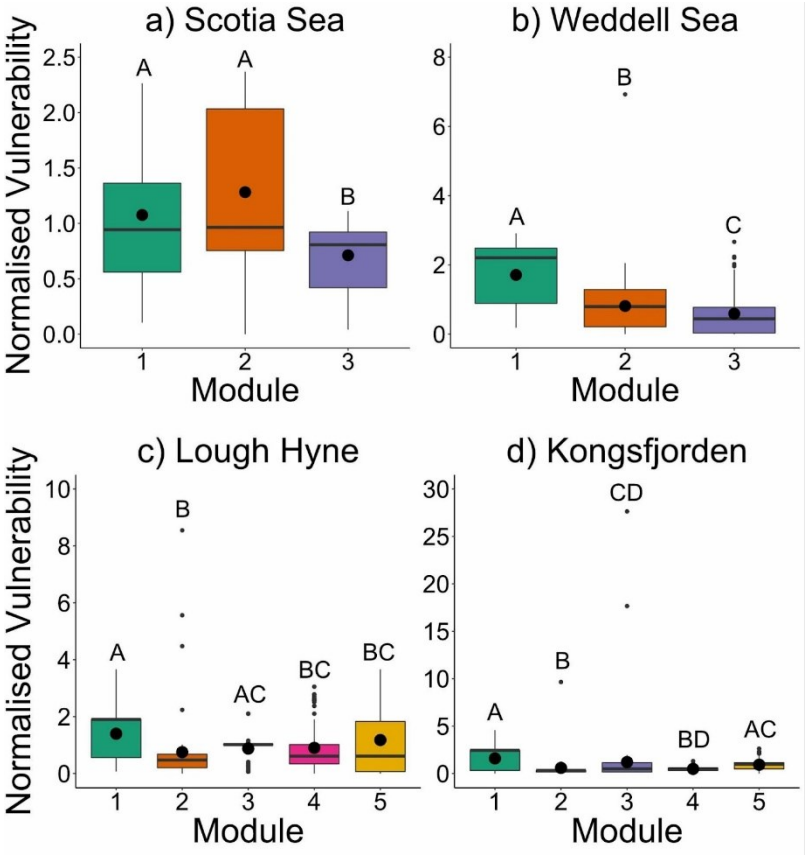

Figure B3: Boxplots of node normalised vulnerability across compartments within each food web. Large black points indicate the mean, thick horizontal lines represent the median, boxes indicate the 25th – 75th percentile range, whiskers are 1.5 × the interquartile range, and outliers beyond this range are indicated as small black points. Boxes not sharing a common letter are significantly different from one another (Dunn's test, $p < 0.05$).

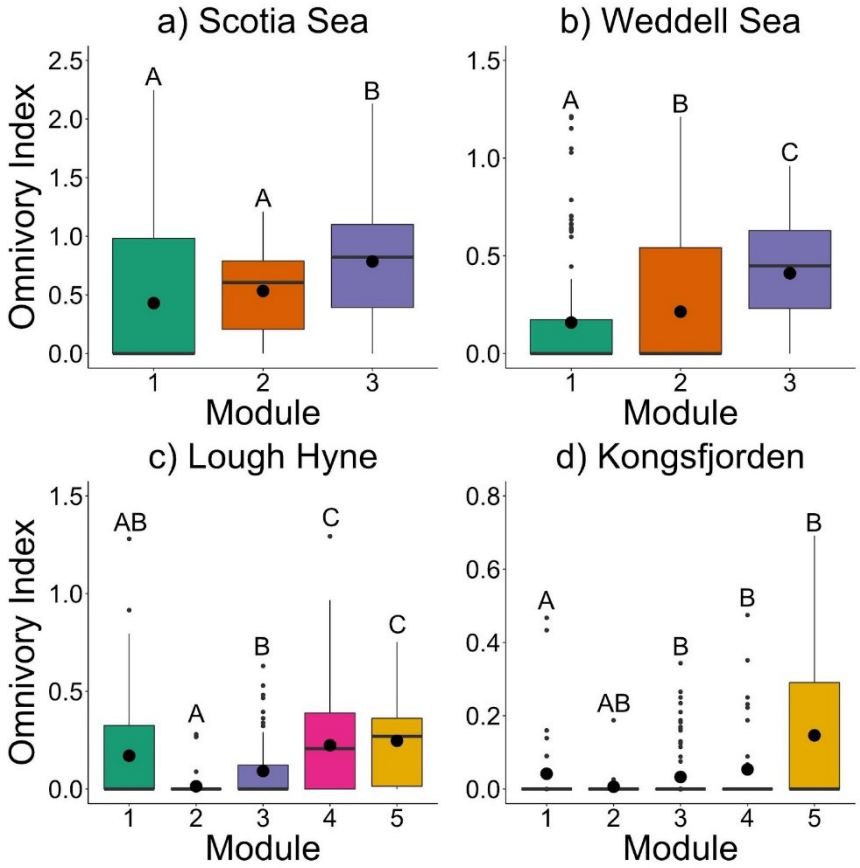

Figure B4: Boxplots of node omnivory index values across modules within each food web. Large black points indicate the mean, thick horizontal lines represent the median, boxes indicate the 25th – 75th percentile range, whiskers are 1.5 × the interquartile range, and outliers beyond this range are indicated as small black points. Boxes not sharing a common letter are significantly different from one another (Dunn's test, $p < 0.05$). Note varying axis scales.

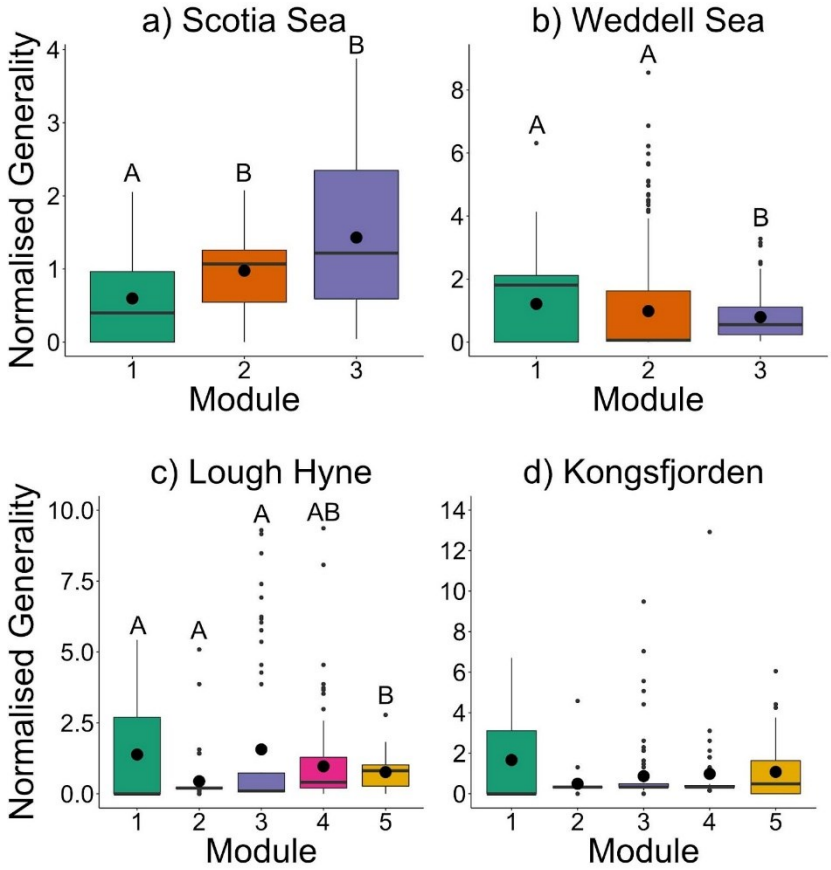

Figure B5: Boxplots of node normalised generality across modules within each food web. Large black points indicate the mean, thick horizontal lines represent the median, boxes indicate the 25th – 75th percentile range, whiskers are 1.5 × the interquartile range, and outliers beyond this range are indicated as small black points. Boxes not sharing a common letter are significantly different from one another (Dunn's test, $p < 0.05$). No significant differences were found for Kongsfjorden. Note varying axis scales.

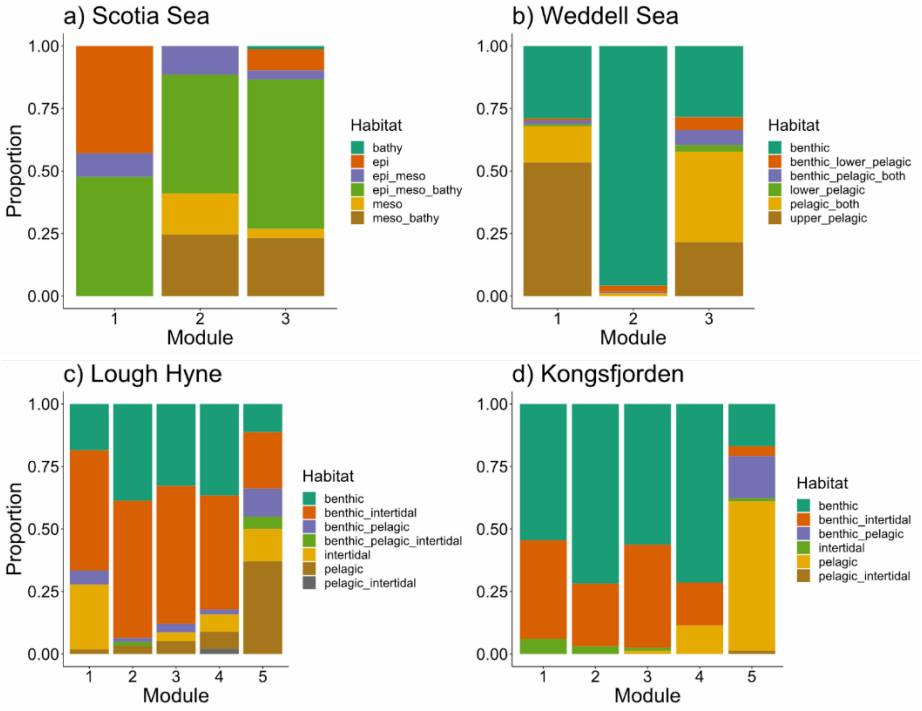

Figure B6: Bar plots displaying the proportion of species within each food web module which were assigned to each foraging habitat. In a), "bathy" represents bathypelagic, "epi" represents epipelagic and "meso" represents mesopelagic. In all plots, habitats joined by "_" indicate that the species forage across multiple habitats.

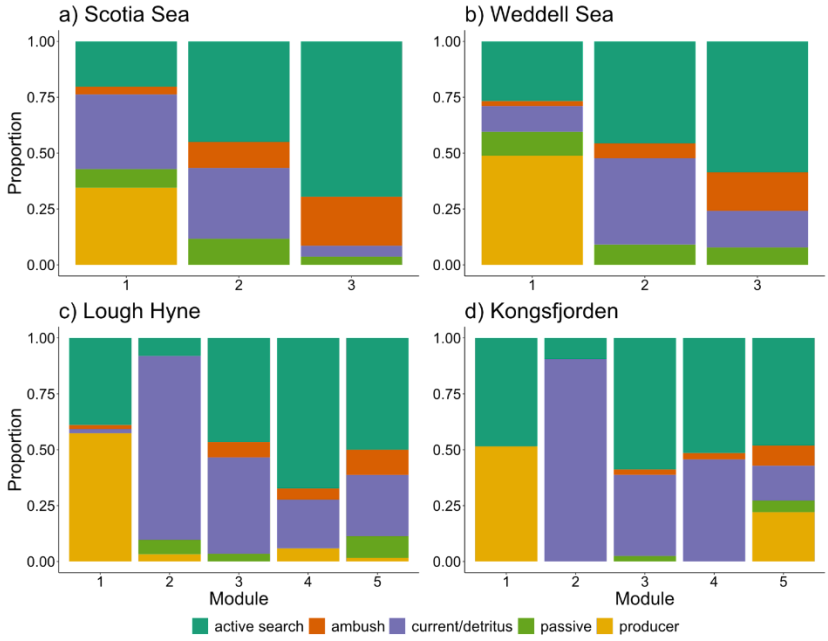

Figure B7: Bar plots displaying the proportion of species within each food web module which were assigned to each prey-capture strategy.

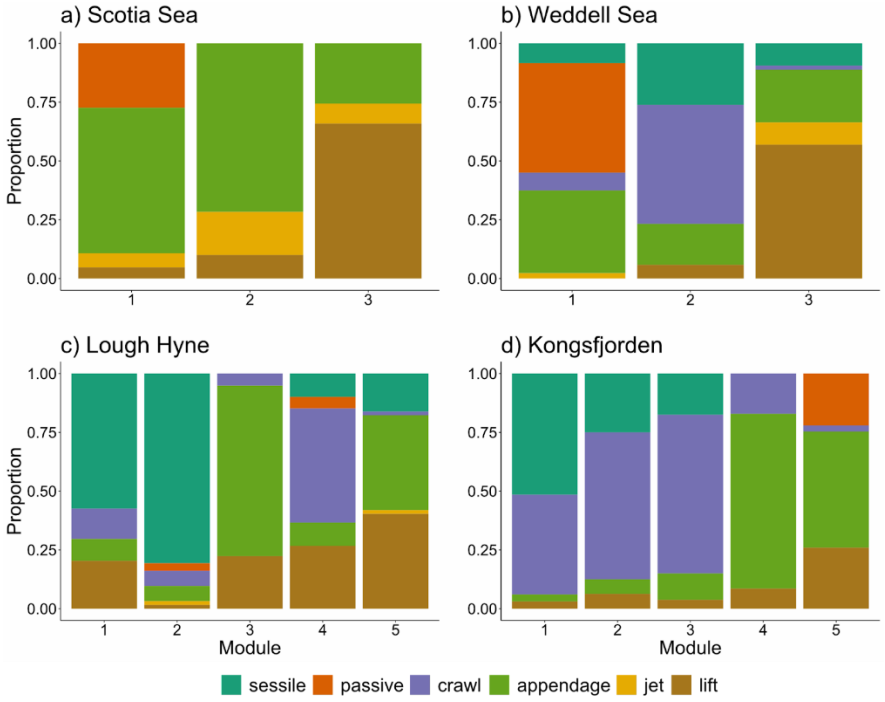

Figure B8: Bar plots displaying the proportion of species within each food web module which were assigned to each movement method.

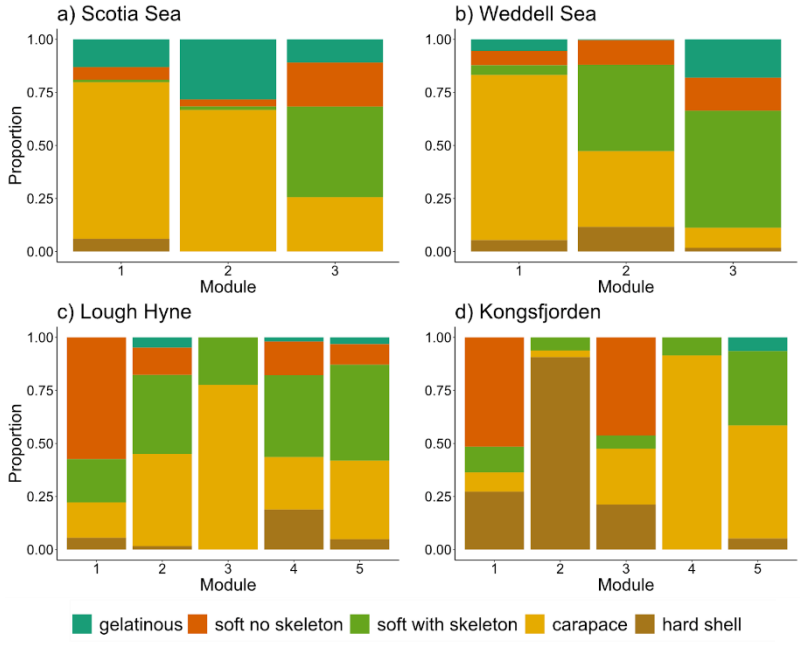

Figure B9: Bar plots displaying the proportion of species within each food web module which were assigned to each body robustness category.

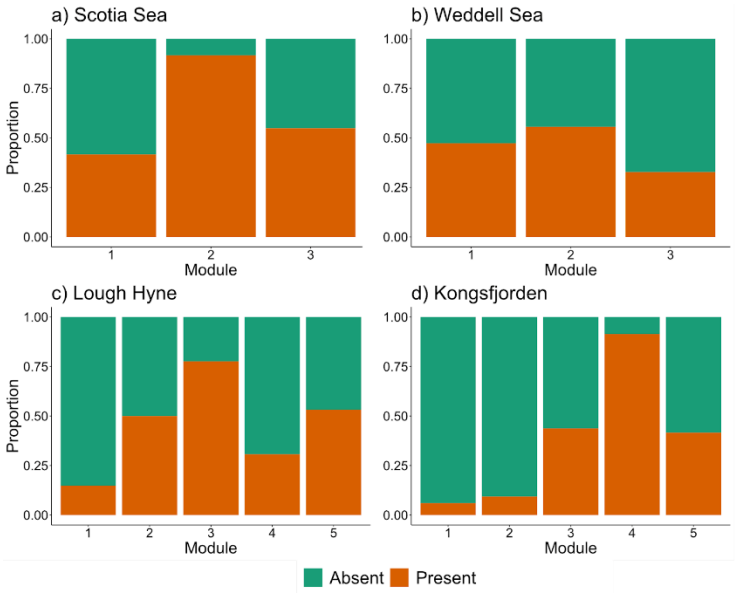

Figure B10: Bar plots displaying the proportion of species within each food web module which were considered to have feeding appendages capable of grasping and manipulating prey.

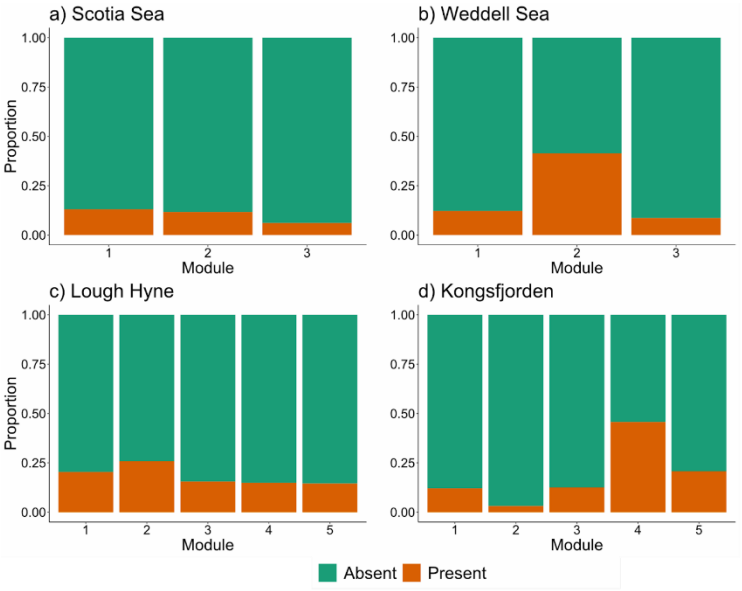

Figure B11: Bar plots displaying the proportion of species within each food web module which were considered to have defensive spines.

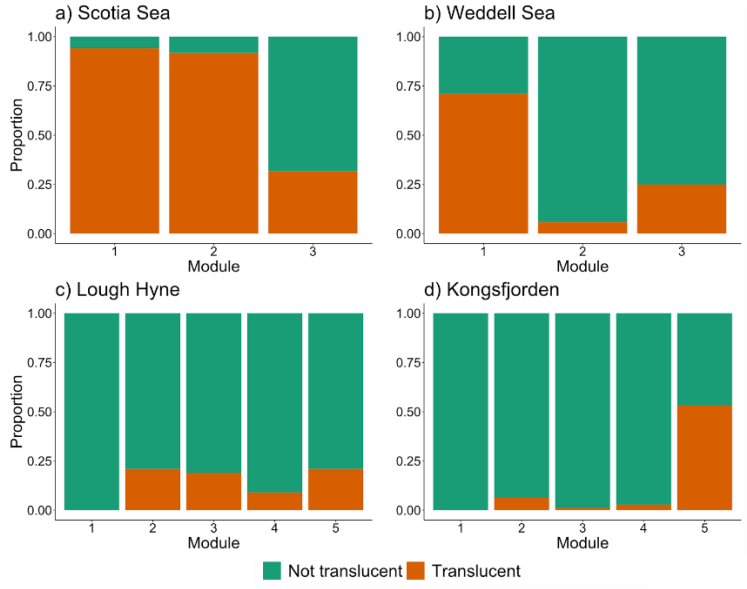

Figure B12: Bar plots displaying the proportion of species within each food web module which were considered to be largely translucent.

Supplementary references:

Brose, U., Archambault, P., Barnes, A. D., Bersier, L.-F., Boy, T., Canning-Clode, J., Conti, E., Dias, M., Digel, C., Dissanayake, A., Flores, A. a. V., Fussmann, K., Gauzens, B., Gray, C., Häussler, J., Hirt, M. R., Jacob, U., Jochum, M., Kéfi, S., Mclaughlin, O., Macpherson, M. M., Latz, E., Layer-Dobra, K., Legagneux, P., Li, Y., Madeira, C., Martinez, N. D., Mendonça, V., Mulder, C., Navarrete, S. A., O'gorman, E. J., Ott, D.,

López-López, L., Genner, M. J., Tarling, G. A., Saunders, R. A. & O'gorman, E. J. 2021. Ecological Networks in the Scotia Sea: Structural Changes across Latitude and Depth. *Ecosystems*.

Rezende, E. L., Albert, E. M., Fortuna, M. A. & Bascompte, J. 2009. Compartments in a Marine Food Web Associated with Phylogeny, Body Mass, and Habitat Structure. *Ecol Lett,* 12**,** 779-88.

Thompson, R. M., Hemberg, M., Starzomski, B. M. & Shurin, J. B. 2007. Trophic Levels and Trophic Tangles: The Prevalence of Omnivory in Real Food Webs. Ecology, 88, 612-617.

Appendix C: Supplementary material for chapter 4

C1: Supplementary figures

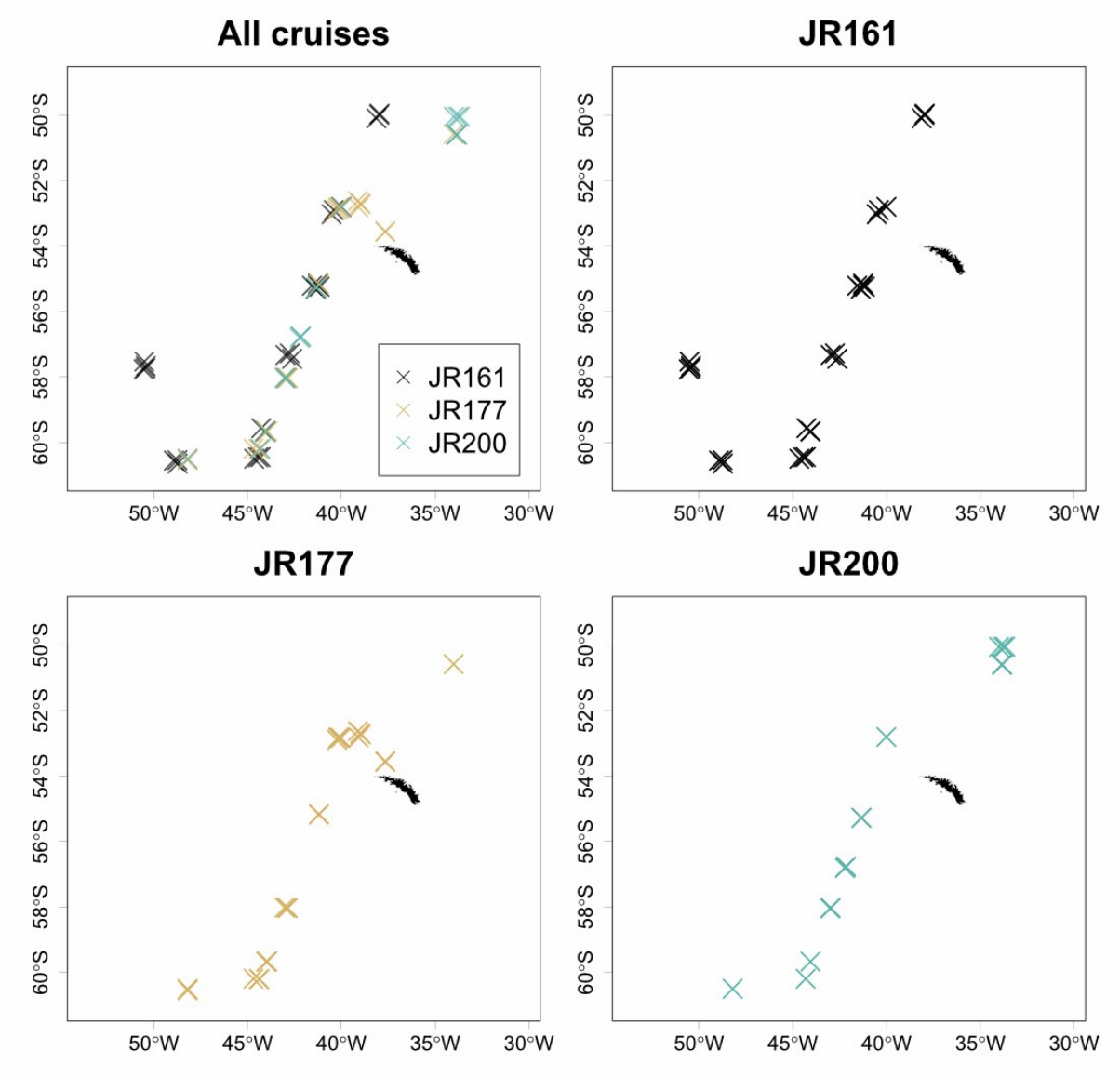

Figure C1: Distribution of myctophid sampling stations from each cruise.

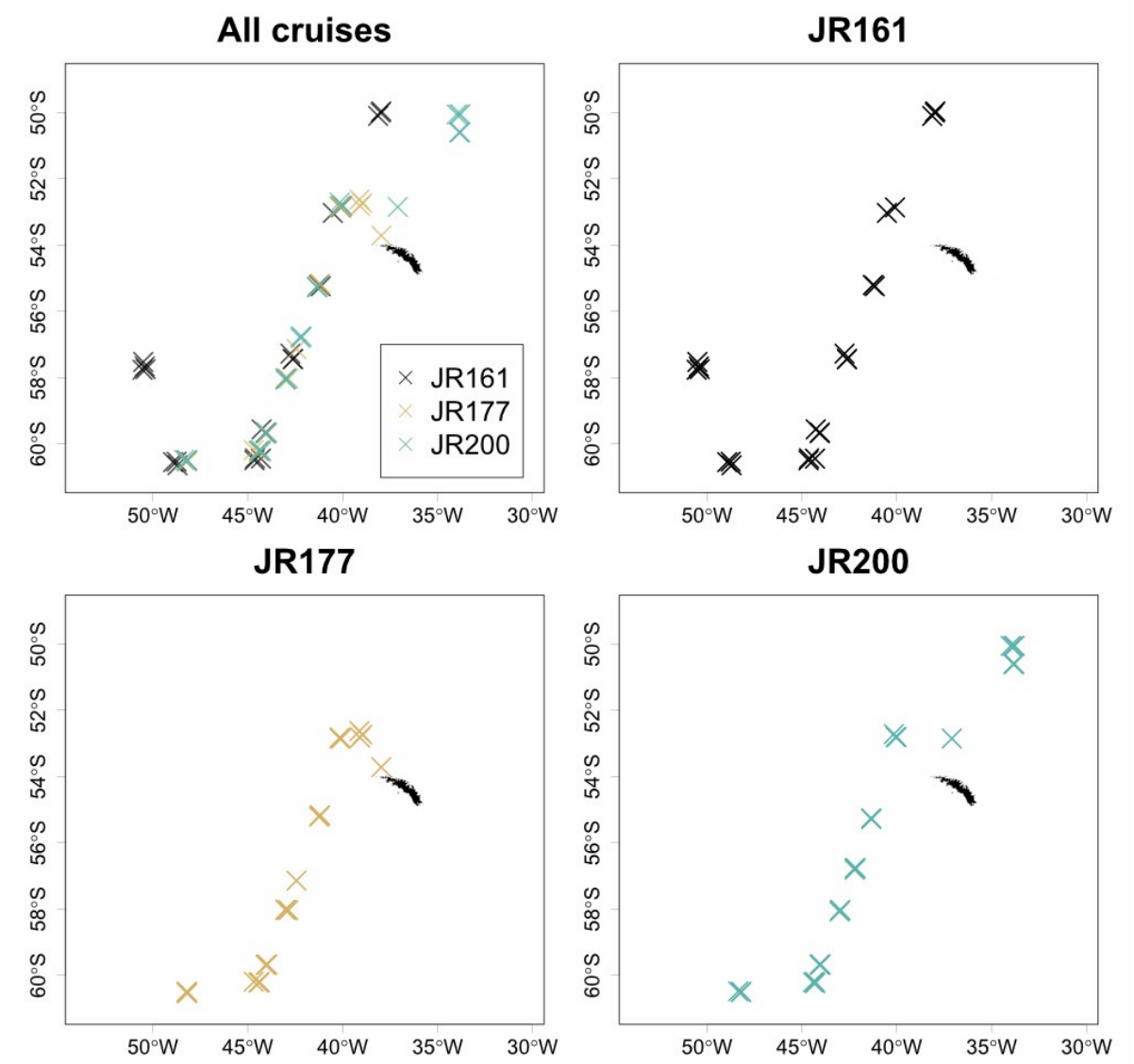

Figure C2: Distribution of zooplankton sampling stations from each cruise.

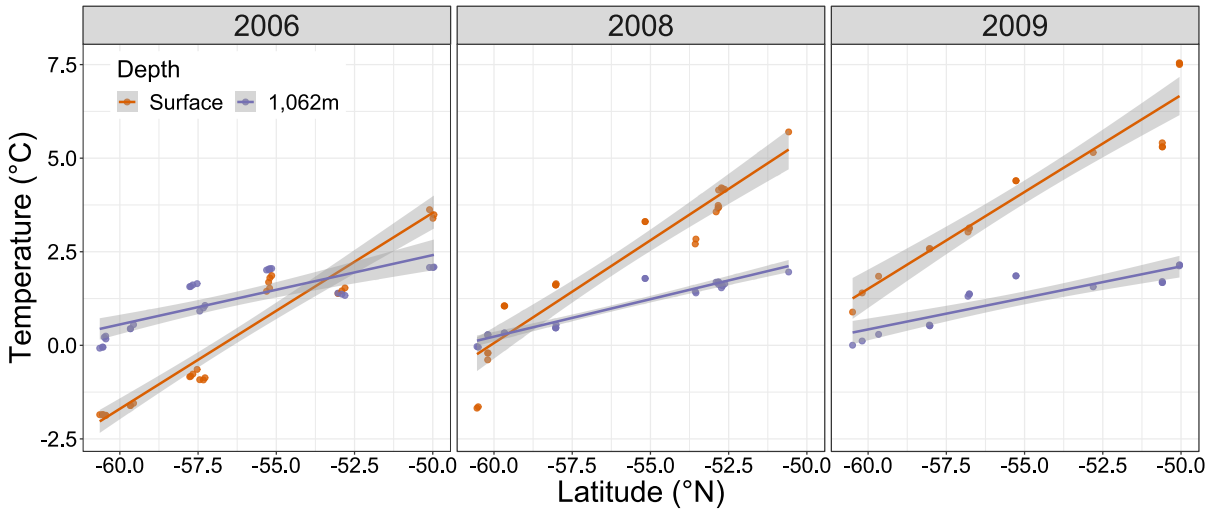

Figure C3: Comparison of temperatures at different depths across the sampling sites. Relationship between temperature (both at the surface and at 1,062m depth) and latitude at each haul location, split by sampling year (n = 27, 25, and 18 sites in 2006, 2008 and 2009, respectively). Lines represent model predicted values and shading represents 95% confidence intervals.

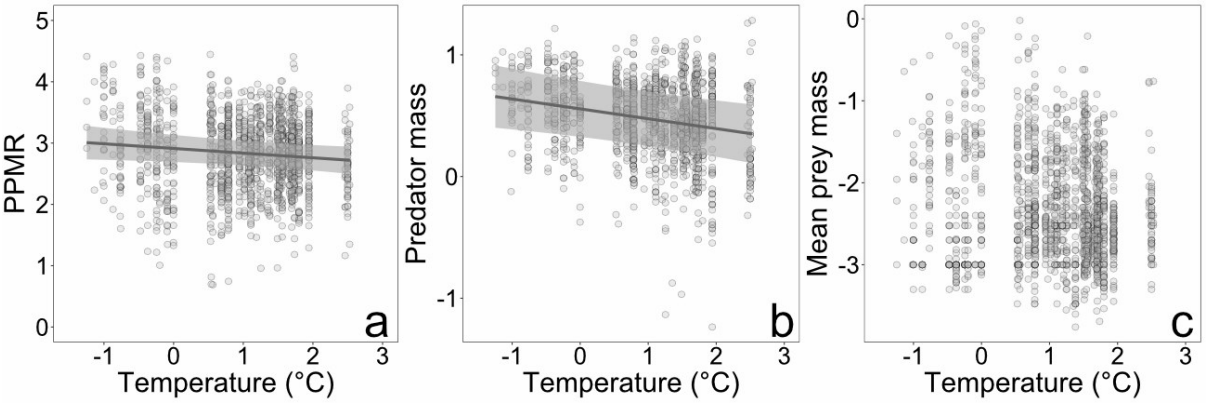

Figure C4: Effects of temperature at 1,062 m depth on predator and prey body mass (n = 1576 fish). (a) partial residual plot from a linear mixed model of the effect of temperature (at 1,062m depth) on prey-averaged predator-prey mass ratio (PPMR); (b) partial residual plot from a linear mixed model of the effect of temperature on predator body mass; (c) scatterplot of the relationship between temperature and abundance-weighted average prey mass in predator stomachs. Y-axis values are in $\log_{10}$ g. Lines represent predicted values at each SST. Shading represents 95% confidence intervals.

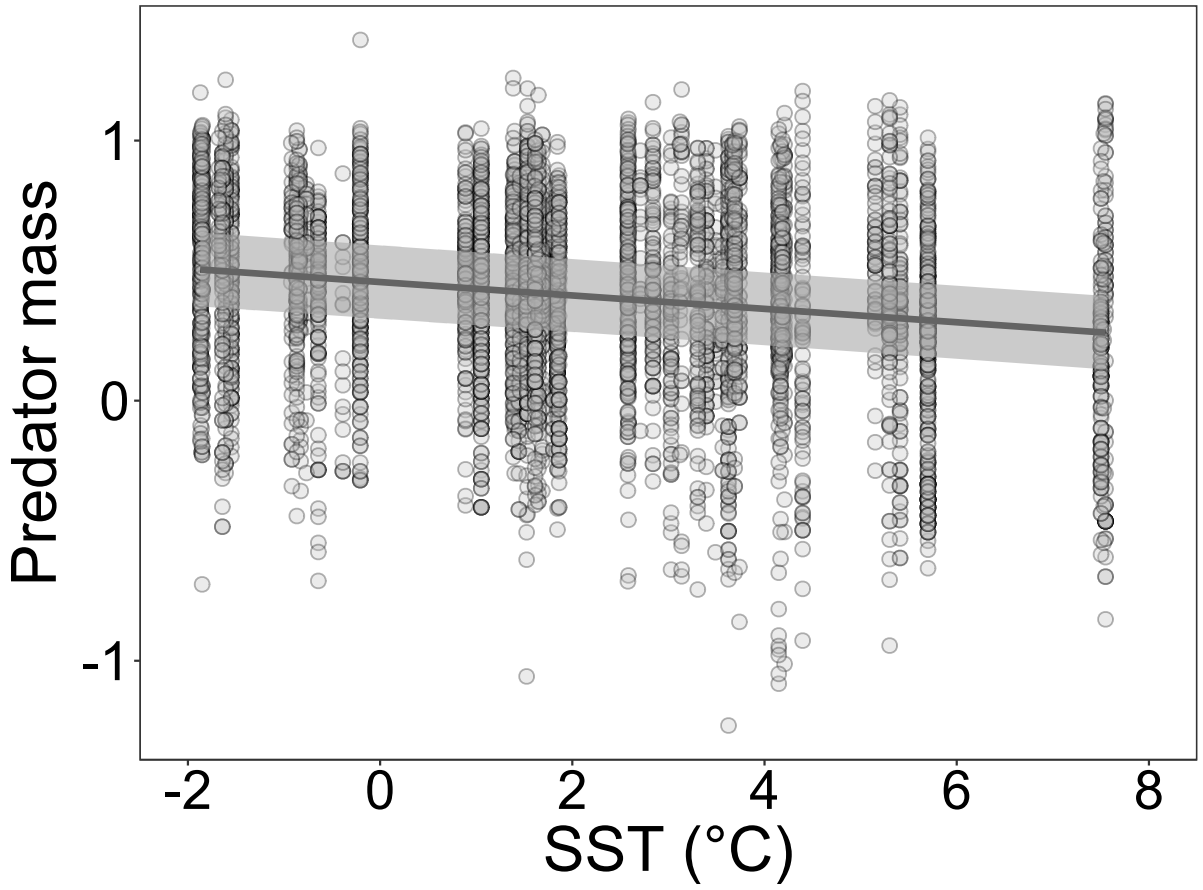

Figure C5: Effects of temperature on predator body mass from a larger dataset. Partial residual plot from a linear mixed model of the effect of sea-surface temperature (SST) on predator body mass using a larger dataset of myctophid body sizes (n = 6,143). Y-axis values are in $\log_{10}$ g. Line represents predicted values of predator mass at each temperature. Shading represents 95% confidence intervals.

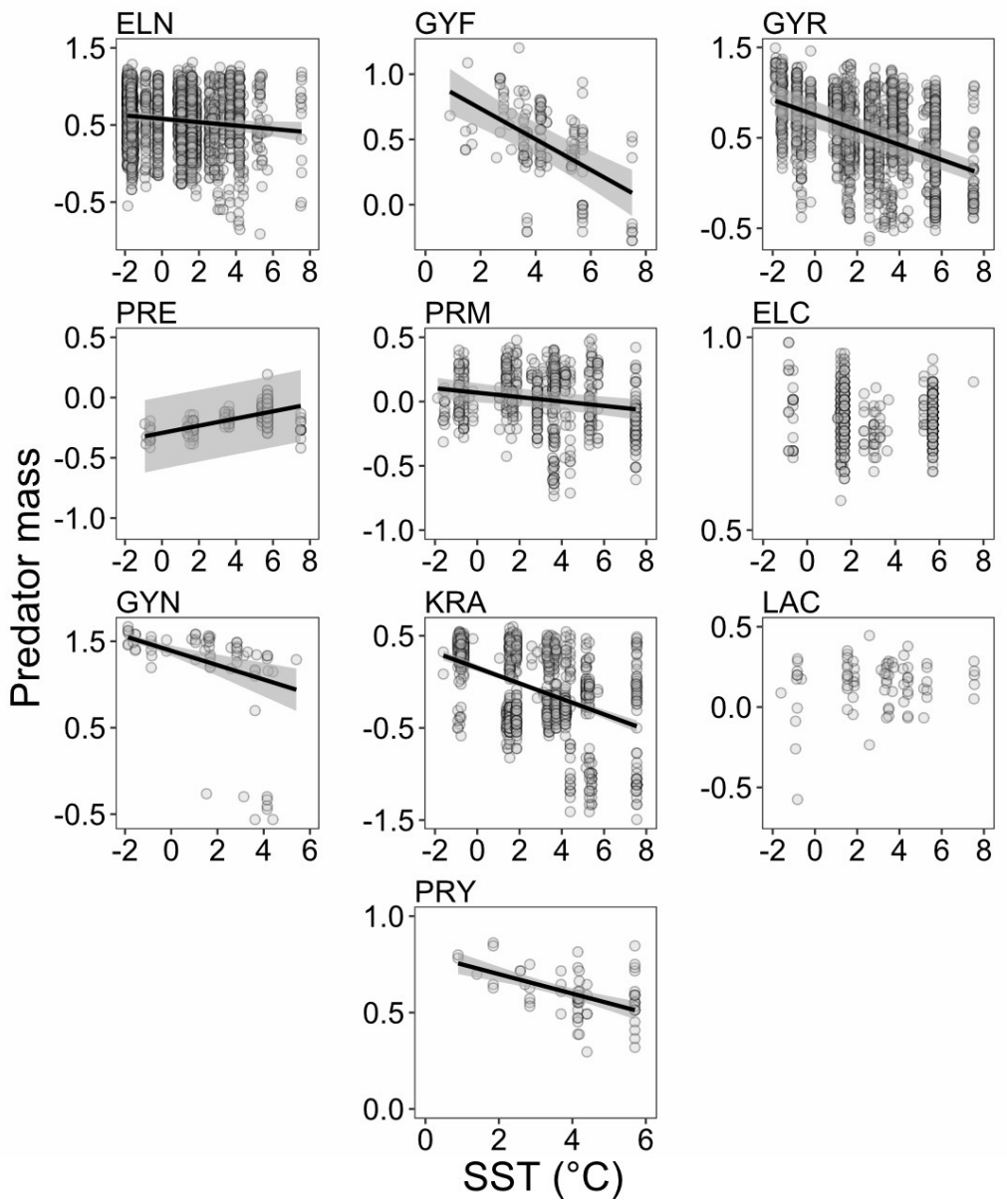

Figure C6: Relationship between predator mass and sea surface temperature (SST) for each species. Panels ELN, GYF, GYR, PRE and PRM are partial residuals plots, the remainder are scatterplots of the raw data with regression lines indicating predicted values from a Generalised Least Squares model. Y-axis values are in $\log_{10}$ g. Panels with no regression lines indicate species for which no significant trend in size with SST was identified. Shading represents 95% confidence intervals. ELC = *E. carlsbergi* (*n* = 486 fish), ELN = *E. antarctica* (*n* = 2,101), GYF = *G. fraseri* (*n* = 143), GYN = *G. nicholsi* (*n* = 68), GYR = *G. braueri* (*n* = 1448), KRA = *K. anderssoni* (*n* = 944), LAC = *N. achirus* (*n* = 76), PRE = *P. tension* (*n* = 217), PRM = *P. bolini* (*n* = 596), PRY = *P. choriodon* (*n* = 64).

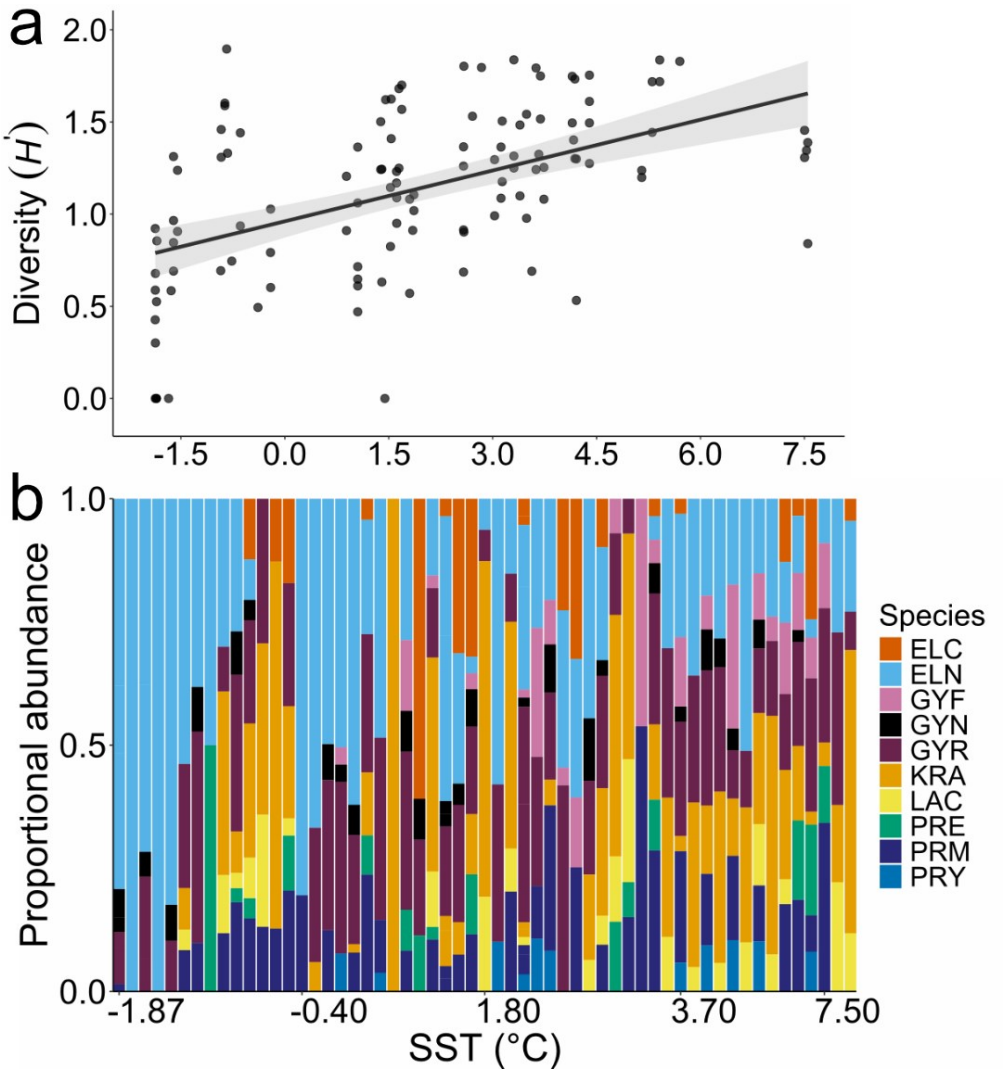

Figure C7: Effects of temperature on myctophid community diversity and the relative abundance of each species. a) Generalised Least Squares regression model predicted values of species diversity (Shannon-Wiener index) versus sea-surface temperature (SST). Shading represents 95% confidence interval. b) stacked bar plot showing the change in proportional sqrt-transformed abundance of each species across SST. Species codes are ELC = *E. carlsbergi* (*n* = 26 individual abundance estimates), ELN = *E. antarctica* (*n* = 101), GYF = *G. fraseri* (*n* = 27), GYN = *G. nicholsi* (*n* = 36), GYR = *G. braueri* (*n* = 91), KRA = *K. anderssoni* (*n* = 64), LAC = *N. achirus* (*n* = 32), PRE = *P. tension* (*n* = 16), PRM = *P. bolini* (*n* = 52), PRY = *P. choriodon* (*n* = 15). A clear shift in species composition can be seen with increasing temperature, from communities dominated by the relatively large-bodied *E. antarctica* at low temperatures to ones with a greater proportion of smaller species like *K. anderssoni* under warmer conditions. Note the discrete x-axis scale for panel b.

C2: Supplementary tables

Table C1: Length-Mass relationships used to estimate body mass of each individual myctophid species. The regressions used to convert standard length (SL, mm) to wet mass (WM, g) follow the equation $WM = a * SL^b$. Lower and upper 95% confidence intervals are provided for each coefficient, along with the overall R^2 for the relationship.

Species	*a*	*Lower*	*Upper*	*b*	Lower	Upper	R^2
E. carlsbergi	2.09×10^{-05}	9.51×10^{-06}	4.59×10^{-05}	2.90	2.72	3.08	0.7214
E. antarctica	3.72×10^{-06}	3.22×10^{-06}	4.30×10^{-06}	3.27	3.24	3.31	0.9599
G. fraseri	3.53×10^{-06}	1.31×10^{-06}	9.51×10^{-06}	3.24	3.00	3.47	0.8811
G. nicholsi	2.87×10^{-06}	2.02×10^{-06}	4.08×10^{-06}	3.25	3.18	3.33	0.9936
G. braueri	4.58×10^{-06}	3.60×10^{-06}	5.82×10^{-06}	3.11	3.06	3.17	0.9326
K. anderssoni	9.05×10^{-06}	7.49×10^{-06}	1.09×10^{-05}	3.02	2.97	3.07	0.9599
N. achirus	8.14×10^{-06}	5.17×10^{-07}	1.28×10^{-02}	2.49	1.45	3.54	0.4259
P. tenisoni	1.39×10^{-05}	9.74×10^{-06}	1.97×10^{-05}	2.94	2.84	3.03	0.9589
P. bolini	1.98×10^{-05}	1.34×10^{-05}	2.92×10^{-05}	2.88	2.77	2.98	0.8926
P. choriodon	1.27×10^{-05}	3.24×10^{-06}	4.94×10^{-05}	2.98	2.66	3.30	0.8779

Table C2: Number of stomachs collected for each myctophid species during each cruise.

Species	JR161	JR177	JR200	TOTAL
Electrona carlsbergi	80	34	27	141
Electrona antarctica	152	178	112	442
Gymnoscopelus fraseri	11	60	27	98
Gymnoscopelus nicholsi	22	11	7	40
Gymnoscopelus braueri	143	94	109	346
Krefftichthys anderssoni	132	44	22	198
Nannobranchium achirus	23	0	0	23
Protomyctophum tenisoni	27	17	0	44
Protomyctophum bolini	106	76	26	208
Protomyctophum choriodon	0	36	0	36
TOTAL	696	550	330	1576

Table C3: Number of individual body mass measurements for each myctophid species during each cruise, from a larger dataset of myctophid sizes (from which only a subset were kept for stomach contents analyses).

Species	JR161	JR177	JR200	TOTAL
E. carlsbergi	195	248	43	486
E. antarctica	568	1023	510	2101
G. fraseri	12	90	41	143
G. nicholsi	30	30	8	68
G. braueri	443	576	429	1448
K. anderssoni	590	162	192	944
N. achirus	43	9	24	76
P. tenisoni	79	98	40	217
P. bolini	261	177	158	596
P. choriodon	0	50	14	64
TOTAL	2221	2463	1459	6143

Table C4: Mean abundances for each broad zooplankton taxon, averaged across sampling sites.

Taxon	Mean density (ind./m^2)	Proportion of total density
Copepoda	13,822.938	0.743
Polychaeta & Chaetognatha	2,645.003	0.142
Pteropoda	1,076.652	0.058
Ostracoda	780.023	0.042
Euphausidae	109.152	0.006
Cnidaria	107.666	0.006
Tunicata	41.255	0.002
Amphipoda	7.266	<0.001
Decapoda	3.692	<0.001
Cephalopoda	0.013	<0.001
Isopoda	0.003	<0.001
Mysidae	0.001	<0.001

Table C5: Identification of the optimal random effects and variance weighting structure for the models involving predator-prey mass ratio (PPMR). The table displays the various random effects and variance weighting structures for the linear mixed effects models describing the relationship between PPMR and the predictors sea-surface temperature (SST) and surface chlorophyl-a concentration (Chl-a), plus their interaction. The most parsimonious model structure based on Akaike's Information Criterion (AIC) is highlighted in grey. NC indicates models with no convergence.

Random effects structure						Variance structure								AIC
~1|Species	~1|Year	~SST|Species	~Chl-a|Species	~SST|Year	~Chl-a|Year	varIdent(~1|Species)	varIdent(~1|Year)	varFixed(~SST)	varFixed(~Chl-a)	varExp(~SST)	varExp(~Chl-a)	varConst(~SST)	varConst(~Chl-a)	
														3174.23
x														2920.04
	x													3167.52
x	x													2862.79
x		x												2923.84
x			x											2921.24
x		x	x											2926.99
	x			x										3156.83
	x				x									3158.10
	x			x	x									3156.01
x	x			x										NC
x	x				x									NC
x	x			x	x									NC
x	x	x												2852.11
x	x		x											2856.31
x	x	x	x											3000.85
x	x		x	x										NC
x	x		x		x									NC
x	x	x		x										NC
x	x	x			x									2856.11
x	x	x												2852.11
x	x	x				x								2746.44
x	x	x					x							2837.77
x	x	x				x	x							2734.96
x	x	x						x						3413.57
x	x	x							x					2823.82
x	x	x								x				2849.13
x	x	x									x			2825.19
x	x	x										x		NC
x	x	x											x	2815.18

Table C6: The results of a Moran's I test on the residuals from each selected linear mixed effects model with sea-surface temperature (SST).

Response	Moran's I	P value
Predator-prey mass ratio	0.003	0.339
Predator mass	-0.002	0.656
Prey mass in the diet	-0.001	0.061

Table C7: Identification of the optimal fixed effects structure for the models involving predator-prey mass ratio (PPMR). The table shows the various fixed effects structures for the linear mixed effects models describing the relationship between PPMR and the predictors sea-surface temperature (SST) and surface chlorophyl-a concentration (Chl-a). Each model includes the optimal random effects and variance weighting structure identified in Table C5. The most parsimonious model structure based on Akaike's Information Criterion (AIC) and retaining only significant fixed effects is highlighted in grey.

Fixed effects structure	AIC
SST*Chl-a	2719.88
SST+Chl-a	2718.18
Chl-a	2726.46
SST	2717.16
Null	2725.11

Table C8: Identification of the optimal random effects and variance weighting structure for the models involving predator body mass. The table shows the random effects and variance weighting structures for the linear mixed effects models describing the relationship between predator mass and the predictors sea-surface temperature (SST) and surface chlorophyl-a concentration (Chl-a), plus their interaction. The most parsimonious model structure based on Akaike's Information Criterion (AIC) is highlighted in grey.

Random effects structure						Variance structure								AIC
~1|Species	~1|Year	~SST|Species	~Chl-a|Species	~SST|Year	~Chl-a|Year	varIdent(~1|Species)	varIdent(~1|Year)	varFixed(~SST)	varFixed(~Chl-a)	varExp(~SST)	varExp(~Chl-a)	varConst(~SST)	varConst(~Chl-a)	
														1714.07
x														807.08
	x													1666.15
x	x													733.51
x		x												759.16
x			x											NC
x		x	x											762.26
	x			x										1662.24
	x				x									1651.06
	x			x	x									1656.18
x	x			x										737.41
x	x				x									737.51
x	x			x	x									743.41
x	x	x												709.89
x	x		x											713.01
x	x	x	x											1498.84
x	x		x	x										NC
x	x		x		x									716.87
x	x	x		x										713.89
x	x	x			x									713.88
x	x	x												709.89
x	x	x				x								167.11
x	x	x					x							650.81
x	x	x				x	x							126.01
x	x	x						x						864.08
x	x	x							x					729.57
x	x	x								x				693.14
x	x	x									x			706.43
x	x	x										x		NC
x	x	x											x	700.55

Table C9: Identification of the optimal fixed effects structure for the models involving predator mass. The table displays the fixed effects structures for the linear mixed effects models describing the relationship between predator mass and the predictors sea-surface temperature (SST) and surface chlorophyl-a concentration (Chl-a). Each model includes the optimal random effects and variance weighting structure identified in Table C8. The most parsimonious model structure based on Akaike's Information Criterion (AIC) and retaining only significant fixed effects is highlighted in grey.

Fixed effects structure	AIC
SST*Chl-a	105.79
SST+Chl-a	103.83
Chl-a	108.06
SST	102.39
Null	106.49

Table C10: Identification of the optimal random effects and variance weighting structure for the models involving dietary prey body mass. The table shows the random effects and variance weighting structures for linear mixed effects models describing the relationship between abundance-weighted prey mass in predator diets and the predictors sea-surface temperature (SST) and surface chlorophyl-a concentration (Chl-a), plus their interaction. The most parsimonious model structure based on Akaike's Information Criterion (AIC) is highlighted in grey. NC indicates models with no convergence.

Random effects structure						Variance structure								AIC
~1|Species	~1|Year	~SST|Species	~Chl-a|Species	~SST|Year	~Chl-a|Year	varIdent(~1|Species)	varIdent(~1|Year)	varFixed(~SST)	varFixed(~Chl-a)	varExp(~SST)	varExp(~Chl-a)	varConst(~SST)	varConst(~Chl-a)	
														3227.59
x														3059.97
	x													3208.49
x	x													2909.48
x		x												3051.49
x			x											NC
x		x	x											NC
	x			x										3181.53
	x				x									3186.04
	x			x	x									NC
x	x			x										NC
x	x				x									NC
x	x			x	x									NC
x	x	x												2888.69
x	x		x											2909.44
x	x	x	x											3055.41
x	x		x	x										NC
x	x		x		x									NC
x	x	x		x										NC
x	x	x			x									NC
x	x	x												2888.69
x	x	x				x								2744.95
x	x	x					x							2868.50
x	x	x				x	x							2732.40
x	x	x						x						3493.64
x	x	x							x					2861.30
x	x	x								x				2869.58
x	x	x									x			2861.37
x	x	x										x		2868.64
x	x	x											x	2851.97

Table C11: Identification of the optimal fixed effects structure for the models involving dietary prey body mass. The table displays the fixed effects structures for the linear mixed effects models describing the relationship between abundance-weighted prey mass in predator diets and the predictors sea-surface temperature (SST) and surface chlorophyl-a concentration (Chl-a). Each model includes the optimal random effects and variance weighting structure identified in Table C10. The most parsimonious model structure based on Akaike's Information Criterion (AIC) and excluding non-significant fixed effects is highlighted in grey.

Fixed effects structure	AIC
SST*Chl-a	2717.49
SST+Chl-a	2715.61
Chl-a	2714.59
SST	2713.76
Null	2712.70

Table C12: Identification of the optimal random effects and variance weighting structure for the models involving predator dietary prey size selectivity. The table shows the random effects and variance weighting structures for linear mixed effects models describing the relationship between predator dietary size preference and the interaction between sea-surface temperature (SST) and predator body mass. The most parsimonious model structure based on Akaike's Information Criterion (AIC) is highlighted in grey. NC indicates models with no convergence.

Random effect structure					Variance structure					AIC
~1|Species	~1|Site	~1|Year	~SST|Species	~SST|Year	varIdent(~1|Species)	varIdent(~1|Year)	varFixed(~SST)	varExp(~SST)	varConst(~SST)	
										288.76
x										263.06
	x									268.13
		x								275.76
x	x									243.02
x		x								238.30
	x	x								266.08
x	x	x								243.80
x			x							264.69
x				x						269.55
	x		x							NC
	x			x						274.13
x	x	x	x							244.75
x	x	x		x						NC
x	x	x	x	x						NC
x		x								238.30
x		x			x					213.95
x		x				x				216.12
x		x			x	x				208.60
x		x					x			226.08
x		x						x		231.49
x		x							x	227.54

Table C13: Identification of the optimal fixed effects structure for the models involving dietary prey size selectivity. The table displays the fixed effects structures for the linear mixed effects models describing the relationship between predator dietary size preference and the interaction between sea-surface temperature (SST) and predator body mass. Each model includes the optimal random effects and variance weighting structure identified in Table C12. The most parsimonious model structure based on Akaike's Information Criterion (AIC) and retaining only significant fixed effects is highlighted in grey.

Fixed effects structure	AIC	Moran's I	P value
SST*predator mass	192.34	-0.025	0.515
SST+predator mass	200.35		
Predator mass	201.51		
SST	232.45		
Null	236.86		

Table C14: Identification of the optimal random effects and variance weighting structure for the models involving predator mass and a larger dataset of myctophid body sizes (n = 6,143). The table shows the random effects and variance weighting structures for linear mixed effects models describing the relationship between predator mass and the predictors sea-surface temperature (SST) and chlorophyll-a concentration (Chl-a), plus their interaction, using the larger dataset of myctophid body sizes. The most parsimonious model structure based on Akaike's Information Criterion (AIC) is highlighted in grey. NC indicates models with no convergence.

Random effects structure						Variance structure								AIC
Year~1	Species~1	Year~ SST	Species~SST	Year~ Chl-a	Species~Chl-a	varIdent(~1|Year)	varIdent(~1|Species)	varFixed(~SST)	varFixed(~Chl-a)	varExp(~SST)	varExp(~Chl-a)	varConst(~SST)	varConst(~Chl-a)	
														7542.835
x														7286.548
	x													4474.619
x	x													4396.677
x		x												7178.632
x				x										7203.550
x		x		x										NC
	x		x											4307.066
	x				x									NC
	x		x		x									4308.701
x	x	x												4349.700
x	x			x										7178.632
x	x	x		x										NC
x	x		x											4245.069
x	x				x									4282.719
x	x		x		x									6738.586
x	x	x	x											4249.069
x	x	x			x									4283.036
x	x		x	x										4183.526
x	x			x	x									NC
x	x		x	x										4183.526
						x								4157.655
							x							2161.584
						x	x							2158.628
								x						5708.168
									x					NC
										x				4129.790

		x		4184.524
			x	4106.948
			x	4186.680

Table C15: Identification of the optimal fixed effects structure for the models involving predator mass and a larger dataset of myctophid body sizes (n = 6,143). The table displays the fixed effects structures for the linear mixed effects model describing the relationship between predator size and the predictors sea-surface temperature (SST) and surface chlorophyll-a concentration (Chl-a), plus their interaction, using the larger dataset of myctophid body sizes. Each model includes the optimal random effects and variance weighting structure identified in Table C14. The most parsimonious model structure based on Akaike's Information Criterion (AIC) and retaining only significant fixed effects is highlighted in grey. The result of a Moran's I test for spatial autocorrelation for the optimal model is also provided.

Fixed effects structure	AIC	Moran's I	P-value
SST*Chl-a	2330.480		
SST+Chl-a	2328.769		
Chl-a	2426.262		
SST	2326.877	0.001	0.161
Null	2424.297		

Table C16: Model statistics for the optimal linear mixed effects model identified in Tables C14-C15 describing the relationship between sea-surface temperature (SST) and predator body mass using a larger dataset of myctophid body sizes (n = 6,143).

Coefficient	Estimate	SE	DF	t-value	p-value
Intercept	0.456	0.072	6113	6.351	<0.0001
SST	-0.026	0.002	6113	-10.397	<0.0001

Table C17: Identification of the optimal random effects and variance weighting structure for the models involving predator mass for each myctophid species. The table shows the random effects and variance weighting structures for linear mixed effects models describing the relationship between predator mass and sea-surface temperature (SST) for each species, using a larger dataset of myctophid body sizes (n = 6,143). The most parsimonious model based on Akaike's Information Criterion (AIC) is highlighted in grey. NC indicates models with no convergence.

Species	Random effect structure		Variance structure				AIC
	Year~1	Year~ sst	varident(~1|Year)	varfixed(~SST)	varexp(~SST)	varConst(~SST)	
E. carlsbergi							- 1288.456
	x						- 1287.623
	x	x					NC
			x				- 1318.993
				x			-1096.769
					x		-1309.503
						x	-1308.141
E. antarctica							1620.508
	x						1615.725
	x	x					1619.725
	x		x				1617.816
	x			x			2093.591
	x				x		1590.430
	x					x	1557.973
G. fraseri							51.531
	x						44.042
	x	x					NC
	x		x				42.658
	x			x			50.821
	x				x		45.530
	x					x	45.833
G. nicholsi							119.246
	x						120.740
	x	x					NC
			x				118.141
				x			94.101
					x		67.816
						x	90.010
G. braueri							1457.564

	x						1405.256
	x	x					1407.795
	x		x				1396.838
	x			x			1670.105
	x				x		1365.444
	x					x	1370.079
							942.875
	x						944.619
	x	x					NC
K. anderssoni			x				840.444
				x			915.442
					x		866.609
						x	880.390
							-47.476
	x						-45.476
	x	x					-41.476
N. achirus			x				-47.247
				x			-2.504
					x		-57.541
						x	-55.363
							-136.615
	x						-428.244
	x	x					NC
P. tenisoni			x				-443.422
				x			-427.005
					x		-443.606
						x	-459.302
							-44.103
	x						-55.174
	x	x					NC
P. bolini	x		x				-63.431
	x			x			-21.393
	x				x		-64.357
	x					x	-70.513
							-77.654
	x						-75.654
	x	x					NC
P. choriodon			x				-75.660
				x			-81.037
					x		-79.060
						x	NC

5123

5124

Table C18: Identification of the optimal fixed effects structure for the models involving predator mass for each myctophid species. The table shows the fixed effects structures for the linear mixed effects models of the relationship between predator size and sea-surface temperature (SST) for each species, using a larger dataset of myctophid body sizes (n = 6,143). Each model includes the optimal random effects and variance weighting structure identified in Table C17. The results of a Moran's I test for spatial autocorrelation are provided for the optimal models, along with the optimal correlation structure implemented based on AIC for any models with significant autocorrelation. No adjustments were made for multiple comparisons.

Species	Fixed effects structure	AIC	Moran's I	Moran's I p-value	Autocorrelation structure
E. carlsbergi	SST	-1340.507			
	Null	-1342.335	<0.001	0.7174	
E. antarctica	SST	1542.642	0.026	<0.0001	Rational
	Null	1569.967			
G. fraseri	SST	34.019	0.060	0.0038	Exponential
	Null	68.081			
G. nicholsi	SST	55.946	0.004	0.6894	
	Null	71.849			
G. braueri	SST	1356.068	0.009	0.0175	Exponential
	Null	1366.125			
K. anderssoni	SST	824.964	-0.010	0.0342	Spherical
	Null	1001.208			
N. achirus	SST	-72.145			
	Null	-73.502	-0.104	0.0914	
P. tenisoni	SST	-469.989	-0.004	0.9498	
	Null	-442.164			
P. bolini	SST	-83.925	-0.013	0.0937	
	Null	-76.457			
P. choriodon	SST	-93.411	-0.021	0.9246	
	Null	-78.834			

Table C19: Outputs of the optimal linear mixed effects models identified in Tables C17-C18, describing the relationship between predator mass and sea-surface temperature (SST) for each species, using a larger dataset of myctophid body sizes (n = 6,143).

Species	*Coefficient*	*Estimate*	*SE*	*DF*	*t-value*	*p-value*
E. carlsbergi	Intercept	0.790	0.003	486	298.685	<0.0001
E. antarctica	Intercept	0.579	0.021	2097	27.425	<0.0001
	SST	-0.022	0.009	2097	-2.479	0.0148
G. fraseri	Intercept	0.887	0.121	139	7.353	<0.0001
	SST	-0.100	0.028	139	-3.536	0.0011
G. nicholsi	Intercept	1.390	0.030	68	45.721	<0.0001
	SST	-0.083	0.019	68	-4.478	<0.0001
G. braueri	Intercept	0.754	0.079	1444	9.578	<0.0001
	SST	-0.083	0.007	1444	-11.213	<0.0001
K. anderssoni	Intercept	0.154	0.019	944	8.287	<0.0001
	SST	-0.085	0.006	944	-14.086	<0.0001
N. achirus	Intercept	0.153	0.015	76	9.965	<0.0001
P. tenisoni	Intercept	-0.294	0.153	213	-1.925	0.0555
	SST	0.030	0.005	213	6.484	<0.0001
P. bolini	Intercept	0.069	0.038	592	1.835	0.0670
	SST	-0.017	0.005	592	-3.406	0.0007
P. choriodon	Intercept	0.800	0.035	64	22.598	<0.0001
	SST	-0.050	0.009	64	-5.464	<0.0001

Table C20: Identification of the optimal random effects and variance weighting structure for the models involving myctophid species diversity. The table shows the random effects and variance weighting structures for the linear mixed effects models describing the relationship between myctophid species diversity (Shannon-Wiener index) and the interaction between sea-surface temperature (SST) and surface chlorophyll-a concentration (Chl-a). The most parsimonious model structure based on Akaike's Information Criterion (AIC) is highlighted in grey. NC indicates models with no convergence.

Random effects structure			Variance structure							AIC
Year~1	Year~ SST	Year~ Chl-a	varIdent(~1|Year	varFixed(~SST)	varFixed(~Chl-a)	varExp(~SST)	varExp(~Chl-a)	varConst(~SST)	varConst(~Chl-a)	
										134.843
x										136.498
x	x									137.938
x		x								139.111
x	x	x								NC
			x							131.819
				x						169.6902
					x					155.0526
						x				132.8421
							x			132.0601
								x		137.1728
									x	129.3736

Table C21: Identification of the optimal fixed effects structure for the models involving myctophid species diversity. The table displays the fixed effects structures for the linear mixed effects models of the relationship between Shannon-Wiener diversity and the interaction between sea-surface temperature (SST) and surface chlorophyll-a concentration (Chl-a). Each model includes the optimal random effects and variance weighting structure identified in Table C20. The most parsimonious model structure based on Akaike's Information Criterion (AIC) and retaining only significant fixed effects is highlighted in grey. The results of a Moran's I test for spatial autocorrelation is provided for the optimal model.

Fixed effects structure	AIC	Moran's I	P-value
SST*Chl-a	114.7948		
SST+Chl-a	115.1217		
Chl-a	148.1829		
SST	114.1337	0.071	0.103
Null	146.3198		

Table C22: Model statistics for the optimal linear mixed effects model identified in Tables C20-C21 describing the relationship between myctophid species diversity and sea-surface temperature (SST).

Coefficient	Estimate	SE	DF	t-value	p-value
Intercept	0.962	0.045	115	21.545	<0.0001
SST	0.090	0.015	115	6.080	<0.0001

Table C23: Identification of the optimal random effects and variance weighting structure for the models involving predator-prey mass ratio (PPMR) and temperature at 1,062 m depth. The table shows the random effects and variance weighting structures for the linear mixed effects models describing the relationship between PPMR and the predictors temperature at 1,062m depth (TAD) and surface chlorophyl-a concentration (Chl-a), plus their interaction. The most parsimonious model structure based on Akaike's Information Criterion (AIC) is highlighted in grey. NC indicates models with no convergence.

Random effects structure						Variance structure								AIC
Species~1	Year~1	Species~TAD	Species~Chl-a	Year~ TAD	Year~Chl-a	varIdent(~1|Species)	varIdent(~1|Year)	varFixed(~TAD)	varFixed(~Chl-a)	varExp(~TAD)	varExp(~Chl-a)	varConst(~TAD)	varConst(~Chl-a)	
														3178.22
x														2942.28
	x													3173.63
x	x													2883.36
x		x												2945.36
x			x											2943.27
x		x	x											2945.37
	x			x										3161.19
	x				x									3161.62
	x			x	x									3153.99
x	x			x										NC
x	x				x									NC
x	x			x	x									NC
x	x	x												2865.27
x	x		x											2877.08
x	x	x	x											2994.12
x	x		x	x										NC
x	x		x		x									NC
x	x	x		x										NC
x	x	x			x									NC
x	x	x												2865.27
x	x	x				x								2762.27
x	x	x					x							2852.23
x	x	x				x	x							2751.60
x	x	x						x						6959.02
x	x	x							x					2836.48
x	x	x								x				2811.59
x	x	x									x			2839.16
x	x	x										x		2833.85
x	x	x											x	2828.41

Table C24: Identification of the optimal fixed effects structure for the models involving predator-prey mass ratio (PPMR) and temperature at 1,062 m depth. The table displays the fixed effects structures for the linear mixed effects models describing the relationship between PPMR and the predictors temperature at 1,062m depth (TAD) and surface chlorophyl-a concentration (Chl-a). Each model includes the optimal random effects and variance weighting structure identified in Table C23. The most parsimonious model structure based on Akaike's Information Criterion (AIC) and retaining only significant fixed effects is highlighted in grey.

Fixed effects structure	AIC
TAD*Chl-a	2740.15
TAD+Chl-a	2738.21
Chl-a	2740.84
TAD	2739.64
Null	2741.57

Table C25: Identification of the optimal random effects and variance weighting structure for the models involving predator body mass and temperature at 1,062 m depth. The table shows the random effects and variance weighting structures for the linear mixed effects models describing the relationship between predator mass and the predictors temperature at 1,062m depth (TAD) and surface chlorophyl-a concentration (Chl-a), plus their interaction. The most parsimonious model structure based on Akaike's Information Criterion (AIC) is highlighted in grey. NC indicates models with no convergence.

Random effects structure						Variance structure								AIC
Species~1	Year~1	Species~TAD	Species~Chl-a	Year~ TAD	Year~Chl-a	varIdent(~1|Species)	varIdent(~1|Year)	varFixed(~TAD)	varFixed(~Chl-a)	varExp(~TAD)	varExp(~Chl-a)	varConst(~TAD)	varConst(~Chl-a)	
														1671.26
x														822.32
	x													1671.09
x	x													734.48
x		x												780.53
x			x											NC
x		x	x											780.29
	x			x										NC
	x				x									1659.41
	x			x	x									NC
x	x			x										NC
x	x				x									NC
x	x			x	x									NC
x	x	x												691.51
x	x		x											712.97
x	x	x	x											NC
x	x		x	x										NC
x	x		x		x									NC
x	x	x		x										NC
x	x	x			x									NC
x	x	x				x								691.51
x	x	x				x								155.92
x	x	x					x							636.45
x	x	x				x	x							113.34
x	x	x						x						3278.38
x	x	x							x					703.20
x	x	x								x				677.66
x	x	x									x			686.63
x	x	x										x		679.64
x	x	x											x	661.70

Table C26: Identification of the optimal fixed effects structure for the models involving predator mass and temperature at 1,062 m depth. The table displays the fixed effects structures for the linear mixed effects models describing the relationship between predator mass and the predictors temperature at 1,062m depth (TAD) and surface chlorophyl-a concentration (Chl-a). Each model includes the optimal random effects and variance weighting structure identified in Table C25. The most parsimonious model structure based on Akaike's Information Criterion (AIC) and retaining only significant fixed effects is highlighted in grey.

Fixed effects structure	AIC
TAD*Chl-a	96.84
TAD+Chl-a	95.57
Chl-a	100.62
TAD	95.07
Null	99.88

Table C27: Identification of the optimal random effects and variance weighting structure for the models involving dietary prey body mass and temperature at 1,062 m depth. The table shows the random effects and variance weighting structures for linear mixed effects models describing the relationship between abundance-weighted prey mass in predator diets and the predictors temperature at 1,062m depth (TAD) and surface chlorophyl-a concentration (Chl-a), plus their interaction. The most parsimonious model structure based on Akaike's Information Criterion (AIC) is highlighted in grey. NC indicates models with no convergence.

Random effects structure						Variance structure								AIC
Species~1	Year~1	Species~TAD	Species~Chl-a	Year~ TAD	Year~Chl-a	varIdent(~1|Species)	varIdent(~1|Year)	varFixed(~TAD)	varFixed(~Chl-a)	varExp(~TAD)	varExp(~Chl-a)	varConst(~TAD)	varConst(~Chl-a)	
														3199.70
x														3057.92
	x													3187.10
x	x													2912.83
x		x												3053.89
x			x											NC
x		x	x											NC
	x			x										3149.94
	x				x									3162.89
	x			x	x									3146.42
x	x			x										NC
x	x				x									NC
x	x			x	x									NC
x	x	x												2881.77
x	x		x											2913.04
x	x	x	x											NC
x	x		x	x										NC
x	x		x		x									NC
x	x	x		x										NC
x	x	x			x									2885.77
x	x	x												2881.77
x	x	x				x								2741.32
x	x	x					x							2861.62
x	x	x				x	x							2728.55
x	x	x						x						7247.49
x	x	x							x					2855.30
x	x	x								x				2782.81
x	x	x									x			2855.72
x	x	x										x		2818.68
x	x	x											x	2845.75

Table C28: Identification of the optimal fixed effects structure for the models involving dietary prey mass and temperature at 1,062 m depth. The table shows the fixed effects structures for the linear mixed effects models describing the relationship between abundance-weighted prey mass in predator diets and the predictors temperature at 1,062m depth (TAD) and surface chlorophyl-a concentration (Chl-a). Each model includes the optimal random effects and variance weighting structure identified in Table C27. The most parsimonious model structure based on Akaike's Information Criterion (AIC) and excluding non-significant fixed effects is highlighted in grey.

Fixed effects structure	AIC
TAD*Chl-a	2717.22
TAD +Chl-a	2715.43
Chl-a	2713.89
TAD	2713.79
Null	2712.36

Table C29: Model statistics for the effects of temperature at 1,062 m depth on predator and prey body masses. Output from linear mixed effects models with predator-prey mass ratio (PPMR), predator body mass and abundance-weighted average prey body mass in predator stomachs as response variables. The temperature variable represents temperature at ~1,062m depth (TAD), while R^2m and R^2c are the Nakagawa's marginal and conditional model R^2 values, respectively.

Model	Coefficient	Estimate	SE	DF	t-value	p-value
PPMR	Intercept	3.017	0.109	1550	27.717	<0.0001
	TAD	-0.131	0.050	1550	-2.596	0.0095
R^2m = 0.025, R^2c = 0.489						
Predator body mass	Intercept	0.566	0.108	1550	5.257	<0.0001
	TAD	-0.071	0.036	1550	-1.984	0.0475
R^2m = 0.012, R^2c = 0.980						
Mean prey body mass	Intercept	-2.357	0.072	1551	-32.600	<0.0001
R^2m < 0.001, R^2c = 0.476						

Table C30: The results of a Moran's I test on the residuals from each selected linear mixed effects model with the temperature at 1,062m depth as the predictor variable.

Response	Moran's I	p value
Predator-prey mass ratio	0.003	0.359
Predator mass	0.001	0.693
Prey mass in diet	0.003	0.312

Appendix D: Supplementary material for chapter 5

D1: Supplementary methods

6.2.5 Re-aggregation of functional groups

Groups were reaggregated using information on biomass and rate parameters available in the supplementary materials for each model. When aggregating groups, the new group biomass was determined by a simple sum of the biomasses of the groups being combined. The final aggregated rate parameters (P/B and Q/B) were averages of the original group-specific parameters, calculated using the group biomasses as weightings. In cases where groups were split to form multiple new groups, the appropriate biomass was assigned to each new group using biomass information in the relevant supplementary material for the published model or wider literature for that region. Unique rate parameters were assigned to the new groups where available in the published supporting information, otherwise the new groups retained the rate estimates from their parent group. Below, we provide an overview of the steps taken to reaggregate each functional group in each regional model.

Whales:

In each model, we reaggregated whale groups to form four functional groups: Toothed whales, humpback whales, minke whales and "other baleen whales".

In the Prydz Bay model, minke whales were already separated and the humpback whale group was extracted from the "baleen whale" group and parameterized using species-level biomass and Q/B information from the supplementary, while retaining the P/B value specified for the original "baleen whale" group. Orca and sperm whales were aggregated into a single toothed whale group.

The Ross Sea model had very similar whale groups to the Prydz Bay model with an additional "toothed whales" group representing two beaked whale species. The same reaggregation steps were taken as for the Prydz Bay model, while "toothed whales", sperm whales and orcas were combined into a single new "toothed whales" group. In this model, P/B and Q/B estimates were available for each species and were used in the reaggregation.

The Prince Edward Islands model represented only orca with no other whale species included, due to their extremely low abundance in the model region. To ensure comparability

with other models, we added minke whale, humpback whale and 'other baleen whale' groups but kept their initial biomasses at zero.

The Kerguelen Plateau model included a toothed whale group (representing southern bottlenose whales and hourglass dolphins), orcas, sperm whales and a baleen whale group representing fin and southern right whales. The only change made to this model was to add the humpback and minke whale groups, again with a negligible biomass to reflect their extremely low current abundance in the model region, and to combine the orcas, sperm whales and 'toothed whales' into a single group.

The South Georgia model included two whale groups: toothed and baleen. Humpback and minke whale groups were extracted from the baleen whale group using biomass and Q/B estimates for each species available in the supplementary, while they retained the P/B estimate from the baleen whale group.

The Antarctic Peninsula model represented each whale species as a separate group. Orca and sperm whales were aggregated into the toothed whale group while baleen whales excluding humpbacks and minkes were aggregated into the "Other baleen whales" group.

Seals and penguins:

In most models, seals and penguins were represented as individual species. These were aggregated into a single seal or penguin group in each model. The exception was the Kerguelen Plateau model, which already aggregated penguins into a single group and therefore required no changes.

Flying birds:

Flying birds were represented to a varying degree of taxonomic resolution across models, ranging from a single functional group to multiple groups representing different feeding guilds, taxonomic distinctions (e.g. albatrosses versus other birds) or even individual species. Models which included multiple flying bird groups were reaggregated to have a single "Flying birds" group.

Fish:

All models included multiple fish groups specified to varying levels of taxonomic resolution. In each model, the groups were combined based on their habitat association to generate two broad functional groups representing demersal and pelagic fish.

Squid:

Squid are known to be poorly represented in most Southern Ocean ecosystem models, due to a lack of information regarding their regional biomass and ecology (REFS). All models included a squid group, with the Prince Edward Islands model distinguishing this group by size. In this latter model the two size classes were aggregated into a single squid group, while no changes were required for the other models.

Zooplankton:

We sought to distinguish between Antarctic krill and all other krill. The Prydz Bay, Ross Sea and Antarctic Peninsula models already provided separate Antarctic krill and other euphausiid groups, though the species represented by the latter differed between models. The Kerguelen Plateau model included a single krill group representing euphausiids other than *Euphausia superba*, as this group is not found in any meaningful numbers in the model region (Yang et al. 2022; Yang et al. 2020). The Prince Edward Islands model did not explicitly model any krill group but according to Hill et al. (2021) the model authors identified that euphausiids make up 88% of the "large crustacean zooplankton" and 20% of the "small crustacean zooplankton" groups. As with the Kerguelen Plateau model, *E. superba* are not present in the model region (Yang et al. 2022; Yang et al. 2020), therefore we redistributed the biomass of the relevant zooplankton groups to produce a single "other krill" group using the above proportions. The South Georgia model included an Antarctic krill group but included other euphausiids in the "Carnivorous macrozooplankton". We estimated the average relative biomass of other euphausiid species in the macrozooplankton from zooplankton samples taken near South Georgia in 2006, 2008 and 2009 during the Discovery cruises (Tarling et al. 2012a). The average proportion of macrozooplankton that was euphausiids was 6.9%, and we extracted the relevant biomass from the "Carnivorous macrozooplankton" group in the South Georgia model and assigned it to a new "Other krill" group.

Three models explicitly included salps and therefore required no further reaggregation to represent this group. In the Prince Edward Islands model, salps represent 5% of the "other zooplankton" group, while in the Ross Sea, salps are estimated to make up 2.6% of macrozooplankton biomass (Hill et al. 2021). The proportion of salps in the zooplankton groups in the Kerguelen Plateau model was not clear, but the source used by the authors to estimate macrozooplankton biomass identifies that salps display extremely patchy distributions in the region, representing between 0.1% and 7% of total macrozooplankton

biomass (Hunt et al. 2011). In the absence of better estimates, we assumed that 7% of macrozooplankton biomass was salps. Salp relative abundance is unlikely to be equivalent to relative biomass as salps are heavier than many other macrozooplankton taxa, but given their patchy distribution we determined that setting their relative biomass to be the maximum estimate of their relative abundance would reasonably capture their approximate biomass in the study region, though with high associated uncertainty. In each of these models, we extracted the relevant biomass from the original groups and assigned these to a new salp group.

We grouped all remaining zooplankton into three size-based functional groups: macrozooplankton, mesozooplankton and microzooplankton. Three models already had this aggregation scheme, and the only adjustments needed were to subtract the estimated salp biomass from the Kerguelen Plateau model. The Ross Sea model included macro- and mesozooplankton groups, but further distinguished flagellates and ice metazoa and protozoa. We merged the mesozooplankton and ice metazoan groups into an aggregate mesozooplankton group, and combined the flagellates and ice protozoa with the heterotrophic microplankton to form a single microzooplankton group. We spit the zooplankton groups in the Prince Edward Islands model following (Hill et al. 2021): macrozooplankton are 12% large crustacean zooplankton, 20% small crustacean zooplankton, 48% other zooplankton; mesozooplankton are 49% small crustacean zooplankton, 43% other zooplankton; microzooplankton are 11% small crustacean zooplankton, 4% other zooplankton. The South Georgia model already incorporated macrozooplankton (carnivorous macrozooplankton minus the biomass representing other krill) and microzooplankton (heterotrophic microzooplankton), and we aggregated the two remaining zooplankton groups ("herbivorous mesozooplankton" and "herbivorous and detritivorous copepods") into a single mesozooplankton group.

Benthos:

All models included at least one benthic functional group. In models that include more than one such group (Ross Sea – megabenthos, macrobenthos and meiobenthos; Prince Edward Islands – benthos and benthic decapods) these were combined into a single benthos group.

Bacteria:

Three models (PB, SG, KP) explicitly modelled bacteria as a single functional group. Another (RS) further split bacteria into ice, water-column and sediment-associated bacterial

groups, which we aggregated into a single group. We did not add bacterial groups to the two remaining models (AP and PE).

Primary producers:

We continued to distinguish between the sea ice algae and other producers in the RS and AP models. All other producer groups were aggregated into a single primary producer group.

Detritus:

All detrital and carcass groups were aggregated into a single detritus group in each model.

6.2.6 Automated balancing routine:

The primary input parameters for the automated balancing algorithm were *B*, *P/B* and *Q/B* and *DC.* Additionally, the assimilation efficiencies of each group were obtained from (Pinkerton and Bradford-Grieve 2010) and held constant across model regions and throughout the balancing process. The balancing algorithm first determines the relative change to each group's *B* by a random draw from a normal distribution with mean = 0 and SD = 0.05. Changes to *B* are therefore small and within a local region around the values at the current step. The final biomass values of each group must remain within the bounds of their pedigree, which was set using the standard Ecopath data pedigree approach (see Table S4). This information was already provided for some of the models (RS, PE, SG), while for the remaining models we assigned pedigrees based on a review of the supplementary information accompanying each published model. The exception to this is the primary producers, for which we set the *EE* values to 0.5 and therefore *B* is calculated based on consumer demand.

Next, a growth efficiency (*GE*) value is drawn from a uniform distribution between a minimum and maximum value determined by group type, based on values in Townsend et al. (2008): endotherm vertebrate (0.001 – 0.05); ectotherm vertebrate (0.05 – 0.2); invertebrate (0.1 – 0.4); bacteria (0.2 – 0.5). This step is included to ensure that energetic parameters comply with general expected ecological relationships. By randomly varying this parameter, rather than fixing it at some predetermined value, we provide further exploration of the range of possible model parameterisations. *P/B* and *Q/B* values are varied within a range of 50% on either side of the model-averaged input values. Because *GE* is determined by the combination of *P/B* and *Q/B* it is only possible to set one of these energetic parameters directly, with the other estimated from the combination with *GE*. To avoid potential bias by only varying one

of these parameters throughout, our algorithm randomly determines, for each group, which of these energetic parameters is randomly sampled at that step. The relevant *P/B* or *Q/B* values are then sampled randomly from a uniform distribution within their specified bounds and used in combination with *GE* to estimate the missing parameters. The exception to this was whale *Q/B*, which was fixed at the lower values calculated from prior estimates of whale consumption to ensure consistency in starting whale consumption across model versions and regions for later analyses.

Random adjustments to the diet composition of each group are then also made. These are achieved by resampling their input balanced diets from a Dirilichet distribution, which ensures that the resulting diet compositions sum to one. A further constraint on the diet resampling is the inclusion of a scaling parameter which restricts the changes to each dietary component, such that diets do not become completely scrambled (i.e. common prey remain common and rare prey remain rare). We found a scaling factor of 50 to provide a good balance between allowing sufficient variation to explore a broad range of plausible prey compositions and preventing excessive reshuffling of diets. For example, for a prey representing 50% of a consumer's diet, a scaling factor of 50 generates values which generally lie within 20% of the original input, with minimum and maximum tails of around 40%. Higher values of the scaling factor increasingly restrict the possible dietary changes (Figure D14).

Once the algorithm has generated a new set of suitable parameter values, the model is evaluated by calculating an objective function, set as the sum of *EE* for all out of balance at that step. This model is accepted if the objective function is lower than that of the previous step. In this case, the biomass values are carried over and used as the basis for determining biomasses at the next step (all other parameters are varied from scratch at each step and therefore do not need to be updated). If the objective function for the new parameter set is higher than that of the previous set, the changes are rejected and the biomass values reset to those of the previous step. To prevent the algorithm from becoming stuck in local optima, steps with higher (worse) objective functions are accepted with a specific probability (P), which is kept constant throughout. The algorithm runs for a specified number of steps (or until a balanced model is found), and a record of the best model (lowest objective function) is kept and updated at each step.

If no balanced model is identified after the specified number of steps, the algorithm switches to targeted, primarily small, adjustments to biomasses and diets to achieve balance. The biomass of the group most out of balance is increased by a small amount and the biomass of the maximal predator of that group is reduced slightly. The diet matrix of the maximal predator is adjusted to slightly reduce the contribution of the focal prey group, with the missing diet contribution randomly redistributed across other prey groups (excluding cannibalistic interactions). The biomass values for the final balanced model are then checked, and the model is rejected if any biomass values fall outside the acceptable bounds set by the pedigree CV. The full balancing process was repeated until a suite of 1000 versions of each regional input model had been generated.

D2: Supplementary figures

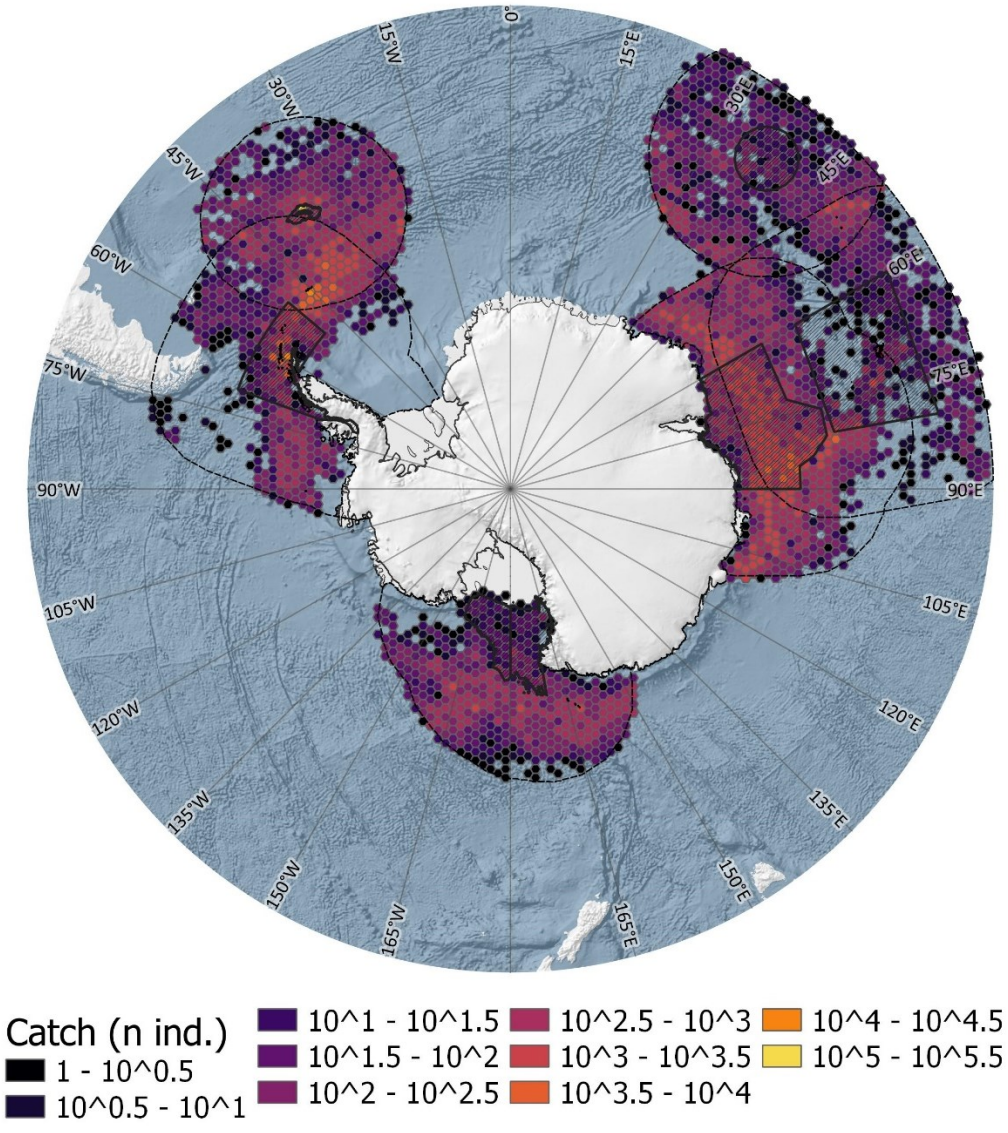

Figure D1: Map of all baleen whale catches (number of individuals) within each of the model regions (solid polygons) and their 1000km buffers (dashed lines). Catches are on a log scale. Hex tiles are 100km^2.

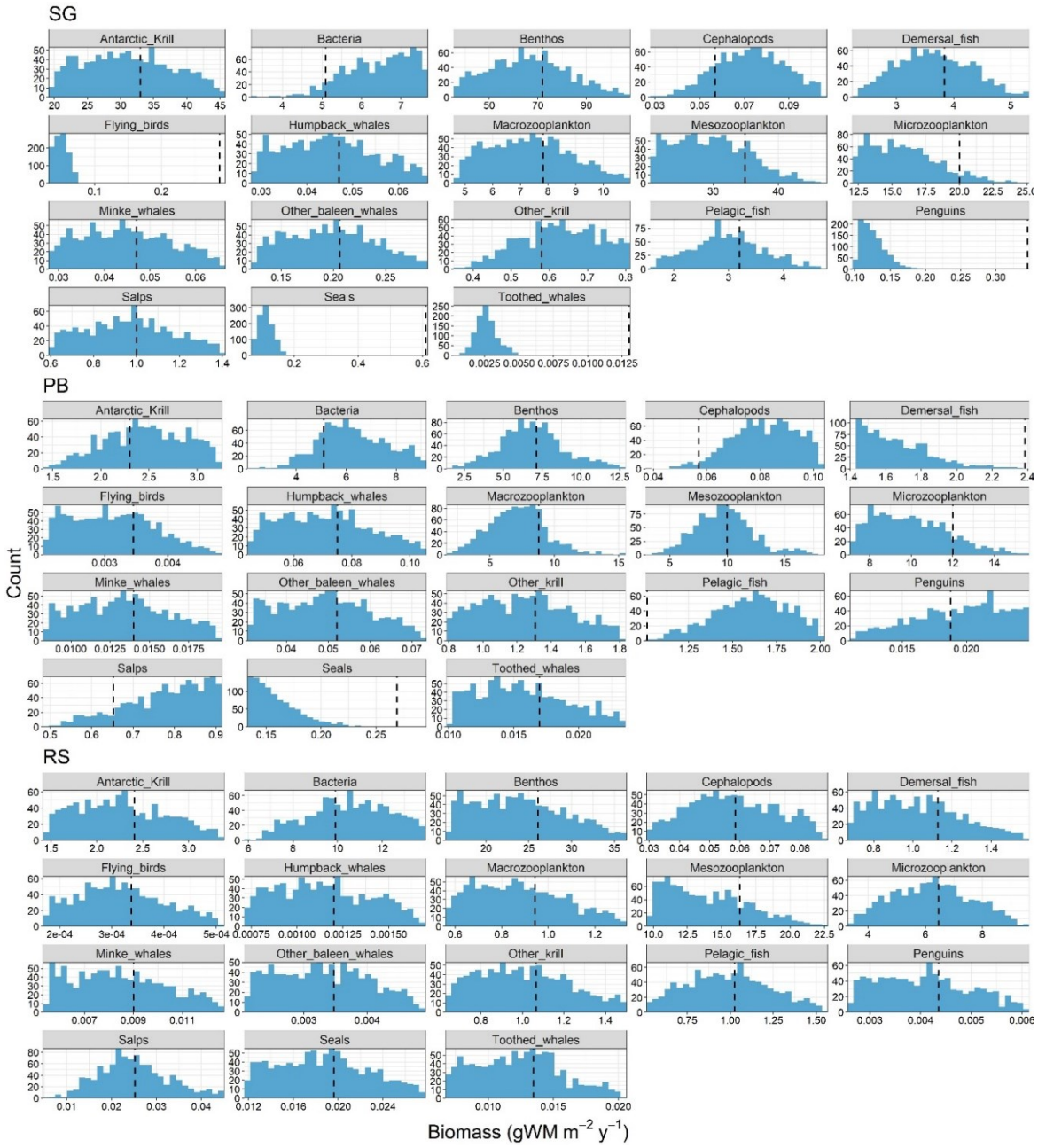

Figure D2: Distribution of biomasses in the balanced versions of each model (n=1000), for PB, RS and SG. Vertical dashed lines display the original value for each parameter in the standardised, reaggregated but unbalanced version of each model.

Figure D3: Distribution of biomasses in the balanced versions of each model (n=1000), for KP, PE and AP. Vertical dashed lines display the original value for each parameter in the standardised, reaggregated but unbalanced version of each model.

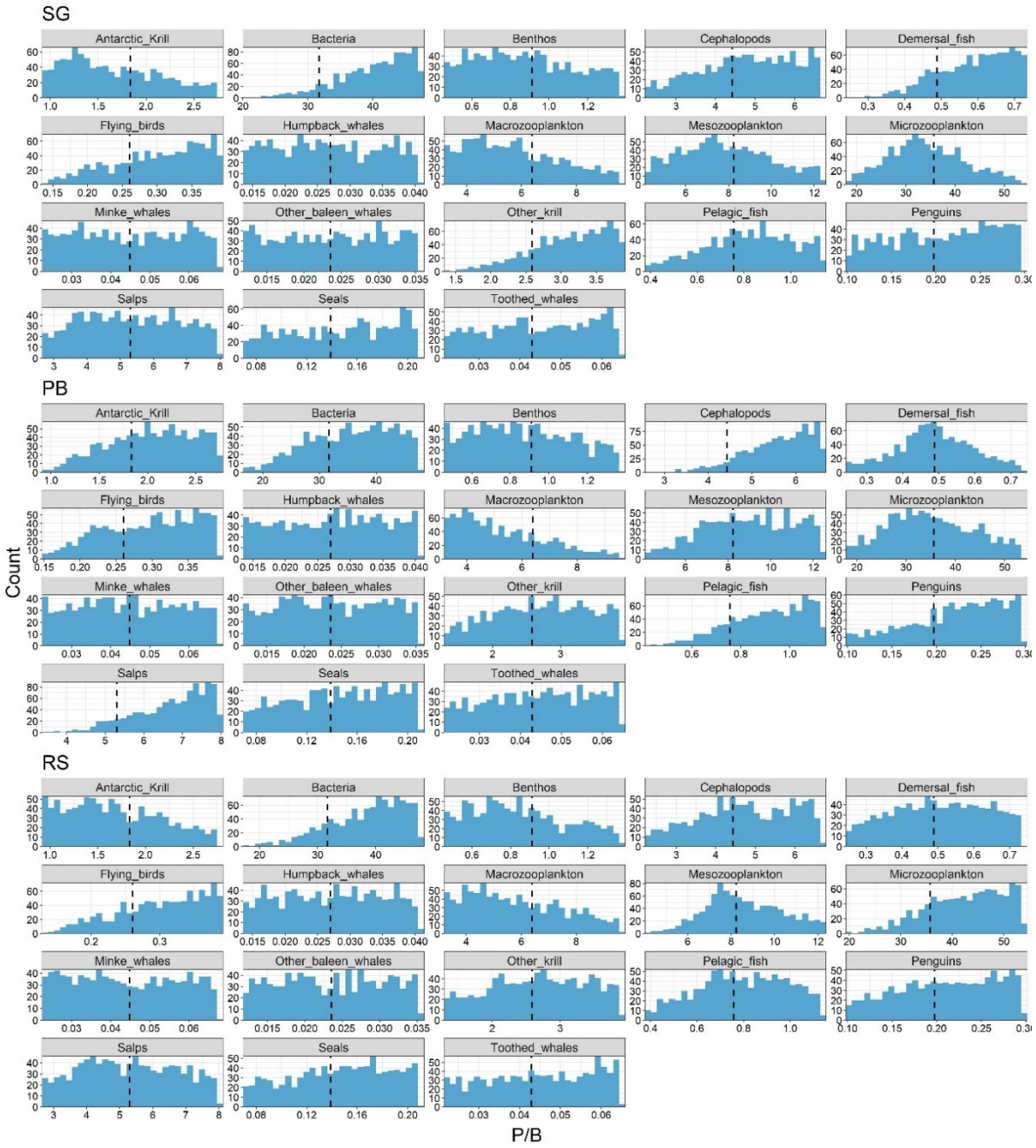

Figure D4: Distribution of production over biomass (*P/B*) in the balanced versions of each model (*n*=1000), for SG, PB and RS. Vertical dashed lines display the original value for each parameter in the standardised, reaggregated but unbalanced version of each model.

5487

5488 Figure D5: Distribution of production over biomass (*P/B*) in the balanced versions of each

5489 model (*n*=1000), for KP, PE and AP. Vertical dashed lines display the original value for each

5490 parameter in the standardised, reaggregated but unbalanced version of each model.

5491

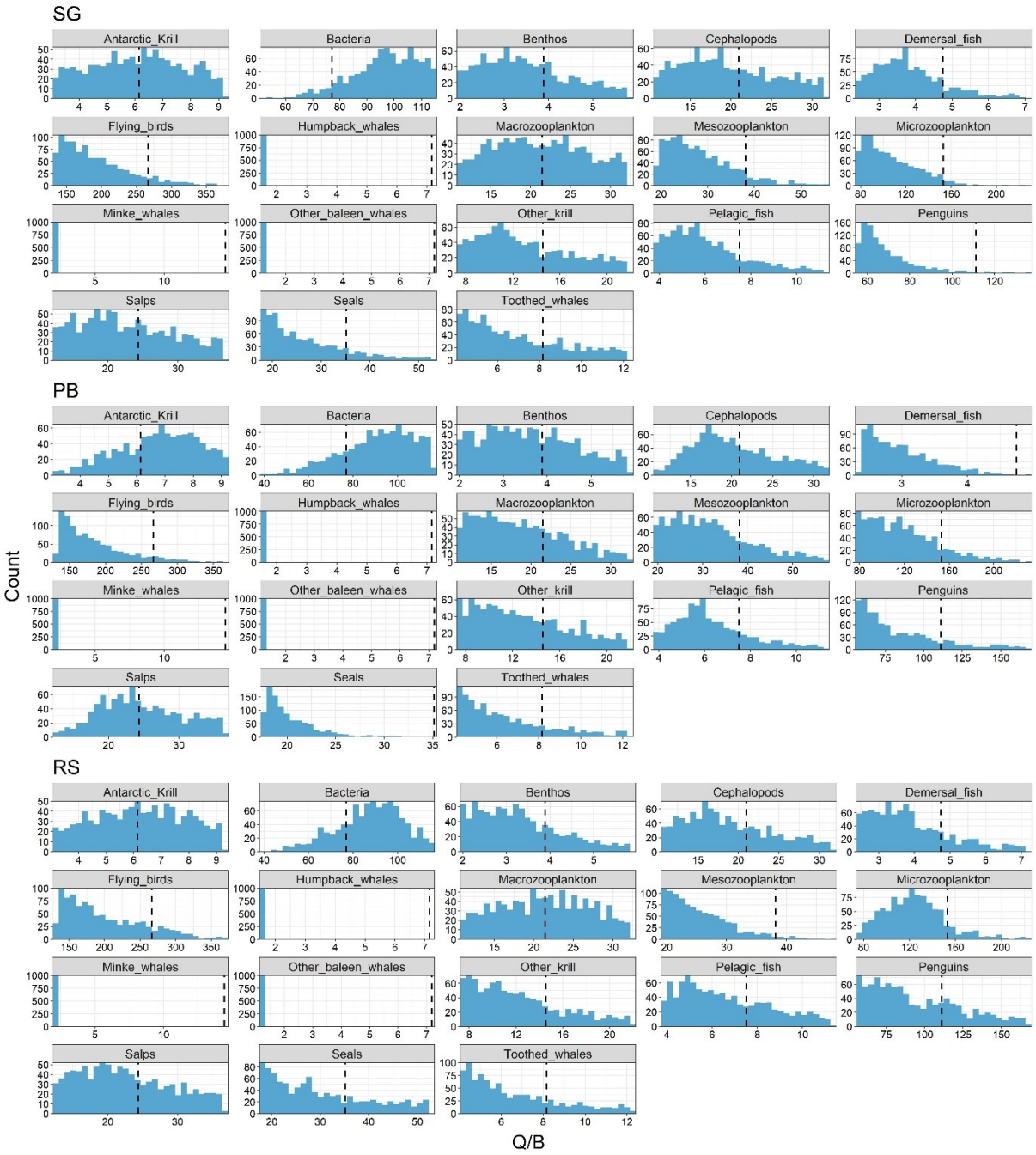

Figure D6: Distribution of consumption over biomass (*Q/B*) in the balanced versions of each model (*n*=1000), for SG, PB, RS. Vertical dashed lines display the original value for each parameter in the standardised, reaggregated but unbalanced version of each model.

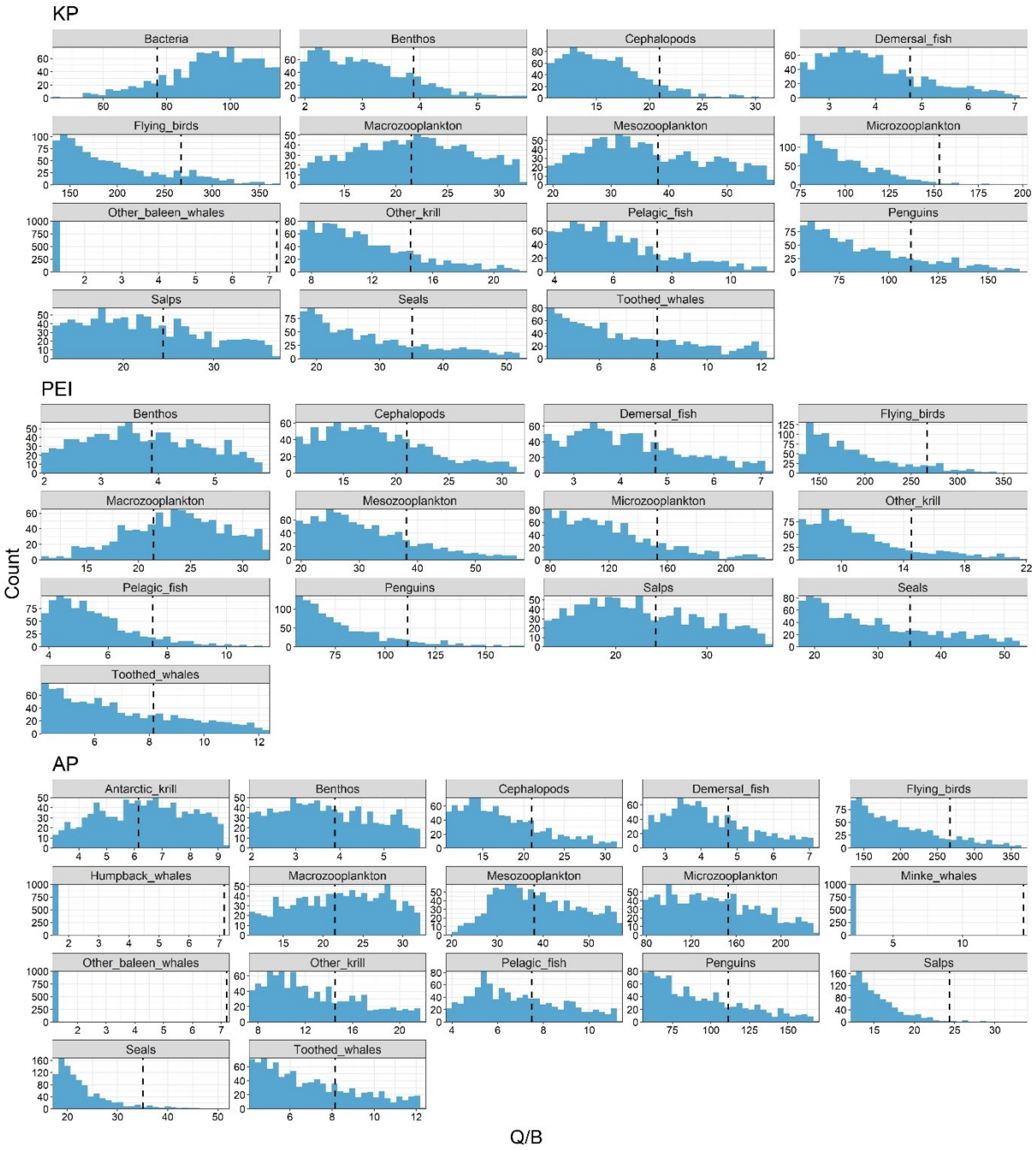

Figure D7: Distribution of consumption over biomass (*Q/B*) in the balanced versions of each model (*n*=1000), for KP, PE and AP. Vertical dashed lines display the original value for each parameter in the standardised, reaggregated but unbalanced version of each model.

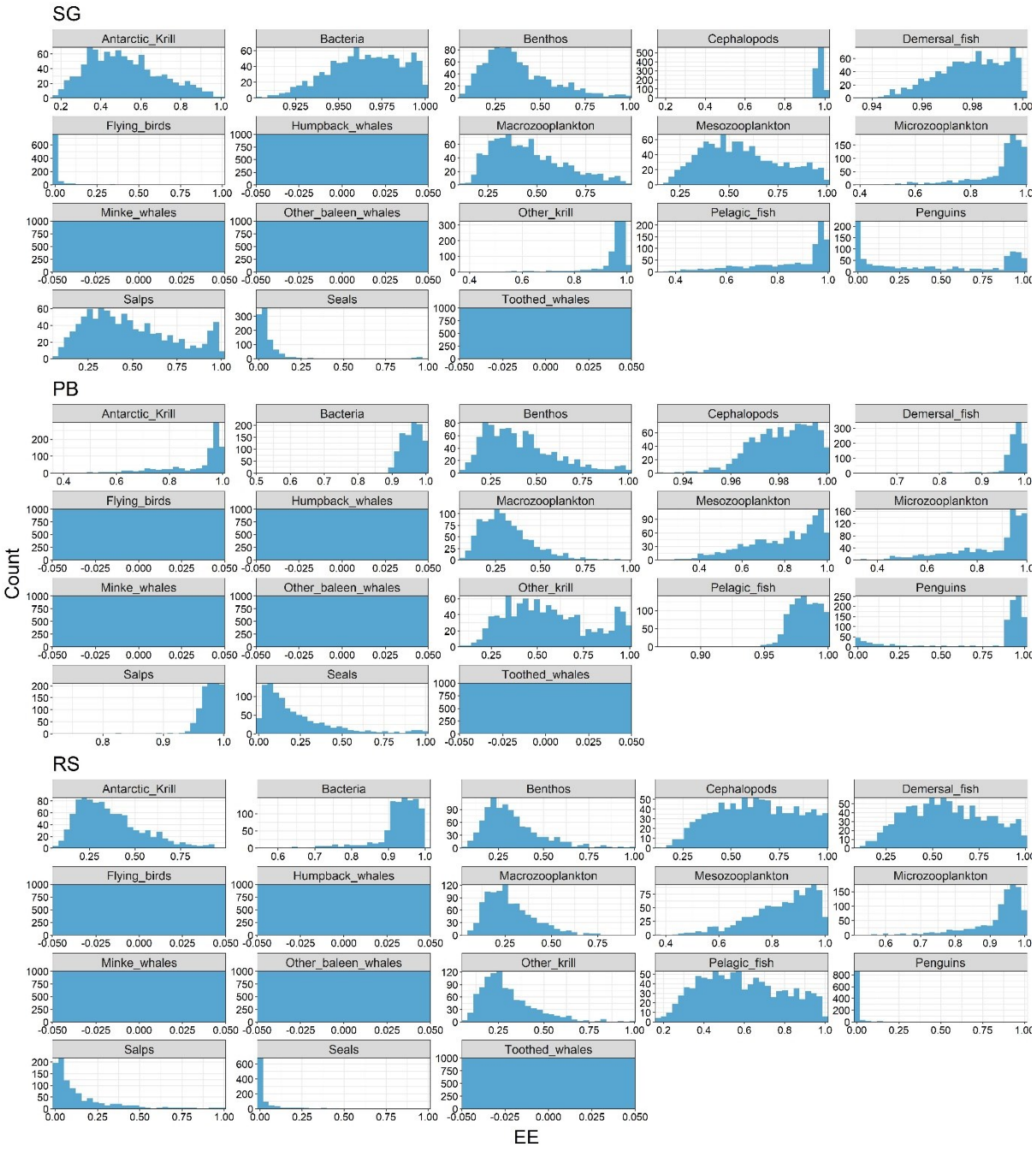

Figure D8: Distribution of ecotrophic efficiency (*EE*) in the balanced versions of each model (*n*=1000), for SG, PB and RS.

Figure D9: Distribution of ecotrophic efficiency (*EE*) in the balanced versions of each model (*n*=1000), for KP, PE and AP.

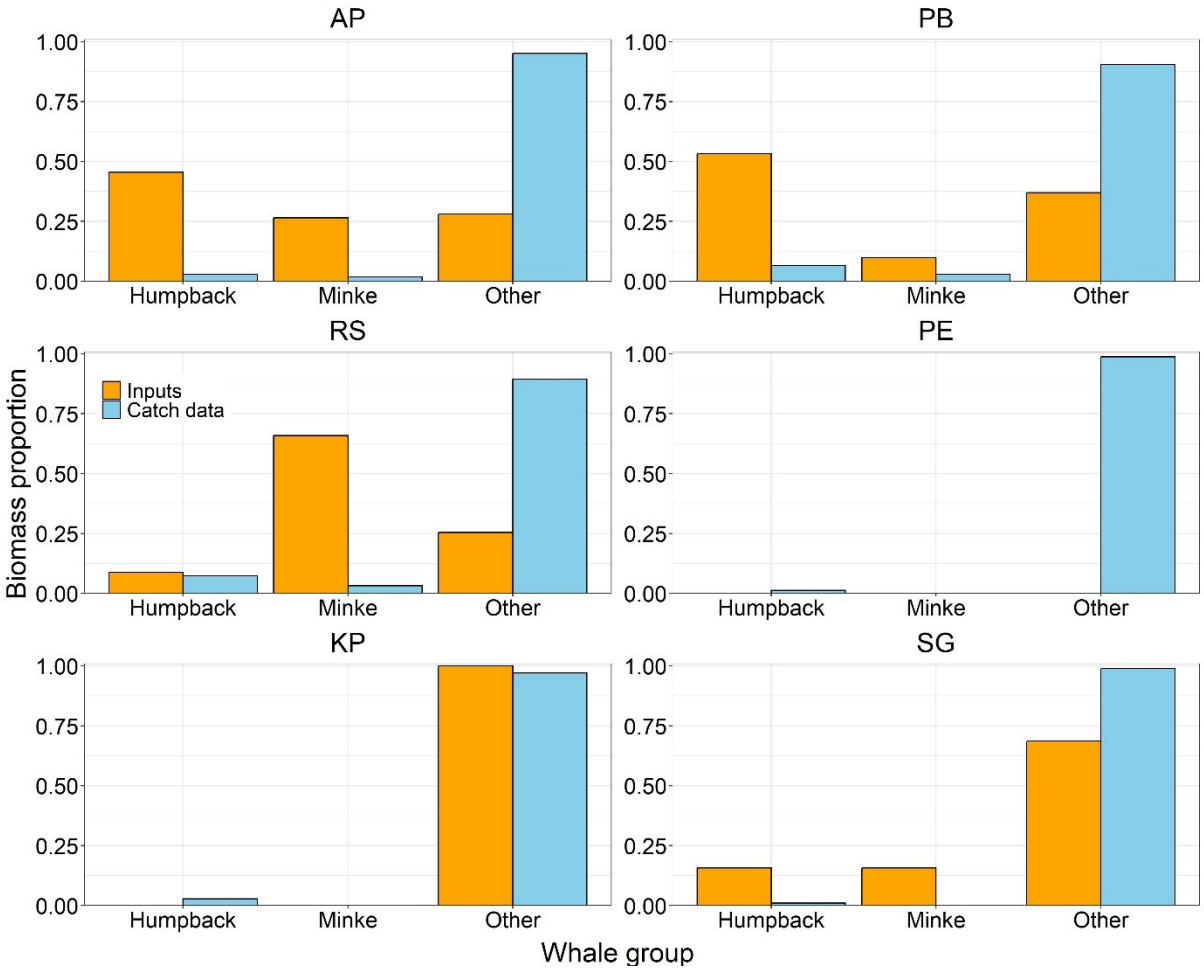

Figure D10: Relative biomass proportion of each baleen whale group for the unbalanced model inputs and for the IWC total catch-derived biomass estimates from the 1000km buffers around each model region.

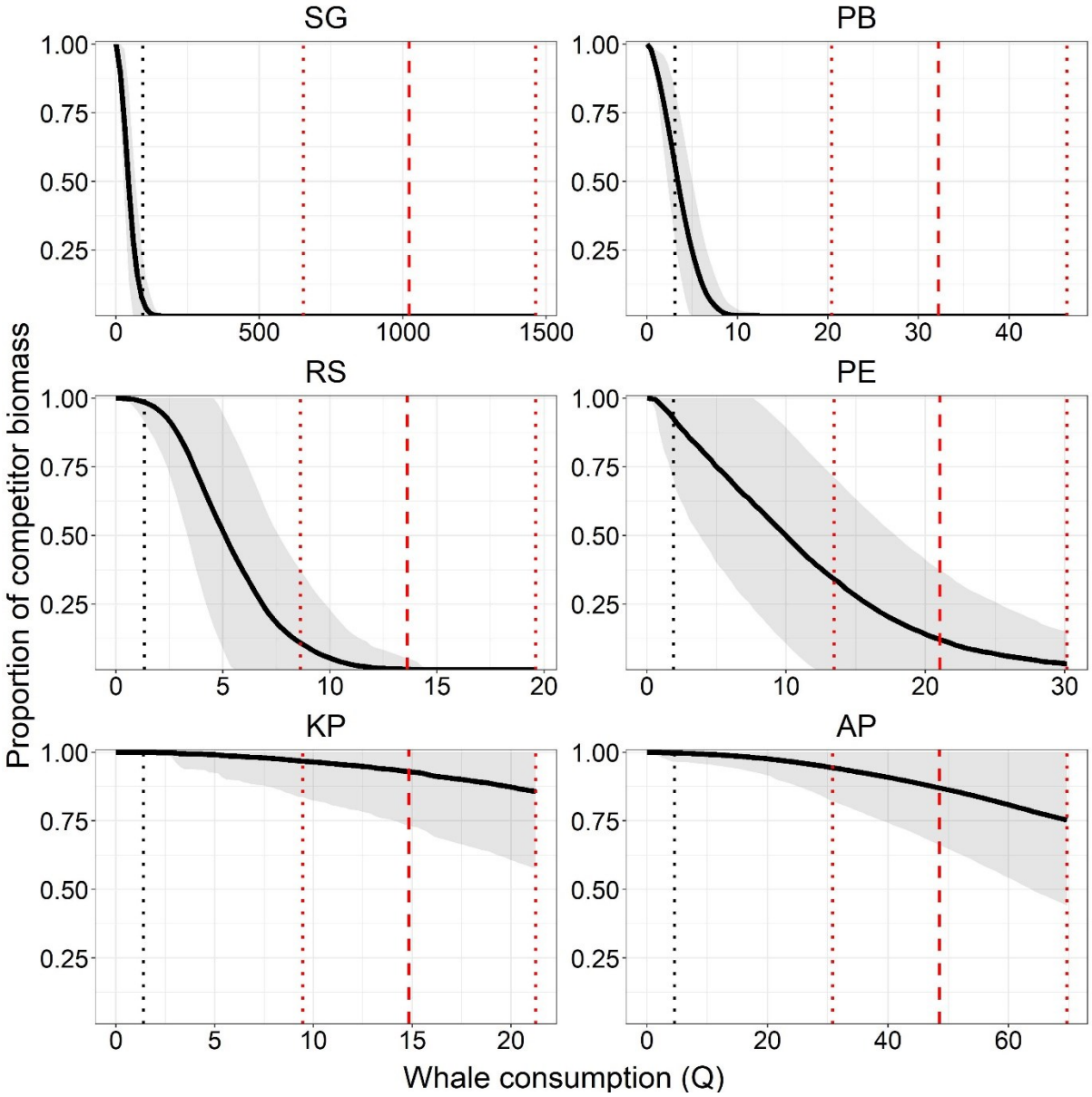

Figure D11: Relationship between competitor biomass proportion and whale consumption (*Q*). Solid black line indicates the ensemble average, and shading indicates standard deviation. Vertical lines indicate the whale *Q* values which represent combinations of catch-derived total whale biomass and estimated *Q/B* values: black dotted = baseline estimates; red dashed = median estimates from Savoca et al. (2021); red dotted = lower and upper estimates from Savoca et al. (2021).

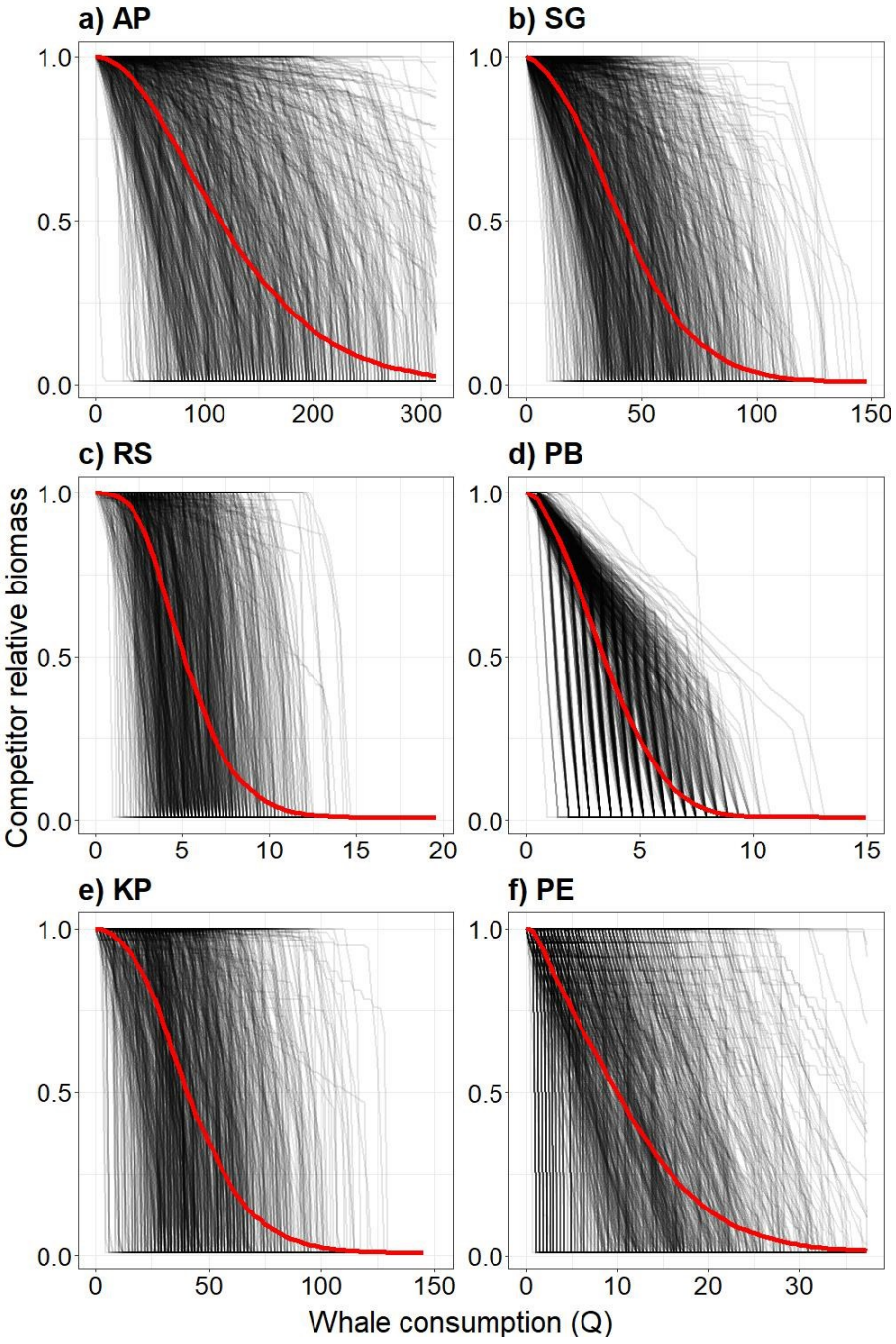

Figure D12: Relationship between competitor biomass proportion and whale consumption (Q) for each of the model ensembles. Black lines represent individual model runs (n=1000), while red lines represent the ensemble average. Note varying x axis scales.

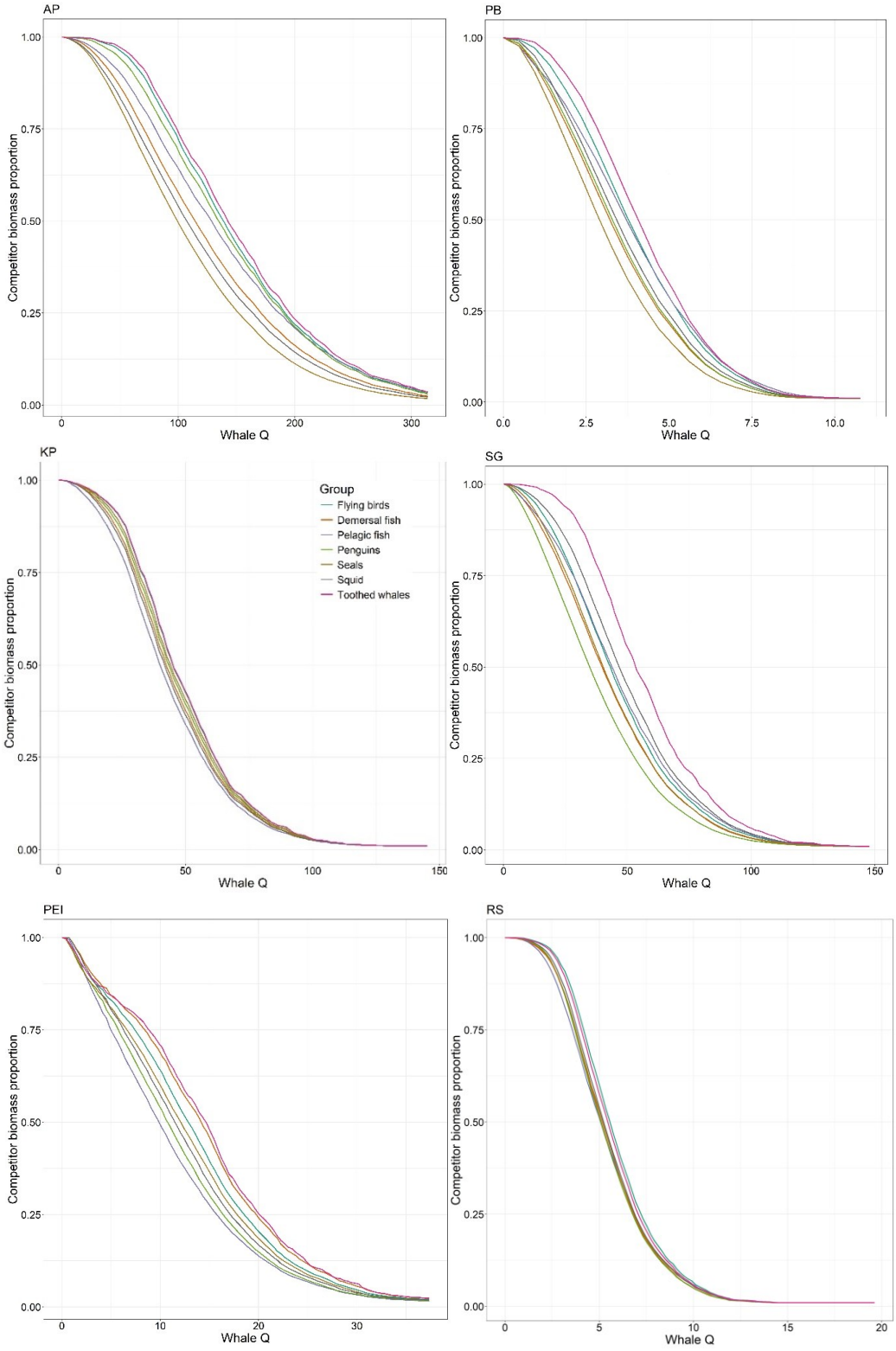

Figure D13: Relationship between total whale consumption (Q) and the proportion of competitor biomass that can be sustained in each model, split by competitor group.

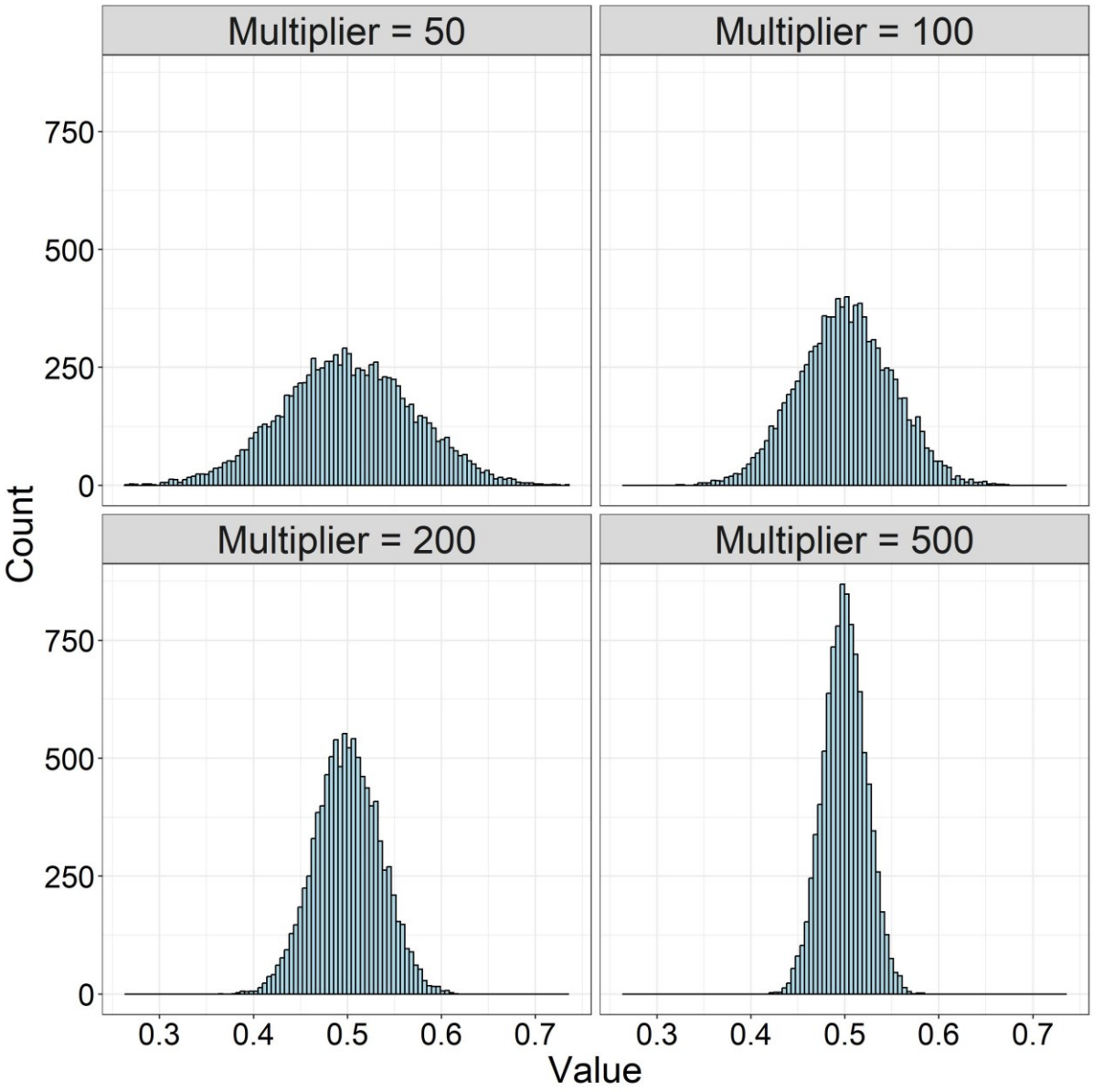

Figure D14: Histograms of the distribution of values generated by resampling the diet of a predator feeding on two prey in equal proportions, under different scaling factors. Each plot displays the values generated for one of the prey.

D3: Supplementary tables

Table D1: Conversion factors used to convert model parameters from to wet weight (gWM $m^{-2}y^{-1}$) to carbon (gC $m^{-2}y^{-1}$).

Functional group	WM:C conversion factor	References and notes
Whales	0.105	Sheehy et al. 2022
Seals	0.162	Horn and de la Vega 2016
Birds	0.181	Horn and de la Vega 2016
Cephalopods	0.087	Ikeda 2016.
Demersal fish	0.105	Horn and de la Vega 2016. Average of benthivorous and piscivorous demersal fish
Pelagic fish	0.170	Horn and de la Vega 2016. Average of planktivorous and piscivorous pelagic fish
Krill	0.107	Kiørboe 2013
Zooplankton	0.049	Kiørboe 2013. Average of ctenophores, tunicates, cnidarians, chaetognaths, gastropods, copepods, euphausids and amphipods
Benthos	0.075	Gogina et al. 2022; Pinkerton and Bradford-Grieve 2010. Based on biomass composition of typical Antarctic benthic communities (Gutt et al. 2016; Pineda Metz 2019).
Bacteria	0.024	Bratbak and Dundas 1984; Finlay and Uhlig 1981
Phytoplankton	0.100	Ullah et al. 2018; Hatton et al. 2021
Macrophyte	0.460	Hill et al. 2021
Detritus	0.450	Hill et al. 2021
Protozoa	0.154	Kiørboe 2013
Salps	0.007	Kiørboe 2013

Table D2: Reaggregated functional groups included in each of the regional models (X indicates that the group is included in the model, • indicates the group is absent from the model).

Functional group	SG	RS	PE	KP	PB	AP
Toothed whales	X	X	X	X	X	X
Humpback whales	X	X	X	X	X	X
Minke whales	X	X	X	X	X	X
Other baleen whales	X	X	X	X	X	X
Seals	X	X	X	X	X	X
Penguins	X	X	X	X	X	X
Flying birds	X	X	X	X	X	X
Demersal fish	X	X	X	X	X	X
Pelagic fish	X	X	X	X	X	X
Cephalopods	X	X	X	X	X	X
Antarctic krill	X	X	•	•	X	X
Other krill	X	X	X	X	X	X
Salps	X	X	X	X	X	X
Macrozooplankton	X	X	X	X	X	X
Mesozooplankton	X	X	X	X	X	X
Microzooplankton	X	X	X	X	X	X
Benthos	X	X	X	X	X	X
Bacteria	X	X	•	X	X	•
Phytoplankton	X	X	X	X	X	X
Ice algae	•	X	•	•	•	X
Detritus	X	X	X	X	X	X

Table D3: Standardised diet composition for each whale group in each model. Separate compositions are provided for krill groups as certain krill groups were absent in some models. Abbreviations are: MW = Minke whales; HW = Humpback whales; OBW = Other baleen whales; SG = South Georgia; PB = Prydz Bay; RS = Ross Sea; AP = Antarctic Peninsula; KP = Kerguelen Plateau; PE = Prince Edward Islands.

	MW	**HW**	**OBW**
Demersal fish	0.029	0.055	0.003
Pelagic_fish	0.128	0.165	0.003
Cephalopods		0.047	
Salps	0.004	0.001	0.003
Macrozooplankton	0.081	0.058	0.083
Mesozooplankton	0.007	0.030	0.160
SG			
Antarctic_krill	0.739	0.634	0.736
Other_krill	0.013	0.011	0.013
PB			
Antarctic_krill	0.479	0.411	0.477
Other_krill	0.272	0.234	0.271
RS			
Antarctic_krill	0.521	0.447	0.519
Other_krill	0.231	0.198	0.230
AP			
Antarctic_krill	0.663	0.569	0.663
Other_krill	0.089	0.076	0.089
KP			
Antarctic_krill	0.000	0.000	0.000
Other_krill	0.752	0.645	0.749
PE			
Antarctic_krill	0.000	0.000	0.000
Other_krill	0.752	0.645	0.749

Table D4: Constants (a) and metabolic scaling exponents (b) used to calculate the average baseline estimates of whale consumption, obtained from Savoca et al. (2021).

a	b
0.1	0.8
0.42	0.67
0.035	1
1.66	0.559
0.123	0.8
0.17	0.773
0.06	0.75

5571 Table D5: Overview of the values used to estimate the *Q/B* for each whale group. Average
5572 body masses are taken from Greenspoon et al. (2023). Daily rations are from Savoca et al.
5573 (2021), multiplied by 90 to estimate annual rations assuming a 90-day feeding period. The
5574 median *Q/B* for each group in the original published models is also shown.

Group	Median Q/B from publish-ed models	Mean mass (kg)	Baseline daily ration (kg)	Baseline *Q/B*	Lower daily ration (kg)	Lower *Q/B*	Median daily ration (kg)	Median *Q/B*	Upper daily ration (kg)	Upper *Q/B*
Minke	10.43	6,566	150.78	2.07	362	4.96	685	9.39	1,085	14.87
Humpback	3.50	30,408	502.13	1.49	1,813	5.37	3,151	9.32	4,926	14.58
Other	3.24	79163	1093.75	1.24	7,765. 50	8.69	12,048	13.60	17,057	19.46

5575

5576 Table D6: Pedigree scheme used to identify confidence intervals for the biomass parameters
5577 for each functional group.

Code	Source	Confidence interval (± %)
1	Estimated by Ecopath	80
2	From other model	80
3	Guesstimate	80
4	Approximate/indirect method	50
5	Local sample, low precision	40
6	Local sample, high precision	10

5578

5579

5580

5581

5582

Table D7: Characteristics of the models. Values represent averages, with brackets indicating the standard deviation.

	PB	SG	RS	AP	KP	PE
Production-weighted mean *EE* of whale prey	0.658 (0.108)	0.526 (0.132)	0.781 (0.108)	0.584 (0.070)	0.636 (0.125)	0.741 (0.108)
Schoener's dietary overlap	0.554 (0.060)	0.642 (0.075)	0.573 (0.048)	0.250 (0.042)	0.717 (0.067)	0.458 (0.059)*

*Based on setting whale biomass to an arbritrarily low value

Table D8: Average total baleen whale biomass (t/km2) across the balanced model ensemble for each region, and total baleen whale catch biomass estimated from the 1000km buffer around each model region and applied to the model's spatial area. Also shown are the whale consumption (*Q*) values estimated from these biomass values when combined with different consumption per unit biomass (*Q/B*) values: Minimum values derived from prior studies (used as the inputs for balancing the models); the lower estimates from Savoca et al. (2021); the upper estimates from Savoca et al. (2021).

	PB	SG	RS	AP	KP	PE
Mean balanced total biomass	0.133	0.288	0.013	0.173	0.026	NA
Total catch biomass	2.44	75.45	1.04	3.62	1.10	1.55
Baseline *Q/B* with balanced biomass	0.195	0.406	0.023	0.271	0.033	NA
Baseline *Q/B* with catch biomass	3.132	94.052	1.333	4.586	1.378	1.937
Lower Savoca *Q/B* with balanced biomass	1.130	2.496	0.110	1.486	0.224	NA
Lower Savoca *Q/B* with catch biomass	20.397	652.781	8.619	30.846	9.458	13.434
Median savoca *Q/B* with balanced biomass	1.776	3.908	0.173	2.331	0.351	NA
Median savoca *Q/B* with catch biomass	32.184	1022.304	13.612	48.482	14.831	21.040
Upper Savoca *Q/B* with balanced biomass	2.552	5.595	0.249	3.343	0.504	NA
Upper Savoca *Q/B* with catch biomass	46.362	1464.142	19.622	69.621	21.266	30.137

5615 Table D9: Conversion of average total whale *Q* into biomass at different reference points of
5616 competitor biomass, using multiple estimates of whale *Q/B*.

Model	Mean initial whale biomass	Catch-derived total whale biomass	Remaining competitor biomass	Total whale *Q*	Whale biomass with baseline *Q/B*	Whale biomass with lower *Q/B*	Whale biomass with median *Q/B*	Whale biomass with upper *Q/B*
PB	0.133	2.44	99%	0.256	0.202	0.030	0.019	0.013
			75%	2.087	1.649	0.246	0.156	0.109
RS	0.013	1.04	99%	1.159	0.914	0.137	0.087	0.061
			75%	3.652	2.880	0.431	0.274	0.191
KP	0.026	1.10	99%	5.172	4.143	0.599	0.383	0.267
			75%	28.095	22.506	3.256	2.078	1.450
PE	0.000	1.55	99%	0.841	0.675	0.097	0.062	0.043
			75%	5.043	4.049	0.582	0.372	0.260
AP	0.173	3.62	99%	2.103	1.675	0.245	0.156	0.109
			75%	70.255	55.956	8.177	5.213	3.636
SG	0.288	75.45	99%	3.091	2.482	0.357	0.228	0.159
			75%	25.943	20.832	2.994	1.912	1.335

5617

5618 Table D10: Primary production required to support the whale consumption (Q) values that
5619 can be achieved by reducing total competitor biomass to either 50% or 10% of starting
5620 values, as identified in Scenario 1. Values are averages across each model ensemble
5621 (*n*=1000), with standard deviations in brackets.

	AP	PB	SG	RS	KP	PE
Mean starting primary production	19,871.53 (4,246.13)	2,251.10 (669.51)	4,372.09 (926.56)	1,073.45 (318.65)	4,094.98 (933.84)	1,075.23 (216.67)
Mean primary production at 75% competitor biomass	19,931.07 (4,240.89)	2,258.79 (669.52)	4,563.84 (974.81)	1,075.19 (318.55)	4,110.01 (935.06)	1,081.85 (217.45)
Mean primary production at maximum whale *Q*	19,931.07 (4,240.89)	2,633.83 (716.51)	28,931.76 (9,626.08)	1,183.00 (332.04)	4,110.00 (935.06)	1,241.15 (267.18)

5622

5623

Table D11: Details of the relationship between whale consumption (Q) and the proportion of extra primary production required to support this increase, for each model.

Model	Max whale Q	Slope
Kerguelen Plateau	21.266	0.000183
Antarctic Peninsula	69.621	0.000046
Prydz Bay	46.362	0.004013
Ross Sea	19.622	0.005649
Prince Edward Islands	30.137	0.005264
South Georgia	1464.142	0.000519